TD

Analytical and in vitro cytotoxicity studies of synthetic cannabinoids found in seized 'herbal incenses'

DOCTORAL THESIS

Vera Lúcia Gouveia Alves
DOCTORATE IN CHEMISTRY

UNIVERSIDADE da MADEIRA
A Nossa Universidade
www.uma.pt

December | 2022

FCT
Fundação para a Ciência e a Tecnologia
MINISTÉRIO DA EDUCAÇÃO E CIÊNCIA

Analytical and in vitro cytotoxicity studies of synthetic cannabinoids found in seized ‘herbal incenses’

DOCTORAL THESIS

Vera Lúcia Gouveia Alves
DOCTORATE IN CHEMISTRY

ORIENTATION
José Sousa Câmara

COORIENTATION
Helena Maria de Sousa Ferreira e Teixeira

Analytical and *in vitro* cytotoxicity studies of synthetic cannabinoids found in seized 'herbal incenses'

A thesis presented to the University of Madeira to obtain the Doctoral degree in Chemistry

Vera Lúcia Gouveia Alves

Under the supervision of:

Professor Doutor José Sousa Câmara

Professora Doutora Helena Maria de Sousa Ferreira e Teixeira

The work presented in this dissertation was performed in Centro de Química da Madeira (CQM) of University of Madeira supported by Fundação para a Ciência e a Tecnologia (FCT) through the PhD grant: SFRH/BD/117426/2016. The support of PROEQUIPRAM - Reforço do Investimento em Equipamentos e Infraestruturas Científicas na RAM (M1420-01-0145-FEDER000008), project M1420-01-0145-FEDER-000005-CQM+ (Madeira 14-20 Program), and FCT throught the CQM Projects: UID/QUI/00674/2015, PestOE/QUI/UI0674/2019. Base Fund UIDB/00674/2020 and Programmatic Fund UIDP/00674/2020, were also acknowledged.

Cofinanciado por:


ACKNOWLEDGMENTS
Agradecimentos

Toda a minha vida tenho-me proposto a vários objetivos e desafios. Contudo a concretização dos nossos sonhos nunca é fácil e é preciso muita dedicação para que tudo seja possível. Este projeto foi sem dúvida um dos maiores desafios que me impus e entre muitos obstáculos, lágrimas, dificuldades e incertezas, não teria conseguido sem o apoio direto ou indireto de várias pessoas. Deste modo gostaria de agradecer…

Ao Professor Doutor José S. Câmara também por ter aceitado uma vez mais na orientação deste projeto, pelo conhecimento transmitido, pela disponibilidade, pela oportunidade de realizar a parte experimental no seu laboratório e pelo apoio prestado ao longo destes anos.

À Professora Doutora Helena Teixeira, por ter aceitado uma vez mais orientar-me e mesmo que à distância esteve sempre disponível para responder às minhas dúvidas/questões e ainda solucionar alguns dos problemas surgidos durante estes 4 anos. Quero agradecer a sua preocupação, atenção, incentivo e paciência ao longo da realização deste projeto.

Ao Doutor Carlos Farinha e à Doutora Maria João Caldeira do Laboratório de Polícia Científica da Polícia Judiciária pela colaboração e pela cedência das amostras.

À Professora Doutora Helena Tomás, por ter aceitado a realização de uma parte do trabalho no Laboratório de Bioquímica e Cultura Celular. Aproveitando também para agradecer à Doutora Mara Gonçalves por todo o conhecimento, ajuda, apoio e paciência nos ensaios de cultura celular.

Ao Professor Doutor João Rodrigues, por ter autorizado a realização das análises de RMN, aproveitando também para agradecer às Doutoras Cláudia Camacho, Dina Maciel e Ana Olival, por toda a ajuda e paciência na realização das análises de RMN.

À Universidade da Madeira e ao Centro de Química da Madeira (CQM) pelas condições fornecidas para a elaboração deste projeto.

À Fundação para a Ciência e a Tecnologia (FCT) pelo financiamento da bolsa de doutoramento (SFRH/BD/117426/2016) sem o qual este projeto não teria sido possível.

Ao Doutor Jorge Pereira e à Doutora Rosa Perestrelo pelo conhecimento e ajuda nos equipamentos e métodos analíticos e pela disponibilidade na resolução de problemas.

Aos colegas de laboratório que acompanharam estes últimos anos, em especial à Mariangie (a paixão) por todo o apoio, disponibilidade, sugestões, colaboração, amizade e pelos sorrisos nos dias de menor ânimo.

Ao meu colega e amigo à mais de 1 década, João Gonçalves, pelo conhecimento, ajuda, motivação, amizade, pelos cafés, pelas risadas, pela partilha de stresses e por também partilhares esta jornada comigo, tu mais do que ninguém sabes os diversos obstáculos que tivemos de enfrentar para prosseguir com as nossas teses.

À minha amiga Joselin, por estares a apoiar desde o início, pela tua amizade, força, ajuda, apoio, motivação, desabafo, risadas, “polacadas”, pela partilha de sobremesas, pelos teus almoços, pelos jantares de Natal e sem dúvida por todo o carinho que sempre me deste e às tuas princesas que tanto gostas.

Ao meu marido Paulo, por todo amor e carinho, pela enorme paciência, pela motivação, força e companheirismo. Obrigada por estares ao meu lado esta última década e por nunca me teres deixado desistir e por seres um excelente pai! Todo o teu apoio e empenho foi essencial para a concretização deste longo e árduo desafio.

À minha mãe Susana, pois sempre teve orgulho na sua primogénita. Obrigada pelos miminhos, por todo o amor, compreensão, dedicação e sacrifício que faz todos os dias para dar o melhor que pode às filhas e às netas.

Ao meu pai Leonel, pelo amor e carinho e por ter me mostrado que nos momentos mais complicados tudo é possível com muita garra e sacrifício. Obrigada por nunca ter desistido mesmo quando tudo parecia impossível de recuperar.

À minha irmã Cristina, a minha 'papaguena', pelo apoio, pelos miminhos, pelas risadas, pela motivação, e por todo o amor por esta tua irmã favorita.

Às minhas avós Lúcia e Isabel, que apesar de já não estarem presentes, em especial a minha 'xarnota' que partiu recentemente, sempre tiveram orgulho em mim. Agradeço-lhes o carinho, a motivação e força que sempre me deram.

E por fim, às minhas filhas gémeas Eliana e Luciana, às quais dedico este projeto, para que de futuro acreditem que os desafios por mais difíceis e que por vezes parecem impossíveis, são possíveis com muita dedicação nossa e apoio dos que nos rodeiam.

PUBLICATIONS AND SCIENTIFIC AWARDS

The following publications were prepared in the scope of this thesis. The author declares to have a major contribution to the conception design and technical execution of the work, acquisition of data, analysis, and interpretation of the results as well as manuscript preparation of the published work included in this thesis.

ARTICLES PUBLISHED IN INTERNATIONAL JOURNALS:

- **Alves V.,** Gonçalves J., Aguiar J., Teixeira H.M., Câmara J.S., The synthetic cannabinoids phenomenon: from structure to toxicological properties. A review, *Critical Reviews in Toxicology* 2020, 50, 359-382, DOI: 10.1080/10408444.2020.1762539.
- **Alves V.,** Gonçalves J., Aguiar J., Caldeira M.J., Teixeira H.M., Câmara J.S., Highly sensitive screening and analytical characterization of synthetic cannabinoids in nine different herbal mixtures, *Analytical and Bioanalytical Chemistry* 2021, 413, 2257-2273, DOI: 10.1007/s00216-021-03199-6.

ORAL COMMUNICATIONS IN SCIENTIFIC MEETINGS:

- **Vera Alves,** João Gonçalves, Joselin Aguiar, Maria J. Caldeira, Helena M. Teixeira, José Câmara, Rapid Screening and Analytical Characterization of Synthetic Cannabinoids in 'Herbal Incenses'. 7th CQM Annual Meeting, 21-22 September 2020, Funchal, Madeira, Portugal.
- **Vera Alves,** João Gonçalves, José Câmara, Helena M. Teixeira, Drogas Sintéticas: Prevalência e Desafios Analíticos na Determinação de Catinonas e Canabinóides Sintéticos. Jornada de Reflexão sobre Novas Substâncias Psicoativas na RAM: - Conhecer, intervir, prevenir, enfrentar, 15 October 2021, Funchal, Madeira, Portugal.
- **Vera Alves,** João Gonçalves, Maria J. Caldeira, Helena M. Teixeira, José Câmara, Identificação, caraterização e isolamento de canabinóides sintéticos de amostras herbais por GC-MS, RMN e UHPLC-PDA. 19º CONGRESSO NACIONAL DE MEDICINA LEGAL E CIÊNCIAS FORENSES / 4ª Reunião da Rede de Serviços Médico-Legais de Língua Portuguesa 18-20 November 2021, Coimbra, Portugal.

POSTER COMMUNICATIONS:

- **Vera L. Alves**, João L. Gonçalves, Maria J. Caldeira, José S. Câmara, Helena M. Teixeira, Characterization Of Synthetic Cannabinoids In 'Herbal Incenses' Products. 57th Annual Meeting of the International Association of Forensic Toxicologists, 2-6 September 2019, Birmingham, UK.
- **Vera Alves,** João Gonçalves, Maria Caldeira, José Câmara, Helena M. Teixeira, Identificação de Canabinóides Sintéticos em Extratos Metanólicos de Misturas Herbais por GC-MS e RMN. 18º

Congresso Nacional de Medicina Legal e Ciências Forenses / 3ª Reunião da Rede de Serviços Médico-Legais de Língua Portuguesa, 21-23 November 2019, Coimbra, Portugal.

- **Vera L. Alves,** João L. Gonçalves, Maria J. Caldeira, Helena M. Teixeira, José Câmara, Screening of 'Spice' Herbal Mixtures using GC-MS and NMR as Complementary Techniques. 11º Encontro Nacional de Cromatografia, 9-11 December 2019, Caparica, Portugal.

SCIENTIFIC AWARDS:

- Poster prize awarded by Analytical and Bioanalytical Chemistry at the 11th Encontro Nacional de Cromatografia, 9-11 December 2019, Caparica, Portugal, with the work: **"**Screening of 'Spice' Herbal Mixtures using GC-MS and NMR as Complementary Techniques".

OTHER PUBLICATIONS/ CONTRIBUTIONS:

ARTICLES PUBLISHED IN INTERNATIONAL JOURNALS:

- Pereira J., Gonçalves J., Porto-Figueira P., Figueira J., **Alves V**., Perestrelo R., Medina S., Câmara J.S., Current trends on microextraction by packed sorbent - fundamentals, application fields, innovative improvements and future trends, *Analyst* 2019, 144, 5048-5074, DOI: 10.1039/c8an02464b. URL: https://pubs.rsc.org/en/content/articlelanding/2019/AN/C8AN02464B#!divAbstract
- Gonçalves J., **Alves V.**, Aguiar J., Teixeira H.M., Câmara J.S., Synthetic Cathinones: An Evolving Class of New Psychoactive Substances, *Critical Reviews in Toxicology* 2019, 49, 549-566, DOI: 10.1080/10408444.2019.1679087. URL: https://www.tandfonline.com/doi/abs/10.1080/10408444.2019.1679087?journalCode=itxc20
- Gonçalves J., **Alves V.**, Aguiar J., Caldeira M.J., Teixeira H.M., Câmara J.S., Structure Assignment of Seized Products Containing Cathinone Derivatives Using High Resolution Analytical Techniques, *Metabolites* 2021, 11, 144, DOI: 10.3390/metabo11030144. URL: https://www.mdpi.com/2218-1989/11/3/144

POSTER COMMUNICATIONS:

- João L. Gonçalves, **Vera L. Alves**, Maria J. Caldeira, José S. Câmara, Helena M. Teixeira, Chemical Characterization of New Psychoactive Substances belonging to the class of Synthetic Cathinones In 'Legal High' Products. 57th Annual Meeting of the International Association of Forensic Toxicologists, 2-6 September 2019, Birmingham, UK.
- João Gonçalves, **Vera Alves**, Maria Caldeira, José Câmara, Helena M. Teixeira, Caracterização Analítica de Catinonas Sintéticas em Produtos Apreendidos em Portugal. 18º Congresso Nacional de Medicina Legal e Ciências Forenses / 3ª Reunião da Rede de Serviços Médico-Legais de Língua Portuguesa, 21-23 November 2019, Coimbra, Portugal.

ABSTRACT

Initially developed as therapeutic agents, synthetic cannabinoids rapidly appeared on drug market as recreational drugs with over 200 substances notified in Europe. Marketed as 'synthetic marijuana', they are usually sold in herbal mixtures, as smoking products. Cheaper, accessible, and with stronger effects compared to cannabis, have led to a dramatic increase in its consumption. New compounds emerge constantly, and the side effects and toxicity of these products have not yet been properly studied, being a challenge for laboratories.

In our study, nineteen seized herbal products provided by the criminal police were analysed by gas chromatography – mass spectrometry (GC-MS) and nuclear magnetic resonance (NMR) techniques. Ten synthetic cannabinoids (JWH-018, JWH-073, JWH-122, JWH-210, MAM-2201, APINACA, XLR-11, UR-144, CP47,497-C8 and 3-epi-CP47,497-C8), and three adulterants (oleamide, vitamin E and vitamin E acetate) were identified.

Subsequently, the determination of eight cannabinoids (MAM-2201, JWH-073, JWH-018, JWH-122, JWH-210, UR-144, XLR-11 and APINACA) in oral fluid samples using microextraction by packed sorbent (MEPS) and µSPEed techniques combined with ultra-high performance liquid chromatography (UHPLC) analysis was developed. Both methodologies were validated, presenting good recovery values (above 70%) and low detection limits (9.5 – 13.2 and 4.4 – 10.3 ng/mL, respectively) and applied to two real samples.

Finally, the cytotoxicity of eight seized herbal extracts and damiana extract was evaluated in A549 lung cell line. A significant concentration-dependent decrease in cell viability was observed after 48h and 72h exposure. Damiana extract and JWH-018 (single compound of one of the samples) significantly induced more reactive species formation and a significant decline in ATP synthesis was observed in damiana and in sample with XLR-11 and APINACA compounds.

In summary, the applied methodologies revealed as promising approaches. Inconsistency in composition was verified among the analysed samples, and *in vitro* results highlighted the potential harmful effects of these synthetic drugs.

Keywords: Synthetic Cannabinoids; Herbal incenses; GC-MS; NMR; MEPS/ µSPEed – UHPLC-PDA; Cytotoxicity

RESUMO

Inicialmente desenvolvidos como agentes terapêuticos, os canabinóides sintéticos apareceram no mercado das drogas como drogas recreativas com mais de 200 substâncias notificadas na Europa. Comercializados como 'marijuana sintética' são geralmente vendidos em misturas de ervas para fumar. Mais baratos, acessíveis e com efeitos mais fortes comparando com a cannabis, levaram ao aumento dramático no seu consumo. Novos compostos emergem constantemente, e os efeitos secundários e a toxicidade destes produtos ainda não foram devidamente estudados, sendo um desafio para os laboratórios.

Neste estudo, dezanove produtos apreendidos pela polícia judiciária foram analisados por cromatografia gasosa - espectrometria de massa (GC-MS) e por ressonância magnética nuclear (RMN). Foram identificados dez canabinóides sintéticos (JWH-018, JWH-073, JWH-122, JWH-210, MAM-2201, APINACA, XLR-11, UR-144, CP47,497-C8 e 3-epi-CP47,497-C8), e três adulterantes (oleamida, vitamina E, e acetato de vitamina E).

Subsequentemente, oito canabinóides (MAM-2201, JWH-073, JWH-018, JWH-122, JWH-210, UR-144, XLR-11 e APINACA) foram determinados em amostras de fluidos orais usando microextração por sorbente embalado (MEPS) e µSPEed, combinadas a cromatografia líquida de ultra eficiência (UHPLC). Ambas as metodologias foram validadas, apresentando bons valores de recuperação (acima de 70%) e baixos limites deteção (9,5 - 13,2 e 4,4 - 10,3ng/mL, respetivamente) e aplicadas a duas amostras reais.

Finalmente, a citotoxicidade de oito amostras apreendidas e extrato de damiana, foi avaliada na linha celular pulmonar A549. Foi observada uma diminuição significativa da viabilidade celular dependente da concentração, após 48h e 72h de exposição. O extrato de damiana e JWH-018 (composto único de uma das amostras) induziram significativamente a formação de espécies mais reativas e um declínio significativo na síntese de ATP pela damiana e pela amostra com os compostos XLR-11 e APINACA.

Em resumo, as metodologias aplicadas revelaram-se promissoras. A inconsistência na composição foi verificada entre as amostras analisadas, e os resultados *in vitro* evidenciaram os potenciais efeitos nocivos destas drogas sintéticas.

Keywords: Canabinóides Sintéticos; Incensos herbais; GC-MS; RMN; MEPS/ µSPEed – UHPLC-PDA; Citotoxicidade

THESIS DESIGN

The present thesis is organized in four main parts:

- **Part 1 – General Introduction**

This first part is divided in two Chapters:

In Chapter I, an overview of the literature on one of the key concepts of this work (cannabinoids) is presented, in order to provide the theoretical basis to understand the main theme of the study. This chapter also includes a review article entitled "The synthetic cannabinoids phenomenon: from structure to toxicological properties. A review".

In Chapter II, an overview of current analytical methodologies for separation and identification of synthetic cannabinoids in different matrices, as well as their advantages and limitations in forensic and toxicological context is discussed.

- **Part 2 – Objectives**

In this part, the justification of the research and the objectives are presented and contextualized.

- **Part 3 – Experimental**

In this part, the studies performed during the research period are presented and divided in three Chapters, which aim to fulfil the objectives of the thesis:

In Chapter I, the chemical characterization studies are described. Part of the results presented in this chapter are published in the article entitled "Highly sensitive screening and analytical characterization of synthetic cannabinoids in nine different herbal mixtures".

In Chapter II, the analytical determination of synthetic cannabinoids in biological samples is described.

And finally, in Chapter III, the cytotoxicity study of synthetic cannabinoids is presented.

- **Part 4 – Final Conclusions**

In this part, the main conclusions and achievements of the thesis are presented based on the proposed objectives.

The remaining data are being prepared to submit for publication in international, peer-reviewed journals soon.

General Index

Figures Index

Tables Index

Abbreviations List Index

$U_{\%\bar{R}}$	Uncertainty in average recovery
t_{crit}	Two-tailed critical value
[C]	Carboxylation
[Glu]	Glucuronidation
[H]	Hydroxylation
[OD]	Oxidative fluorination
·OH	Hydroxyl
^{13}C NMR	Carbon Nuclear Magnetic Resonance
^{19}F NMR	Fluor Nuclear Magnetic Resonance
^{1}H NMR	Proton Nuclear Magnetic Resonance
$^{1}O_2$	Singlet oxygen
2,4-DNPH	2,4-dinitrophenylhydrazine
2-AG	2-arachidonoylglycerol
3-epi C47,497-C8	2-[(1S,3S)-3-Hydroxycyclohexyl]-5-(2-methyl-2-nonanyl)phenol
4F-MDMB-BINACA	Methyl (S)-2-(1-(4-fluorobutyl)-1H-indazole-3-carboxamido)-3,3-dimethylbutanoate
5F-AKB-48	N-(adamantan-1-yl)-1-(5-fluoropentyl)-1H-indazole-3-carboxamide
5F-APICA	N-benzyl-1-(5-fluoropentyl)-1H-indole-3-carboxamide
5F-Cumyl-PINACA	1-(5-Fluoropentyl)-N-(2-phenylpropan-2-yl)-1H-indazole-3-carboxamide
5F-MDMB-PICA	Methyl (2S)-2-[[1-(5-fluoropentyl)indole-3-carbonyl]amino]-3,3-dimethylbutanoate
5F-MDMB-PICA	Methyl (2S)-2-[[1-(5-fluoropentyl)indole-3-carbonyl]amino]-3,3-dimethylbutanoate
5F-MDMB-PINACA	Methyl (S)-2-[1-(5-fluoropentyl)-1H-indazole-3-carboxamido]-3,3-dimethylbutanoate
5F-PB-22	Quinolin-8-yl 1-pentyfluoro-1H-indole-3-8-carboxylate
A549	Human lung cell line
AB-001	1-Pentyl-3-(adamant-1-oyl)indole
AB-CHMINACA	N-[(2S)-1-Amino-3-methyl-1-oxobutan-2-yl]-1-(cyclohexylmethyl)indazole-3-carboxamide
AB-FUBINACA	N-[(2S)-1-Amino-3-methyl-1-oxobutan-2-yl]-1-[(4-fluorophenyl)methyl]indazole-3-carboxamide
AB-PINACA	N-[(1S)-1-(Aminocarbonyl)-2-methylpropyl]-1-pentyl-1H-indazole-3-carboxamide
ACN	Acetonitrile
AM-1220	(R)-(1-((1-Methylpiperidin-2-yl)methyl)-1H-indol-3-yl)(naphthalen-1-yl)methanone
AM-1248	1-[(N-methylpiperidin-2-yl)methyl]-3-(adamant-1-oyl)indole
AM-2201	1-[(5-Fluoropentyl)-1H-indol-3-yl]-(naphthalen-1-yl)methanone
AM-2232	5-(3-(1-Naphthoyl)-1H-indol-1-yl)pentanenitrile

AM-2233	1-[(N-methylpiperidin-2-yl)methyl]-3-(2-iodobenzoyl)indole
AM-251	1-(2,4-Dichlorophenyl)-5-(4-iodophenyl)-4-methyl-N-(1-piperidyl)pyrazole-3-carboxamide
AM-4030	6H-Dibenzo(b,d)pyran-9-methanol, 3-(1,1-dimethylheptyl)-6a,7,8,9,10,10a-hexahydro-1-hydroxy-6-((1E)-3-hydroxy-1-propenyl)-6-methyl-, (6S,6aR,9R,10aR)
AM-630	1-[2-(Morpholin-4-yl)ethyl]-2-methyl-3-(4-methoxybenzoyl)-6-iodoindole
AM-679	(2-Iodophenyl)(1-pentyl-1H-indol-3-yl)methanone
AM-694	1-[(5-Fluoropentyl)-1H-indol-3-yl]-(2-iodophenyl)methanone
AMB-FUBINACA	Methyl (2S)-2-{[1-[(4-fluorophenyl)methyl]indazole-3-carbonyl]amino}-3-methylbutanoate
AMP	Adenosine Monophosphate
anandamide	N-arachidonoylethanolamine
ANOVA	Analysis of variance
APICA	N-(1-adamantyl)-1-pentylindole-3-carboxamide
APINACA	N-(1-Adamantyl)-1-pentylindazole-3-carboxamide
APS	Aminopropyl Silane
ATP	Adenosine Triphosphate
BCA	Bicinchoninic Acid solution
BEH	Bridged Ethylene Hybrid
Bias	Mean relative error of the estimated concentration
BIN	Barrel Insert and Needle Assembly
BSA	Bovine Serum Albumin solution
C_{18}	Octadecyl-silica
C_{18EC}	End-capped octadecylsilane
C_2	Ethyl-silica
C_8	Octyl-silica
cAMP	Cyclic adenosine monophosphate
CAR/PDMS	Carboxen/polydimethylsiloxane
CB_1	Cannabinoid receptor type 1
CB_2	Cannabinoid receptor type 2
CBD	Cannabidiol
CBG	Cannabigerol
CBN	Cannabinol
CD_3OD	Deuterated Methanol
CI	Confidence interval
CNS	Central nervous system
CO_2	Carbon dioxide
COSY	Correlation Spectroscopy
CP 47,497	2-[(1S,3R)-3-hydroxycyclohexyl]-5-(2-methyloctan-2-yl)phenol
CP 55,940	cyclohexylphenol
CP 47,497-C8	2-[(1S,3R)-3-hydroxycyclohexyl]-5-(2-methyloctan-2-yl)phenol

CRA-13	Naphthalen-1-yl-(4-pentyloxynaphthalen-1-yl)methanone
CRM	Certified reference materials
CSA	Controlled Substances Act
CSH	Charged Surface Hybrid
CV_r	Coefficient of repeatability variation
CV_{si}	Coefficient of intermediate precision
CYP	Cytochrome P450 enzymes
d	Duplet
Da	Dalton
DAD	Diode Array Detector
DART-MS/MS	Direct Analysis in Real Time-tandem Mass Spectrometry
DCF	2',7'-dichlorofluorescein
DCFH	Dichlorofluorescein
DCFH-DA	2',7'- dichlorofluorescin diacetate
DCM	Dichloromethane
dd	Double duplet
DEA	Drug Enforcement Administration
DESI-HRMS	Desorption Electrospray Ionization-High Resolution Mass Spectrometry
DI-SPME	Direct Extraction - Solid Phase Microextraction
DLLME	Dispersive Liquid-Liquid Microextraction
DMSO	Dimethyl Sulfoxide
DS^2	Difference of variances
Dspe	Dispersive Solid Phase Extraction
DTT	Dithiothreitol
DUID	Driving under the influence of drug
EAM-2201	(4-ethyl-1-naphthalenyl)[1-(5-fluoropentyl)-1H-indol-3-yl]-methanone
EDTA	2,2',2'',2'''-(Ethane-1,2-diyldinitrilo) tetra acetic acid
EE (%)	Extraction Efficiency
EI	Eletron Impact Ionization
EMCDDA	European Monitoring Centre For Drugs And Drug Addiction
F-12K	Ham´s F-12 medium - Kaighn's modification
FA	Formic Acid
FBS	Fetal Bovine Serum
F-test	Fisher/Snedecor test
GCB	GRAPHITISED CARBON BLACK
GC-MS	Gas Chromatography Mass Spectrometry
GP	Glutathione Peroxidase
GR	Glutathione Reductase
GSH	Reduced Glutathione
GSSG	Oxidized Glutathione
H_2O_2	Hydrogen Peroxide
HBSS	Hank's Balanced Salts Solution
$HClO_4$	Perchloric acid
HDVB	Highly Cross-Linked Divinylbenzene Polystyrene

HL	High Level
HMBC	Heteronuclear Multiple Bond Spectroscopy
HOCl	Hypochlorous acid
HPLC-MS/MS	High Performance Liquid Chromatography–Tandem Mass Spectrometry
HPLC-UV	High-Performance Liquid Chromatography-Ultraviolet
HSQC	Heteronuclear Single Quantum Spectroscopy
HS-SPME	Headspace - solid phase microextraction
HU-210	1,1-Dimethylheptyl- 11-hydroxy-tetrahydrocannabinol
HU-211	(6aS,10aS)-9-(Hydroxymethyl)-6,6-dimethyl-3-(2-methyloctan-2-yl)-6a,7,10,10a-tetrahydrobenzo[c]chromen-1-ol
HU-308	[(1S,2S,5S)-2-[2,6-Dimethoxy-4-(2-methyloctan-2-yl) phenyl]-7,7-dimethyl-4-bicyclo [3.1.1] hept-3-enyl]methanol
HU-433	[(1R,5R)-4-[2,6-dimethoxy-4-(2-methyloctan-2-yl) phenyl]-6,6-dimethyl-2-bicyclo [3.1.1] hept-2-enyl]methanol
IC_{25}	25% inhibitory concentration
IC_{50}	Half maximum inhibitory concentration
IE	ion exchange
J	Spin coupling
JWH-015	(2-Methyl-1-propyl-1H-indol-3-yl)-1-naphthalenylmethanone
JWH-018	Naphthalen-1-yl-(1-pentylindol-3-yl) methanone
JWH-019	1-Hexyl-3-(naphthalen-1-oyl)indole
JWH-030	Naphthalen-1-yl-(1-pentylpyrrol-3-yl)methanone
JWH-073	Naphthalen-1-yl-(1-butylindol-3-yl) methanone
JWH-081	4-Methoxynaphthalen-1-yl-(1-pentylindol-3-yl)methanone
JWH-122	(4-methyl-1-naphthyl)-(1-pentylindol-3-yl) methanone
JWH-133	(6aR,10aR)-3-(1,1-Dimethylbutyl)-6a,7,10,10a-tetrahydro -6,6,9-trimethyl-6H-dibenzo[b,d]pyran
JWH-151	1-propyl-2-methyl-3-(6-methoxy-1-naphthoyl)indole
JWH-184	3-[(4-Methyl-1-naphthalenyl)methyl]-1-pentyl-1H-indole
JWH-192	4-(2-(3-((4-methylnaphthalen-1-yl)methyl)-1H-indol-1-yl)ethyl)morpholine
JWH-196	2-Methyl-3-(1-naphthalenylmethyl)-1-pentyl-1H-Indole
JWH-200	(1-(2-Morpholin-4-ylethyl)indol-3-yl)-naphthalen-1-ylmethanone
JWH-203	2-(2-Chlorophenyl)-1-(1-pentylindol-3-yl)ethanone
JWH-210	4-ethylnaphthalen-1-yl-(1-pentylindol-3-yl) methanone

JWH-250	2-(2-Methoxyphenyl)-1-(1-pentylindol-3-yl)ethanone
JWH-251	2-(2-Methylphenyl)-1-(1-pentyl-1H-indol-3-yl) ethan-1-one
JWH-307	(5-(2-Fluorophenyl)-1-pentylpyrrol-3-yl)-naphthalen-1-ylmethanone
$KHCO_3$	Potassium bicarbonate
LC	Liquid Chromatography
LC-MS/MS	Liquid Chromatography with Tandem Mass Spectrometry
LC-QTOF/MS	Liquid Chromatography-Quadrupole-Time of Flight Mass Spectrometry
LC-TOF-MS	Liquid Chromatography Time-of-Flight Mass Spectrometry
LL	Low Level
LLE	Liquid-Liquid Extraction
LOD	Limit of Detection
LOQ	Limit of Quantification
LPC	Laboratório de Polícia Científica
m	Multiplet
m/z	Mass-to-charge ratio
M1	Mixed-mode
MA	Maleic Acid
MAM-2201	(1-(5-fluoropentyl)-1H-indol-3-yl) (4-methyl-1-naphthalenyl)-methanone
MDMB-4-en-PINACA	Methyl 3,3-dimethyl-2-(1-(pent-4-en-1-yl)-1H-indazole-3-carboxamido) butanoate
MDMB-FUBINACA	Methyl (2S)-2-{[1-[(4-fluorophenyl) methyl] indazole-3-carbonyl]amino}-3,3-dimethylbutanoate
ME (%)	Matrix effect
MeOH	Methanol
MEPS	Microextraction By Packed Sorbent
$MgSO_4$	Magnesium Sulphate
MIPs	Molecular Imprinted Polymers
ML	Medium Level
MS	Mass spectrometry
MTT	3-(4,5-Dimethylthiazol)-2,5-diphenyltetrazolium
NAD^+	Nicotinamide Adenine Dinucleotide
NADPH	Nicotinamide Adenine Dinucleotide Phosphate Hydrogen
NaOH	Sodium Hydroxide
NIST	National Institute of Standards and Technology
NMR	Nuclear Magnetic Resonance Spectroscopy
$NO^{\cdot}$	Nitric Oxide
NO_2	Nitrogen Dioxide
NP	Normal Phase
NPS	New Psychoactive Substances
$O_2^{\cdot}$-	Superoxide
O_3	Ozone

$ONOO^{\cdot}$	Peroxynitrite
PB-22	1-pentyl-1H-indole-3-carboxylic acid 8-quinolinyl ester
PBS	Phosphate Buffered Saline
PDA	Photodiode Array Detector
PDMS	Polydimethylsiloxane
PDMS	Polydimethylsiloxane
PEP	Polar Enhanced Polymer
PNS	Peripheral Nervous System
PP	Protein Precipitation
ppm	Parts per million
PSA	Primary Secondary Amine
PS-DVB	Highly Cross-Linked Polystyrene Divinylbenzene Copolymer
PTFE	Polytetrafluoroethylene
PV-DVB	Polystyrene-Divinylbenzene Copolymer
QSM	Quaternary Solvent Manager
QuEChERS	Quick, Easy, Cheap, Effective, Rugged and Safe
quint	Quintet
r	Correlation coefficient
R (%)	Extraction recovery
R^2	Determination coefficient
R-AX	Polymeric DVB partially functionalized with quaternary amine groups
RCS-4	2-(4-methoxyphenyl)-1-(1-pentyl-indol-3-yl)methanone
R-CX	Polymeric DVB partially functionalized with sulfonic acid groups
Rf	Retention factor
RF	Radio frequency
RI	Retention indices
RMN	Ressonância Magnética Nuclear
RNS	Reactive Nitrogen Species
RO-	Alkoxyl
$RO_2^{\cdot}$	Peroxyl
ROS	Reactive Oxygen Species
RP	Reversed Phase
Rs	Resolution
RSD or *CV*	Relative Standard Deviation or Coefficient of Variation
Rt	Retention Time
s	Singlet
SAX	strong anion exchange
SCs	Synthetic Cannabinoids
SCX	Strong Cation Exchange
SD	Standard Deviation
SEM	Standard Error of the Mean
S_i	Standard Deviation of Intermediate Precision

SICAD	Serviço de Intervenção nos Comportamentos Aditivos e nas Dependências
SLE	Supported Liquid Extraction
SPE	Solid Phase Extraction
SPME	Solid Phase Microextraction
S_r	Standard Deviation of Repeatability
SR141716A	5-(4-Chlorophenyl)-1-(2,4-dichlorophenyl)-4-methyl-N-(piperidin-1-yl)-1H-pyrazole-3-carboxamide
SR144528	5-(4-Chloro-3-methylphenyl)-1-[(4-methylphenyl) methyl]-N-[(1S,2S,4R)-1,3,3-trimethylbicyclo[2.2.1]heptan-2-yl]-1H-pyrazole-3-carboxamide
SWGDRUG	EI-MS Library of the Scientific Working Group for the Analysis of Seized Drugs
$S_{y/x}$	Residual standard deviation
t	Triplet
t_{exp}	*t-Student* test
TFA	Trifluoroacetic Acid
THJ-2201	[1-(5-Fluoropentyl)-1H-indazol-3-yl](1-naphthyl)methanone
TLC	Thin Layer Chromatography
TV	Test value
UGT	UDP-glucuronosyltransferases
UHPLC	Ultra-High Performance Liquid Chromatography
UHPLC-MS/MS	Ultra-High Performance Liquid Chromatography-Tandem Mass Spectrometry
UNODC	United Nations Office on Drugs and Crime
UR-144	(1-pentylindol-3-yl)-(2,2,3,3-tetramethylcyclopropyl) methanone
UV-Vis	Ultraviolet/visible
WHO	World Health Organisation
WIN55,212-2	(11R)-2-Methyl-11-[(morpholin-4-yl) methyl]-3-(naphthalene-1-carbonyl)-9-oxa-1-azatricyclo [6.3.1.04,12] dodeca-2,4(12),5,7-tetraene
XLR-11	(1-(5-fluoropentyl)-1H-indol-3-yl) (2,2,3,3-tetramethylcyclopropyl) methanone
β-NADPH2	β-nicotinamide adenine dinucleotide phosphate
δ	Chemical Shift
Δ9-THC	Δ9-tetrahydrocannabinol
θ_{max}	Maximal observed effects
θ_{min}	Minimal observed effects
µ-SPE	Miniaturized Solid Phase Extraction

Part 1- GENERAL INTRODUCTION

CHAPTER I - Cannabinoids

1. Cannabinoids: from natural to synthetic

According to the World Health Organization (WHO), cannabis (Figure 1) is the most commonly cultivated, trafficked, and abused illicit drug and, its consumption has an annual prevalence rate of approximately, 147 million individuals or nearly 2.5% of the global population [1].

Figure 1. Cannabis leaf (adapted from [2])

Being the most thoroughly studied plant of all time, cannabis have been used for recreational, medicinal, or scientific purposes due to its bioactive components [3]. Cannabis plant is chemically complex, containing more than 500 components, of which over 120 cannabinoids have presently been identified and isolated [4]. Most of the biological activity attributed to cannabis have so far been linked to cannabinoids. The term 'cannabinoids' represented the group of typical terpenophenolic C_{21} compounds present in cannabis plant, their carboxylic acids, analogues, and transformation products. However, an extended classification comprising new classes, groups, and subgroups of cannabinoids was proposed for better representation of their structural variety [5]. Cannabinoids, now constitute the whole set of herbals, endogenous, natural and synthetic ligands of the cannabinoid receptors (CB_1 and CB_2), belonging to a wide variety of chemical families [6-8]. Based on their source of production, cannabinoids can be classified into three groups: endogenous cannabinoids (or endocannabinoids), phytocannabinoids and synthetic cannabinoids (Figure 2) [9].

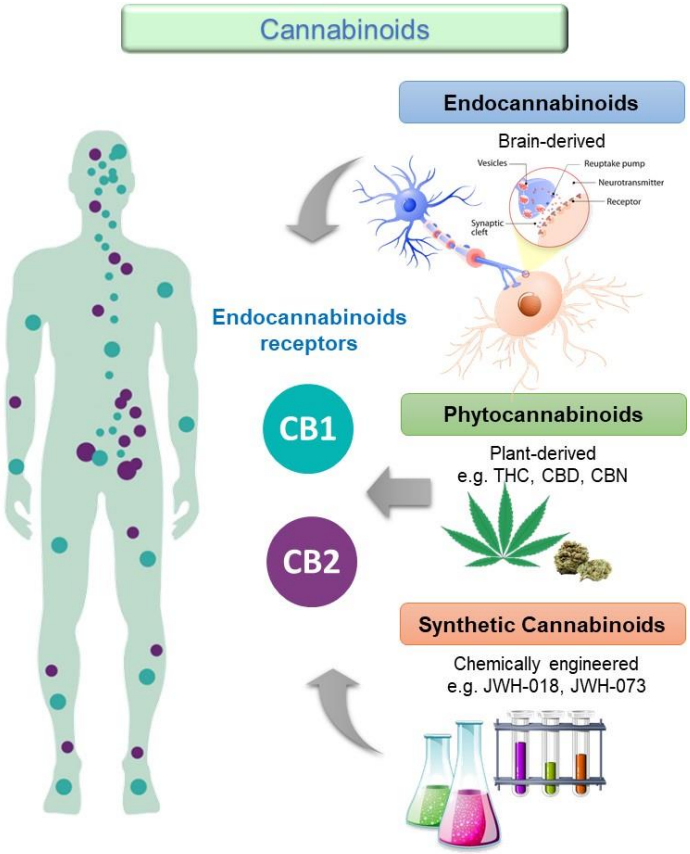

Figure 2. Types of cannabinoids (adapted from [10]).

Endocannabinoids have been identified as having roles in various physiological and pathological processes. Largely due to the association of the effects of cannabis administration on mental states, the impact of the endocannabinoid system on central nervous system (CNS) has been the most intensively studied. Defined as endogenous lipids that activate cannabinoid receptors, this group of cannabinoids affects the behaviour in a way that at least partially recapitulates the effects produced by the psychoactive components of cannabis [11, 12].

N-arachidonoylethanolamine (anandamide and 2-arachidonoylglycerol (2-AG) (Figure 3) the first endogenous agonists to be discovered, are saturated or unsaturated acid amides that present physiological properties very similar to natural and synthetic exogenous cannabinoids, such as those found in cannabis plant [5, 13].

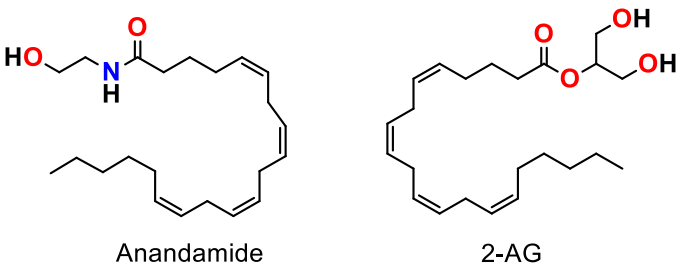

Figure 3. Molecular structure of two major endocannabinoids

These natural agonists are lipid-based molecules containing long-chain polyunsaturated fatty acids, amides, esters and ethers, and act as neuromodulators or retrograde neurotransmitters that bind to cannabinoid receptors and cannabinoid receptor proteins that are expressed throughout the mammalian CNS (including the brain) and peripheral nervous system (PNS) [9, 11, 14, 15].

Phytocannabinoids, are only known to occur naturally in significant quantity in cannabis plant [16]. The total number of natural compounds identified or isolated from cannabis has continued to increase over the last few decades being Δ9-tetrahydrocannabinol (Δ9-THC), cannabinol (CBN), cannabidiol (CBD) and cannabigerol (CBG) the most abundant phytocannabinoids (Figure 4) [17-19].

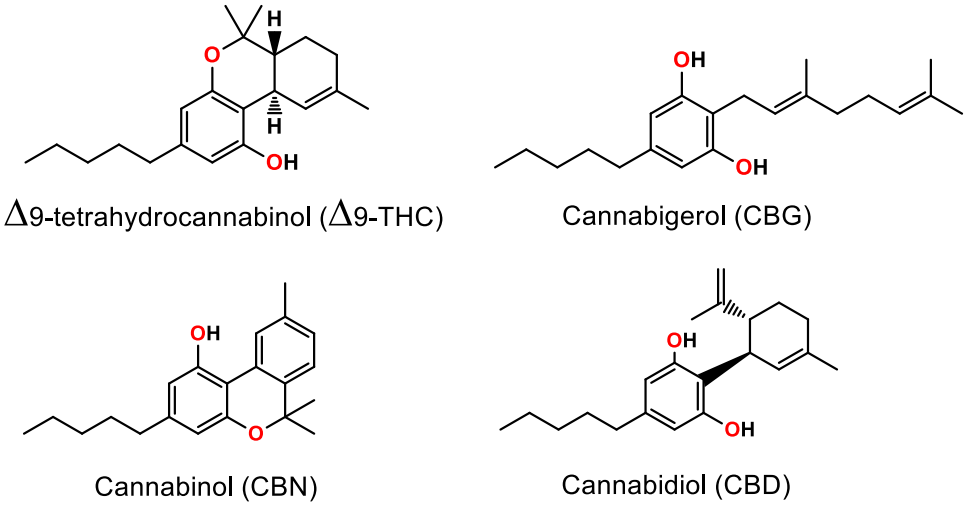

Figure 4. Most abundant phytocannabinoids.

The potential therapeutic and clinical application of phytocannabinoids has been greatly appreciated in pharmaceutical and medical fields, since its metabolites show potent bioactivities on human health [14, 20]. Since the discovery of Δ9-THC, the pharmaceutical industry undertook several studies for the development of synthetic analogues, with the aim of creating compounds that retain the biological activity of natural cannabinoids but devoid of psychoactive side effects. These new molecules included not only compounds structurally similar to the already known phytocannabinoids, but also compounds with different chemical structure. These human-made mind-altering chemicals were called synthetic cannabinoids (SCs) [21].

Given the growing popularity of cannabinoid-based drugs use, there is a lack of comprehensive scientific studies on SCs toxicity and abuse liability, posing a threat to public health, once the risks correlated to its consumption are often unexpected and unknown, so further research is needed in this field [22-24]. Clinical and forensic toxicology laboratories are continuously confronted by analytical

challenges when dealing with this kind of substances. The huge number of potential compounds to be investigated, the lack of available chemical reference standards and the evolving nature of these substances, are some of the major challenges faced in clinical and forensic toxicology laboratories [25].

2. The emergence of Synthetic Cannabinoids

SCs emerged in the 1970s when researchers were first exploring the endocannabinoid system and attempting to develop new treatments for cancer pain [26, 27]. The first SCs were synthesized by academic laboratories or the pharmaceutical industry [27]. The synthesis of selective cannabinoid receptor agonists with particular reference to their antinociceptive activity started at Pfizer, in 1974, with cyclohexylphenol (CP 55,940) followed by the HU-210 compound (or 1,1-Dimethylheptyl-11-hydroxy-tetrahydrocannabinol), synthetized in 1988, by Mechoulam's group at the Hebrew University [28].

John W. Huffman (Figure 5), a professor emeritus of chemistry at Clemson University, in South Carolina, and his team of researchers were involved in the synthesis of novel cannabinoids with some of the properties of Δ9-THC [29]. Huffman's research focused on synthesizing small molecules that could be applied as new pharmaceutical analgesics, particularly molecules that bind to cannabinoid brain (CB_1) and peripheral (CB_2) receptors.

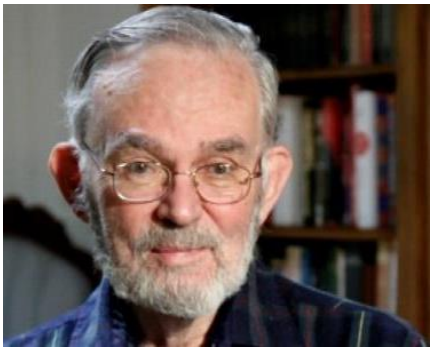

Figure 5. Professor John W. Huffman (adapted from [30]).

JWH-018 is one among several hundred analgesic drug candidates synthesized by him [31, 32].

More than 450 SCs compounds were synthesized over the course of twenty years, and many of the SCs have the initials of the person/ institution responsible for its synthesis, for example, 'JWH' compounds by John W. Huffman, AM-2201 by Alexandros Makriyannis, HU-210 at Hebrew University, CP 47,497 by Charles Pfizer or WIN55,212-2 at Sterling - Winthrop, Inc. (Figure 6) [27].

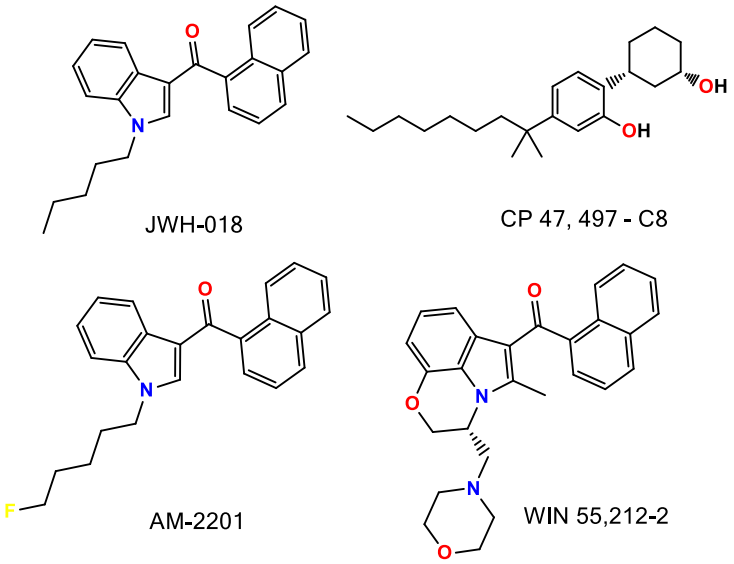

Figure 6. Structure of first SCs

Scientists' continuing development of synthetic variants of Δ9-THC as research tools, provided better understanding of the physiological cannabinoid control system in the human body and brain and opened a path of elucidating this natural regulatory mechanism in health and disease. As these compounds were discovered, the information was made public through publications or patents, and it resulted in great advances in the understanding of the endocannabinoids system and in potential therapeutic options without the adverse side effects. Unfortunately, multiple underground laboratories have utilized this research for clandestine purposes with the production of illicit compounds used as alternatives for marijuana. Moreover, the rejected substances as drug candidates from pharmaceutical industry, have instead appeared on the drug market as unregulated and illicit drugs [14, 33].

The structure of the cannabinoid system makes it receptive to a diverse set of compounds, making it an easier target for a set of synthetic drugs when compared to other systems. In this sense, the research on SCs compounds is involuntarily responsible for the growing epidemic of these synthetic drugs, with no signs of stopping [14].

2.1. Synthetic Cannabinoids as drugs of abuse

2.1.1. Epidemiology and legal status

Around the year 2000, SCs appeared on the illicit drug market, where their prevalence had long been underestimated. However, it wasn't until 2008 that, forensic investigators in Germany and

Austria first detected the synthetic cannabinoid JWH-018 in an herbal product. Since then, their place in the market has steadily increased [26, 34].

Being part of a group of drugs called 'new psychoactive substances' (NPS), SCs constitute the largest category in terms of the number of different substances monitored by the EU Early Warning System with a total of 224 substances notified since 2008, including 11 reported for the first time in 2020 [35] (Figure 7). In 2019, SCs and synthetic cathinones accounted for almost 60% of the number of seizures reported by EU Member states. According to the European Monitoring Centre for Drugs and Drug Addiction (EMCDDA) cannabis cultivation and synthetic drug production within the European Union continued at pre-pandemic levels during the year 2020. Lockdown measures in 2020 appear to have led to the domestic cultivation of cannabis, as well as the rise of cannabis adulterated with SCs [35].

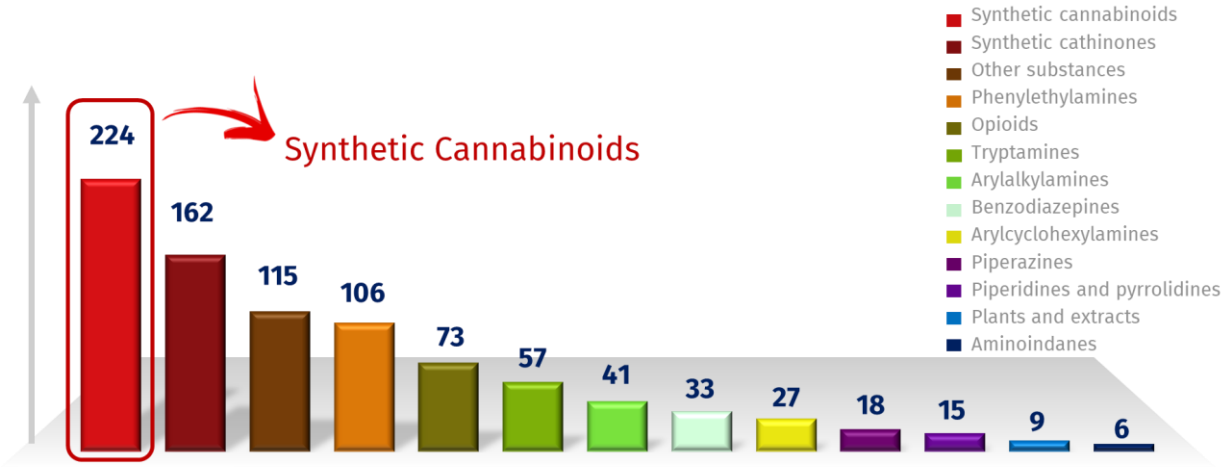

Figure 7. Number of NPS notified to the EU Early Warning System until the end of 2022 (adapted from [35]).

As the number of NPS detected globally has risen exponentially, the policy response of assessing and prohibiting each new substance individually has become increasingly unworkable [36].

In response to health-related problems associated with the consumption of SCs, across Europe and US government agencies have taken legal actions to limit the sale and distribution of these substances [37]. In early 2009 SCs started to be banned and their use controlled, with Austria and Germany being the first concerned countries [38, 39].

In the UK, the so-called 'first generation' of SCs, including JWH-018, was controlled at the end of 2009 and further legislation to control the "second generation" products, including AM-2201 and UR-144, was enacted on February 2013 [40]. Far from stopping their sales, manufacturers of these products developed new cannabimimetic substances, such as PB-22, 5F-PB-22, 5F-APICA and 5F-AKB-

48, to replace those that were banned under previous controls [40, 41]. Currently, these substances are permanently controlled in the UK as Class B drugs under the Misuse of Drugs Act 1971 [42].

Given the complexity and highly dynamic nature of the NPS market, Portugal adopted specific legislation to stop the rapid proliferation of NPS. The Autonomous Region of Madeira was the first region of the country to take specific action against NPS. According to regional news, it is suspected that NPS were responsible for 4 deaths and around 190 hospitalizations up until October 2012, forcing the government of Madeira to take legal measures through the implementation of the Legislative Decree nº. 28/2012M of 25th October, which prohibited the sale and distribution of such substances, hindering their trade and mitigating the number of emergency cases related to NPS in the region [43]. In the following year, new legislation was introduced in Portugal (Decree-Law nº. 54/2013 of 17th April), which prohibited the production, export, advertisement, distribution, and sale of 159 NPS, 45 of them are SCs. These measures have helped to reduce the supply of NPS by seizing stock and closing the so-called 'smartshops' [44].

In the US, prior to 2010, SCs were not controlled by any State or at the Federal level. However, with the evident harm caused by K2 products, along with the initial analytical studies identifying JWH-018, JWH-073, JWH-200, CP-47,497 and cannabicyclohexanol, as the main psychoactive components in these products, promptly led the Drug Enforcement Administration (DEA), on March 1, 2011 to temporarily place these five compounds on the list of controlled substances under Schedule I of the Controlled Substances Act (CSA) [45].

By 2012, the banned compounds were replaced by structurally related ones, such as AM-2201, JWH-122, JWH-203, JWH-210 and RCS-4, apparently indicating that manufacturers of these products have remained one step ahead of SCs regulation [46, 47].

Despite the legislative efforts against the NPS problem, new SCs continue to emerge on the clandestine drugs market. Differences in country-specific legislation and its capacity to implement them open opportunities for trafficking NPS and pose a major obstacle for effective law enforcement interventions [48].

Figure 8 summarizes the main historical events associated with SCs to date.

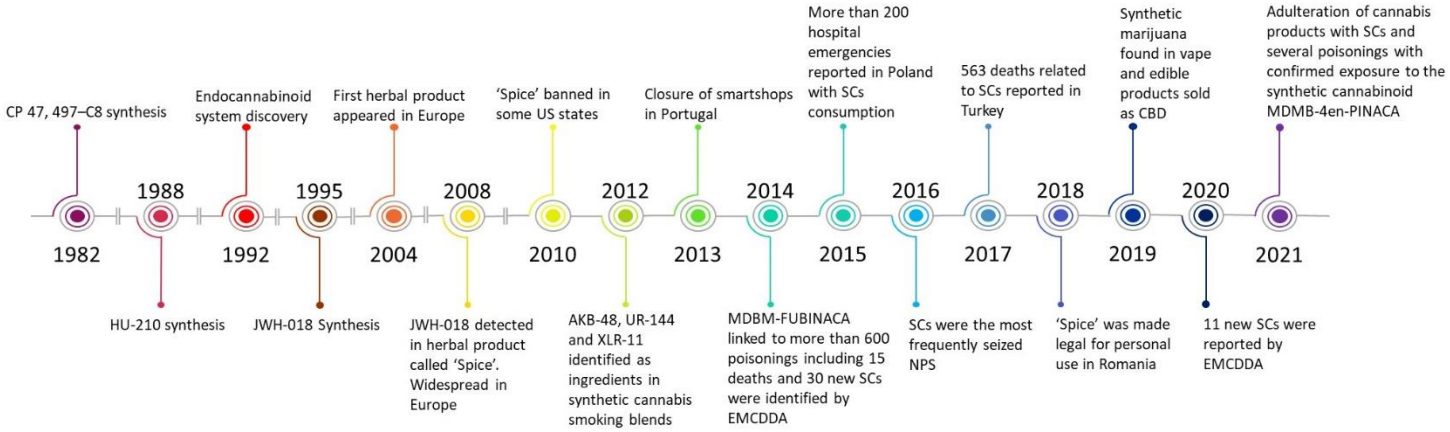

Figure 8. Timeline of major historical events associated with SCs to date (adapted from [10]).

2.1.2. Pattern of use and commercial appearance

Commonly known as synthetic marijuana since its introduction into the drug market, SCs have been sold as 'herbal incenses' or 'herbal smoking mixtures' under different brand names. 'Spice' and 'K2' were the earliest in a series of SCs products sold in many European and US countries [47, 49]. Since then, a high number of similar products such as 'Kronic', 'Cloud 9', 'Black Mamba', 'Zombie', 'Sence', 'Blue Lotus', 'Mojo', 'Moon Rocks', 'Kaos', 'Voodoo', among others, have been developed [27, 50-52].

In general, SCs products are sold in brightly coloured metal-foil packages containing about 0.5 to 3 g of finely cut green/brown plant material [53]. Damiana (*Turnera diffusa*) and Lamiaceae herbs such as *Melissa*, *Mentha* and *Thymus* are commonly used as the plant base for the smoking mixtures [34] (Figure 9).

Figure 9. Example of commercially available herbal incenses and some of the most common base plants used.

The dried plants present in these blends have no psychotropic effects in most cases, just giving the illusion of being of natural origin, being no more than mere vehicles for SCs. SCs are usually added to the plant material by soaking or spraying, normally on an industrial scale using solvents such as acetone or ethanol to dissolve these substances; however, in some cases, their solid form (crystalline powder) is added to plant material, leading to an inhomogeneous mixture [34, 54]. Once the solvent evaporates and the plant material is dried with SCs attached to it, the product can be crushed and packaged, and frequently in very different concentrations within the same package (originating parts where the concentration of SCs is very high, called 'hot spots') [49, 55]. Then, the products are ready to be sold on the internet by 'legal high' retailers in bricks-and-mortar head shops, and usually labelled with a disclaimer indicating that the contents are not for human consumption [17, 34, 56].

The herbal mixtures that are sprayed with SCs and are proposed as legal alternatives to marijuana are often smoked by users. Currently, other available SCs preparations look like hashish or are found in the form of capsules, tablets, powders, and more recently, in liquid-filled cartridges for use in electronic cigarettes (e-cigarettes), as a new alternative for tobacco withdrawal, and as a more discreet way of consumption. This new trend is called, 'buddha-blue', 'C-Liquid', 'Herbal e-Liquid', etc and is discussed on drug-user forums [34, 53, 57, 58]. Apart from herbal smoking blends, some consumers prefer homemade mixtures, using some "purified" powders of SCs sold on websites, solved in alcohol and sprayed on herbals [58].

A recent report of EMCDDA highlighted the seizure of several cannabis products that have been adulterated with SCs. These substances are being mis-sold as Δ9-THC and CBD vaping liquids or being used to adulterate low- Δ9-THC cannabis products. Users do not know that a product contains SCs can led to higher health risks [59].

In addition to SCs, some herbal mixtures have been shown to contain numerous other compounds, such as fatty acids amides (e.g. oleamide, palmitoyethanolamide), vitamin E, etc to mask detection of SCs, flavours (e.g. menthol, eucalyptol, vanillin), various preservatives (e.g. benzophenone, benzyl benzoate, hydroxybenzoic acid) [60], sympathomimetic agents such clenbuterol, a potent β-adrenergic receptor agonist, *o*-desmethyltramadol and mitragynine which are μ-opioid receptor agonists, and sedative benzodiazepines such as phenazepam [61, 62]. Unknown to users, SCs have also been sold as ecstasy/MDMA and other illicit drugs and in some cases, this has led to severe poisoning [63].

Comparing with other new drugs, there is a particularly remarkable increasing in consumption of SCs [26]. Motivations for their use are typically associated with curiosity, low cost, positive drug effects

including relaxation and feeling a pleasant high, belief of the products general safety, and the potential for passing drug testing [22].

Regarding to routes of administration, inhalation by smoking SCs remains the most common used method, due to the rapid onset of pharmacological effects [64, 65]. The adaptation of e-cigarette devices to vape e-liquids infused with SCs has been gaining popularity over the last few years, especially among young people [34, 66-68]. Oral administration is another way to use SCs, but leads to a delayed onset of the effects due to extensive hepatic metabolism, before reaching systemic circulation [65, 69]. Rectal absorption has also been reported in the literature but is less commonly used [70].

Estimations on the prevalence of SCs use are very difficult to attain and the available data is limited to the analysis of case reports, calls to poison control centres, emergency department visits and drug use surveys [34, 62].

2.2. Chemistry of Synthetic Cannabinoids

Mostly lipophilic and nonpolar, in general SCs consist of about 22 to 26 carbon atoms, which makes them volatile when smoked with a side chain of 4-9 saturated carbon atoms, being a common finding in these compounds [71]. From the chemical point of view, many of the SCs are not structurally related to the so-called 'classical' cannabinoids like Δ9-THC. In fact, the main differences lead to possess increased biological activity [34, 72].

In order to systematize the chemical structures of the SCs, EMCDDA presented a model describing the diverse structural types. This generic model structure, shown in Figure 10, consists of four key structural elements, namely "the core and substituents", "the link", "the ring and substituents" and "the tail", which denote altering positions. This method of assigning a code name to each component allows the chemical structure of the cannabinoid to be identified without the long chemical name [34].

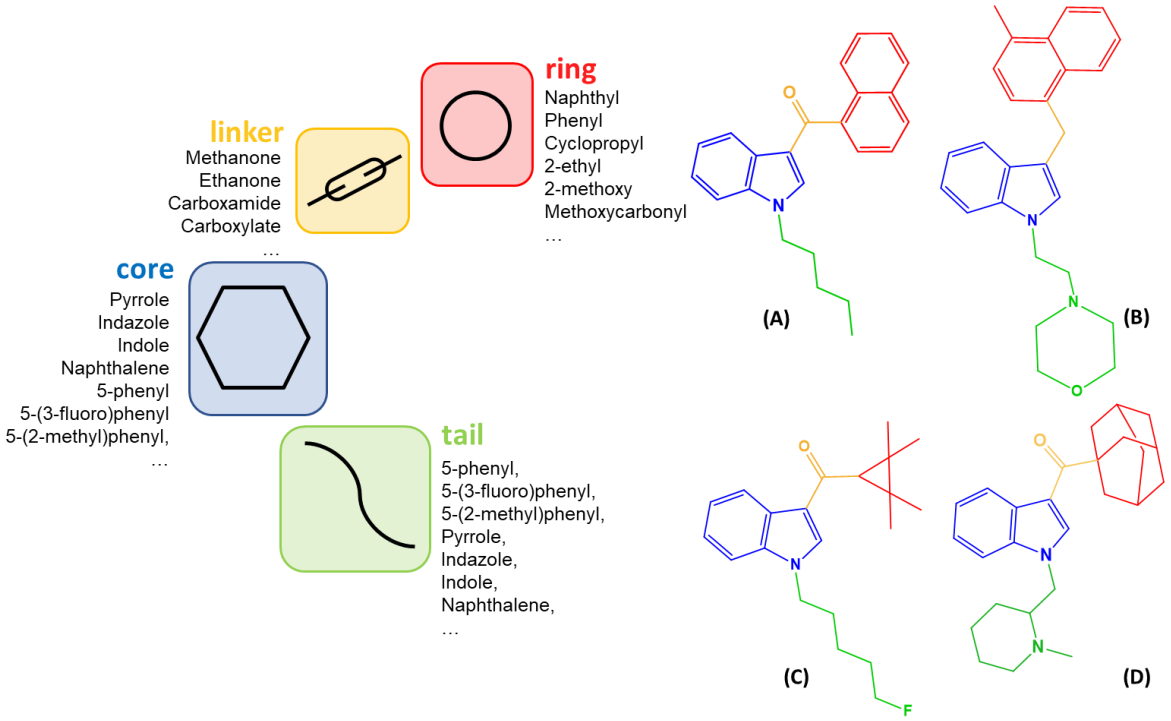

Figure 10. General chemical structure of SCs. (A-D) Structures of the SCs JWH-018, JWH-192, XLR-11 and AM-1248 according to EMCDDA model, respectively (adapted from [73]).

Even though most of the reported cannabinoids follow the general structure (Figure 10), there are also other SCs with affinity for the cannabinoid receptor that have other base structures [74].

SCs family is extremely large, including numerous substances belonging to various chemical groups and subgroups. This variety of diverse structures served as the basis for a classification system that became, at the beginning of the 21st century, the current standard [75]. Table 1 present the main classes and some examples of SCs according to this classification system, namely classical cannabinoids, nonclassical cannabinoids, hybrid cannabinoids, aminoalkylindoles, eicosanoids and miscellaneous cannabinoids.

Table 1.The main classes of SCs (adapted from [21, 65, 76, 77]).

Synthetic Cannabinoid Class		**Examples**
Classical Cannabinoids	Similar structure to Δ9-THC; Derivatives of dibenzopyran	HU-210; HU-211; HU-208; HU-311; AM-906, AM-411, O-1184
Nonclassical Cannabinoids	Structure quite similar to classical cannabinoids; Derivatives of cyclohexylphenol; Bicyclic and tricyclic analogues to Δ9-THC	CP 47,497 and its analogues; CP 55,940, CP 55,244
Hybrid Cannabinoids	Combine structural features of both classical and nonclassical cannabinoids	AM-4030
Aminoalkylindoles	No structural similarity with Δ9-THC	WIN 55,212-2; AM-1241, JWH-015
Eicosanoids	Synthetic analogues of endocannabinoids such as anandamide	methanandamide
Others	Cannabinoids constituting no classes in their own right: diarylpyrazoles, naphtoylpyrroles, naphthoylpyrroles and naphthylmethylindenes.	SR141716A; SR144528

Developed in the 1960s, classical cannabinoids were originally the only cannabinoids synthesized. HU-210, and others from HU series are synthetic analogues of the compounds that occurs naturally in cannabis plant and are based on a dibenzopyran ring [78-80].

Cannabinoids defined as 'nonclassical' include bicyclic and tricyclic structures, as well as cyclohexylphenol (CP) derivatives. The CP compounds are more similar to the structure of Δ9-THC with regard to the alkyl chain attached to the central phenol moiety of the compound. This plays a significant role in the interaction of these compounds with the cannabinoid receptors [5, 21, 77].

Hybrid cannabinoids have a combination of classical and nonclassical cannabinoid structural features. AM-4030, a derivative of HU-210, is an example of this class of cannabinoids because it has the dibenzopyran ring that is common to classical cannabinoids and an aliphatic hydroxyl group

common in the CP family of nonclassical cannabinoids [65]. The structures of classical, nonclassical and hybrid cannabinoids are shown in Figure 11.

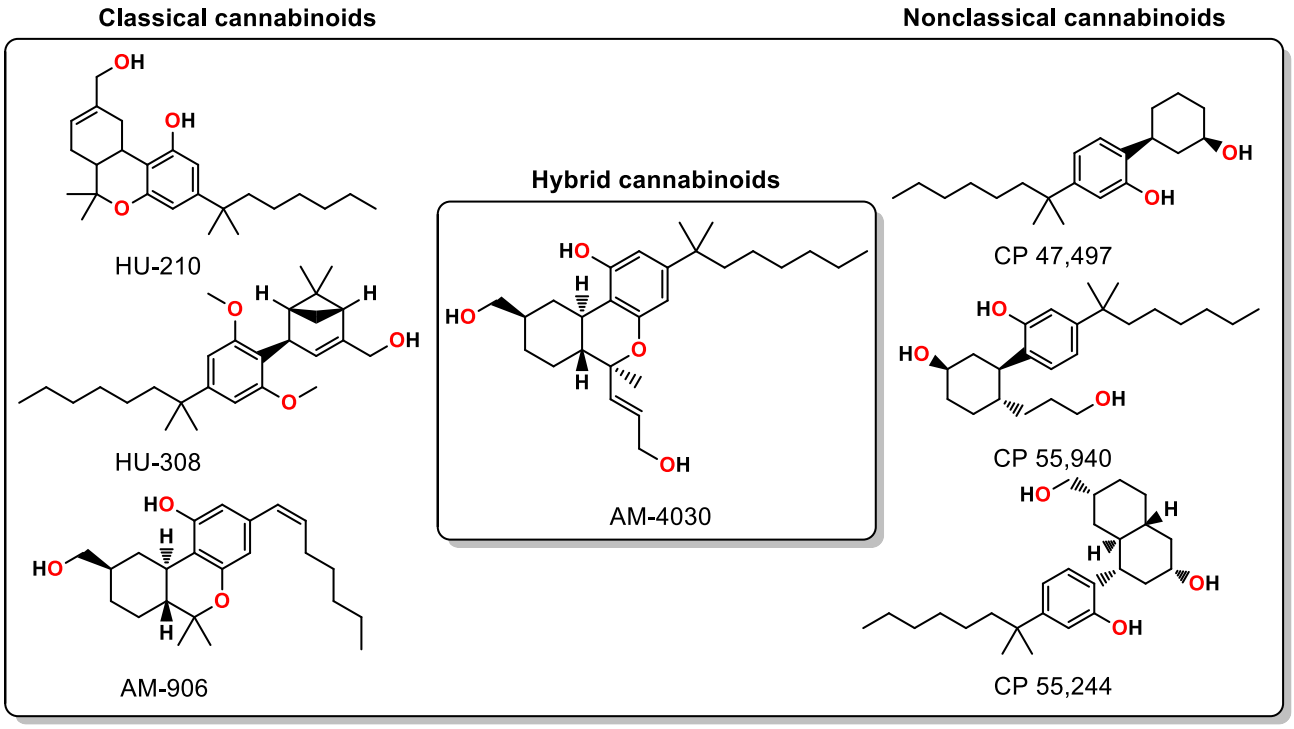

Figure 11. Chemical structures of some examples of classical cannabinoids, nonclassical cannabinoids and hybrid cannabinoids (adapted from [10]).

Aminoalkylindoles are structurally different of Δ9-THC but with cannabimimetic properties, and are considered to be the most common SCs found in blends, likely due to the fact that these molecules are easier to be synthesized than classical and nonclassical cannabinoids [5, 9]. This class is further divided into naphthoylindoles (e.g. JWH-015, JWH-018, JWH-073, JWH-081, JWH-122, JWH-200), phenylacetylindoles (e.g. JWH-250, JWH-251), benzoylindoles (e.g. AM-694, RSC-4), naphthylmethylindoles (e.g. JWH-184, JWH-196, JWH-192), cyclopropoylindoles (e.g. UR-144, XLR-11), adamantoylindoles (e.g. AB-001, AM-1248), indole carboxamides (e.g. APICA, 5F-APICA) [5, 58, 65, 81]. In Table 2 are shown some examples of the structures of the classes previously mentioned, as well as the general structure of each class.

Table 2. Chemical structures of the different subgroups of aminoalkylindoles [adapted from [5, 58, 65]).

Aminoalkylindoles	
Subclass	***Examples***
Naphthoylindoles 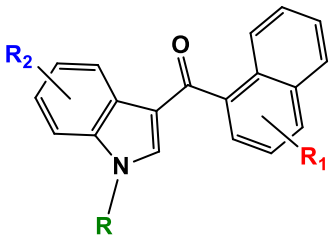	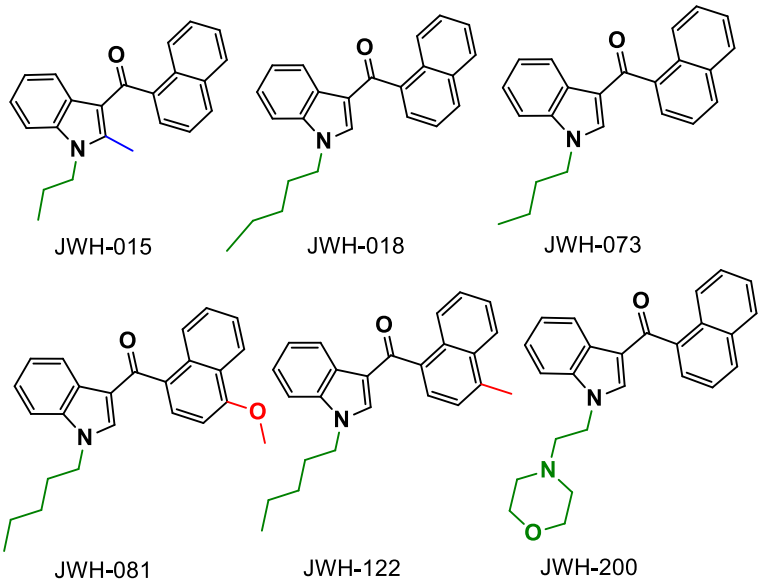 JWH-015 JWH-018 JWH-073 JWH-081 JWH-122 JWH-200
Phenylacetylindoles 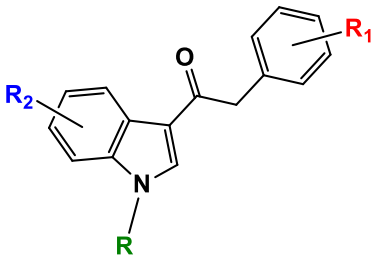	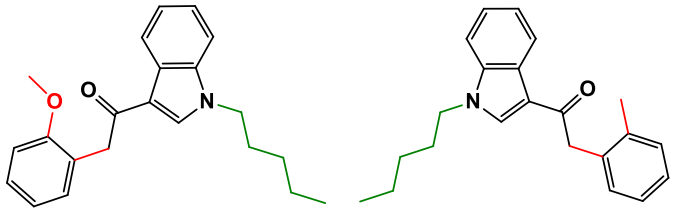 JWH-250 JWH-251
Benzoylindoles 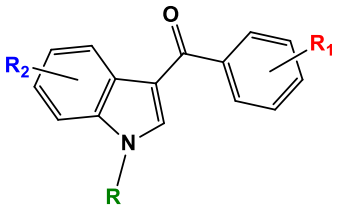	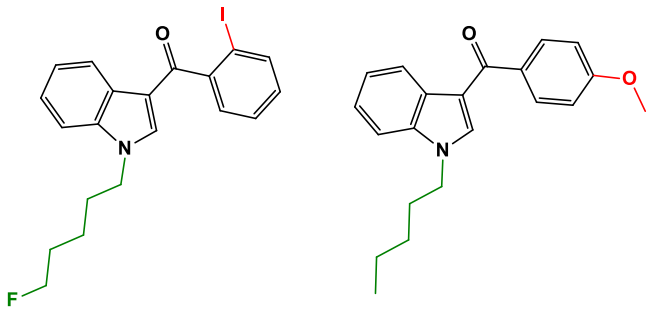 AM-694 RSC-4

Naphthylmethylindoles 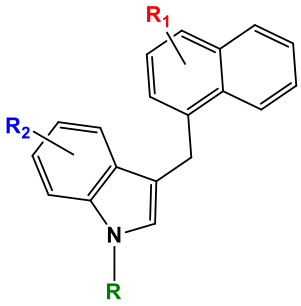	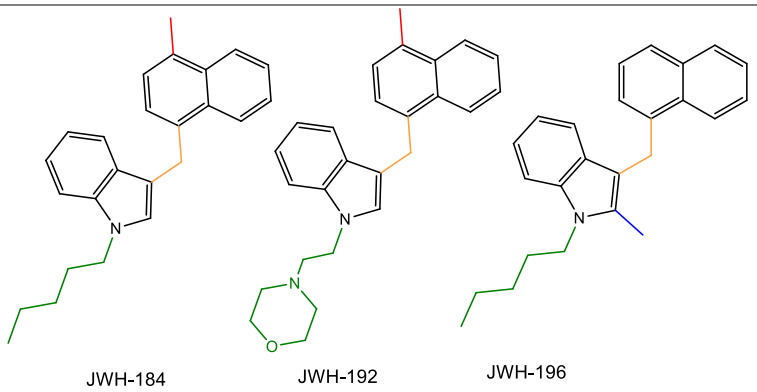 JWH-184 JWH-192 JWH-196
Cyclopropoylindoles 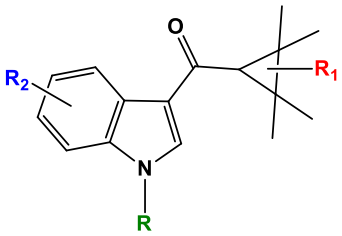	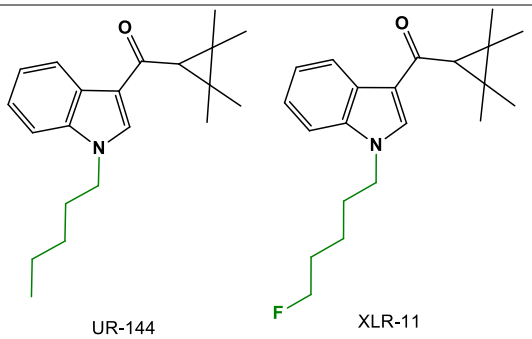 UR-144 XLR-11
Adamantoylindoles 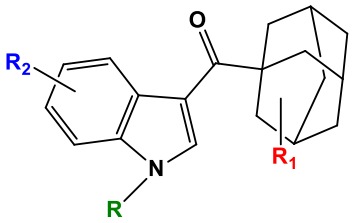	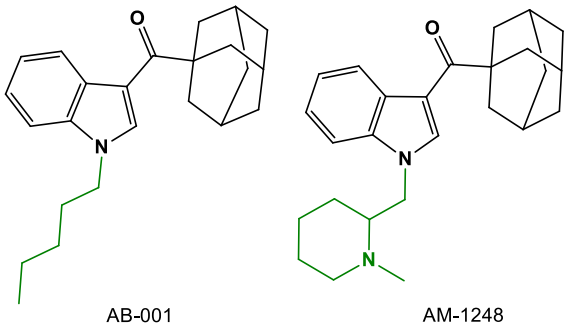 AB-001 AM-1248
Indoles Carboxamides 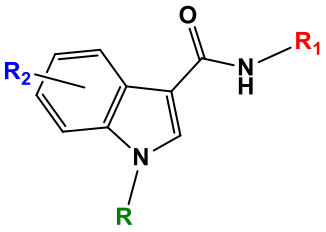	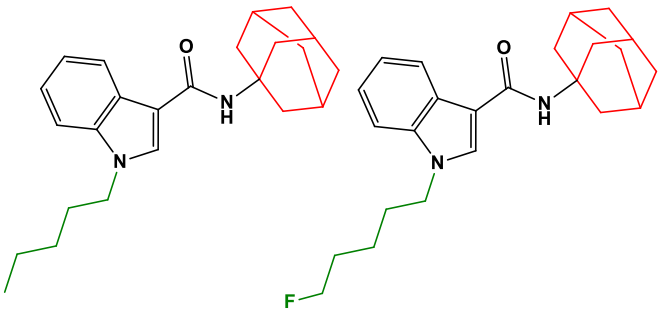 APICA 5F-APICA

Eicosanoids, another class of SCs, are synthetic analogues of endocannabinoids, such as anandamide (e.g. methanandamide). Finally, the cannabinoids that do not constitute a class by itself are grouped into 'miscellaneous cannabinoids or others', like diarylpyrazoles (e.g. SR141716A), naphthoylpyrroles (e.g. JWH-307) and naphtylmethylindenes or derivatives of naphthalene-1-yl-(4-pentyloxynaphthalen-1-yl) methanone (e.g. CRA-13) (Figure 12) [5, 65].

Several classifications have been described since the beginning of the SCs development; however, some of the classifications were imperfect due to the number of new compounds that can belong to unknown chemical classes and that emerge constantly, making the inventory of existing products infinite [5, 58]. Recently, an extensive and more complete classification was presented. Many derivatives and analogues in the above classes of compounds could be synthesized by the addition of a halogen, alkyl, alkoxy, or other substituents to one of the aromatic ring systems. Also, it is possible to make some variations on the length and arrangement of the alkyl chain without losing the cannabinoid activity or change an indole to indazole (e.g. AM-2201 to THJ-2201), as well as a terminal fluorine replacement allowing the development of new compounds [5, 76, 82]. In Figure 13 is presented the general structure of indole and indazole derivatives [58].

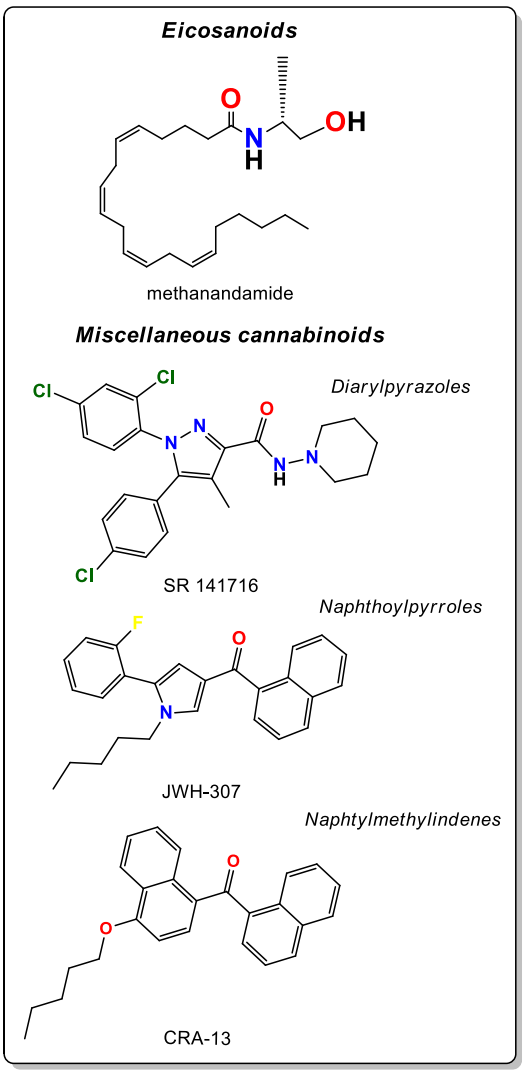

Figure 12. Chemical structures of eicosanoids and miscellaneous cannabinoids (adapted from [10]).

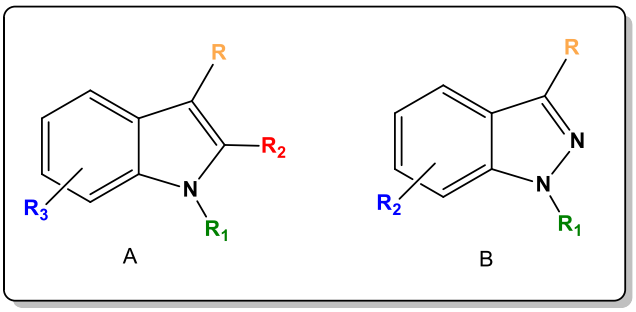

Figure 13. General structure of indole and indazole derivatives.

According to Elsohly *et al.* [76] recent review, SCs are categorized into nine different classes. Carbazoles, indoles, indazoles, pyrroles and URB-class are the new categories that join into the standard classification.

It is quite understandable that the classification of these substances cannot be static, due to the constant development of new SCs, and any new suggested classification system will inevitably require updating, including the determination of new and separate groups and classes [5, 83]. Furthermore, these structural changes result in compounds with unpredictable pharmacological or toxicological properties [84].

2.3. Pharmacology and toxicology aspects

Comparing the pharmacological similarities between SCs and Δ9-THC has been a topic of great interest among scientists and lawmakers [85]. However, little is known about the detailed pharmacology and toxicology of the SCs and few formal human studies have been published [71].

Considering the potential risks associated with SCs, pharmacodynamic and pharmacokinetic studies are needed to document consumption in clinical and forensic cases [86].

2.3.1. Synthetic cannabinoid receptor agonists and antagonists

Due to the lipophilic nature of cannabinoids, it was initially thought that these compounds exert several biological effects by breaking the cell membrane non-specifically. However, after the discovery of Δ9-THC and subsequent emergence of the several chemically synthesized cannabinoids, the successful mapping and pharmacological characterization of cannabinoid binding sites in the brain revealed that its pharmacological effects are considered to be mediated through, at least, two G-protein coupled transmembrane receptors, namely CB_1 and CB_2 [14, 71].

SCs are referred to as substances with structural features which exhibit higher binding affinity at both CB_1 and CB_2 receptors, and also to display varying intrinsic activity relative to Δ9-THC, both in cellular assays and animal studies [65, 85]. CB_1 is thought to be responsible for most of the pharmacological effects of cannabinoids and is found mainly, in the central and peripheral nervous systems, but also is expressed in bone, heart, liver, lung, vascular endothelium, and reproductive system [65, 87, 88]. The other receptor, CB_2, was originally identified from macrophages present in the spleen and is primarily expressed in the periphery, but also in the CNS at lower levels than CB_1, and may mediate many physiological processes involving immune responses, and influence the body´s resistance to infectious, allergic, and oncological diseases. The unequal distribution of cannabinoid receptors in the CNS may explain, to some extent, the psychoactive effects of cannabinoids, since there is evidence of the direct relationship between the affinity of cannabinoid for these receptors and their narcogenic potential [5, 14].

Several studies reported that Δ9-THC is a potent activator of the CB_1 receptor, while the non-psychoactive CBD does not bind directly with either CB_1 or CB_2 receptors, instead, it stimulates both types of receptors. Despite this fact, CBD modulate the effect of Δ9-THC via direct blockade of CB_1 receptor. This modulation leads to a reduction in unwanted side effects from the consumption of Δ9-THC, such as anxiety, dysphoria, panic reactions and paranoia, and is also known to improve the Δ9-THC therapeutic activity [4, 89, 90]. In contrast to cannabis, which mainly contains a mixture of agonist

and antagonist cannabinoids, SCs compounds show differences in their selectivity, their potency and their function, being more potent and efficacious cannabinoid receptor agonists than Δ9-THC [12, 22]. Also, these synthetic substances are lack of cannabinoids such as CBD, that may otherwise counteract psychoactive properties of Δ9-THC [91].

The activation of CB_1 receptor decreases cellular cyclic adenosine monophosphate (cAMP) levels and elicits cannabimimetic responses. SCs agonists interact with voltage-gated ion channels and inhibit potassium, sodium, and N- and P/Q-type-calcium channels by reducing membrane potentials [88].

The complex molecular architecture of the cannabinoid receptors allow a single receptor to recognize multiple classes of compounds [58]. Due to the large variety of chemical structures, SCs bind to the two types of cannabinoid receptors with different affinities being classified in CB_1/CB_2 agonists, CB_2 selective agonists, peripherally restricted CB_1/CB_2 agonists, CB_1/CB_2 antagonists, and inverse agonists. Moreover, many SCs present chiral centres and stereoisomer forms that may differ in their pharmacological potencies [58]. The cannabis-like bioactivity of SCs is mostly due to the fact that they are mainly agonist of CB_1, like JWH-210, HU-308 and WIN55,212-2. On the other hand, these psychoactive substances have also the ability to bind to cannabinoid receptors without producing cannabis-like effects, but simply blocking these receptors for other substances, acting as antagonists, like SR 141716A and SR 144528 [65, 75].

The majority of SCs detected in herbal products possessed higher affinity and lower inhibitory constant (Ki) values than Δ9-THC at the CB_1 receptor. SCs affinities for CB_1 and CB_2 receptors have been determined in displacement assays using tritiated cannabinoid receptor ligands and membranes obtained from brain (CB_1-rich), spleen (CB_2-rich), or using culture cells transfected with CB_1 or CB_2 receptors. Ki values of SCs collected from literature are grouped in Table 3 [22, 58, 88].

Table 3. CB1 and CB2 binding affinity of several SCs (adapted from [88, 92]).

Chemical Class	Compound	Activity	CB_1 Ki (nM)	CB_2 Ki (nM)	Ref.
Classical cannabinoids	HU-210	CB_1 and CB_2 agonist	0.2	0.4	[93]
	HU-308	CB_2 agonist	-	22.7	[94]
Naphthoylindoles	JWH-015	CB_2 agonist	336	13.8	[95]
	JWH-018	Full CB_1 agonist	1.22	2.9	[96]
	JWH-019	Full CB_1 agonist	9.8	5.6	[95]
	JWH-030	Partial CB_1 agonist	87.0	-	[97]
	JWH-073	Full CB_1 agonist	8.9	38.0	[95]
	JWH-081	CB_1 and CB_2 agonist	1.2	12.4	[95]
	JWH-122	CB_1 agonist	0.7	1.2	[87]
	JWH-151	Full CB_2 agonist	-	30	[87]
	JWH-200	CB_1 agonist	42.0	-	[98]
	JWH-203	CB_1 and CB_2 agonist	8.0	7.0	[87]
	JWH-210	CB_1 and CB_2 agonist	0.5	0.7	[87]
	AM-1220	CB_1 agonist	3.9	73.4	[99]
	AM-2201	Full CB_1 agonist	1.0	2.6	[99]
	AM-2232	CB_1 and CB_2 agonist	0.3	1.5	[99]
	AM-2233	Full CB_1 agonist	2.8	-	[100]
	EAM-2201	CB_1 and CB_2 agonist	0.380	0.371	[75]
	MAM-2201	Full CB_1 agonist	1.86	0.59	[101]
Phenylacetylindoles	JWH-250	CB_1 and CB_2 agonist	11.0	33	[102]
	JWH-251	CB_1 agonist	29.0	146	[102]
Naphthoylpyrroles	JWH-307	CB_1 and CB_2 agonist	7.7	3.3	[103]
Aminoalkylindoles	WIN55,212-2	CB_1 and CB_2 agonist	62.3	3.3	[87]
	PB-22	Full CB_1 agonist	0.318	0.433	[104]
	5F-PB-22	Full CB_1 agonist	0.468	0.633	[104]

Tetramethylcyclo-propyl indoles	UR-144	Full CB_2 agonist	29.0	4.5	[105]
	XLR-11	CB_1 and CB_2 agonist	24.0	2.1	[105]
Indazole carboxamide	AB-FUBINACA	CB_1 and CB_2 agonist	0.9	23.2	[106]
	MDMB-FUBINACA	Full CB_1 agonist	1.14	0.1228	[84]
	APINACA	Full CB_1 agonist	304.5	-	[99]
	AB-PINACA	CB_1 and CB_2 agonist	2.87	0.88	[106]
	AB-CHMINACA	CB_1 and CB_2 agonist	0.78	0.45	[107]
Pyrazole	AM-251	CB_1 antagonist	7.5	-	[108]
Benzoylindoles	AM-679	CB_1 agonist	13.5	49.5	[99]
	AM-694	Full CB_1 agonist	0.08	1.44	[109]
Adamantylindoles	AM-1248	CB_1 and CB_2 agonist	11.9	4.8	[99]
Cyclohexylphenols	CP 47,497	CB_1 agonist	0.8	-	[110]
	CP55,940	CB_1 and CB_2 agonist	1.1	-	[110]

The majority of compounds used as drug of abuse have Ki in the range 1 to 10 nM or 10 to 100 nM for both CB_1 and CB_2 receptors. Higher affinity of SCs to the cannabinoid receptors produce a stronger effect than phytocannabinoids [111]. The family of the JWH compounds is the most numerous and, although their chemical structures differ greatly from those of Δ9-THC, they have a higher affinity to CB_1 and/or CB_2 receptors and are more potent than Δ9-THC [112]. JWH-018 has 4 times the affinity for CB_1 receptors and 10 times the affinity for the CB_2 receptors, while JWH-015 acts as a selective CB_2 receptor agonist, being 28-fold higher for CB_2 than for CB_1 [113]. Other naphthoylindoles like, AM-2201, produce psychoactive effects similar to Δ9-THC, but with a binding affinity 40 times higher at CB_1 and 14 times higher at CB_2 [86]. The binding affinity of the SCs to the CB_1 receptor can range from being similar to Δ9-THC, like JWH-200, to 90 times higher, like JWH-210. The affinity of indol compounds to cannabinoid receptors was explained by a three-point bond for each compound with Δ9-THC natural ligand regions, being the three key regions the naphthalene ring, the carbonyl group and the indole N-alkyl substituent. The replacement of the naphthalene by a methyl-, methoxy-, fluoro-, chloro- or bromo-substituted phenylacetyl group resulted in an increased selectivity for the CB_1 receptor, depending on the nature and location of the substituent on the aromatic ring [111].

The cyclohexylphenols CP 55,940 and CP 47,497, as well as their n-alkyl homologues also act as CB_1 receptors full agonists. CP 47,497 does not have the classical cannabinoid chemical structure

(tricyclic benzopyran system) and presents 3 to 28 times higher potency [112]. HU-210 is one of the most potent synthetic cannabinoids, being 100-800 times more potent than Δ9-THC, despite a slow initial effect, it has a long duration of action due to binding to both CB_1 and CB_2 receptors [71, 86, 114, 115].

In vitro experiments have demonstrated that the selective agonists JWH-015, JWH-133, and HU-308, and the mixed CB_1–CB_2 receptor agonists WIN55,212-2 and HU-210 reduce the release of pro-inflammatory cytokines in microglial cell cultures exposed to different species of the toxic Aβ peptide, preventing cognitive impairment and neuronal loss in Alzheimer's disease [116, 117]. On the other hand, HU-211 the enantiomer of HU-210, does not act as a cannabinoid receptor agonist but instead produces antagonist effects in N-methyl D-aspartate receptors, protecting cells from neurotoxicity induced by it ligand [117]. Also, HU-433 and HU-308, two synthetic cannabinoid enantiomers are specific CB_2 agonists, however HU-433 binding to CB_2 receptor is substantially lower compared with HU-308, being more potent than HU-308 in its CB_2-mediated anti-osteoporotic and anti-inflammatory effects. A molecular-modelling analysis suggested that HU-433 and HU-308 have two different binding conformations within CB_2, with one of them possibly responsible for the affinity difference. Hence, different ligands may have different orientations relative to the same binding site [118].

The two indazole carboxamide AB-CHMINACA and AB-PINACA also exhibited higher efficacy than most known full agonists of the CB_1 receptor, leading to potential interest as research tools due to their unique chemical structures and high CB_1 receptor efficacies [118].

Little is known about the detailed pharmacological profiles of most SCs in humans, and its abuse as well as the case reports of adverse effects have raised concerns about the pharmacologic mechanisms underlying *in vivo* effects [111, 119].

2.3.2. Pharmacokinetics

In forensic toxicology, the clarification of pharmacokinetic and pharmacodynamic properties of SCs is important in order to interpret analytical results obtained from intoxicated or poisoned individuals, particularly post-mortem [120].

Due to their highly lipophilic nature, SCs are present in 'herbal' product in small proportions and after being smoked (their main administration form), SCs reach peak blood concentration very quickly [65, 121]. The instant absorption via the lungs and redistribution into other organs like brain in a short time, onset of action usually occurs within minutes. In case of oral consumption, the absorption process as well as the onset of action is delayed due to food intake, digestion activity and variations

in the extent of the first pass effect. High volumes of distribution can be expected for these lipophilic compounds and as a result, after chronic consumption, fat accumulation in the body is very likely [65, 111].

Despite the restriction of studies on controlled administration of SCs in humans, a few works with SCs intake in humans have been published. In Teske *et al.* [122] work, a human study was performed in which two subjects smoked 50 $\mu g.kg^{-1}$ of JWH-018, reaching a blood peak concentration of 10 $\mu g.L^{-1}$ after 5 minutes, rapidly decreasing in the following 3 hours, becoming barely traceable after 24 hours. The results allowed to conclude that the synthetic drug reached peak blood concentration very quickly, then being redistributed to other tissues such as the brain. The same was observed in Kacinko *et al.* [123] study, with one of the six subjects smoking over 30 minutes 0.3 g herbal blend containing 17 $mg.g^{-1}$ JWH-018 and 22 $mg.g^{-1}$ JWH-073. Blood peak concentration was reached 19 minutes after smoking with 4.8 and 4.2 $mg.L^{-1}$, respectively, with a quickly declining to 1.5 $mg.L^{-1}$ JWH-018 and 1.0 $mg.L^{-1}$ JWH-073 at 53 minutes, and 0.2 $mg.L^{-1}$ for both at 107 minutes. These studies allowed to calculate the half-live of JWH-018 and JWH-073 from the concentration data measured.

A self-experiment was reported in Hutter *et al.* [124] work, in which one of the authors ingested 5 mg of pure AM-2201, and serum as well as urine samples were analysed subsequently. The serum plasma peak was 0.56 $\mu g.L^{-1}$ at 1.5 hours, decreasing after 21 hours but remaining detectable for 5 days. Additionally, the smoke condensate from a cigarette laced with pure AM-2201 was also investigated and urine samples of patients after known consumption of AM-2201 or JWH-018 were evaluated. In another similar study, an adult male volunteer orally ingested a 5 mg dose of pure AM-2201, and the AM-2201 serum concentrations was reported to decreased from 1.4 µg/L at approximately 1 hour to 0.7 µg/L at 5 hours after ingestion. AM-2201 was still detectable in serum 25 hours after administration. The half-life of AM-2201 was estimated to be approximately 4 hours. [125].

These studies showed that SCs are significantly more efficacious and have a faster onset and shorter duration of action relative to Δ9-THC. HU-210, another compound identified in herbal blends, is also more potent and efficacious than Δ9-THC, yet its duration of action is nearly five times longer and its onset of action is significantly slower. Although slow onset and long duration of action of the HU-210 do not necessarily predict a higher risk of abuse relative to cannabis, it is suggested that it is capable of producing protracted withdrawal symptoms similar to what is observed with long-acting opioid agonists, predicting significant adverse effects associated with SCs dependence and withdrawal [119]. These findings highlight the pharmacological characteristics of a few of the dozens

of compounds found in 'herbal products' that predict significant clinical physiological and behavioral risks in relation to cannabis [17].

SCs undergo extensive metabolism and clearance through the liver, which is the most important organ for SCs metabolism, although other organs may also be involved in drug biotransformation such as intestine, lung, brain, and kidney [82, 126].

Although many of the SCs available in 'herbal products' have not been fully characterised regarding their metabolism, there is data from several representatives demonstrating extensive oxidative metabolism. Based on the recent evidence, SCs are extensively metabolized in phase I and phase II biotransformation reactions. These substances are firstly oxidized by cytochrome P450 enzymes (CYP), whereby oxidized metabolites are formed and then served as substrates for a second metabolic phase, namely glucuronidation and/ or sulfation by a class of enzymes called UDP-glucuronosyltransferases (UGT) and finally, renal excretion [82, 111, 127, 128]. In Figure 14 is illustrated a schematic summary about absorption, distribution, metabolism, and excretion of SCs, with main metabolites produced by CYP and UGT enzymes.

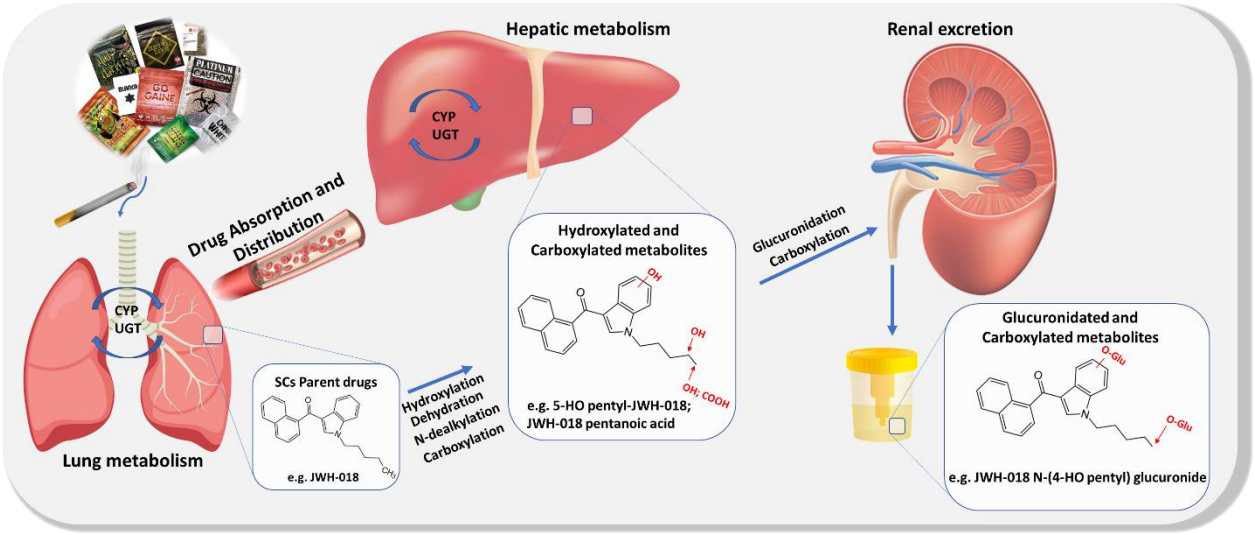

Figure 14. Schematic summary of the absorption, distribution, metabolism, and excretion of SCs (adapted from [10]).

In general, oxidative metabolism forms are preferably mono-, di-, and tri- hydroxylated, carboxylated and N-dealkylated compounds. Hydroxylation process takes place on the aliphatic chain, the indole, the naphthalene, or the substituted aromatic rings that can be secondarily metabolized to carboxylic acids then conjugated to glucuronic acid [82, 85, 126, 129].

The earliest reports of SCs metabolism were published in the early 2000s and focused on the *in vitro* metabolism of WIN-55,212-2 [130], AM-630 [131] and JWH-015 [132] synthetic compounds. However, the popularity of JWH-018 as a recreational drug soon brought human *in vivo* metabolism

to the forefront. Sobolevsky *et al.* [133] identified two major JWH-018 monohydroxylated metabolites in urine using gas and liquid chromatography combined with tandem mass spectrometry. Metabolites of JWH-018 were observed to be excreted almost entirely as glucuronide conjugates, as in the *in vitro* studies of Chimalakonda *et al.* [134]. More recently, Toennes *et al.* [135] performed a pilot study to assess adverse effects of JWH-018. In this study, the pharmacokinetic properties of JWH-018 and of its metabolites were determined using blood samples taken during 12 h after controlled inhalation of 2 and 3 mg of the cannabinoid. Concentrations of JWH-018 in blood reached its maximum within minutes after inhalation and their time course suggests a multi-compartment distribution/elimination. The same was verified to six metabolites of the cannabinoid detected in the blood samples, whose levels of concentration were ten times lower than the parent compound. With these studies it was possible to confirmed that the prevailing metabolites of JWH-018 are monohydroxylated, typically on the terminal carbon of the alkyl group (N-5-hydroxypentyl-JWH-018 and N-4-hydroxypentyl-JWH-018) by two main lung and liver CYP1A2 and CYP2C9 isozymes and with minimal contributions from CYP2C19, 2D6, 2E1, and 3A4 [136, 137].

Also, commonly detected in human urine are metabolites that are monohydroxylated on the alkyl site, monohydroxylated on the indole group, or carboxylated on the alkyl site (5-hydroxyindole-JWH-018, 6-hydroxyindole-JWH-018 and 7-hydroxyindole-JWH-018 and N-pentanoic acid-JWH-018, a major human urinary metabolite) [138, 139]. In the second metabolic phase, glucuronidated metabolites are formed, N-Hydroxypentyl-JWH-018 glucuronide is formed from N-hydroxypentyl-JWH-018 by UGT2B7, and N-pentanoic acid-JWH-018 is metabolized to N-pentanoic acid glucuronide-JWH-018 by UGT1A3 and UGT2B7. 5-Hydroxy-JWH-018 glucuronide, 6-hydroxy-JWH-018 glucuronide and 7-hydroxy-JWH-018 glucuronide are also formed through the metabolism of its respective substrates (Figure 15) [138, 140]. Interestingly, N-dealkylated and N-dealkyl monohydroxylated metabolites of JWH-018 are abundant in rat urine but rare in human samples [139].

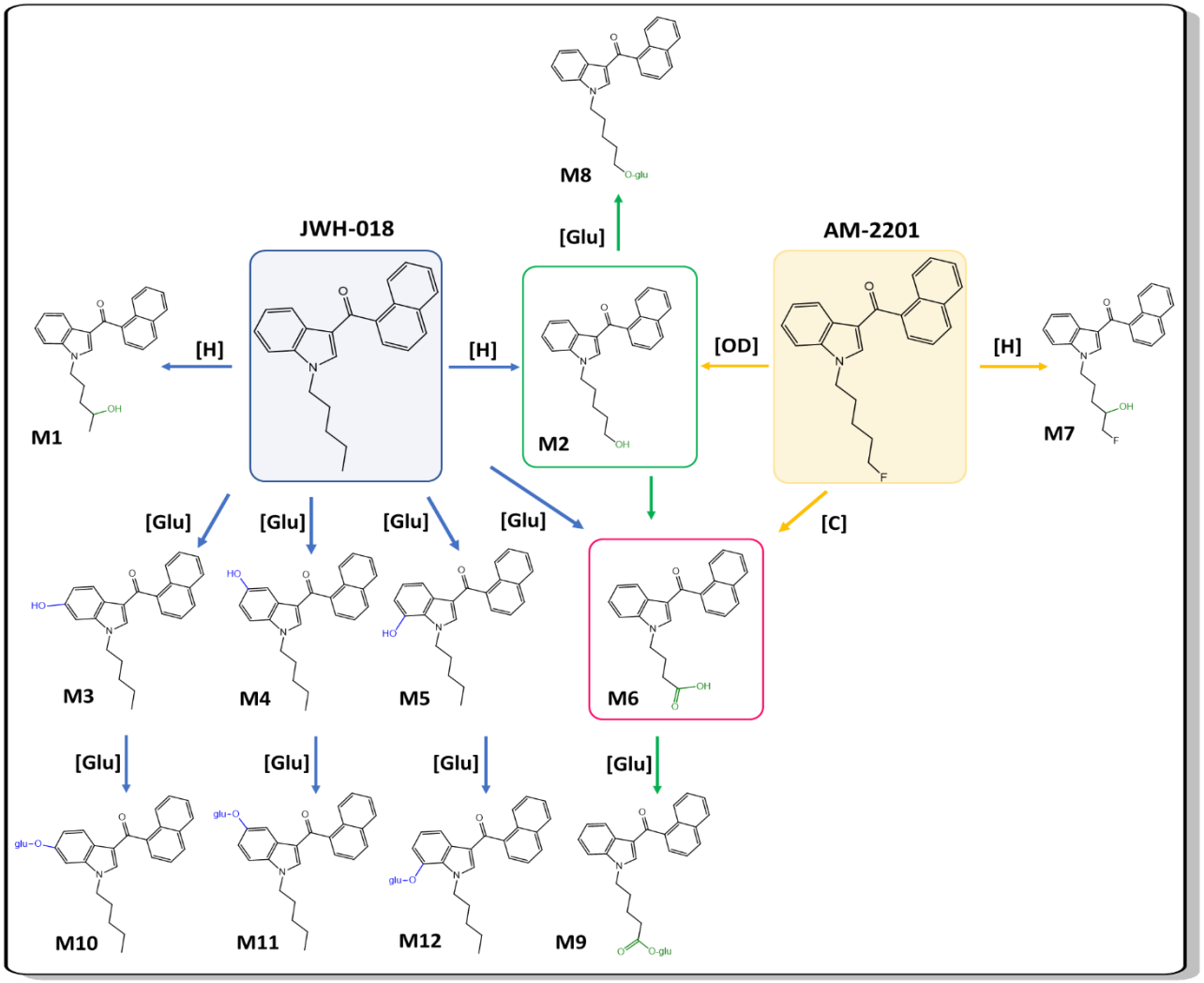

Figure 15. Merging metabolic pathways for JWH-018 (blue arrows) and AM-2201 (yellow arrows). Green arrows indicate the metabolic phase II in common to both compounds. M1- N-4-hydroxypentyl-JWH-018; M2- N-5-hydroxypentyl-JWH-018; M3- 6-hydroxyindole-JWH-018; M4- 5-hydroxyindole-JWH-018; M5- 7-hydroxyindole- JWH-018; M6- N-pentanoic acid-JWH-018; M7- N-4-hydroxyfluoropentyl-AM-2201; M8- N-5-hydroxypentyl-JWH-018 glucuronide; M9- N-pentanoic acid-JWH-018 glucuronide; M10- 6-hydroxy-JWH-018 glucuronide; M11- 5-Hydroxy-JWH-018 glucuronide; M12- 7-hydroxy-JWH-018 glucuronide. [H] hydroxylation; [C] carboxylation; [OD] oxidative defluorination; [Glu] glucuronidation (adapted from [10]).

N-5-hydroxypentyl-JWH-018 and N-pentanoic acid-JWH-018 are also metabolites of synthetic cannabinoid AM-2201. Chimalakonda *et al.* [134] studied the oxidative metabolism of JWH-018 and its fluorinated analogue AM-2201 using human liver microsomes and human recombinant CYP. The authors concluded that both synthetic substances appear to be metabolized similarly to produce several ring and alkyl side chain oxidized metabolites that are excreted in human urine as glucuronic acid conjugates.

AM-2201 undergo oxidative defluorination to N-5-hydroxypentyl-JWH-018. Other metabolites are also produced, like N-pentanoic acid-JWH-018, N-4-hydroxyfluoropentyl-AM-2201, dihydroxy-AM-2201, dihydrodiol-AM-2201 and despentyl-AM-2201. Hydroxy-AM-2201 and glucuronides of

hydroxy-AM-2201 and dihydrodiol-AM-2201 were also detected *in vitro* and *in vivo* [134, 136, 138]. N-4-Hydroxyfluoropentyl-AM-2201 activates CB_1 receptors with nanomolar affinity and is a distinctive marker of differentiation between AM-2201 and JWH-018 abuse [138].

Different studies have been published on the metabolism of other JWH-type compounds, such as JWH-015 [141], JWH-073 [142, 143], JWH-081 [143], JWH-098 [141], JWH-122 [143], JWH-200 [144], JWH-201 [145], JWH-210 [143], JWH-250 [146], JWH-251 [141, 145] and JWH-307 [141]. Like JWH-018, each of these contains an aminoalkylindole group and both JWH-015 and JWH-073 compounds have a naphthoyl group in common with JWH-018 [139]. The *in vitro* metabolism of JWH-015 produces 22 products reminiscent of those detected following similar treatment of JWH-018.

The diversity of products generated by this method greatly exceeds those typically reported from urine, as in the studies examining the human urinary metabolites of JWH-073. As JWH-073 differs structurally from JWH-018 solely in alkyl chain length (butyl for pentyl), the human urinary metabolites are naturally comparable: monohydroxylation of the indole group or alkyl site or carboxylation of the alkyl chain. Again, all monohydroxylated forms are fully glucuronidated while only a fraction (<50%) of the carboxylated products are glucuronidated [139]. Figure 16 shows the sites of modification of the major metabolites of JWH-015, JWH-073 and JWH-250.

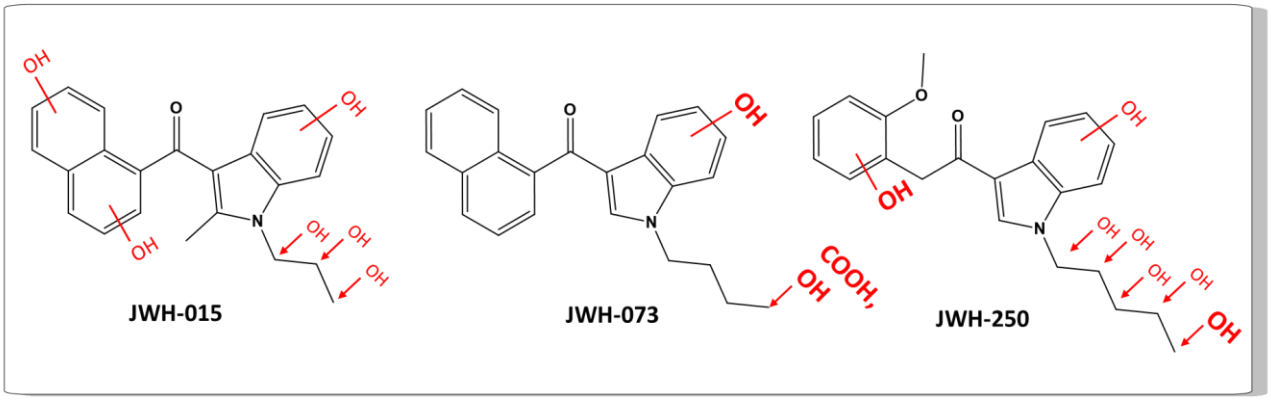

Figure 16. Sites of modification in the metabolism of JWH-015, JWH-073 and JWH-250 with major metabolites given in larger font (adapted from [10]).

The metabolites of JWH-018 and JWH-073 also maintain their *in vitro* activity at CB_2. It is therefore reasonable to assume that other SCs are also biotransformed into molecules with various levels of activity at the CB receptors. These active metabolites may prolong the parent compound's psychotropic and physiological effects and may contribute to its toxicity profile [147].

CYP3A4 has been recently demonstrated to be the major CYP enzyme responsible for the metabolism of APINACA, 5F-APINACA, APICA, and 5F-APICA. This enzyme is, preferentially, responsible for hydroxylation on the adamantyl group [138, 148, 149].

In UR-144 and XLR-11 metabolism, CYP3A4 also shows the highest level of metabolism activity, preferentially at the tetramethylcyclopropyl moiety. XLR-11 is the fluorinated form of UR-144 and a derivative of AM-2201 and both compounds differ from JWH-018 by the substitution of a naphthyl group with a 2,2,3,3-tetramethylcyclopropyl group [138]. These two cyclopropoylindoles are extensively metabolized by monohydroxylation at pentyl, indole, or 2,2,3,3-tetramethylcyclopropyl groups, dioxidation followed by internal hydration at tetramethylcyclopropyl group, dihydroxylation at pentyl and tetramethylcyclopropyl group, carboxylation at tetramethylcyclopropyl or pentyl groups, dioxidation followed by internal hydration, glucuronidation, and combinations of these reactions [138, 150, 151]. As the 2,2,3,3-tetramethylcyclopropyl group can undergo ring opening when heated or smoked, the pyrolytic product of UR-144, 1-(1-pentyl-1H-indol-3-yl)-3-methyl-2-(propan-2-yl)but-3-en-1-one and its several urinary metabolites have been reported along with metabolites of UR-144 [150]. Thirteen urinary metabolites of the pyrolytic product of XLR-11 have been tentatively identified, and the UR-144 degradation product N-pentanoic acid is a major metabolite [138, 151, 152].

The indazoles AB-CHMINACA and AB-FUBINACA are extensively metabolized by hydrolysis of the amide group, mono-, di-hydroxylation, N-dealkylation, glucuronidation, and combinations of these reactions. Dehydrogenation, defluorobenzylation, and epoxidation followed by hydrolysis are also reactions that occur in AB-FUBINACA metabolism. Hydroxylation on the indazole ring and amino-3-methyloxobutane moiety of AB-FUBINACA are major pathways, but there is no modification of the fluorobenzyl moiety. AB-CHMINACA and AB-FUBINACA carboxylic acid metabolites are formed by carboxylesterase enzymes (CES) and were identified as major metabolites in human hair and urine samples [153-155].

Ashino *et al.* [156] suggested that SCs, especially naphthoylindole derivatives, are capable of inhibiting CYP1A enzymatic activity as do the major metabolites present in cannabis, CBN and CBD. Introduction of novel functional groups and substructures could potentially convert the resulting compounds into substrates for other CYP enzymes than the reported ones or subject them to non-CYP-mediated biotransformation. Therefore, metabolism studies on novel emerging SCs are essential. [58, 137].

Of note, some hydroxylated urinary metabolites are even more toxic than the parent synthetic drug. As example, JWH-018 major metabolites, N-4-hydroxypentyl-JWH-018 and N-5-hydroxypentyl-JWH-018, and AM-2201 metabolite, N-4-Hydroxyfluoropentyl-AM-2201 remained full agonists in nanomolar concentrations [134]. The exact mechanisms through which SCs produce their wide-ranging effects and toxicities are not fully understood. Furthermore, the extent to which these effects are

caused by either the parent compounds or their metabolic and thermolytic degradants is unknown [84]. Although, the duration of effects in humans compared to Δ9-THC differs, (shorter for JWH-018 (1 to 2 hours), and longer for CP-47,497 or its C8 homologue (5 to 6 hours) [80], in general SCs have longer half-lives, leading to prolonged toxicological effects [111]. Greater knowledge of the activity of relevant metabolites from a broader set of SCs may allow us to gain a better understanding of the contribution of these active metabolites to the toxicity observed with SCs [147].

2.3.3. Recreational and adverse effects

In contrast to the decline in the use of many NPS such as the cathinones and piperazines, it appears that the number of cannabimimetic drug users is increasing. Although SCs mimic the psychotropic effects of cannabis, these compounds are accepted to be more potent than natural cannabinoids and human data concerning the induction and duration of adverse effects remain limited [22, 111].

The continuously changing composition of these synthetic drugs by the producers, in order to avoid detection and regulation, makes treating SCs toxicity particularly challenging because the individual compounds vary in potency, efficacy, and duration of action, making their effects unpredictable, resulting in different experience to the users [17, 47]. Some users report a feeling of sedation while others experience agitation, fatigue, and flushes [22]. Hudson *et al.* [157]detailed the analytical detection of 11 different SCs across 40 batches of 16 different incense products in various combinations and proportions from brand to brand and from batch to batch, even within brands. The authors concluded that the cannabinomimetic content profile of the 40 products highlighted differences between the products and the fact that the cannabinomimetic content of sachets of the same labeled product can vary significantly and may explain the different reported effects. Compared with the intoxication of organic cannabis products which have a slow effect and gradually fade, SCs have a shorter duration and peak earlier. In the majority of cases the duration of clinical effects is shorter than 8 hours, whereas it lasts longer than 24 hours in some cases [111].

Numerous complications have been observed in SCs users. Similar to cannabis, the psychoactive effects of SCs range from pleasant and desirable euphoria to anxiety, relaxation, agitation, and changes in cognitive abilities, such as perceptual alteration, altered sense of time, and mild cognitive impairments [17, 22]. Some users also related sickness, hot flushes, burning eyes and xerostomia along with mydriasis and tachycardia. This clinical variability could be explained by some SCs being more associated with the development of stimulant-like acute toxicity while others may be more

associated with the development of cannabis-like chronic toxicity. The type of compound used, the individual susceptibility to the drug effects, the dose, or multi-factorial scenario, are potential factors too [111].

SCs can produce a wide range of physiological and psychiatric adverse effects, which vary in duration and severity. Case reports and retrospective studies of acute intoxication indicate that severe effects that have been noted include seizures, cardiovascular damage, renal damage, stroke, psychosis, paranoia, aggression, anxiety attacks, dependence, or even death (through suicide, adverse reaction, or overdose) [111, 158].

Acute cardiac toxicities are relatively common among SCs users, being tachycardia/bradycardia and chest pain the most commonly reported findings after SCs intake [159]. Supraventricular tachycardia with heart rates as high as 172 bpm were reported in a 24-year-old after ingestion of e-cigarette fluid mixed with SCs [160]. Acute myocardial infarction was also reported in adolescents and adults and cardiovascular fatalities associated with SCs use were described in the literature [159]. Most of patients arriving at Emergency Departments presented at least one psychiatric effect. Among them, anxiety and hallucinations were the most reported. Confusion, amnesia, unconsciousness, paranoid delusion and disorganized behaviour were also observed following use of SCs. According to several case reports, the use of SCs may also be associated with an increased risk of suicidal ideation [22, 158]. In Patton *et al.* [161] and Shanks *et al.* [162] work, two men without history of psychiatric disorders, committed suicide shortly after smoking herbal products containing SCs including JWH derivatives and AM-2201. In both cases, drug screening was negative for other licit and illicit substances [158].

Psychosis and psychosis-like conditions seem to occur relatively often following the use of SCs, presumably due to their high potency and the absence of CBD in the preparations. Studies on the relative risk of SCs compared with natural cannabis to induce or evoke psychosis are urgently needed [163].

The neurotoxicity of SCs abuse is well documented in the literature. An acute ischemic infarction was revealed after a 25 years old individual had stroke symptoms after smoking a product containing SCs called ‘freeze’ [164]. Seizures, aggressive behaviour, and rhabdomyolysis are another severe adverse effects occurring with SCs, but they are rarely reported with cannabis use given THC's weak affinity for the cannabinoid receptors [159].

The use of SCs can also lead to a variety of renal and gastrointestinal problems. A number of cases demonstrated nephrotoxic effects with kidney damage and intrinsic acute renal failure after

exposure to XLR-11 and/or UR-144 [165, 166]. Symptoms such as emesis, nausea, abdominal pain, diarrhea, excessive thirst, xerostomia and persistent cannabinoid hyperemesis syndrome have been described [158].

Ocular and metabolic disturbances are less common, and a small number of side effects have been described. Among these, mydriasis was frequently observed in ocular side effects and leukocytosis as well as more severe complications including hypokaliemia and metabolic/respiratory acidosis were reported in intoxications with SCs consumption [158]. Table 4 summarizes the several reported adverse effects with synthetic cannabinoid intoxication.

Table 4. Summary of clinical side-effects with SCs use (adapted from [17, 22, 114, 158-160, 163, 166, 167]).

Physiological damage	Side-effect
Cardiovascular	Tachycardia/bradycardia, hypertension, myocardial infraction, arrhythmias, chest pain, and palpitations. Risk of cardiovascular disease.
Neuropsychiatric	Severe psychotic symptoms like agitation, aggression, catatonia, paranoia, auditory and visual hallucinations, perceptual alterations, and persistent psychosis episode. Risk of psychotic disorders.
Cognitive	Severe cognitive impairments like memory alteration, attention difficulties, and amnesia. Executive function deficits of working memory and attention.
Neurologic	Dizziness, somnolence, seizures, hypertonicity, hyperflexion, hyperextension, sensation changes, and fasciculations. Structural and functional CNS alterations.
Renal	Acute kidney injury, abdominal pain, miosis, mydriasis, xerostomia, hyperthermia, fatigue, rhabdomyolysis, cough, deficits of driving ability. Kidney diseases, insomnia, nightmares, dependency, tolerance, and withdrawal.
Gastrointestinal	Nausea, emesis, appetite change, abdominal pain, diarrhea, excessive thirst, xerostomia and persistent cannabinoid hyperemesis. Severe weight-loss after prolong use.
Ocular	Mydriasis
Metabolic disturbances	Leukocytosis, hypokaliemia and metabolic/respiratory acidosis

Recently in the US, there has been an outbreak of severe bleeding events leading to at least 4 deaths due to the ingestion of synthetic cannabinoid products tainted with brodifacoum (a rodenticide). To increase sales, SCs are being mixed with other substances, including other psychoactive substances, such as bath salts or ecstasy/Molly by dealers. This new trend poses a huge health risk, thus raising concerns about the increased toxicity of these dangerous substances that are being incorporated into these products [168].

Several studies demonstrate an association between repeated cannabis use and long-lasting cognitive impairments, and an increase in risk for developing a variety of mental disorders, such as bipolar disorder, depression, and schizophrenia. There is growing evidence that SCs are associated with severe negative psychiatric and medical conditions. This evidence demonstrates that repeated exposures to these synthetic drugs induce overall negative side-effects, which are more severe and long-lasting than those related with Δ9-THC [22]. Despite a number of clinical trials with promising results, for some cannabinoids there are still a relative scarcity of data on long-term tolerability and efficacy [28]. However, chronic use of cannabinoids have been associated with structural and functional neuronal alterations, which lead to addiction syndrome and withdrawal symptoms [111]. Impaired cognitive and emotional function was also observed in chronic SCs users. SCs users have shown impairments in working and long-term memories, response inhibition, as well as an elevation of depressive and anxiety symptoms [169]. The same was observed in Livny *et al.* [170] work. The study showed impairment in the neural brain mechanisms responsible for working memory in SCs users and the results also showed reduced grey matter volume in chronic SCs users.

Adverse effects of intoxication have been reported to occur even in those who only used SCs once, whereas withdrawal from SCs has been reported to occur only in daily users. Symptom management for acute intoxication is frequently treated with supportive care and intravenous fluids to treat electrolyte and fluid disturbances [17]. Treatment is usually individualized and directed at the specific clinical presentation. Decisions regarding hospitalization, extent of observation, and treatment modalities are based on the symptoms, their severity, and comorbidities present [171].

Many adverse effects associated with acute intoxication are identical to some withdrawal symptoms; consequently, they are treated similarly. Benzodiazepines are recommended for controlling agitation, anxiety and seizures as a first-line treatment. However, quetiapine is administered in treating withdrawal symptoms in patients who failed to respond to benzodiazepines [17, 111]. Neuroleptics are also administered for acute psychosis and agitation and mania with psychotic symptoms. Although not always effective, antiemetics have been administered for hyperemesis [17].

Combined use of SCs with other psychoactive products such as alcohol, cannabis, or tobacco was also reported, which suggest that the clinicians must be aware about it when dealing with an intoxicated patient. Furthermore, because most of the intoxicated patients have increased activity, they are reported to be at high risk for rhabdomyolysis, elevated creatine kinase, and subsequent renal failure [111]. In addition, physicians need to remember that SCs are not detected by common commercial drug screenings and a negative drug screening result for SCs may not necessarily mean

that the patient is free of these drugs, since the list of SCs types is constantly growing. Therefore, the use of SCs should be suspected if a patient arrives at clinical departments with adverse effects similar to those of cannabis and a negative drug screening for other drugs of abuse, including natural cannabinoids [158].

3. Concluding remarks

Initially developed as therapeutic agents, often for the treatment of pain, SCs rapidly appeared on the illicit drug market, where their prevalence had long been underestimated. Since then, their place in the market has steadily increased, with more than 560 synthetic psychoactive substances identified worldwide on the illicit market [26]. Usually labelled as "not for human consumption" or "for aromatherapy use only" to circumvent legislation, SCs are commonly called 'synthetic marijuana' due to the fact they are produced with the goal of mimicking or enhancing the effects of Δ9-THC [172].

In light of the growing popularity of commercial synthetic cannabinoid products, it has become critically important to reevaluate our understanding of cannabinoid abuse. Increasing evidence suggests that there is a strong abuse potential for the high efficacy of these compounds, at least comparable to that of cannabis itself. Furthermore, these synthetic drugs are readily accessible and can be purchased easily from the comfort of home through the internet [173]. As long as there is a market for SCs, competitive pricings and attractive gimmicks will be used to increase sales and the appearance of electronic cigarette as an alternative to traditional tobacco cigarettes rapidly become a popular method of use for administration of SCs [68, 173].

In Europe the production is closely monitored, however current legislation is frequently defeated and outwitted by manufacturers who regularly modify their chemical formulations, resulting in rapid turnover of SCs. Indeed, each synthetic compound is replaced by newer analogues within a year or two, making the inventory of existing products endless and requiring constant updating of the classification system by new and separate groups and classes [5, 26, 83].

There are several common features among different compounds of SCs which can highlight the risk potential which these drugs have and their related adverse effects. Firstly, SCs act as full agonists to CB_1 receptors and some also bind to CB_2 receptors. Secondly, SCs are much more potent, easily cross the blood-brain barrier and have more affinity compared to organic psychoactive cannabinoids like Δ9-THC [22].

To date, several studies based on behavior, neurochemistry, and electrophysics have helped the forensic and clinic community to understand the pharmacological mechanisms of action of synthetic

compounds. However, many of them have been focused on the acute toxicological consequences of its use. As they are relatively new and novel, there are no epidemiological studies to show the long-term effects of these psychoactive compounds [174]. Moreover, since the chemical composition of many SCs is unknown and/or is changing from one batch to another, the effects may differ between consumers. Several of these substances may have addictive potential, higher than cannabis, producing greater acute and long-term toxicity, leading to serious adverse effects [175].

Given the prevalence of consumption there is an urgent need to better understand the pharmacology and toxicology of SCs. In particular, the role of intrinsic efficacy in abuse-related effects and adverse effects should be targeted in future studies [172]. Very limited information is available on the safety of SCs in humans, and the occurrence of serious health damage in their abusers is highly probable.

Analytical laboratories are challenged with SCs identification in biological matrices due to structural diversity and similarity. Unidentified synthetic compound in a patient's sample, makes it difficult to definitively evaluate the clinical effects of SCs or develop specific treatments. Given the evidence of the damage caused by SCs and the risk of adverse complications, more epidemiological and clinical studies are needed to investigate the risk factors associated with the abuse of these substances in order to integrate such information into the prevention and treatment programs. In addition, clinicians should be aware of the effects of the use of these substances and their possible complications in order to offer a more appropriate approach to treatment [88, 175].

Given the worldwide spread of these herbal mixtures, an international cooperation system is mandatory for sharing analytical information and improving monitoring of the global drug market [112].

CHAPTER II – Analytical methodologies used for determination of Synthetic Cannabinoids

1. Analytical challenges

Throughout this chapter will be discussed an overview of current analytical methodologies for separation and identification of SCs in different matrices, as well as their advantages and limitations in forensic and toxicological context.

The consumption of recreational drugs has increased in recent years. Internationally, policymakers and governmental authorities have struggled with this problem as a public health issue for decades, and from an analytical point of view, the correct identification of these synthetic drugs is a major challenge. Forensic and toxicological analytical approaches can detect, identify, and, depending on the technique, quantify substances in seized or biological samples. However, it is important to understand that conventional methods to illicit drug response may not be appropriate for these synthetic molecules, and proper identification is crucial in the assessment of suspected seized samples and in the evaluation of possible intoxication cases, which requires the use of reliable and accurate identification methods [176].

In recent years, the presence of new compounds in herbal products, which were not previously identified, has been more frequent. The variety of modifications in molecules and the speed which they enter on the market are challenges in SCs assessment. In fact, new compounds emerge faster than regulatory agencies as well as the development of analytical protocols [177].

One of the main analytical problems is the lack of certified standards for reference. Since clandestine laboratories are the producers of these substances, they are always one step ahead of chemical companies, since they are not able to produce synthetic cannabinoid standards as fast as new derivatives are produced. And to obtain reliable qualitative and quantitative results, every analysis must use a reference material. Due to the lack of standards for these chemicals, the identification process for these compounds has become complicated and very expensive [178, 179]. Furthermore, SCs are frequently combined with other recreational drugs or alcohol, making it difficult to relate an effect to a specific product. Besides that, the standard routine toxicology screening procedures, especially those targeted for cannabis detection, are unable to detect the presence of SCs. This presents an analytical problem for most laboratories, since more specific and more sensitive methods are required for their identification and quantification in biological samples, and the growing diversity of new products makes the constant updating of databases unbearable to most laboratories [180].

2. Analytical approaches for determination of SCs

2.1. Matrices

Fast detection and quantification of SCs is very important in forensic laboratories. The difficulties persist in screening and quantifying novel SCs with enough speediness and minimal cost-effective planning and clean-up measures [181]. One of the parameters to consider in drug analysis is the sample, depending on availability of specimens and the purpose of analysis [177].

SCs have been detected in different matrices, such as seized or biological samples. Each matrix requires specific treatment according to the investigated compounds [177].

2.1.1. Seized samples

2.1.1.1. Herbal incenses

As described in Chapter I, the most common types of seized products are ready-to-smoke mixtures of plant material infused with SCs. They usually contain more than one active substance and may have about six or more in the same product [182].

Since SCs are frequently found on the surface of the plant material, sample preparation of herbal mixtures appears to be quick and simple. However, when the material is soft and light, it is more difficult to obtain a representative sample for quantitative analysis. In addition, the plant and SCs content of herbal blends varies between commercial products, so the analysis strategy may differ to some extent from the analysis of traditional herbal drugs such as cannabis or drugs in other forms such as heroin, cocaine, and amphetamine-type stimulants.

Frequently, the main procedure for the extraction of compounds from herbal products is with organic solvents like ethanol, methanol, chloroform, dichloromethane, or acid/base extraction, followed by sonication for more effective extraction [182, 183].

In West *et al.* [184] study, a rapid and simple method to extract SCs from leafy substrates is described, where four different solvents (dimethyl sulfoxide, chloroform, methanol, and ethanol) were tested to extract SCs from doped damiana leaves, as well as different extraction times. The authors determined that the extraction of a small amount of substance (approximately 10 mg) with ethanol and 30 s of shaking would yield enough synthetic cannabinoid compounds for further analysis techniques. Extraction studies were also carried out in this work and are described in Part 3, Chapter I.

Modified sample procedures may be required when dealing with herbal combinations, especially when a high number of distinct brands are detected in the same seizure. It should be noted that the content of a specific product brand may change over time [182]. In Brent *et al.* [47] review, several studies were described, analysing the same brand of herbal incense, namely 'K2 products', and detected different compounds between them. Hudson *et al.* [185] detected four SCs of the 'JWH series' in K2 products purchased online, while Uchiyama *et al.* [186] identified cannabicyclohexanol, along with CP-47,497, oleamide, JWH-018 and JWH-073 compounds, in K2 products purchased in Japan.

2.1.1.2. Powders

Powder forms are also common and are frequently used for large scale production of herbal preparations or by particular users who mix their own herbal blends. Uchiyama *et al.* [187] analysed two different products that were purchased online as chemical and herbal product. Approximately, 2 mg of the chemical product was used for extraction with methanol under ultrasonication. The herbal material was crushed into powder and then extracted with methanol, also under ultrasonication, with the identification of two SCs, APICA and APINACA. Other study [188], analysed a brown powder and different product packages of "spice-like" herbal incenses were identified and characterized the synthetic compound 5F-MDMB-PICA.

2.1.1.3. E-liquids

In recent years, e-liquids used in electronic cigarettes have become a popular alternative to smoking tobacco. Instead of smoking cannabis or herbal mixes laced with SCs, e-liquids containing SCs are becoming increasingly popular [189, 190]. Angerer *et al.* [190] analysed 21 e-liquids bought online and ten of them contained one or more SCs; in 3 of them an unknown compound was detected which, after analysis was identified as 5F-Cumyl-PINACA. More recently, 13 commercial e-liquid formulations provided by customs seizures were screened by nuclear magnetic resonance, being detected 5 SCs [189].

2.1.1.4. Infused papers

The infused papers are designed to evade detection and facilitate smuggling. This new trend is currently circulating and are highly prevalent in prisons and the nature of the substances as well as their concentrations are variable both between paper samples and across individual sheets. Unlike

other sample substrates like powders and herbal materials, infused papers cannot be homogenized before sampling and therefore must be sampled in a representative manner, being a challenge to obtain a representative qualitative data [191].

In Portugal, according to Serviço de Intervenção nos Comportamentos Aditivos e nas Dependências (SICAD) report [192], in 2017 the main form of presentation of SCs was the herbaceous mixture, being the powder presentation almost equally frequent, also identifying the presence of the synthetic cannabinoid AMB-FUBINACA in micro-stamps.

Very recently, SCs were detected in infused paper sheet samples in some prisons. Norman *et al.* [191] reported the analysis of 354 individual seized paper samples originated from 168 seizures from three Scottish prisons, in which, 41% contained, at least, one synthetic cannabinoid, and 23% of these papers contained multiple SCs. For qualitative analysis, approximately 1 cm^2 of sample area was cut from opposite corners and placed in a glass vial with methanol, followed by sonication for 5 minutes, whereas for quantitative analysis a 3 mm diameter hole punch sample was collected. The collected paper was placed in a screw-cap glass vial, and sequentially extracted with a dichloromethane/methanol solution. The extract was weighed, and the total volume calculated. In this study, 5F-MDMB-PINACA, 5F-MDMB-PICA, 4F-MDMBBINACA and MDMB-4-en-PINACA were the prevalent compounds.

Another recent research [193], also described the identification of SCs in 56 infused paper sheet samples, seized mainly in Brazilian prisons between 2016 and 2020. Seven different SCs were identified in the samples, with MDMB-4en-PINACA and 5F-MDMB-PICA being the most frequently ones.

Figure 17 shows the different seized samples previously mentioned with SCs.

Figure 17. Different seized samples with SCs. A – herbal incenses; B – powder form; C – e-liquids; D – micro-stamp.

2.1.2. Biological samples

2.1.2.1. Blood

The selection of a biological fluid for drug analysis depends on the specific purpose of the testing. Blood is usually, the preferred biological fluid for detecting drugs in the "under-the-effects" period, as most substances are only present for a few hours [194]. Other advantage is that blood can also be used to determine the amounts and ratios of the parent drug and its metabolite, which can provide useful information on acute or chronic drug usage [177]. Kneisel *et al.* [195], published a broad study where 833 authentic serum samples were analysed with the dentification of 30 SCs. The preparation procedure was based on a simple liquid-liquid extraction with n-hexan/ethylacetate (90:10) mixture.

Very recently, Ji *et al.* [196] established a rapid screening method for 23 SCs in human whole blood by direct analysis in real time-tandem mass spectrometry. According to the authors the method is simple, efficient, quick, and environmentally friendly, and it gives useful data for the rapid screening of these compounds in forensic research. However, there are significant difficulties, such as crime scene screening and manual error.

Another recent work [197] reported the simultaneous analysis of 29 SCs and metabolites, amphetamines, and cannabinoids in human whole blood. Samples were prepared by supported-liquid-extraction followed by liquid chromatography –tandem mass spectrometry analysis with positive electrospray ionization. The described method was successfully applied to the analysis of 564 ante- and post-mortem blood samples, with 132 of them with positive findings of at least one synthetic cannabinoid. The findings showed that metabolites are present in blood at higher quantities than unmodified parent SCs, highlighting the need for forensic screening technologies that can detect both parent substances and metabolites at the same time.

In blood, parent compounds can be detected using either a targeted or non-targeted analytical technique; however the detection time window is shorter than in urine. The low concentrations and short half-life of exogenous substances in this sample, demands a series of pre-requisites for the analytical techniques used, such as 10- to 100-fold more sensitive procedures than those used for urine. Furthermore, the invasiveness of the sampling technique, the need for specially trained staff for sample collection and the high cost of blood drug testing are the main drawbacks for this matrix [194].

2.1.2.2. Urine

Among the different biological fluid for drug detection, identification and quantification, urine is one of the most widely used in forensic toxicology. Some of the benefits of this sample are: easily accessible by non-invasive procedures; the concentrations of analytes are often higher when compared with blood or oral fluid; and almost all drug metabolites are eliminated in the urine, where they can be detected for longer periods of time than in the blood [180, 194]. The prevalence of positive results in urine specimen for some compounds is higher than those observed in blood due to the longer detection window in urine samples [177]. However, the detection of these substances in urine is not always possible. As described in Chapter I, SCs are rapidly transformed to a large number of metabolites, which are not yet known or fully characterized [180]. Because of the extensive metabolism of SCs, the parent drugs are rarely observed in the urine; rather, their metabolites are excreted, making detection more difficult, since there is a lack of reference metabolic patterns [10, 180].

The detection of the parent drug is crucial in body fluid analysis, because once the parent drug has been metabolized, the consumption of the drug cannot be confirmed without data on the metabolites [111]. Depending on the dose and period after intake, metabolites may be detected in the blood; however, many urinary metabolites generated from multiple SCs ingestions may be present, while only one substance may be present in the blood causing urine metabolite data confusing [126, 194]. Furthermore, metabolites may derive from more than one parent synthetic cannabinoid, which makes the analysis of SCs from urine samples more complicated [177, 194].

Regarding urine sample preparation for SCs, hydrolysis with acids or enzymes is required, since it was discovered that the hydroxylated metabolites of JWH-018, JWH-073 and JWH-250 are excreted in conjugated form in a high percentage [177]. The major metabolites of SCs are often extensively glucuronidated, and for this reason β-glucuronidase is the most used enzyme for hydrolysis [180]. Knittel *et al.* [198] presented a validated procedure for identification and quantification of 15 parent SCs in blood along with their corresponding urine metabolites. Prior to extraction, the urine samples were hydrolysed with phosphate buffer and β-glucuronidase solution. After incubation, an acid solution among with chlorobutane were added and centrifuged. The upper organic layer was transferred, evaporated, and finally reconstituted with mobile phase. According to the results 15 SCs were identified in blood samples and 17 corresponding metabolites in urine samples. The authors suggest a strong correlation between the metabolites detected in urine and the parent compounds found in blood.

A study with a large dataset of authentic workplace drug testing urine specimens was published with 290 urine specimens collected. Urine specimens were hydrolysed with β-glucuronidase, and proteins precipitated with acetonitrile. Analytes were eluted with ethyl acetate, dried completely under nitrogen and reconstituted in mobile phase before analysis. According to this study, 22 alkyl hydroxy and carboxy metabolites from 11 parent SCs (JWH-018, JWH-073, JWH-081, JWH-122, JWH-210, JWH, 250, JWH-398, AM2201, MAM2201, RCS-8, and UR-144) were quantified, being the JWH-018 pentanoic acid compound the one with the highest concentration. The authors reported that JWH-018 and AM2201 metabolites were the predominant analytes quantified in urine specimens and no parent drug was identified. Multiple metabolites were present from a single parent compound and hydroxy and carboxy metabolites provided suitable urinary metabolite targets for most SCs present in the samples; however, this may vary for newly emerging compounds [199].

As the pharmacodynamics of this class of drugs matures, blood analytical data can identify the precise parent synthetic cannabinoid used and may also allow conclusions about impairment. The urine results, on the other hand, can be utilized to determine past exposure to SCs and, in certain cases, provide information concerning the consumed synthetic cannabinoid. SCs with structural similarities appear to go through similar metabolic changes, according to latest evidence [198]. As a result, one of the most difficult aspects of urine synthetic drugs testing is that new compounds are constantly emerging, and their metabolic profiles are unknown. Prior to developing targeted screening methods, it is necessary to identify urinary marker metabolites [194].

2.1.2.3. Oral fluid

Another biological specimen that has been applied for the determination of SCs is the oral fluid. This sample is an alternative with increasing interest in forensic and clinical toxicology. Its collection is fast and easy, non-invasive, no medical staff is needed for sampling, as is mandatory for blood withdrawal, the risk of infection is much lower compared to blood and reduced risk of adulteration or manipulation due to the direct observation of specimen collection [180, 194, 200]. Furthermore, oral fluid containing parent SCs is an excellent choice for testing, when metabolite references are unavailable or the target metabolites are still unknown [177].

However, there are some disadvantages, such as small sample volume, reduced salivation after intake of drugs with sympathomimetic properties, and lower concentrations when compared to urine [200]. In terms of window of detection, oral fluid shows, in general, a shorter window (hours) compared to urine (days), which could be appropriate to detect drugs in the “under-the-effects” phase [194, 200].

Using sensitive methods for oral fluid analysis can improve the overlap between detection times in oral fluid and urine. Additionally, the detection window for drugs in oral fluid may be expanded after repeated ingestion of high doses of drugs of abuse [200].

Blandino *et al.* [200] compared urine and oral fluid as biological matrices to monitor recent exposure to SCs and classic drugs among HIV+ homeless individuals. They concluded that 5 oral fluid samples were positive for AB-FUBINACA and 4 urine samples tested positive for PB-22, 5-Fluoro-PB-22, AB-FUBINACA, and metabolites UR-144 5-pentanoic acid and UR-144-4-hydroxypentyl synthetic compounds. According to the authors, only one case matched oral fluid and urine results, with AB-FUBINACA compound being identified in both specimens. Regarding sample preparation, urine samples were initially treated as in the papers mentioned above, while oral fluid samples were vortexed, loaded onto supported liquid extraction (SLE) cartridges, eluted ethyl acetate, evaporated and reconstituted in mobile phase before analysis.

Oral fluid collection can be achieved via spitting, drooling or collection via various types of absorbent swabs (Figure 18).

Figure 18. Different swab-based devices for oral fluid collection (adapted from [201]).

Oral fluid collectors are favoured for sanitary reasons, as well as the fact that they feature stabilizing buffers that ensure correct analysis. On the other hand, there are some drawbacks in using those special devices like drug losses due to the dilution effect connected with the use of stabilizing buffers, the detection window, and the possible adsorption effects [183, 202]. Kneisel *et al.* [203] studied the detection of 30 SCs in oral fluid using a collection device for sample collection. 264 authentic oral fluid samples were tested, being 31 positives for at least one synthetic cannabinoid. JWH-210 was identified in 31 samples, whereas JWH-122, JWH-081 and JWH-018 were identified in 17, 8 and 7 samples respectively. Despite the suitability of the method for the analysis of SCs in oral fluid samples, analyte recovery studies from unstabilized collection devices revealed significant drug loss after a

few minutes, probably due to adsorbing of analytes on the pad surface. Stabilization of the pads using ethanol led to satisfactory recoveries of at least 43% after three days of storage.

Expectoration or spitting produces clean oral fluid without the need for buffer dilution, which improves assay sensitivity. Although this collecting method is less expensive than others, it can be unpleasant for donors and collectors. Oral fluid that has been expectorated is viscous and contains mucus, food particles, and/or other oral debris. Prior to laboratory examination, samples must be centrifuged to remove precipitant material, and this may decrease drug concentration due to drug loss in the pellet or adsorption to the tube [204]. In Williams *et al*. [205] study, a validated method for the detection of 19 SCs in oral fluid with minimal sample preparation is presented. The authors reported that the major advantage of the method is the rapid run time, minimal sample volume and preparation and the ability to add new drugs quickly as the standards become available and can be readily applicable to a routine laboratory. The oral fluid samples were collected by direct expectoration into a sterile tube. The stability and recovery studies revealed that overall SCs are most stable when stored in glass tubes (without buffer) either refrigerated or frozen.

2.1.2.4. Hair

Other alternative specimens have gained popularity in drug testing like, hair, sweat as well as in post-mortem samples such as vitreous humor, bile or stomach content [194]. Some studies have reported the determination of SCs in hair samples [206-208]. Hair can provide long-term histories via segmental analysis due its larger detection window when compared with all the other types of specimens (up to months). Another benefit of using hair as biological sample is the low risk of donor manipulation. However, environmental contamination, such as the one caused by drug smoking, may affect hair analysis, resulting in false-positive results [177].

A recent work [209], reported a comprehensive method validation for 72 SCs in hair samples. Hair strands were washed in deionized water, acetone, and petroleum ether. After air drying, 1.5 mL of MeOH were added to 50 mg of hair segment and then cut by into 1–2 mm pieces in the solvent. The extraction was performed by 3h of ultrasonication. The validation demonstrated low quantification limits (0.5–5.0 pg/mg) however, high matrix effects were taken into consideration as a major limitation of the method. The analysis of 294 authentic samples resulted in 163 positive samples. According to the authors, hair analysis can be a suitable tool as it provides a larger detection window compared with body fluids (e.g. blood, oral fluid, or urine) and non-invasive sampling can easily be performed. The main drawback of hair analysis consists in the complex interpretation of analytical

findings due to the difficulty to differentiate external contamination from incorporation of the drug via systemic uptake. Table 5 summarizes the different biological samples most used for the detection of SCs.

Table 5. Summary of the biological samples most used for the detection of SCs.

Specimen type	Detection Window	Collection process		Target compounds	Sample preparation	Advantages/ disadvantages
Blood	hours – 1 or 2 days	Invasive		Parent drugs and metabolites	Liquid extraction with organic solvents and centrifugation/ ultrasonication	Parent substances and metabolites can be detected /Needs specially trained staff
Urine	hours – days	Non-invasive		Metabolites	Hydrolysis with acids or enzymes (β-glucuronidase) and centrifugation	Easily accessible and longer detection window/ Only metabolites can be detected and the need of sample preparation procedures before analysis
Oral fluid	minutes – 12 hours	Non-invasive		Parent drug	Dilution and centrifugation	Easily and rapid accessible and reduced risk of adulteration/ Short detection window, only parent substances can be detected
Hair	days - months	Non-invasive		Parent drugs and metabolites	Several washing steps; extraction with organic solvent and ultrasonication	Low risk of manipulation/ Environmental contamination; difficulties with correlating measured concentrations in hair to the amount of drug consumed

2.2. Sample preparation techniques

The analysis of drugs or other substances in biological samples such as blood, urine, saliva, etc., requires a pre-treatment of the sample, due to the complexity of the matrix, since they normally contain proteins, salts, acids, bases and various organic compounds that may be similar to the analyte of interest. Furthermore, they cannot always be analysed directly, due to their incompatibility with

chromatographic systems and many of the compounds to be analysed are found in trace concentrations [210, 211].

Sample preparation is an essential part of the analytical process to convert the biological material into a form that can be studied analytically. The extraction stage is the most important aspect of the sample preparation method, since it decreases background noise by removing interfering matrix molecules. Furthermore, it concentrates the target compounds, resulting in increased sensitivity and reduced detection limits [177, 180]. In general, sample treatment improves the precision, accuracy, and robustness of analytical procedures, which is the goal when developing methods for determining synthetic drugs in a variety of biological matrices, notably for SCs [180].

Several sample pre-treatment procedures have been used for the removal of interfering compounds and pre-concentration of analytes. These techniques can be divided into conventional sample preparation techniques (most commonly used in routine analysis), including liquid-liquid extraction (LLE), solid phase extraction (SPE) and protein precipitation, and in current sample preparation techniques where reduced sample and solvent consumption and increased specificity and extraction selectivity are favoured when compared to traditional techniques [180, 211].

The choice of a sample preparation technique must be carefully considered, taking into account some analytical requirements, including matrix complexity, chromatographic separation, polarity of target analytes, and the need for high performance.

2.2.1. Protein Precipitation (PP)

PP has been proven to be useful when analysing protein rich matrices, such as whole blood, serum and plasma [177].

To reduce the solubility of the solute and precipitate the protein, an organic solvent is added to the specimen, which can then be removed by centrifugation or filtration. For SCs the solvents most used are acetonitrile, and perchloric and trichloroacetic acids [180]. In Wohlfarth *et al*. [212] study, acetonitrile was used as precipitant solvent to determine nine SCs and twenty metabolites in urine samples by liquid chromatography with recoveries ranging from 53 to 95%. The same organic solvent was applied in Patton *et al.* [161] in post-mortem blood samples, being detected AM-2201 metabolites.

PP is a rapid and simple extraction technique; however, it does not remove many of the matrix interferences [177].

2.2.2. Liquid-liquid extraction (LLE)

LLE is used to separate, concentrate, and purify organic compounds existing in a liquid phase. It is based on the distribution of a substance between two immiscible phases placed in contact, where in one of the phases the analyte is dissolved (aqueous phase, biological sample) and the other is an organic solvent (extracting solvent). The hydrophilic compounds have a greater affinity for the polar aqueous phase, while the hydrophobic compounds will be found mainly in the organic solvent [213, 214].

In SCs extraction, LLE is usually used because of their high hydrophobicity, being applicable with most types of matrices. The solvent selection is determined by the polarity range of analytes included in the analytical procedure, as well as the biological matrix. [177, 180]. Several solvents have been reported for SCs extraction, such as t-butylmethyl ether [143, 215], chloroform [216, 217], and diethyl ether [133, 218, 219]. However, solvent mixtures are the most widely described. Gottardo *et al.* [208] applied a user-friendly procedure with a mixture of n-hexane and ethyl acetate for the analysis of eight SCs in hair samples. Another study [207] used the same solvent mixture for the extraction of 23 SCs, also in hair samples. Before extraction procedure hair samples were digested with sodium hydroxide. In Ji *et al.* [196] study, blood samples were processed by adding a mixture of acetonitrile/methanol (v/v, 4:1) for the analysis of 23 SCs.

LLE offers better clean up than protein precipitation and it also removes protein. In addition, it can be optimised for different compound classes. However, it requires an evaporation step prior to analysis to eliminate excess solvents, which can be difficult to automate and the tendency to form emulsions and the fact of being laborious and time-consuming are some of LLE drawbacks [177, 220].

2.2.3. Solid Phase extraction (SPE)

SPE is a technique that has been proven to be a very effective method for sample pre-treatment and clean-up in biological matrices in clinical and toxicological drug analysis in recent years [177]. In this technique the analytes are extracted after passing a solid phase (sorbent), which is usually contained in a reservoir in the form of a syringe or cylinder (cartridge) [214].

The extraction process is based on the same principles as LLE, since it requires the partitioning of analytes into two phases. However, instead of two immiscible liquid phases as in LLE, in SPE the analyte partition takes place between a liquid phase (matrix) and a solid phase (sorbent) [221]. Compared with LLE, SPE has several advantages, such as high selectivity, clean extracts, absence of

emulsions, less use of solvents and higher yield by automation. In addition, it has a wide variety of sorbents that allow the development and improvement of extraction procedures [214]. The polarity or ionic charge of the analyte of interest determines the choice of the most suitable sorbent and solvent. Thus, SPE can be divided into 4 categories, according to the extraction mechanism: adsorption (normal and reversed phase), ion exchange and mixed-mode [222, 223]. In Figure 19, it is schemed the different types of SPE and its properties.

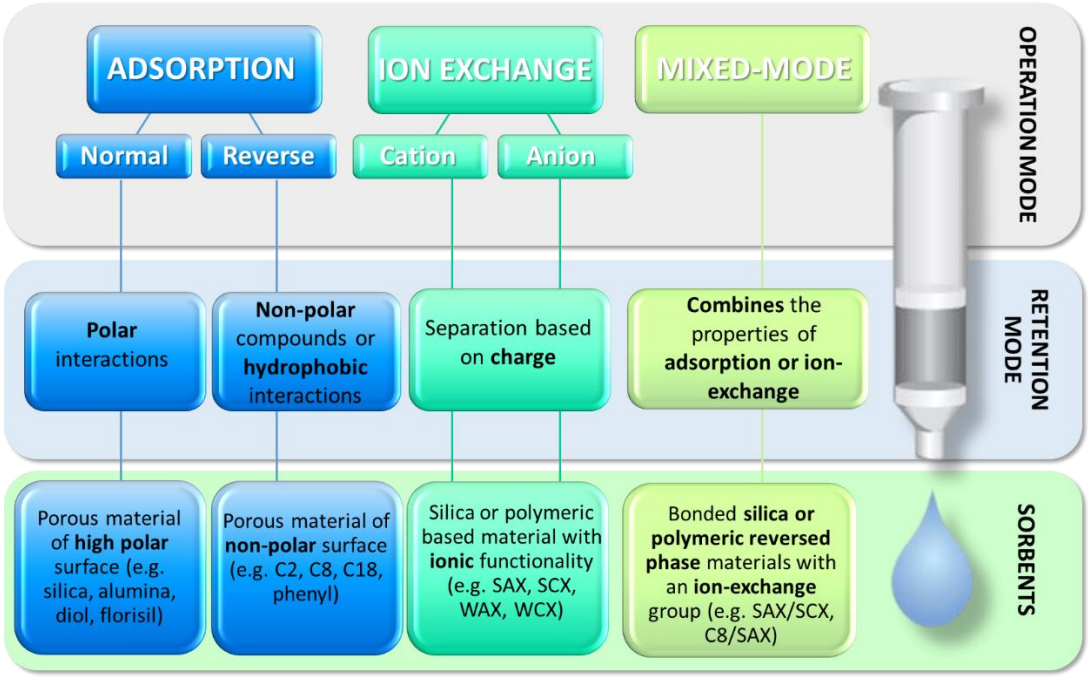

Figure 19. Different SPE extraction modes (adapted from [223]).

Normal phase is commonly used when the analyte of interest has low to high polarity or is neutral. The separation process is based on polarity, with the least polar components eluting first. The matrix is usually non-aqueous, and the sorbent is a polar material, such as silica. On the other hand, reversed phase SPE techniques are optimal for analytes with moderate to low polarity. The separation of analytes is based on hydrophobicity with the most polar compounds eluting first. SPE with reversed phase sorbents is often used since many analyses involve analytes dissolved in an aqueous sample (e.g., urine or plasma) [214, 223].

In ion-exchange SPE, the sorbent is composed by anionic or cation-exchange functional groups, responsible for the electrostatic interactions that occur between the charged functional group of the analyte and the charged functional groups attached to the sorbent. The analyte, as well as the functional groups attached to the sorbent, must be ionized by adjusting the sample pH [221].

Finally, mixed-mode combines the capabilities of ion-exchange and reversed-phase SPE for an enhanced separation. This type of SPE extraction can enhance analyte retention and/or reduce matrix impurity contamination and is commonly used in the separation of basic, acidic, and neutral compounds in a mixture, being strongly applied in the isolation of drugs and metabolites from urine and blood samples [221, 223].

SPE method generally, comprises the following steps: conditioning of the stationary phase, application of the sample (adsorption of the analyte to the sorbent), washing of the stationary phase (elimination of the interferents) and finally the elution (recovery of the analyte) as described in Figure 20.

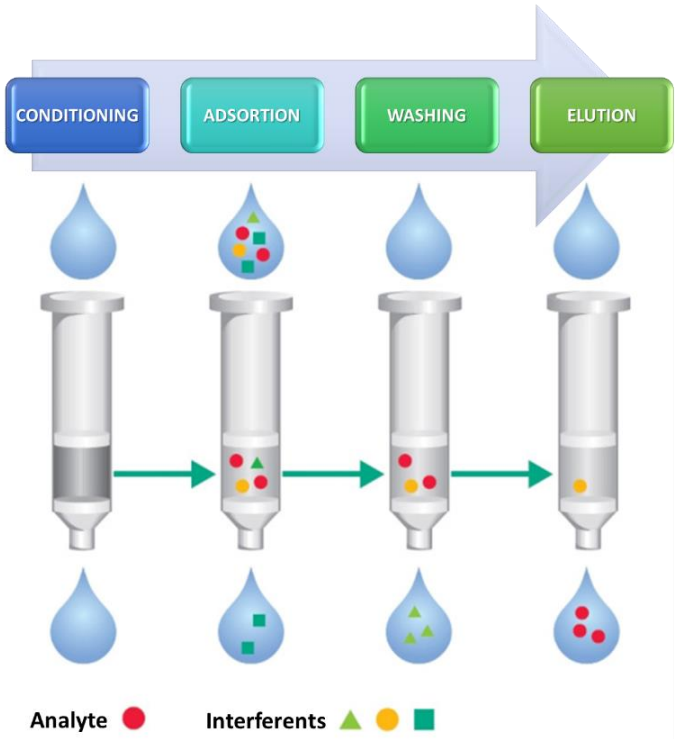

Figure 20. Schematic representation of the SPE procedure (adapted from [221]).

In the first step, the solid phase is conditioned with a suitable solvent, usually methanol, whose purpose is to solvate the functional groups of the stationary phase, thus ensuring the interaction of the matrix with the sorbent. Next, the sample is transferred to the SPE cartridge using vacuum or positive pressure. In this process, impurities are eluted while the analyte is retained due to chemical interactions with the stationary phase. The clean-up step is essential to eliminate compounds from the matrix, which can interfere with the analytical method. Finally, a solvent is applied to remove the analyte retained in the stationary phase. The selection of elution solvent is an important parameter and is directly related to the polarity of the analyte and the sorbent used in the SPE extraction, which

should be able to break the interactions between the analyte and the stationary phase and recover it in the smallest amount of time and volume [221].

Regarding to the extraction of SCs using SPE as extraction technique, several reports have been published in different biological samples [177]. Guale *et al.* [224] developed a screening method that utilizes automated SPE to purify a wide array of analytes, including SCs in spiked blood and urine samples. The analytes were loaded with a polymeric strong cation-exchange SPE sorbent and eluted in two steps using mixed organic solvents (a hexane/ethyl acetate mixture for the first elution, and a methylene chloride–isopropanol–ammonium hydroxide mixture for the second fraction). Simões *et al.* [225] reported the analysis of nine SCs in urine samples using a polymeric reversed-phase sorbent and ethyl acetate as elution solvent. Another study [226], also used a polymeric reversed-phase sorbent for the extraction of seven SCs and Δ9-THC in oral fluid. Elution was performed with an organic solvent mixture (2-propanol/dichloromethane/acetic acid).

Although SPE is an extraction technique that removes endogenous compounds which can cause technical problems such as coelution and matrix effects, the cost and time spent on method development and extraction are the main disadvantages [180].

Another technique developed for sample pre-treatment is QuEChERS. This technique was presented in 2003 by Anastassiades *et al.* [227], being developed with the aim of obtaining a method that allowed the simultaneous analysis of several pesticide residues present in fruit and vegetable samples that was also easy and quick to perform, with low costs. The name QuEChERS comes from the combination of its main characteristics, being a quick, easy, cheap, effective, robust and safe technique. It has less sample preparation time when compared to traditional techniques, providing fewer process steps and reducing the amount of sample and solvents. Unlike many other sample preparation techniques, which are adapted for the selective extraction of target analytes, QuEChERS strategy is primarily focused on matrix removal. Basically, this method comprises 2 phases: sample extraction/partition and a sample clean up step by dispersive SPE [221].

In recent years, QuEChERS has grown in popularity, with some modifications to its procedure, to adapt to new analytical challenges. From a forensic toxicology case, Hasegawa *et al.* [228], developed a method for the identification and quantification of metabolites of the synthetic cannabinoid MAB-CHMINACA in urine sample with or without β-glucuronidase hydrolysis, using QuEChERS methodology as extraction technique. The results of the application or not of hydrolysis process were practically the same. Satisfactory recovery rates were obtained for the compounds examined (between 96.3 and 97.6%) and a good linearity in the range of 0.5–20 ng/ml was achieved.

According to our research, few studies were reported using QuEChERS methodology as extraction technique for SCs. The fact of this technique is being used mainly for the determination of pesticide residues in the food and agricultural fields and the need to modify the original method to minimize degradation of some compounds to guarantee the efficient extraction of pH-dependent compounds, could be some of the factors for the reduced exploitation of the technique [180].

Many improvements have been introduced in recent years; however, these procedures that we described above, are still quite time-consuming and laborious, requiring large amounts of sample and, in many cases, the use of toxic organic solvents to achieve satisfactory analytical limits. Moreover, many of these extraction procedures were designed to work offline, which is a limiting step to obtaining fast bioanalysis [229].

2.2.4. Microextraction approaches

Currently, researchers are following a new trend of 'greener' extraction procedures with the use of miniaturized or micro techniques for the extraction of new substances such as SCs [180]. Microextraction techniques represent a key step in these analytical methodologies by providing samples in the suitable volumes and purification levels necessary for the characterization of the target analytes. The use of small amounts of sample and organic solvents, as well as the reduction of solvent waste (both of which have clear environmental benefits), and the ability to reuse the extraction equipment (in some of the techniques) are the main advantages [180, 230].

Several approaches have been employed, including solid phase microextraction (SPME), microextraction by packed sorbent (MEPS), miniaturized solid phase extraction (μ-SPE), among others, as powerful sample preparation techniques, characterized by their reduced time of analysis, low solvent consumption, and broad application [194, 230].

2.2.4.1. Solid-Phase Microextraction (SPME)

SPME is a unique sample preparation technique based on sorption extraction. This technology has proven to be very promising since its creation in the early 1990s by Janusz Pawliszyn [231], and fitting well into the 'green chemistry' concept. SPME has been extensively researched as a simple, adaptable, and low-cost alternative sample preparation for chromatographic analysis, retaining all of the advantages of SPE, such as simplicity, easy automation, and, in addition, ease of field sampling and reduced solvent use [214].

In SPME the analytes are retained in an organic polymeric phase coated on the outer surface of a fused silica fiber (Figure 21) [230].

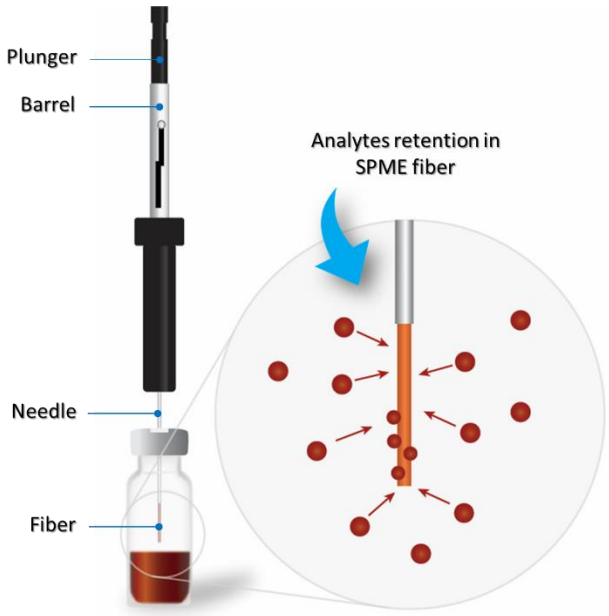

Figure 21. SPME technique using a commercial device (adapted from [232]).

Depending on the nature of the coating, analytes present in the sample are absorbed or adsorbed. As in SPE, the appropriate choice of fiber coating (sorbent) is crucial for the effectiveness of the analytical method, as the type of fiber used affects the selectivity of the extraction [232]. In its most common format, the fused silica SPME coated fiber can be introduced into the sample by direct extraction (DI-SPME) or by headspace (HS-SPME). In DI-SPME, the coated fiber is directly immersed in the aqueous samples, and the analytes are transported directly from the sample matrix to the extracting phase. In the HS-SPME mode the analytes are extracted from the gas phase above a gaseous, aqueous or solid sample [230]. This second approach protects the fiber from adverse effects caused by non-volatile, high molecular-weight substances present in the sample matrix (e.g. proteins) and also allows matrix modifications (including pH adjustment) without affecting the fiber [230].

SPME has been widely employed in many areas, including anti-doping and drug of abuse determinations [194]. A recent study [233], proposed a SPME approach for the determination of SCs in oral fluid, using direct immersion mode with a polydimethylsiloxane (PDMS) fiber, obtaining a LOQ of 10 $\mu g.L^{-1}$ and good precision. Another approach was presented by Cox *et al.* [234] using the HS-SPME mode for the rapid and reliable detection and identification of herbal smoking mixtures containing SCs using a carboxen/polydimethylsiloxane (CAR/PDMS) SPME fiber. More than 25 herbal products were analysed being identified several active compounds, such as JWH-073, 019, 018, 081, AM-694

and WIN-48,098 (pravadoline). The authors concluded that the minimization of sample preparation inherent in SPME analysis allows for ease and rapid access to the analysis of the herbal products and SCs.

SPME is a well-known approach that completely avoids the use of organic solvents in gas chromatography determination for the elution step, making it a highly environmentally friendly tool with very high enrichment factors [228]. Despite the advantages that characterize SPME, this technique has some limitations, highlighting its fragility and the range of commercially available fibers. The quality of fibers depends on the manufacturer and sometimes their performance varies from batch to batch, which requires the optimization of each fiber before its use [235]. Particularly in the analysis of drugs in biological fluids, the main limitations are related to the low stability of the fibers in the presence of organic solvents, which is a huge disadvantage when it comes to analysing these compounds by liquid chromatography, and the irreversible adsorption of compounds from high molecular weight that change the properties of the fiber leaving it unusable [236]. Also, the use of immersion mode could increase matrix effect and reduce lifetime of SPME fibres [194].

2.2.4.2. Miniaturized solid phase extraction (µ-SPE)

Miniaturized solid phase extraction (µ-SPE) is a SPE-based technique typically carried out with pipette tips containing a small amount of packed sorbent material. Instead of vacuum systems, micropipettes are used to circulate the loading, cleaning, and elution solutions. Monolithic materials are commonly used as sorbents, whether they are bought commercially or manufactured at home [194].

Compared to conventional SPME, µ-SPE has several advantages, such as efficiency in extracting analytes from suspensions or semi-solid/solid samples, due to the porous membrane preventing particles from contaminating the sorbent phase; lower costs as much less organic solvent is needed, and each device can be reused up to 20 times and finally the ease of handling and less time consuming [220].

µ-SPE has been employed for the extraction of several NPS in biological samples. Montesano *et al.* [24] reported the development of a method to determine simultaneously different classes of NPS including SCs and their metabolites, directly on whole blood without anti-coagulants, using µ-SPE as a clean up. Before µ-SPE, the samples were treated with a ACN:MeOH (50:50, v/v) solvent mixture, then sonicated for 10 min and centrifuged (10,000g for 10 min). 200 µL of supernatant was then mixed with 350 µL of H_2O, split in 2 tubes and finally processed by µ-SPE. For extraction an automatic

pipette with a OMIX C_{18} tip was used and methanol with 0.1% formic acid (MeOH 0.1% FA) was the elution solvent. The authors also compared µ-SPE performance with different clean up strategies, such as PP, LLE, PP/SPE hybrid, concluding that µ-SPE and PP were comparable in terms of recovery, being the microscale SPE more convenient due to its rapidity and lower matrix effect.

Another study [237], presented a µ-SPE using molecular imprinted polymers (MIP) for SCs assessment in urine followed by liquid chromatography–tandem mass spectrometry. The MIP- µ-SPE device was conditioned by sonication with 5 mL of 0.1 M/0.1 M KH_2PO_4/NaOH buffer solution (pH 5.0) for 10 min. Elution was performed by placing the MIP-µ-SPE device into a flask containing 2 mL of heptane/2-propanol/ammonium hydroxide mixture (75:20:5, v/v/v), followed by ultrasounds for 8 min. The developed MIP-µ-SPE has been shown to be a convenient, cost-effective and fast sample pre-treatment method, without the need for previous urine sample treatment such as PP.

µ-SPE also addresses some disadvantages of SPME such as analyte carryover and fiber fragility. Despite that, several micro SPE approaches are continuously being developed using different supports to accommodate small amounts of sorbents that will contact the sample solution [229, 237].

2.2.4.3. Microextraction by Packed Sorbent (MEPS)

MEPS, is a simple, fast and user- and environmentally-friendly miniaturization of SPE. Indeed, it has been demonstrated that MEPS can easily replace SPE in the majority, if not all, of the prior applications. It can do so by reducing sample and solvent usage, which is considerably lowered without compromising the extraction efficiency [238].

Its high selectivity and simplicity, combined with the use of reduced volumes, have made this technique an attractive option and a powerful tool in sample preparation in performing analytical and bioanalytical challenges. In addition, it combines sample extraction, concentration and clean-up steps in a single device, which can be easily connected with liquid or gas chromatography systems, providing a fully automated method [229].

In MEPS, the conventional SPE cartridge is replaced by a miniaturized column (≈1 cm × 0.2 mm internal diameter) with approximately 1-2 mg of packaged solid material, connected to a micro syringe needle, as illustrated in Figure 22. The analytes present in the sample are retained after passing through the stationary phase (sorbent), packed in a microcolumn also called a BIN (Barrel Insert and Needle Assembly) or MEPS cartridge [221, 229].

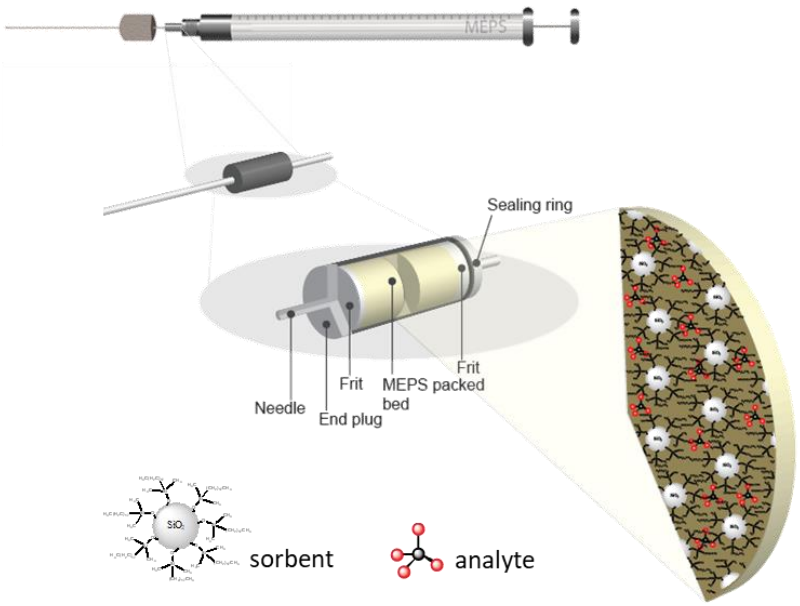

Figure 22. MEPS syringe and sorbent overview (adapted from [229]).

SPE cartridges are generally used once and discarded; on the other hand, MEPS sorbents, depending on the complexity of the sample, can be reused 50 to 100 times. The benefit of miniaturizing the extraction system in MEPS is that the analytes retained in the microcolumn can be eluted (desorbed) from the extractor phase in a single step using a few microliters of organic solvent or mobile phase, which can be injected directly into the analytical instrument [238].

The sorbent selection is an important factor to achieve high recovery rates. Since its development, numerous sorbent materials were made commercially available for MEPS. Traditional silica matrices (unmodified silica, C_2, C_8 and C_{18}), functionalized strong and weak cation and anion exchange C_{18} versions (SCX, SAX) and mixed sorbents (C_8/SCX) are essentially the MEPS sorbents.

More recently, the polymeric sorbent, polystyrene-divinylbenzene copolymer (PV-DVB), modified or functionalized to meet different retention abilities and target analytes, became available, as well as MIP. Table 6 presents some of the properties of the most popular commercially available sorbents for MEPS.

Table 6. Overview of the MEPS sorbents properties (adapted from [229]).

Sorbent type		Name	Phase	Properties
SILICA	**Unmodified**	**Silica**	NP	Highly polar.
	Modified	**C_2**	RP	Relatively non-polar sorbent (short chain length of functional group).
		C_8		Less retentive than C_{18} for non-polar compounds.
		C_{18}		Highest hydrophobic and least selective sorbent. Extremely retentive for non-polar compounds, retaining most organic analytes from aqueous matrices.
	Functionalized	**SCX**	Mixed-mode (RP, IE)	Suitable for weakly basic compounds.
		SAX		Suitable for weakly acidic compounds.
		M_1		Dual retention mechanisms broaden retention for a range of neutral, basic, acidic and compounds. Higher selectivity for basic compounds from biological fluids.
		APS		Very polar silica-bonded aminopropyl phase used as an ion-exchanger in both normal-phase and ion-exchange applications. Rapid release of very strong anions such as sulfonic acids that may be retained
Carbon		**Hypercarb**	RP	100% porous graphitic carbon material. Retention of extremely polar compounds. Recommended for pesticides extraction from different matrices
POLYMERIC	**Unmodified**	**SDVB**	RP	Highly retention of non-polar compounds.
	Modified	**HDVB**	RP	Hydrophobic polymeric sorbent offering 100% reversed phase interaction.
	Functionalized	**PEP**	Mixed-mode (RP, IE)	Polymeric PS-DVB modified with urea functional groups to give balanced retention of polar and non-polar analytes. Ideal for a wide range of applications, such as drugs and metabolites in biological fluids.
		R-CX	IE	Polymeric PS-DVB material partially functionalized with sulfonic acid groups to give balanced retention of basic and non-polar analytes. Ideal for the retention of a wide range of drugs of abuse, including basic and neutral drugs.
		R-AX		Polymeric PS-DVB material partially functionalized with quaternary amine groups to give balanced retention of acidic and non-polar analytes. Ideal for the retention of Δ9-THC and its metabolites.

Abbreviations: APS – aminopropyl silane; C18 – octadecyl-silica; C2 – ethyl-silica; C8 – octyl-silica; HDVB – highly cross-linked divinylbenzene polystyrene; IE – ion exchange; M1 – mixed-mode; NP – normal phase; PEP – polar enhanced polymer; PS-DVB – highly cross-linked polystyrene divinylbenzene copolymer; R-AX – polymeric DVB partially functionalized with quaternary amine groups; R-CX – polymeric DVB partially functionalized with sulfonic acid groups; RP – reversed phase; SAX – strong anion exchange; SCX – strong cation exchange.

MEPS is commercially available in off-line and on-line formats (Figure 23). The manual syringe was the first commercially available format and is the most widely used in the scientific community

among the three types. Its simplicity, low-cost and easy design and operation are certain factors behind such popularity [229].

The semi-automatic version (eVol®) was recently introduced by SGE Analytical Science and Thermo Fisher Scientific, making it a big step forward in the development of analytical methods as it is more reliable than manual MEPS. The combination of a digitally controlled and programmable electronic drive with an analytical syringe and the fact that it can be calibrated by the user allows greater precision and greater automation of possibilities for the MEPS extraction process. In addition, it provides customizable and precise flow volumes and velocities facilitating repeatable extraction of target analytes.

Finally, fully automated MEPS can be easily achieved using the same analytical syringes in autosamplers. These robotic platforms allow the automation of sample preparation with high precision. Its online use with analytical systems, facilitates and minimizes user intervention [229].

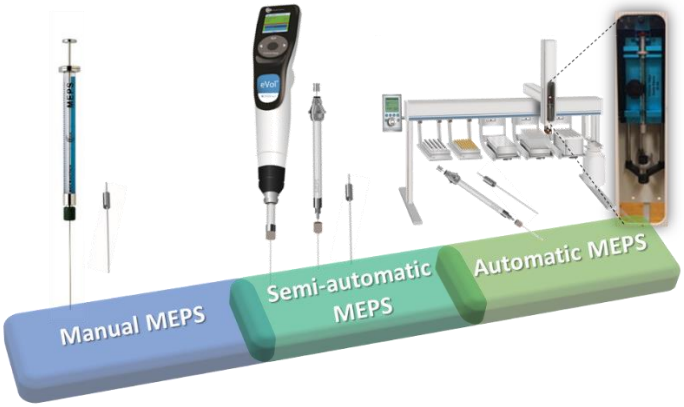

Figure 23. MEPS formats commercially available: manual, semi-automatic and on-line (fully automatic) (adapted from [221]).

Regarding MEPS procedure, the extraction follows the same steps as SPE, namely, conditioning of the stationary phase, sampling (passage of the sample through the sorbent), washing and elution. In Figure 24 is presented the schematic representation of the different steps of MEPS procedure.

Unlike conventional SPE, where the sample and solvents flow in one direction only (top to bottom), in MEPS extraction the aspiration and dispensing of the solutions is in two directions (from the bottom). Double-passing the sample and solvents significantly reduces the fraction weakly bound to the sorbent resulting in considerable improvements in selectivity and sample clean up. Furthermore, the idea of incorporating a microcolumn (BIN) into an analytical syringe, allowing the "cycling" of various sample aliquots through the sorbent, has a major impact on the recovery of the analytes of interest [239]. Another difference, is the conditioning step which allows the sorbent activation when it is used for the first time or its clean up and regeneration for a new sample

extraction cycle, which is an advantage over traditional SPE which has single-use sorbent cartridges [229].

Figure 24. Different steps in MEPS procedure.

MEPS has been widely employed in different fields of research, with special interest in clinical and forensic toxicology. In the last years, MEPS has been applied in different biological samples for the determination of new psychoactive substances [194, 240]. Regarding SCs, few studies are published, however there is a particular interest for the determination of these compounds in oral fluid samples. Very recently, Sorribes-Soriano *et al.* [241] described a procedure for the determination of 5F-MDMB-PINACA and four other SCs in oral fluid samples using MEPS as extraction technique followed by gas chromatography-mass spectrometry. The extraction was performed using a semi-automatic MEPS analytical device (eVol XR) with a C_{18} packed sorbent. A high sensitivity was obtained for the proposed procedure with limits of detection from 10 to 20 µg/L. The obtained results demonstrated the high potential of semi-automated MEPS for the selective and sensitive determination of SCs in oral fluid samples.

In addition to MEPS miniaturization, to accommodate small quantities of sorbents that will contact the sample solution, several microextraction techniques are constantly being developed employing various supports or automation procedures [238].

More recently, a new improvement of MEPS was introduced in the market by ePrep® company (Victoria, Australia). This variant, named µSPEed extraction, is a promising solid phase microextraction technique and represents a major upgrade by including several important modifications to MEPS extraction.

Contrary to MEPS, the µSPEed cartridges contain an efficient pressure-driven one-way check valve, which allows an ultra-low dead volume connection and a single way flow path through the sorbent bed in every extraction. As a result, when the plunger is drawn back, the only option to produce aspiration is by vacuum, which eliminates the need to pass through the bed and instead bypasses the sorbent. Another modification in µSPEed is the use of smaller sorbent particles (3 µm or smaller) in a small cartridge, instead of the 50 µm diameter particles normally used in traditional MEPS [238]. In Figure 25, is shown the MEPS and µSPEed main architecture differences.

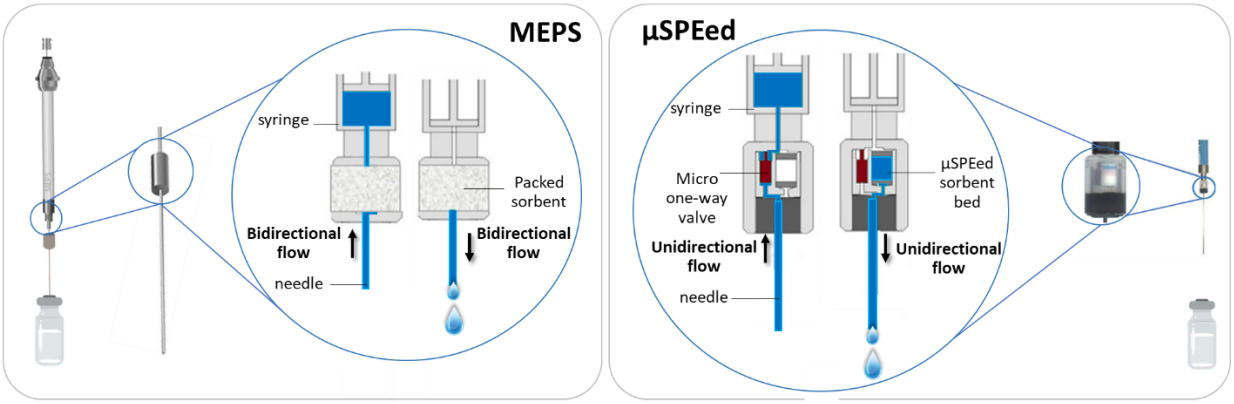

Figure 25. Comparison of MEPS and µSPEed sorbents (adapted from [238, 242]).

According to our research, no studies were found, to date, in the literature, for the determination of SCs using the µSPEed approach. In this work an optimized and validated method for the determination of SCs in oral fluid samples using µSPEed and MEPS as extraction techniques is presented in Part 3, Chapter II.

A summary of the published methods for extraction and determination of SCs in different matrices is described in Table 7.

Table 7. Sample preparation procedures for the determination of SCs in different matrices.

Sample preparation technique	Matrix (sample volume/ mass)	SCs	Extraction Parameters	LOD (ng/mL)	Recovery (%)	Analytical Methodology	Ref.
PP	Urine (100 µL)	JWH-018, JWH-073, JWH-081, JWH122, JWH-210, JWH-250, RCS-4, AM-2201, MAM-2201 and their metabolites	50 µL of 0.4 M ammonium acetate buffer (pH 4.0) + 20 µL β-glucuronidase + 190 µL ACN	0.5 – 10	53 - 95	LC-MS/MS	[212]
	Post mortem blood (100 µL)	AM-2201	400 µL ACN	-	-	LC-MS/MS	[161]
LLE	Hair (~100 mg)	JWH-018, JWH-073, JWH-081, JWH-250, and JWH-122	1 mL sodium hydroxide (0.5M) + 5 mL hexane/ethyl acetate (9:1)	10×10^{-3}	> 61	LC-QTOF-MS	[208]
	Hair (10 mg)	WIN 48,098, AM-1220, JWH-200, WIN 55,212-2, AM-694, AM-2201, JWH-015, RCS-4, JWH-250, JWH-073, JWH-203, JWH-251, JWH-018, JWH-081, JWH-007, JWH-307, RCS-8, JWH-122, JWH-019, HU-210, JWH-210, JWH-398, and JWH-020	1 mL sodium hydroxide (0.5M) + 5 mL hexane/ethyl acetate (9:1)	$0.2 – 24 \times 10^{-3}$	84 - 114	UHPLC-MS/MS	[207]
	Blood (200 µL)	JWH-073, JWH-019, JWH-122, MDMB-4en-PINACA, MAM-2201, 5F-UR-144, 5F-AB-PINACA, PB-22, 5F-CUMYL-PINACA, MDMB-CHMINACA, AB-PINACA, AB-CHMINACA, 4F-MDMB-BINACA, AB-FUBINACA, 5F-EMB-PICA, EAM-2201, JWH-081, FUB-JWH-018, STS-135, AMB-FUBINACA, MDMB-FUBINACA, AM694, and SKF525	1 mL ACN-MeOH (v/v, 4:1)	0.01 – 1	72 - 106	DART-MS/MS	[196]
	Postmortem blood (1 mL) urine (6 mL)	5F-MDMB-PINACA and MMB-FUBINACA	2 mL ACN + 6 mL ethyl acetate + 1 mL sodium hydroxide (1M)	25	99.6	GC-MS HPLC-UV	[243]
	Oral fluid (500 µL)	AM-2201, AM-2233, AM-694, HU-210, JWH-015, JWH-018, JWH-019, JWH-073, JWH-081, JWH-122, JWH-200, JWH-203, JWH-210, JWH-250, JWH-251, MAM-2201, PB-22, RCS-4, RCS-4-C4, RCS-8, STS-135, UR-144, URB 754, WIN 55,212-2, XLR-11, 5f-APINACA, and 5F-PB-22	10 mL triton- X100 (0.1%) + 250 mL ammonium carbonate buffer (pH 9.3) + 1.3 mL ethyl acetate:heptane (4:1, v/v)	-	-	LC-MS/MS	[244]
SPE	Blood (1 mL) Urine (1 mL)	RCS-4, JWH-073, JWH-019, JWH-122, AM-2201, JWH-210, JWH-081, RSC-8,	Strata-X-drug B column (polymeric strong cation-exchange sorbent)	-	15 - 50	LC-TOF-MS	[224]

		JWH-200, JWH-251, JWH-015, JWH-250, JWH-203, JWH-022, JWH-018, JWH-016, JWH-007, JWH-018-6-MeO, WIN-48098, JWH-098, AM-1241, AM-694	Conditioning: 3 mL MeOH + 3 mL dest. H_2O, 1st elution: 3 mL of a hexane –ethyl acetate (1:1), 2nd elution: 3 mL of a methylene chloride–isopropanol – ammonium hydroxide (78:20:2, v/v/v)				
	Urine (1 mL)	JWH-073-4-OH, JWH-073-3-OH, JWH-018-5-OH, JWH-018-5-hydroxyindole, JWH-073, JWH-250, JWH-018, JWH-018-4-hydroxyindole, and HU-210	Oasis® HLB 3 cc (polymeric reversed-phase sorbent) Conditioning: 2 mL MeOH + 2 mL dest. H_2O, washing: 2 mL of H_2O/ACN/ ammonia solution (90:10:1, v/v/v), elution: 2 mL ethyl acetate	0.01 – 0.5	58 - 105	UPLC-MS/MS	[225]
	Oral fluid (500 µL)	JWH-200, JWH-250, JWH-073, JWH-018, HU-211, CP 47,497, and CP 47,497-C8	Strata X cartridge (polymeric reversed-phase sorbent) Conditioning: 2 mL MeOH + 2 mL acetic acid (0.1M), washing: 2 mL acetic acid (20%) + 2 mL H_2O/MeOH (50:50, v/v), elution: 2-propanol:dichloromethane:acetic acid (24.5:75:0.5, v/v/v/)	0.025 – 1	65.4 – 105.6	LC-MS/MS	[226]
	Oral fluid (100 µL)	JWH-018, JWH-073, XLR-11, AB-FUBINACA, AB-PINACA, MAM-2201, MMB-FUBINACA, AM-2233, JWH-081, PB-22, JWH-122, AM-2201, AB-CHMINACA, UR-144, AM-694, NPB-22, SDB-006, FUB-PB-22, MDMB-CHMCZCA, THJ-2201, MN-18	Bond Elut Certify (C_8/SCX) Conditioning: 2 mL MeOH + 2 mL acetic acid (0.1M), elution: 1 mL 1-butanol:methylene chloride:acetic acid (24.5:75:0.5) and 1 mL methanol:ammonium hydroxide (98:2)	-	80 - 113	LC-MS/MS	[245]
	Urine (1 mL) Blood (1 mL)	AM-694	Bond Elut Certify (C_8/SCX) Conditioning: 2 mL MeOH + 2 mL phosphate buffer, elution: 2 x 1 mL of a dichloromethane:isopropanol (8:2,v/v)	-	90 - 94	GC-MS	[246]
QuEChERS	Urine (1 mL)	MAB-CHMINACA metabolites: 4-monohydroxycyclohexylmethyl and dihydroxyl (4-hydroxycyclohexylmethyl and *tert*-butyl hydroxyl)	Organic solvent: ACN dSPE with PSA + C_{18EC} + magnesium sulphate and dSPE without PSA	0.1	96.3 – 97.6	LC-MS/MS	[228]
SPME	Oral fluid (1 mL)	JWH-019, JWH-200, JWH-081, JWH-122, JWH-250, AM-2201, UR-144, CP,47-497 (C8) and CP,47-497 (C7)	DI-SPME; PDMS fiber Immersion: 15 min at room temperature and desorbed at 270 °C, 15 min.	1 - 10	-	GC-MS	[233]

	Herbal samples (50 mg)	JWH-018, JWH-073, JWH-250, JWH-081, JWH-019, Pravadoline, AM-694, AM-2201	HS-SPME; CAR/PDMS fiber: 5 min incubation at 200°C and desorbed 15 min.	-	-	GC-MS	[234]
µ-SPE	Blood (100 µL)	JWH-073, JWH-018, JWH-018-5-OH, JWH-081, JWH-081-5-OH, JWH-122, JWH-200, JWH-250, UR-144, UR-144-5-OH, XLR-11, XLR-11-4-OH, AB-005, MAM-2201	Automatic pipette; OMIX C18 tip; Tip washing: 100µL H_2O:ACN (50:50, v/v); Loading: 5 x mixture supernatant and water;) conditioning: 100µL H_2O:ACN:MeOH (80:10:10, v/v); washing 100µL MeOH:H_2O (80:20, v/v); elution: 3 x 100µL MeOH (0.1% FA).	0.25 – 250	21 - 70	LC-MS/MS	[24]
	Urine (1 mL)	AM-2201, AM2233, JWH-015, JWH-018, JWH-018-4-OH, JWH-019, JWH-073, JWH-073 COOH, JWH-073-5-OH, JWH-081, JWH-098, JWH-122, JWH-203, JWH-210, JWH-250, JWH-250 5-OH, JWH-302, RCS-4, RCS-8	Cone-shaped device; MIP - polypropylene porous membrane-protected; Conditioning: 5 mL 0.1 M/0.1 M KH_2PO_4/NaOH buffer solution (pH 5.0); loading: 2 mL KH_2PO_4/NaOH buffer solution (pH 5.0); elution: 2 mL heptane/2-propanol/ammonium hydroxide mixture (75:20:5, v/v/v)	0.03 – 0.75	85 - 102	HPLC–MS/MS	[237]
MEPS	Oral fluid (100 µL)	5F-ADB, MMB-CHMICA, THJ-2201, CUMYL-4CN-BINACA, MDMB-CHMCZCA	Semi-automatic MEPS; C_{18} sorbent; Conditioning: 100 µL 2-propanol + 100 µL dest.H_2O; loading sample: 5 x 100 µL; washing: 100 µL dest.H_2O + 100 µL clean air; elution: 5 x 50 µL 2-propanol	10 – 20	66 - 104	GC-MS	[241]
	Oral fluid (50 µL)	UR-144, JWH-250, JWH-081	Semi-automatic MEPS; C_{18} sorbent; Conditioning: 10 x 50 µL MeOH; loading sample: 5 x 50 µL; no washing step; elution: 25 x 50 µL dichloromethane:2-propanol:NH_4OH (78:20:2, v/v/v)	-	85 - 115	DESI-HRMS	[247]
	Oral fluid (90 µL)	AM-220, JWH-200, AB-005, JWH-018 N-pentanoic acid, JWH-018 5-OH, XLR-11 4-OH, MAM-2201 N-pentanoic acid, JWH-073, WIN-55, UR-144-5-OH, MAM-2201, JWH-250, XLR-11, JWH-018, JWH-081, JWH-122, UR-144	Manual MEPS; C_{18} sorbent; Conditioning: 3 x 250 µL H_2O/MeOH (75:25, v/v); loading sample: 5 x 250 µL; washing: 3 x 200 µL H_2O/MeOH (90:10, v/v); elution: 5 x 100 µL MeOH (0.1% FA)	0.005 – 0.275	49 - 96	UHPLC-MS/MS	[248]

Abbreviations: ACN - acetonitrile; CAR/PDMS - carboxen/polydimethylsiloxane; DART-MS/MS - direct analysis in real time-tandem mass spectrometry; DESI-HRMS - desorption electrospray ionization-high resolution mass spectrometry; GC-MS - gas chromatography–mass spectrometry; HPLC-MS/MS - high performance liquid chromatography–tandem mass spectrometry; HPLC-UV - high-performance liquid chromatography-ultraviolet; LC-MS/MS-liquid chromatography with tandem mass spectrometry; LC-QTOF/MS - liquid chromatography-quadrupole-time of flight mass spectrometry; LC-TOF-MS - liquid chromatography time-of-flight mass spectrometry; LOD – limit of detection; PDMS - polydimethylsiloxane; UHPLC-MS/MS - ultra high performance liquid chromatography-tandem mass spectrometry.

2.3. Analytical Methods

In recent years, rapid identification and quantification of SCs have emerged as crucial issues for forensic laboratories. The issues persist in screening and quantifying these synthetic compounds with sufficient pace and with minimum and cost-effective planning and clean-up measures [181].

2.3.1. Colorimetric tests

Along with a range of portable tools used by security services to detect explosive substances or drugs, colorimetric methods are the most popular because they are simple to use and inexpensive. Colorimetric techniques typically do not call for specialized equipment, elaborate protocols, or specialized apparatus because they are sufficiently sensitive and selective to allow for the quick, low-cost detection of a variety of analytes. There are test kits available for drugs of abuse such as marijuana, heroin, cocaine, and amphetamine [249]. However, these presumptive tests are non-specific and non-quantitative for SCs due to low concentrations of the analytes in the herbal mixtures, possible interferences by the sample matrix and the limited selectivity. Despite that, there are some commercially available presumptive tests for a few specific SCs [182, 249].

SCs with a similar molecular structure to Δ9-THC, give positive results to known marijuana tests (e.g. Duquenois-Levine and Fast Blue B salt tests), whereas for most SCs that do not have a similar structure to classical cannabinoids, the test is negative [249, 250]. The van Urk colour test, which is used to identify indole-containing drugs of abuse, is also negative for these compounds.

In Isaacs work [251], it is reported positive results with the use of Brady's reagent, 2,4-dinitrophenylhydrazine (2,4-DNPH) as an alternative colour test reagent, which reacts with the keto moiety instead indole group, for presumptive identification of SCs. At least 10 mg of sample powder or 50 mg of plant material was suspended in MeOH. Then, the supernatant was diluted with 2,4-DNPH reagent and heated to 60-65^{o}C for 5-10 min. A positive test result was indicated by the formation of a bright orange-red solution with or without eventual formation of a brick red precipitate. The author concluded that the presented test was capable to presumptively indicate synthetic cannabimimetics from the naphthoylindole, phenylacetylindole, benzoylindole and cyclopropoylindole classes in either powder form or adsorbed onto plant material and the speed of visualization could possibly be correlated to structural, steric and electronic features of the specific drug. However, colour changes in plant material with SCs was not always pronounced as those observed with powders due to variability in concentration. Also, the variations between batches

affected the speed of the colour test reaction. Despite these results, the test does not react with cannabimimetics without a ketone carbonyl group.

The Marquis reagent, is another colorimetric test which reacts with all nitrogen-containing drugs, giving positive results for cyclohexylphenols and the JWH series [250]. Although it is possible to detect SCs with each reagent in these screening tests, it is difficult to detect small amounts or mixtures of SCs. There are currently no presumptive tests which cover the whole range of SCs and the emergence of new synthetic compounds in the drug market makes it difficult for the rapid screening of these substances [182, 250].

2.3.2. Immunoassays

Immunoassay is a rapid method used as a preliminary screening test to eliminate negative samples, being very popular in clinical and forensic toxicology laboratories due to their ability to provide quickly and easily test results [177, 252].

Today's market offers a variety of immunoassay types, all of which are based on the interaction of an antigen (the target molecule) and an appropriate antibody [253]. Competitive immunoassay techniques are frequently utilized in drug testing. In these situations, a mixture of the sample analyte and the labelled analyte competes for a limited number of antibody-binding sites. As a result, the relationship between the amount of labelled analogue bound and the analyte concentration in the sample is inversely proportional [254].

Despite being fast, it has limitations, such as lower specificity. Furthermore, cross-reactivity and false positives can occur, being recommended to repeat the immunoassay tests and confirm the results by chromatographic analysis [177].

Different commercial kits are available for detecting SCs and metabolites in different biological samples, such as oral fluid, urine, and blood. Barnes *et al.* [255] demonstrated the utility of the homogenous enzyme immunoassay for monitoring of SCs by targeting the JWH-018 N-pentanoic acid metabolite on over two thousands authentic urine samples. The optimized performance of the immunalysis for the identification of SCs in urine was evaluated and compared to an LC–MS/MS assay for 29 SCs and metabolites. Despite being simple, cost-effective and rapid sample preparation, there are some limitations. The antibodies can identify first generation SCs based on the targeted napthoylindole structure, however, may not cross react with the most recent compounds on the market. The same conclusion was obtained by Rodrigues *et al.* [256]. In this work an ELISA targeting JWH-200 in oral fluid was evaluated. The assay was validated and applied to 32 authentic oral fluid

specimens previously analysed using LC–MS-MS. The authors reported that the immunoassay is predominantly targeted at the JWH-structured compounds and showed limited cross-reactivity to the newer SCs such as XLR-11 and also, stated that the ability to identify these synthetic compounds continues to be difficult as more compounds are detected in herbal products on a regular basis.

In conclusion, these devices/ kits are more useful than the colorimetric methods, because they do not require special reagents or tools, and the results are easily and quickly obtained. The devices also can detect older types of SCs, such as JWH-018 or JWH-073, but, unfortunately, the main limitation of immunoassay is the inability to cross-react with newer analogues of SCs as they become more widely used [177, 250].

2.3.3. Thin-layer chromatography (TLC)

TLC is one of the separation techniques for fast and simple screening of drugs, although gas and liquid chromatography have replaced it in many laboratories [182, 183].

The stationary phase is a thin adsorbent material layer, usually silica gel or aluminum oxide, coated onto an inert plate surface, typically glass, plastic, or aluminum. The sample is spotted onto one end of the TLC plate and placed vertically into a closed chamber with an organic solvent (mobile phase). Through capillary forces the mobile phase travels up the plate and the sample components migrate varying distances based on their differential affinities between the stationary and mobile phases (Figure 26). The plate is removed from the chamber when the solvent reaches the top of it and dried. The spots on the plate represent the separated components, and each component's retention factor (Rf) is measured [257].

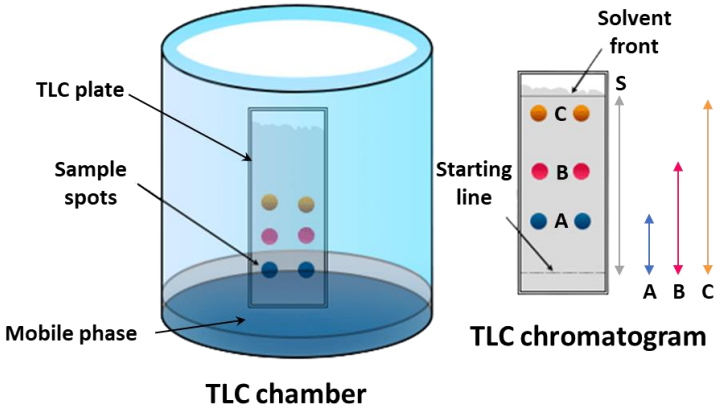

$$Rf = \frac{\text{distance travelled by the component (A, B or C)}}{\text{distance travelled by the solvent (S)}}$$

Figure 26. Illustration of a TLC separation and Rf calculation (adapted from [258]).

Accessible to a wide variety of substances in base and salt form, ranging from the most polar to non-polar materials, inexpensive, quick, and, flexible in the selection of both the stationary and mobile phase are some advantages. Also, TLC plates are single-use products, unlike LC columns, which are susceptible to contamination (of the stationary phase) by matrix compounds (such as fatty acid derivatives) [182, 183].

Several works use TLC for separation and identification of common abused drugs (such as amphetamines, natural cannabinoids, opiates, etc.). Regarding the analysis of SCs, some studies have been published using TLC as a separation technique of these synthetic compounds in herbal blends [241].

In UNODC report [182], 3 solvent system are presented for the separation of SCs, namely, n-hexane/diethylether (2:1, v/v), toluene/diethylamine (9:1, v/v) and ethyl acetate/DCM/MeOH/NH_4OH (18.5:18:3:1, v/v/v/v). For qualitative analysis of herbal products, no homogenization is required prior TLC assay. The plant material is usually extracted with MeOH or ACN under ultrasonication least 10 min and subsequently centrifuged. After TLC assay, UV light at 254 nm, iodine or iodoplatinate are the commonly used method to visualize/ detect the spots.

Logan *et al.* [259] work focused on the separation and detection of SCs in herbal incense blends by TLC. Two of the system solvents reported by UNODC were tested separately as mobile phases using Silica Gel for the separation of 21 SCs. All studied compounds exhibit UV absorbance at 254 nm and some of SCs exhibit white (AM-2201, RCS-4) or yellow, 366 nm (JWH-018, JWH-019, JWH-081, JWH-073, JWH-200, JWH-398, WIN 55,212-2, WIN 55,212-3) fluorescence. Iodoplatinate was the most effective reagent for the detection of studied SCs.

Kneisel *et al.* [260] also used TLC to analyse herbal blends samples. Two spots were revealed, indicating a mixture of two substances with highly similar physicochemical properties. The following LC–MS/MS experiments indicated two naphthoylindoles featuring different heterocyclic substituents at the indole nitrogen.

Despite the unquestionable superiority of High-Performance Liquid Chromatography (HPLC) due to higher performance and automatization, TLC has some important advantages like simplicity, significantly reduced cost and time of analysis, lower consumption of solvents and reagents, and ability to simultaneously handle dozens of samples. Therefore, this method is also attractive from "green chemistry" viewpoint. Finally, in contrary to HPLC, TLC analysis can be performed without any complicated instrumentation. For this reason, it is still widely used and is one of the most popular techniques for practical separation technique. However, the main limitation is the fact is not suitable

to differentiate certain closely related compounds due to their similar chromatographic properties. It is essential that other more selective methods be used to confirm the presence of these substances [182, 261].

2.3.4. Gas Chromatography coupled to mass spectrometry (GC-MS)

GC-MS is one of the most, commonly, used technique for the identification of drug samples in forensics [177].

In gas chromatography a chemically inert gas (usually helium, nitrogen, or hydrogen) is used as mobile phase. The gas flows through the entire system, passing through a heated column and bent in a spiral, containing the stationary phase, where the separation takes place. The samples are introduced with a syringe that passes through a rubber septum, existing in the injector. In general, the injection system consists of a metallic cylinder that is heated to a specific temperature, causing the evaporation of the sample components to be carried by the gas into the chromatographic column [214].

The column is located inside an oven, with programmable temperatures, usually linearly increased. The sample is dragged along the column interacting with the stationary phase at different speeds that will depend on the volatility of the analyte leading to chromatographic separation. The stationary phase together with the column temperature can affect the migration of analytes. Also, the solubility and volatility of the analytes are two crucial factors that will determine how the analytes are separated from the samples. The substance's volatility decreases with increasing molecular weight and polarity, which increases analysis complexity [214, 262].

After passing the analytes through the column, the detectors determine a physical or chemical property, generating an electrical signal of intensity proportional to the amount detected. The electrical signal produced by the detector is transmitted and recorded through chromatograms in a computerized system for data processing. In Figure 27 is presented a schematic diagram of a GC-MS system.

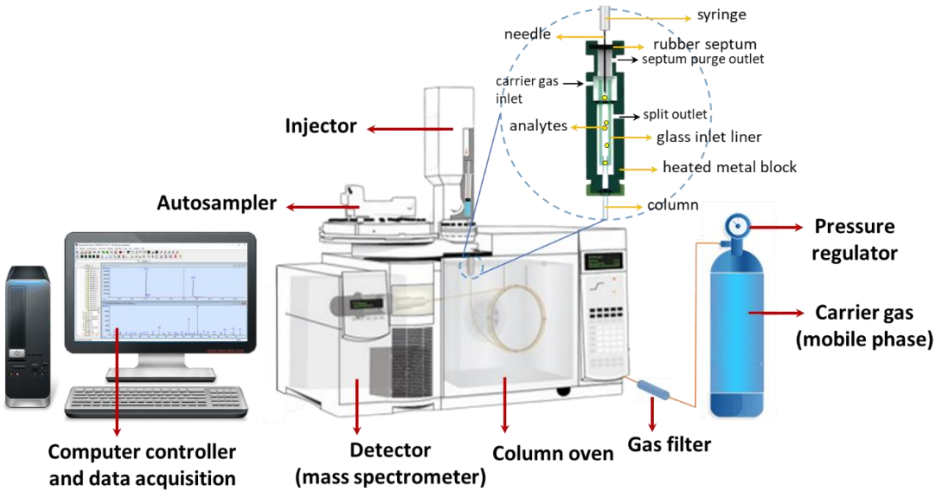

Figure 27. Schematic of a GC-MS system (adapted from [265]).

Several detectors are available for gas chromatography, however gas chromatography coupled to a mass spectrometer is considered the 'gold standard' technique and is used for broad spectrum drug screening [263, 264].

Mass spectrometry (MS) is one of the most sensitive and specific method available for drug detection, without the need of special reagents, which is an important advantage due to the ever-growing availability of clandestine synthetic drugs [264]. Since many drugs have relatively low molecular weight and/or nonpolar or volatile characteristics, these substances are especially suitable for gas chromatography analysis. Unknown compounds can be identified by matching full mass spectrum of unknown peaks with a mass spectral library or a database.

Basically, a MS detector generates multiple ions from the sample being studied, separates them based on their mass-to-charge ratios (m/z), and then records the relative abundance of each ion type. The major components of a MS detector are: an ion source, which splits the sample molecules into ions; a mass analyser, which sorts the ions according to their masses by applying electromagnetic fields; a detector, which measures the value of an indicator quantity and thus provides data for calculating the abundances of each ion present; and a computer, which regulates the mass analyser and manages the data derived from the detector [266].

Electron impact (EI) and chemical ionization (CI) are the most common ionization techniques in GC-MS. Most of EI fragments molecules at 70 eV, producing several fragmentations of molecules which can provide useful structural information. Due to the wide range of chemical structures among SCs, their mass spectra under EI circumstances differ greatly from one another [177].

Advantages of GC-MS are low cost and the universal availability of several commercial drug identification libraries [263]. However, the requirement that chemicals must be sufficiently volatile to allow transfer from the liquid phase to the mobile carrier gas and, consequently, to elute from the analytical column to the detector, is one of the limitations of GC-MS [267]. In addition, compounds which are thermally labile might decompose in the GC injection port. Many compounds with a polar functional group such as an amino or hydroxyl groups can also cause a polar interaction between the compound and the column stationary phase that leading to poor detection of the analyte. In many cases to overcome these problems a derivatization step is added onto the extraction method for these compounds to create sufficiently volatile forms of compounds [177, 267]. Derivatisation can change the functional groups and chemical properties of the molecule, making them less reactive with the stationary phase and more stable. However, this adding step consumes more time and reagent which can be toxic, and beyond that, may introduce another source of possible error [201].

Several studies have been published for the analysis of SCs in different biological samples using GC-MS (Table 7). The simultaneous analysis of different SCs in seized products has also been reported. In Choi *et al.* [268] work, a rapid and simple GC-MS method was developed and validated to identify and quantify SCs in seized samples. 10 mg of ground powder of dried leaves, tablets or bulk powders were extracted with 10 ml of MeOH under ultrasonication for 10 min. The extracts were centrifuged for 5 min at 3,000 rpm, and the supernatants were filtered and 1 µl was injected into the GC–MS system. The separation was carried out using helium as carrier gas, a HP-5MS capillary column and the injector operated in splitless mode.

As a result of the analysis, ten species of SCs were identified using some reference materials or using the in-house GC-MS library and consulting previous reports. No derivatisation step was needed, and the validated GC-MS methodology demonstrated to be useful to rapidly identify and quantify designer drugs in legal highs.

2.3.5. High Performance Liquid Chromatography (HPLC)

Liquid chromatography (LC) is the most popular technique for the analyses of different types of biological samples containing SCs and their metabolites [177]. Although GC is very useful to separate SCs or other synthetic drugs, the decomposition problems caused by the high injector temperatures are not seen in LC.

Basically, LC consists of a liquid mobile phase that crosses along the stationary phase in a defined direction. The analytes are retained in the stationary phase according to their affinity, with the

compounds with lower affinity being less retained and traveling faster, while those that establish stronger interactions with the stationary phase, leave more slowly until the complete separation of the sample components [269].

Early in the 1960s, a development of traditional LC emerged. HPLC uses sophisticated equipment that can be fully automated, making it indispensable in many laboratories. In HPLC the stationary phase is made up of small particles with a large surface area packed inside a column. The samples are dissolved in a suitable solvent and analysed in solution that then, introduced into the system and dragged by the mobile phase, under high pressure through the stationary phase [214, 270]. The wide variety of combinations between mobile and stationary phases makes HPLC an extremely versatile technique.

An HPLC system, essentially, consists of a pump, an injection system, a column, and a detector, all connected in an installation resistant to high pressures, which can go up to 300 atm. One or more solvent reservoirs for mobile phase and a computer system for data analysis are also part of the HPLC components [269]. In Figure 28 is illustrated a typical HPLC system.

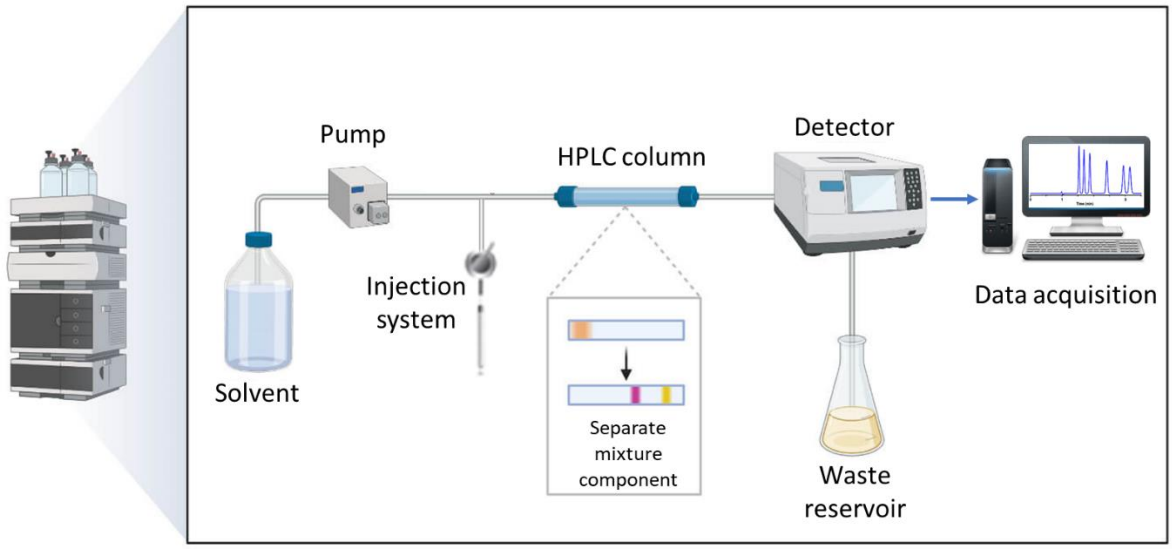

Figure 28. Schematic diagram of a typical HPLC system (adapted from [271]).

The sample is introduced into the system by an injection system. This system usually comprises an injector with a valve system that can be automated.

The chromatographic separation takes place in a column containing the stationary phase that can be inside a compartment that can be heated, allowing the use of heating to optimize the chromatographic separation.

Depending on the nature of the stationary phase, four main types of chromatographic processes in HPLC can be considered: adsorption, ion exchange, exclusion and partition. In Table 8 is presented the principal mechanisms of LC separation.

Table 8. Principal mechanisms of LC separation (adapted from [214]).

Types of separation	Illustration	Properties
Adsorption	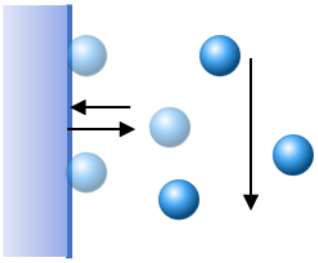	• Stationary phase is an adsorbent (e.g. silica gel) and the separation is based on repeated adsorption/desorption processes.
Ion-exchange	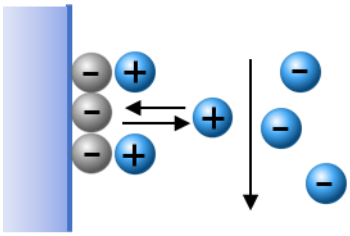	• Based on electrostatic interaction between the solute and stationary phase. • Used exclusively in ionic or ionizable samples. • Columns are characterized by the presence of charged groups covalently attached to the stationary phase. Anionic exchangers contain bound positive groups, whereas cation exchangers contain bound negative groups.
Partition	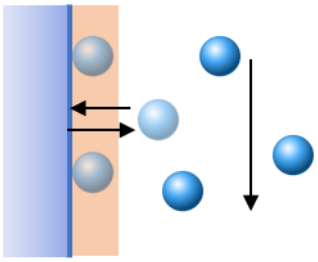	• Stationary phase is a liquid that coats small diameter silica particles. • Separation is based on the differential solubility of the analytes in the stationary phase and mobile phase. • Two main types: normal phase (very polar stationary phase and a non-polar mobile phase) and reversed phase (non-polar stationary phase and a polar mobile phase).
Exclusion	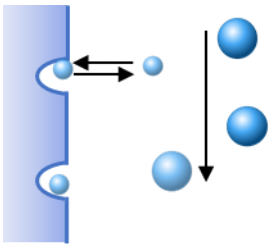	• Stationary phase is made up of a material with pores of a precise size and separation occurs according to the molecular size of the analytes. • Larger molecules do not fit in the pores and are eluted first, whereas smaller molecules penetrate the pores and are eluted later.

The pump (or pump system), associated with a controller, then, transports the liquids contained in the reservoirs in the selected proportions (eluent or mobile phase), and with the required flow

throughout the entire chromatographic system, ensuring that the flow of the mobile phase remains constant and reproducible. Elution can be done in isocratic mode when a mobile phase composed of a single solvent or a mixture of solvents with the same composition is used or gradient mode, where a variation in the composition of the mobile phase throughout the chromatographic separation is programmed in order to, obtain the best resolution in shorter time of analysis. The system can be binary, ternary or quaternary depending on the number of reservoirs. Finally, data is recorded by a detector [214].

Several detectors can be used in LC. The combination of LC with MS can yield a powerful analytical tool for identification of drugs in biological samples. Since its major advantage is its high sensitivity, makes this technique an excellent method of choice for many laboratories identify/ confirm unknown components in a sample. Despite these benefits, MS is still quite expensive and typically has a higher operational cost, which is not accessible to many laboratories. Absorbance detectors are a significantly less expensive and more user-friendly option to mass spectrometers. Ultraviolet/visible (UV-Vis) spectrophotometers are the most common used detectors for LC [214]. Based on the absorption of UV-Vis light by the sample when electromagnetic radiation passes through it. It is a selective detector for molecules that have chromophores. Fixed wavelength photometers, spectrophotometers, and photodiode array detectors (PDA) or simply diode array detectors (DAD) are the three types of equipment that operate according to this principle. Fixed-wavelength photometers, as the name implies, have their application restricted to molecules that absorb at the wavelength at which they work. On the other hand, spectrophotometers are more versatile, as they allow the choice of the most suitable wavelength for each analysis [272].

PDA detectors employs a reverse optics system, that is, the diffracting grating is placed between the sample and the detector and not between the radiation source and the sample. Thus, in the PDA, the polychromatic radiation falls on the sample and is then dispersed in a fixed monochromator at different wavelengths that are monitored simultaneously by the diodes. This fixed monochromator configuration brings some advantages, allowing the PDA spectrophotometer to acquire a spectrum without distortion and in a few milliseconds, as well as measuring wavelengths with high repeatability [273]. Another important factor for these detectors is the fact they have different sensitivities for different wavelengths, operating between 190 and 500 nm, so it is necessary to specify in which region of the spectrum to work, but the spectral resolution depends of the type and number of diodes that make up the array [274]. It is recommended to use the maximum wavelength of the analyte, as

long as it is greater than 220 nm, because below this value, mobile phase interference is usually observed.

Although detectors that provide spectral data on the compounds under analysis are increasingly common, as is the case with mass detectors, PDA equipment is accessible to most laboratories and has been designed for a range of laboratory applications, including detection and quantification of trace impurities, identification of compounds and development of methods [275].

Regarding to SCs analysis, Table 7 presents some works that used LC or HPLC as methodology techniques for the determination of SCs in biological samples.

Duranovic *et al.* [276] reported the isolation and purification of the synthetic cannabinoid AM-2201 from the methanolic extract of a seized product using a preparative HPLC coupled to a DAD with a scan range from 200 to 400 nm. A mixture of MeOH/water (70:30, v/v) was used as mobile phase, with a flow of 1mL/min and 40^{o}C as oven temperature. The injection volume was 10 µL and the run time 45 minutes. Given the difficulty of laboratories to access all possible reference materials needed for the unequivocal identification of the unknown compounds in seized products, the presented methodology proved to be suitable for use in most analytical laboratories.

More recently, the quantification of 5F-QUPIC (or 5F-PB-22) in the herbal extract was determined by HPLC-DAD based on total hydrolysis and measurement of the hydrolytic product (8-hydroxyquinoline) at 292 nm. Firstly, the seized plant material was analysed by GC-MS and nuclear magnetic resonance for the presence of SCs. Two SCs (5F-QUPIC and MDMB-CHMICA) were identified and determined by direct and indirect procedures using HPLC-DAD for the determination of 5F-QUPIC. The mobile phase was composed of ACN and 10 mM triethylamine – phosphate buffer, pH 5.2 (60:40 v/v) operated at a flow rate of 1 mL/min and C_{18} column was used as stationary phase. According to the authors, this combined analytical strategy can be further extended if SCs on the surface of herbal products meet the requirements for presented protocols.

In both studies, the combination of HPLC with other analytical techniques such as GC-MS and/or nuclear magnetic resonance was performed. The use of complementary techniques enables the proper identification and determination of the compounds when the reference materials are not available.

2.3.6. Nuclear Magnetic Resonance (NMR)

While SCs are relatively well studied by separation techniques such as LC or GC with MS identification, few works deal with spectral methods. The fact that many SCs are structurally similar,

effective analytical tools may be required to provide the structural information essential for their differentiation. NMR can play an important role for identification of "unidentified" peaks, which occur in LC–MS or GC–MS, enabling not only the identification but also the structural elucidation of unknown compounds [182, 183].

The fundamental concept behind NMR spectroscopy is that all nuclei are electrically charged and have multiple spins [277]. Interactions between nuclear spins and applied magnetic fields are quantised and only two orientations are allowed (aligned 'with' and aligned 'against' the applied magnetic field) (Figure 29). Application of radio frequency (RF) radiation causes 'resonance' between the lower and upper energy spins states and a signal appears in the NMR spectrum [278].

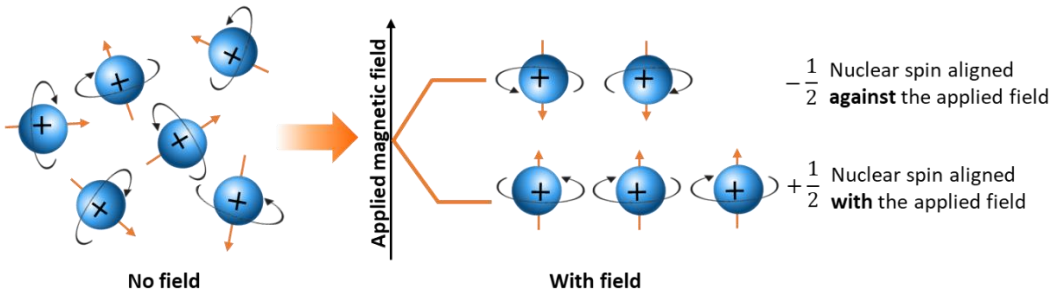

Figure 29. The different spin states of a nucleus with and without a magnetic field (adapted from [278]).

Basically, an NMR equipment consist of a superconducting magnet. This must be kept at low temperatures, so needs to be emerged in liquid helium, which is prevented from evaporating by vacuum and nitrogen jackets. The probe, containing the RF coil sits in the bottom of the magnet within its bore. The sample is always contained within the NMR tube; it is gently dropped into the probe on a cushion of air. Here the superconducting magnet causes the protons to spin and the RF coil sends RF pulses to excite them and collects the free-induction decay as they relax back to equilibrium. The pulse programs are created using the computer and sent to the console, which acts both as a RF transmitter and receiver. The signals are amplified on transmission and receipt. The FIDs are Fourier transformed (mathematically deconvoluted) to produce the NMR spectra of intensity versus chemical shift (δ) using the computer [279]. In Figure 30 is illustrated a simplified diagram of an NMR spectrometer.

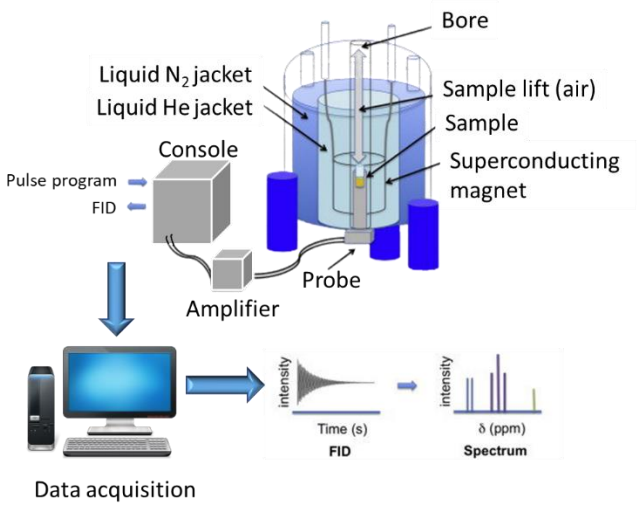

Figure 30. Simplified diagram of an NMR spectrometer (adapted from [279]).

The use of NMR spectroscopy as a method for drug analysis, has several advantages such as: rapidity, small sample volume requirement, straightforward quantitation, and the simultaneous detection of many compounds with little or no sample pre-treatment. However, the primary disadvantage is a higher detection limit than other techniques such as mass spectrometry (MS) or HPLC. So, trace amounts of compounds are usually not detected. However, this lack of sensitivity might not be important in emergency toxicology testing because only those drugs or metabolites in larger amounts are commonly associated with clinical symptoms. Besides that, NMR is a non-destructive technique which provides essential structural information that cannot easily be obtained from these other methods. Recent advances in technology have allowed the interfacing of NMR instruments with other equipment such as HPLC devices to provide even more robust analytical methodology [280, 281].

Several publications focused on the combination of separation and spectral data analysis for rapid and accurate identifications of SCs [183]. Moosmann *et al.* [282] reported the characterization of JWH-412 and the identification of 1-[(5-fluoropentyl)-1H-indol-3yl]-(4-methylnaphthalen-1-yl)methanone] as compound that was found out along with AM-2201. A flash chromatography for isolation and purification of the target compounds was used before the NMR step. Another study [283] used a combination of GC–MS, LC–MS, NMR, infrared (IF) and UV spectral data for separation and identification of two SCs JWH-018 and JWH-122, in herbal blends. Additionally, they revealed a new active ingredient which was JWH-307. Its structure was confirmed by NMR measurements. Simolka *et al.* [284] also elucidated by NMR spectroscopy and further characterized by MS and UV and IF spectroscopy, the structures of eight SCs identified in seven commercial “spice-like” products available on the German market.

The reason to use such a combination lies in the complexity of the sample. Most of the herbal samples are mixtures of SCs with other compounds and thus the separation step before the identification is necessary. The physiological activity (on the human body) of different isomers can be different. Thus, the elucidation of the SCs structure in obtained material is very important [284].

Part 2-
OBJECTIVES

1. Justification of the research

Synthetic drug availability and use have dramatically increased over the past few years, as well as their distribution, especially in Portugal. With the appearance of an average of 10 new synthetic drugs per year, the islands of Madeira and Azores have been the focus of the emergence of NPS. Curiosity, low cost, similar effects to 'traditional' drugs, are some of the motivations that have led to an increase in consumption. However, the situation is disturbing, with a significant increase in hospitalisations due to the use of these substances in Madeira.

Among the different NPS groups, SCs are the largest group with more detected substances in Europe. These specific substances are produced by suppliers with the aim of mimicking or even enhancing the effects of Δ9-THC, making each synthetic cannabinoid disposable. When a substance is, or is about to be, legally controlled, producers have already one or more substitute substances ready for sale.

Given the growing popularity of the use of cannabinoid-based drugs in recent years, the number of SCs, their chemical diversity and the speed how quickly they appear, make this group of compounds particularly challenging in terms of detection, monitoring, and response. Furthermore, since they are manufactured without any controls, it is extremely important to identify and quantify the composition of the seized samples, since the actual content of these products is unknown. Despite concerns about the toxicity associated with SCs being long established, the real danger of these drugs consume is not elucidated. Some of these compounds may be more addictive than phytocannabinoids, which could result in higher acute and long-term toxicity levels, leading to serious adverse effects.

2. Aims and objectives

The overall goal of this work was to conduct a cytotoxic and analytical analysis of SCs found in seized samples sold as herbal incenses.

In order to achieve the general objective, the following research design (figure 31) was established with specific objectives:

- Chemical characterisation of seized products by the Portuguese police, using GC-MS and NMR as complementary techniques, identifying synthetic drugs, as well as potential adulterants;
- Evaluation of the best extraction conditions of SCs from herbal samples, namely different solvents and extraction times;

- Evaluation of the best separation, resolution, and analysis time conditions by UHPLC-PDA, including selection of chromatographic column, column temperature and flow rate;
- Isolation of SCs from herbal seized samples by UHPLC-PDA;
- Development of a new analytical methodology, based on the microextraction technique µSPEed followed by UHPLC-PDA analysis, for determination of SCs in oral fluid samples;
- Development of MEPS technique followed by UHPLC-PDA analysis, for determination of SCs in oral fluid samples;
- Optimization of different experimental parameters such as the chemical nature of the sorbent material, the sample volume, the number of extraction cycles, the solvent and elution volume;
- Validation of the optimised methodologies using the principles proposed in analytical toxicology;
- Application of the µSPEed and MEPS methodologies to real samples provided from recreational drug users;
- Evaluation of the toxicity induced in lung cells (A549 cell line) using herbal products extracts applying the MTT assay;
- Assessment of oxidative stress in lung cells induced by herbal products extracts;
- Assessment of energetic disturb state in lung cells induced by herbal products extracts;
- Comparison of *in vitro* assays between the seized samples and the damiana extract.

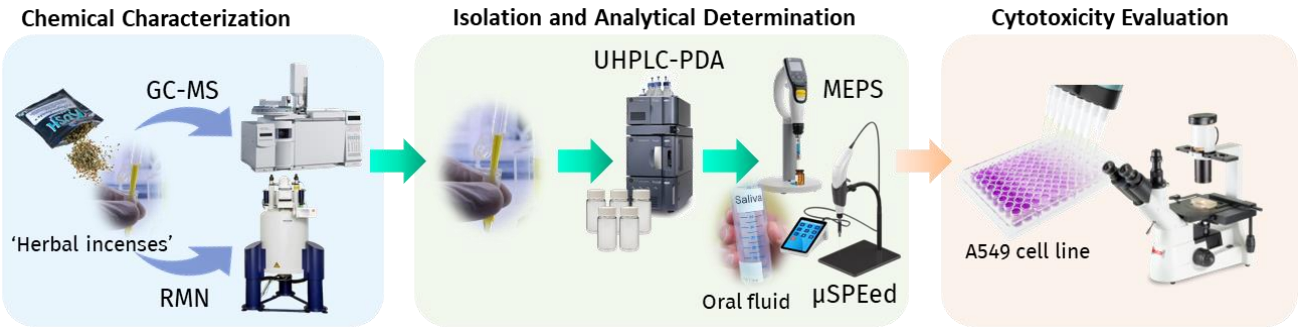

Figure 31. Research design of the thesis.

Part 3-
EXPERIMENTAL PART

CHAPTER I – Chemical Characterization Studies

1. Introduction

As previously mentioned in Part 1, SCs are usually sold in an herbal mixture, advertised as herbal incenses, as a smoking product, being the most widespread products on drug market, especially in Madeira. Moreover, according to EMCDDA several cannabis products have been adulterated with SCs and being mis-sold as Δ9-THC and CBD [59].

The speed of the emergence of SCs has resulted in several analytical challenges for clinical and forensic laboratories. As already mentioned, reference material for use in positive identifications is not readily available, and since the SCs products are frequently combined with other illicit drugs or substances can increase the difficulty in identifying them. In this sense the GC-MS method was chosen, being one of the methods recommended by the UNODC in order to analyse qualitatively such substances in this type of samples [182].

In this chapter the identification and characterization of herbal incenses suspected to contain SCs by GC-MS and NMR is described.

2. Materials and Methods

2.1. Chemicals and Reagents

All chemicals were of analytical grade. MeOH, acetone, ACN, ethanol, DCM and chloroform of HPLC gradient grade (>99% purity) were purchased from Fisher Chemicals (Loures, Portugal). Deuterated methanol (CD_3OD, 99.9%), maleic acid (MA) and trifluoroacetic acid (TFA, 99.0%) were acquired from Sigma Aldrich (Steinheim, Germany). Certified standard for the mixture of n-alkanes (C_7-C_{40}) was supplied by Labodidática (Açores, Portugal).

2.2. Herbal samples

Nineteen seized herbal products suspected to contain SCs were provided by the Forensic Science Laboratory of Portuguese Criminal Police (LPC-PJ) under special permission. In addition, 2 samples referenced with the compounds JWH-018 and XLR-11, were also provided by LPC-PJ (Figure 32). Dried damiana leaves (*Turnera aphrodisiaca*) were purchased online at chasdomundo.pt.

Figure 32. Seized material provided by LPC-PJ.

2.3. Qualitative screening by GC-MS

2.3.1. Sample preparation

For GC-MS analysis, the extraction procedure was carried out according to the method described by Uchiyama *et al.* [186] and UNODC recommended methods [81]. Two mL of MeOH was added to 50 mg of each homogenised herbal mixture. After vortexing for 1 min and sonication for 10 min in an ultrasonic bath the supernatant extract was decanted. 500 µL of the supernatant was then filtered through a 0.22 µm PTFE filter and diluted with methanol (1:1).

2.3.2. GC-MS analysis

An Agilent Technologies 6890N Network gas chromatograph equipped with 7683B autosampler connected to an Agilent 5975 quadrupole mass selective detector was used for determination of the mass spectrum of the substances (Figure 33).

Figure 33. Agilent GC-MS equipment and temperature ramp used.

The GC column was an HP 5 (5% phenyl 95% dimethylpolysiloxane) from Agilent J&W supplied by SGE (Darmstadt, Germany) (30 m × 0.32 mm i.d., 0.25 µm film thickness) with helium (Air Liquid, Portugal) as the carrier gas at a flow rate of 1.3 mL/min (column-head pressure: 12 psi). Injections were performed in split mode (40:1) and the injector port was heated to 250°C. An initial oven temperature of 80 °C was set for 4 min, ramping at 8 °C/min until it reached 300°C and held for 10 min. The total run time was 41.5 min. For the MS system, the temperature of the transfer line was set 230 ºC, electron impact mass spectra were recorded at 70 eV and the ionization current was approximately 30 µA. The acquisitions were performed in full scan mode (40-600 m/z) with an injection volume of 2 µL.

2.3.3. Identification process

All mass spectra were compared with the NIST 14 MS library and SWGDRUG MS library version 3.9. using MSD ChemStation software for data acquisition and processing.

To improve the reliability of the compounds identification in the herbal products, and in order to facilitate their subsequent identification in such samples, the chromatographic retention indices (*RI*) were determined as Kovats' indices calculated from the measurement of an *n*-alkane mixture (Equation 1).

$$RI = 100\,(n) + 100(m-n)\frac{t_{ri} - t_{rn}}{t_{rm} - t_{rn}} \qquad \textit{Equation 1}$$

Where:

i is the analyte that is being analysed; n is the carbon number of the alkane which elutes before "i"; m the number of carbons of the alkane which elutes after "i"; t_{ri} the retention time of "i"; t_{rn} the retention time of the alkane which elutes before "i" and t_{rm} is the retention time of the alkane which elutes after "i" [285].

2.4. Structural elucidation by NMR analysis

2.4.1. Sample preparation

For the acquisition of NMR spectra, approximately 50 mg of each herbal product was placed into 1 mL of CD_3OD containing 2 mg of the internal standard MA for ^{1}H NMR and ^{13}C NMR analysis and

the internal standard TFA for ^{19}F NMR. The solution was then vortexed 1 min and sonicated during 10 min and then transferred to an NMR sample tube.

2.4.2. NMR analysis

The NMR experiments were recorded on a Bruker Avance II 400 MHz spectrometer (Figure 34). Chemical shifts (δ) were expressed as parts per million (ppm) and referenced to the signal of MA (δH = 6.37, δC = 167) and coupling constants (*J*) were reported in units of Hertz (Hz). The structure's identification with the respective assignment of the proton and carbon signals was based on the analysis of NMR spectra obtained by 1D (^{1}H and ^{13}C) and 2D (COSY, HMBC and HSQC) techniques. For samples 2 and 4, a ^{19}F NMR spectrum was also recorded, and the chemical shifts were referenced to the TFA resonance at -78 ppm.

Figure 34. NMR Bruker equipment used.

For NMR purity assessment, the ^{1}H signal integration for each compound was calculated calibrating for 100 the area of MA resonance peak. In each sample, the cannabinoid amount was calculated by applying the following Equation:

$$amount\ of\ cannabinoid\ (mg) = \frac{m_{IS} \times N_{IS} \times I_X \times FW_X}{I_{IS} \times FW_{IS} \times N_X} \qquad \textit{Equation 2}$$

where m_{IS} and m_X are the mass of internal standard (*IS*) and the compound of interest (*X*), I the integrated area, N the numbers of protons represented by the selected signal for integration and FW the molecular weight (in g.mol^{-1}). The calculated mass of cannabinoid is

divided by the amount of sample (in grams) initially weighed to express the concentration in mg of compound per gram of sample herb.

2.4.3. Identification process

NMR data was processed using the Bruker TopSpin 3.6.1 software. The structural identification with respective assignments of the proton and carbon signals was based on the analysis of NMR spectra obtained by 1D (^{1}H, ^{13}C, ^{19}F) and 2D (including the COSY, HMBC and HSQC experiments) techniques.

In Figure 35 is illustrated the procedure used for the chemical characterization of the herbal products.

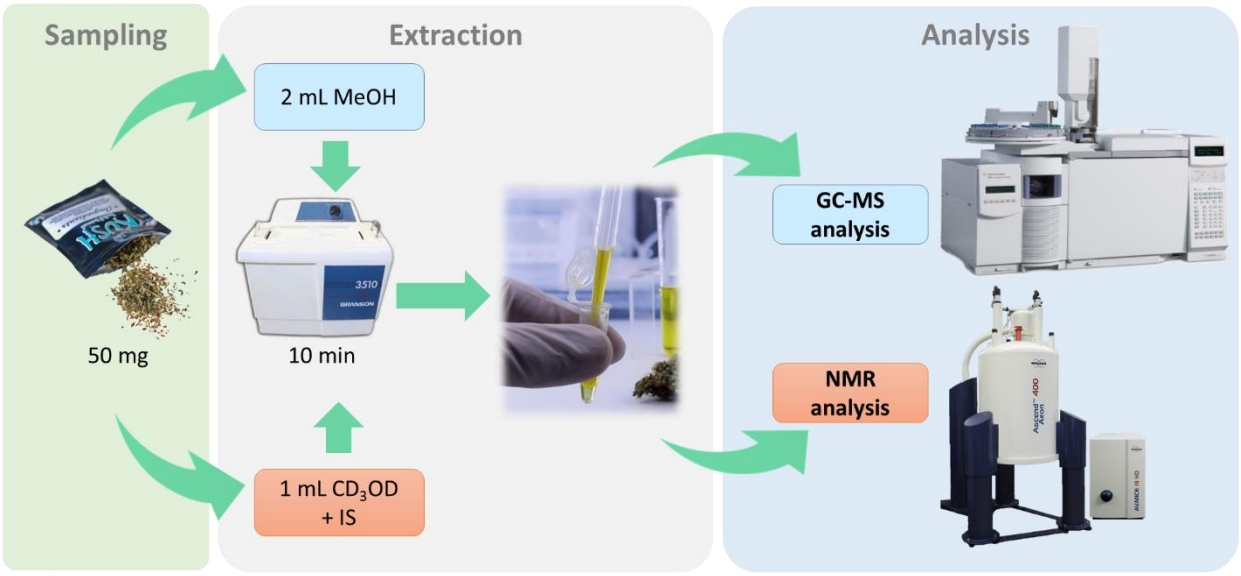

Figure 35. Schematic representation of the procedure used in the chemical characterization of seized herbal products.

2.5. Synthetic cannabinoid extraction studies

2.5.1. Extraction solvent and extraction time

Five different solvents, namely, chloroform, MeOH, ethanol, acetone, DCM were tested for their ability to extract SCs from seized herbal products and different extraction times (1, 5, 10 and 15 min) were analysed. All extraction studies were performed with 50 mg of sample B54 sonicated with 2 mL of solvent. The extract was filtered through a 0.22 µm PTFE filter and analysed in triplicate by GC-MS.

3. Results and Discussion

3.1. Screening of synthetic cannabinoids in “herbal incenses” and Chemical characterization

In this study, a total of nineteen seized herbal products were provided by LPC-PJ. The samples were in the form of greenish plant material composed of frayed leaves and branches (Figure 36).

Figure 36. Content of one of the samples analysed in this study.

Seventeen of them were presented in brightly coloured metal-foil packages under different brand names with the indication ‘not for human consumption’ or ‘do not eat’, they were produced in European Union and two of the samples were presented in a plastic bag without any information. Regarding the composition indicated on the packaging, different plant mixtures are described in several samples, highlighting the damiana plant that is described in 8 of them. In order to investigate potential herbal interferences, damiana leaves were purchased online (Figure 37) and processed using the same sample preparation methods.

Table 9 describes the different seized herbal products analysed in this study, as well as the code names assigned to each sample.

Table 9. Herbal products analysed in this study.

Sample code	Product name	Description/ appearance	Quantity indicated on the label (g)	Ingredients indicated on the label
H1	Caramba	Herbal incense	1	Damiana*; Canavalia maritima; Nymphaea caerulea; Nelumbo nucifera; Leonurus sibiricus*
H2	MAÚI	Herbal incense	0.4	*Canavalia maritima; Althaea officinalis; Leonurus cardiaca; Pedicularis canadensis; Rosa damascena; Leonotis Leonurus*
H3	Mandala	Herbal incense	1	Damiana*; Canavalia maritima; Leonotis Leonurus; Nelumbo nucifera; Zornia latifolia*
H4	Maya 2012	Herbal incense	1	*Leonorus cardiaca; Tussilago;* Damiana*; Althaea officinalis;* Coconut leaf
H5	Esfinge	Herbal incense	1	Damiana*; Leonotis Leonurus*
H6	Atomic Bomb (strawberry)	Incense	1.5	Vanilla*;* Indian warrior (*Pedicularis densiflora);* Maconha brava *(Zornia latifolia);* Marshmallow *(Althaea officinalis);* Blueberry *(Vaccinium corymbosum);* Strawberry *(Fragaria);* Wild cherry *(Prunus avium);* Damiana *(Turnera aphrodisiaca)*
H7	Atomic Bomb (blueberry)	Incense	0.4	Vanilla*;* Indian warrior (*Pedicularis densiflora);* Maconha brava *(Zornia latifolia);* Marshmallow *(Althaea officinalis);* Blueberry *(Vaccinium corymbosum);* Strawberry *(Fragaria);* Wild cherry *(Prunus avium);* Damiana *(Turnera aphrodisiaca)*
H8	Radioactive (strawberry)	Incense	3	Vanilla*;* Indian warrior (*Pedicularis densiflora);* Maconha brava *(Zornia latifolia);* Marshmallow *(Althaea officinalis);* Blueberry *(Vaccinium corymbosum);* Strawberry *(Fragaria);* Wild cherry *(Prunus avium);* Damiana *(Turnera aphrodisiaca)*
H9	Radioactive (blueberry)	Incense	0.4	Vanilla*;* Indian warrior (*Pedicularis densiflora);* Maconha brava *(Zornia latifolia);* Marshmallow *(Althaea officinalis);* Blueberry *(Vaccinium corymbosum);* Strawberry *(Fragaria);* Wild cherry *(Prunus avium);* Damiana *(Turnera aphrodisiaca)*
C54	Troll – colletors product	-	-	Dried leaves and flowers mixed with aroma extracts
C56	Reggae Love – Collectors product	-	-	Dried leaves and flowers mixed with aroma extracts
C58	Shaman Pipe	Incense	-	Incense composed of natural aromatic herbs and essential oils
C60	Pulse ultra – novelty	Incense	1.5	Incense composed of natural aromatic herbs and essential oils

	collector's item			
C61	Pulse ultra – novelty collector's item	Incense	0.4	Incense composed of natural aromatic herbs and essential oils
C66	Ice Bud – Super cold	Incense	1.5	Incense composed of natural aromatic herbs and essential oils
B23	Pacman	Solid incense	3	Puncture vine resin; *Centella asiatica*; *Leonurus sibiricus*; Scutellaria; Licortice; aromatizers
B43	Rainbow	Incense	0.4	Incense composed of natural aromatic herbs and essential oils
B54	No commercial name	Herbal mixture	-	-
B63	No commercial name	Herbal mixture	-	-

Figure 37. Purchased damiana leaves.

According to EMCDDA, damiana (genus *Turnera*) and Lamiaceae herbs such as Melissa, Mentha and Thymus are commonly used as the plant base for the smoking mixtures [34]. In fact, Ogata *et al.* [286] investigated the origins of botanical materials in 62 herbal products distributed on the illegal drug market in Japan, by DNA sequence analyses and BLAST searches, being these two types of plants the most frequently detected among analysed products.

The labels of these herbal products usually indicate common plant names to create the illusion that the content is natural, but several psychoactive plants are also added to enhance the effects [286]. However, there is no precise information on their contents, and generally, no information about SCs is indicated.

Since the products labelled as "herbal incenses" are suspected to contain SCs, we started this work by studying the chemical profiling of different seized products.

3.1.1. GC-MS analysis

GC-MS technique was firstly chosen to separate and identify the various compounds present in the "herbal incenses" samples. The methanolic solutions of the herbal products were analysed using the conditions described in the experimental section and the different chromatographic profiles, as well as the EI mass spectra of the identified compounds are presented in Supplementary Material (Figure S1 and S2). All peaks were considered for the products characterization. Through comparison of the mass spectra information was achieved for each chromatographic peak (e.g. base peak, molecular ion) with the spectra databases NIST14 and SWGDRUG, the literature and by analysing their fragmentation pattern, the initial analysis revealed the presence of 10 SCs, as well as other substances (Table 10). Additionally, RI were determined to increase the accuracy of the identification of the compounds in the herbal products (Table 11). A n-alkane (C_7-C_{40}) mixture was injected into GC-MS system under the same conditions used for the seized samples. RI values were then compared with those reported in the literature [287, 288].

Table 10. Preliminary GC-MS identification of compounds present in 19 herbal products.

	Compounds										
Samples	JWH-018	JWH-073	JWH-122	JWH-210	MAM-2201	APINACA	XLR-11	UR-144	CP47, 497, C8	3-epi CP47, 497, C8	Others
H1	x		x	x							**1**
H2	x		x	x	x						**2, 3**
H3	x		x								**2, 3**
H4						x	x				**2**
H5			x	x							**2**
H6	x	x									**2**
H7	x	x									**2**
H8	x	x							x	x	
H9	x	x							x	x	
C54					x		x				
C56							x				**2**
C58					x		x				
C60	x	x							x	x	
C61	x	x							x	x	**2**
C66	x	x							x	x	
B23	x										**2**
B43	x	x	x								**2**
B54						x		x			
B63	x		x	x							**2**

1 vitamin E acetate

2 oleamide

3 vitamin E

The EI mass spectra of the compounds were consistent with the fragmentation pattern of SCs (Figure S2). As a matter of fact, their molecular ion is not only present in the MS, as it is, in most of the cases, the base peak [250]. The primary analysis of the SCs detected by GC-MS is shown in Table 11.

Table 11. GC-MS results of initial analysis.

Compound	Molecular Formula	No. of detections	Rt (min)	Base Peak (m/z)	Characteristic Ions (m/z)	RI
UR-144	$C_{21}H_{29}NO$	1	25.098	214	311 [M^+], 296, 214, 144	2529
XLR-11	$C_{21}H_{28}FNO$	4	26.468	232	329 [M^+], 314, 232, 144	2674
3-epi CP 47, 497-C8	$C_{22}H_{36}O_2$	5	27.063	233	332 [M^+], 233, 215, 161, 81	2741
CP 47, 497-C8	$C_{22}H_{36}O_2$	5	27.202	215	332 [M^+], 233, 215, 161, 81	2756
JWH-073	$C_{23}H_{21}NO$	8	30.973	327 [M^+]	310, 284, 200, 127	3216
APINACA	$C_{23}H_{31}N_3O$	2	31.112	215	365 [M^+], 337, 294, 215, 145	3234
JWH-018	$C_{24}H_{23}NO$	13	31.488	341 [M^+]	284, 214, 127	3284
JWH-122	$C_{25}H_{25}NO$	6	32.748	355 [M^+]	338, 298, 214, 144	3434
JWH-210	$C_{26}H_{27}NO$	4	33.390	369 [M^+]	352, 312, 214, 144	3502
MAM-2201	$C_{25}H_{24}FNO$	3	33.912	373 [M^+]	298, 232, 144, 115	3549

According to the results, it was observed that the majority of the SCs detected by GC-MS analysis contain naphthalene, indole or indazole rings as part of their structure.

Among the identified compounds, JWH-018 was detected in 13 samples. As described in Part 1 - Chapter I, this compound was one of the 'JWH-series' synthesized by John W. Huffman, while studying cannabinoid receptor pharmacology, being discarded due to the existent undesirable psychoactive properties and, thus, has not been approved for human use. However, in 2008, it was reported as one of the active components in an herbal product named 'spice', which has been sold as incense in several countries around the world [142]. JWH-018 belongs to the naphthoylindole family and four other compounds identified in the different herbal products also belong to the same family, namely JWH-073, JWH-122, JWH-210 and MAM-2201.

As they belong to the same chemical class, it should be expected that its structure, as well as their spectrometric behaviour, would be similar. In fact, these 5 compounds besides belonging to the same family, only differ in the 'tail' or in the 'ring' parts. All contain an indole and a naphthalene substructure unit and the only difference between JWH-018 and JWH-073 is that JWH-018 contains a pentyl alkyl chain, whereas JWH-073 contains a butyl alkyl chain [289, 290].

JWH-122 and JWH-210 compounds are structurally closely related to JWH-018, with the difference of a methyl and an ethyl substitution in the para-position, respectively. MAM-2201 has a similar structure to JWH-122 but with a fluorine atom at the end of the chain. Despite the similarity of the fragmentation patterns between these naphthoylindoles, they present slight differences in retention times. On the other hand, the appearance of a distinct molecular peak is very useful for differentiating compounds with similar structures except for regioisomers [291].

The EI mass spectra of these 5 SCs show that the most abundant peak is the molecular ion. This fact was a starting point for the identification of the compounds, providing additional details of each of them, when compared with the fragmentation pattern.

In Figure 38 a proposed fragmentation route of naphthoylindoles under EI conditions is presented, and Table 12 describes the major fragment ions of 5 the naphthoylindoles identified in this study.

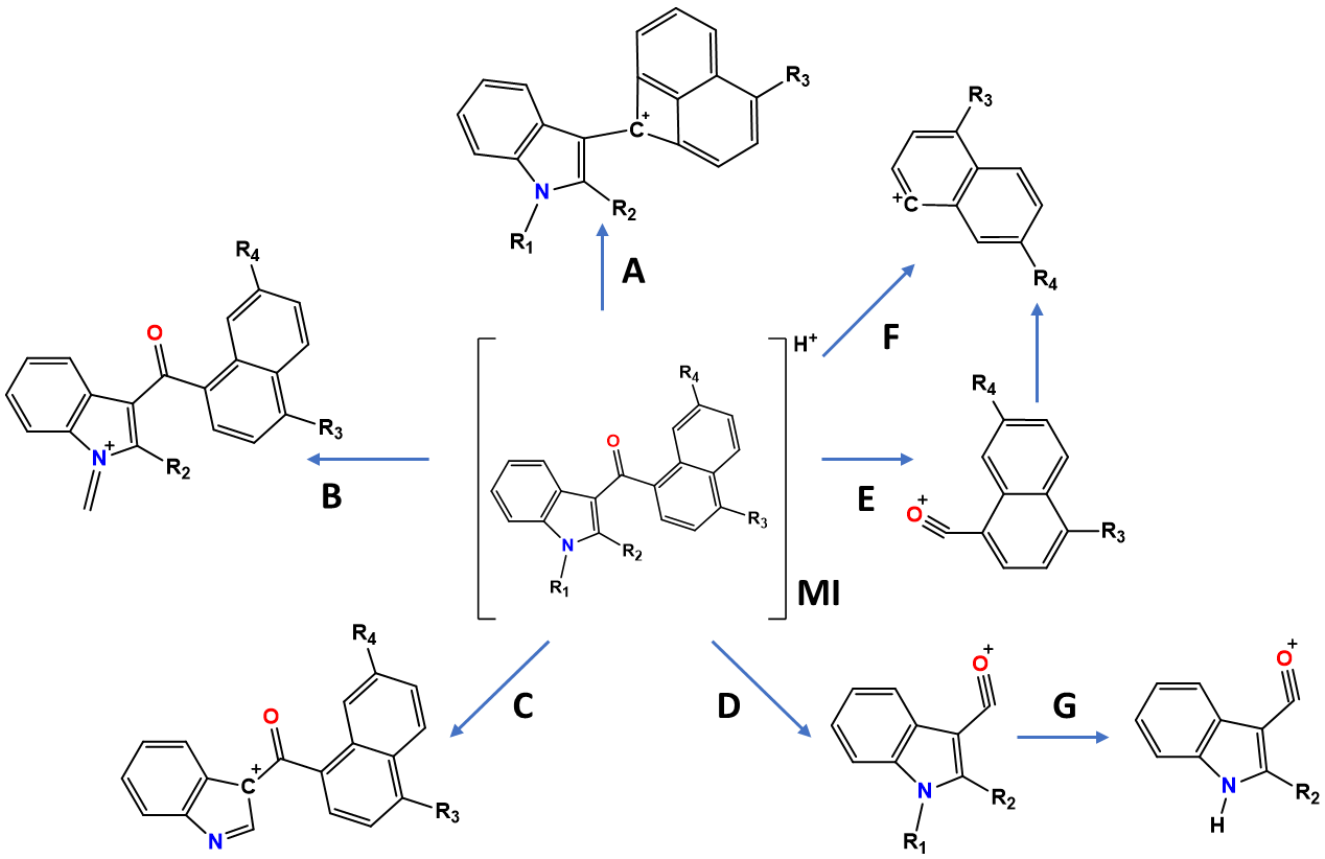

Figure 38. Proposed fragmentation pattern of naphthoylindoles under EI conditions with major fragment ions (A-G), MI – molecular ion (adapted from [292, 293]).

Table 12. Major fragment ions of JWH-018, JWH-073, JWH-122, JWH-210 and MAM-2201 in the EI-MS (adapted from [289, 292]).

Fragment	JWH-018	JWH-073	JWH-122	JWH-210	MAM-2201
MI	341	327	355	369	373
A	324	310	338	352	356
B	284	284	298	312	298
C	270	270	284	298	284
D	214	200	214	214	232
E	155	155	169	183	169
F	127	127	141	155	141
G	144	144	144	144	144

The main primary fragmentations of these compounds occur in the indole group with the loss of the pentyl substitution in the nitrogen atom (R_1), the loss of the naphthalene group with transfer of charge to the carbonyl oxygen atom or even the loss of the carbonyl group [293].

The carbonyl group fragment ions (fragment A) are typically observed, due to the α-cleavage of the alkylamino group of the indole, resulting in a loss of 17 Da [M-17]+, which is certainly observed in naphthoylindole compounds [250].

The SCs JWH-018 and JWH-073 present a similar EI mass spectra. The fragment ions at m/z 284, 270, 155, 144 and 127 are the major ions (except the molecular ion) in common with these two compounds. In Xing *et al.*[289] work, the fragmentation pathways of JWH-018 and JWH-073 were studied, and the full scan spectrum of both compounds showed similar results with the present study. The main ion peak m/z 341 was reported as the molecular ion of JWH-018 and the presence of fragment ions at m/z 310 and 200 in JWH-073 is due to having one less methylene. According to the authors, the m/z 327 ion in JWH-073 fragmentation pathway could lead to the m/z 310 ion through an isomerization and dehydroxylation process.

The m/z 270 and 284 fragments are present in all 5 naphthoylindoles identified in this study with different intensities. The fragment ion m/z 270 represents the loss of the entire side chain (R_1) from the molecular radical ion while the m/z 284 is the iminium cation resulting from the loss of the C_4H_7 radical (57 Da) from the molecular ion [293]. m/z 155, 127 and 214 fragment ions are also common in indole-derived SCs [294]. Comparing with our results, m/z 127 is one of the major ions in JWH-018 and JWH-073 and m/z 214 one of the major ions in JWH-018, JWH-122 and JWH-210. The presence of these ions confirms the acyl substituent on the indole ring as the naphthoyl moiety [293].

Other relatively low mass ions m/z 144, 186 and 214 were seen in EI mass spectra. These ions represent indole containing fragments following the loss of the acyl moiety from the molecular ion. m/z 214 represents the loss of 127 Da ($C_{10}H_7$, naphthyl group) from the molecular radical ion due to the cleavage of the bond between the carbonyl carbon and the naphthyl group [293]. The m/z 144 ion is an interesting fragment which results from a secondary fragmentation and is present in all 5 naphthoylindoles (see Table 12). This ion is formed by an hydrogen rearrangement product of the fragment D resultant from the elimination of a C_5H_{10} alkene or its structural equivalent and does not come directly from the molecular radical ion [295]. Therefore, it is suggested that fragment G could suffer a tertiary fragmentation, losing the carbonyl group and leading to a fragment with an m/z 116 ($C_8H_6N^+$) [296, 297]. This smaller fragment is difficult to observe in EI mass spectra, due to the presence of m/z 115 ion with higher intensity.

MAM-2201 compound was identified in H2, C54 and C58 samples. In H2 sample, this compound was presented in highest abundance when compared to the other SCs also detected in this sample. This naphthoylindole is considered the fluorine derivative of JWH-122. The fragmentation pattern is very similar between the two compounds, and the presence of the base peak as molecular ion (m/z 373) indicates the probable replacement of fluorine in JWH-122, due to the difference of 18 Da in relation to the molecular ion of JWH-122 (m/z 355). Besides that, the presence of a peak at m/z 115, confirms the methyl substitution in MAM-2201 ($C_9H_{12}^+$).

Another interesting compound identified in this work is APINACA (or AKB-48). This synthetic compound was identified in samples H4 and B54. APINACA was first identified by Japanese laboratories in March 2012 as an ingredient in synthetic cannabis smoking blends, along with a related compound APICA [187]. This compound belongs to the adamantoylindazole family and are structurally different from naphthoylindoles with an adamantyl group linked to an indazole [298]. Regarding to the EI mass spectra, several fragment ions were observed, which were very diagnostic for characterizing the molecule. The presence of the intense fragments at m/z 337, 294, 215, 145 and 135, as well as the molecular ion peak (m/z 365), allowed us to assume that the analysed molecule is APINACA (Figure 39). An interesting fact, unlike naphthoylindoles, the base peak is not the molecular ion. The predominant fragment ion at m/z 215 is a result from the cleavage of the carbonyl-adamantane bond producing the N-pentylindazole acylium ion ($C_{13}H_{15}N_2O^+$) [299, 300]. This peak is characteristic of an indazole group and can be derived from the characteristic peak m/z 214 ($C_{14}H_{16}NO^+$) of an indole group, since the difference between these two groups is the addition of a nitrogen atom and the loss of a carbon and hydrogen atoms.

Further loss of the pentyl side chain resulted in indazole acylium ion at m/z 145 ($C_8H_5N_2O^+$), which is also characteristic of an indazole moiety [299].

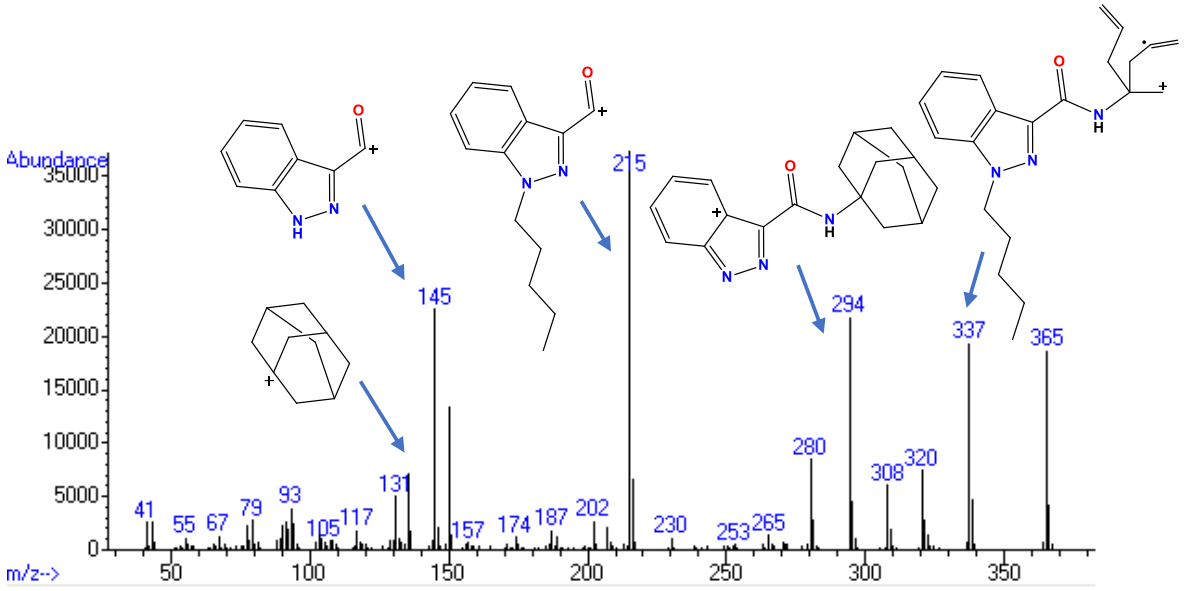

Figure 39. EI-MS spectra of APINACA compound with major fragment ions represented.

In samples H4 and B54 two other compounds were identified, XLR-11 and UR-144, respectively. XLR-11 was also identified in samples C54, C56 and C58, being the only synthetic cannabinoid in C56 sample. Like APINACA, these two compounds were first reported to the EMCDDA in 2012, being detected in herbal incenses and spread very quickly all over the world [104, 301]. UR-144 was among the most popular SCs in the past year, found in herbal blends, resinous samples (with macroscopic appearance similar to that of hashish), and powders [301].

Both XLR-11 and UR-144 compounds contain a tetramethyl cyclopropyl group in their structure, being XLR-11 the UR-144 analogue with a fluoride group at the end of pentyl chain [302]. In contrast to the previously analysed naphthoylindoles, the base peaks of XLR-11 and UR-144 do not correspond to their molecular ion. The fluor substitution on the aliphatic chain of XLR-11 compound increases all the correspondent peaks in 18Da. Therefore, m/z 232 fragment ion ($C_{14}H_{15}FNO^+$) is the base peak and results from the α-cleavage of the molecular ion m/z 329 ($C_{21}H_{28}FNO^+$) where fluor is present, whereas in UR-144 compound, the characteristic fragment of a pentyl-substituted indole with the charge on the oxygen atom of the carbonyl group at m/z 214 ($C_{14}H_{16}NO^+$) is the base peak [303]. Figure 40 illustrates the comparison of XLR-11 and UR-144 fragments.

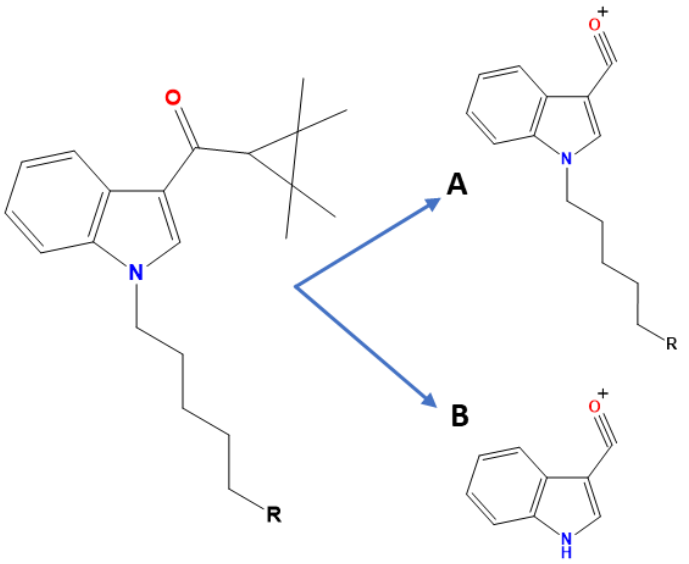

UR-144 (MW = 311)	
R = CH_3	
A	214
B	144
XLR-11 (MW = 329)	
R = CH_2F	
A	232
B	144

Figure 40. Comparison of UR-144 and XLR-11 fragments (MW – molecular weight) (adapted from [303]).

According to GC-MS results, a less intense peak is observed just after the peaks of XLR-11 and UR-144 compounds. These peaks were identified as XLR-11 and UR-144 cyclopropyl rearrangement products (peaks 9 and 15 respectively in Figure S1). Also called as XLR-11 or UR-144 degradants, these molecules are common impurities observed during GC-MS analysis that results from the cleavage of the cyclopropyl ring structure into a pyrolyzed compound [304, 305]. The rearrangement products are artifacts induced by the high temperatures of the GC injection port [303]. However, during the smoking process (burning and heat), both XLR-11 or UR-144 compounds undergoes thermal degradation leading to a thermodynamic product where the cyclopropyl ring is thermally opened [304-306].

The fact that the cyclopropane fraction is thermally unstable produces a characteristic GC-MS behaviour. The molecular ions are the same as parent compounds, however the presence of an abundant fragment 15Da, greater than the base peak in both compounds, m/z 247 ($C_{15}H_{18}FNO^+$) in XLR-11 degradant and m/z 229 ($C_{15}H_{19}NO^+$) in UR-144 degradant product, can explain the rearrangement on the cyclopropyl, followed by cleavage [303, 307].

The EI-MS of the XLR-11 and UR-144 cyclopropyl rearrangement products are shown below (Figure 41).

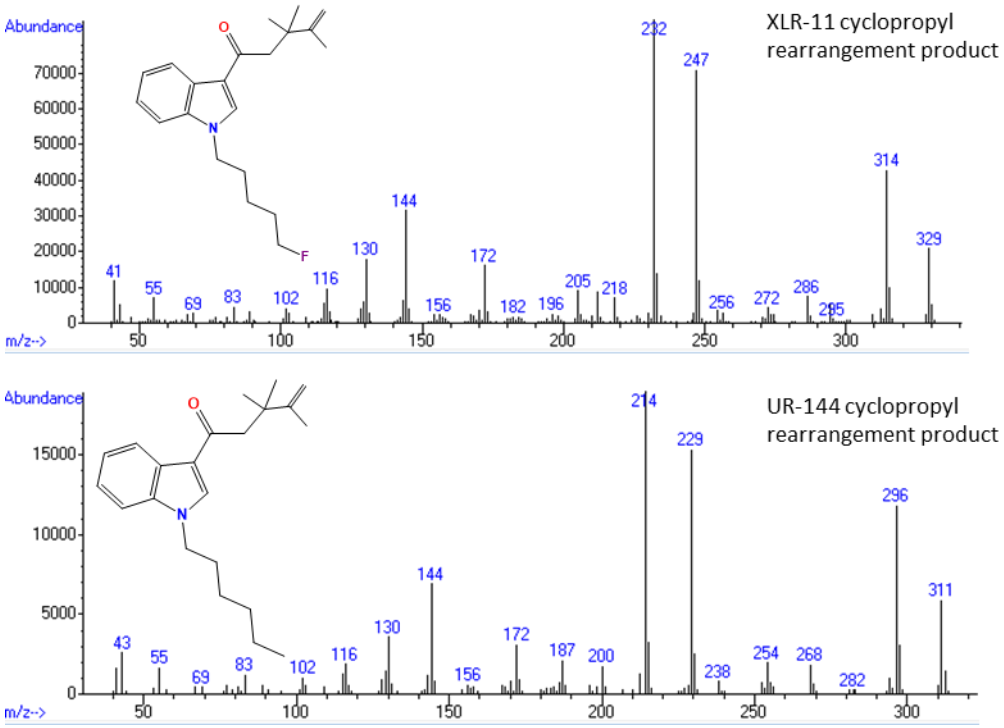

Figure 41. EI-MS of XLR-11 and UR-144 cyclopropyl rearrangement products.

In samples H8, H9, C60, C61 and C66 two small peaks were observed in the ion chromatogram at 27.063 and 27.202 min. According to the MS libraries, these two peaks correspond to 3-epi CP47,497-C8 homolog and CP47,497-C8 homolog, respectively. CP47,497-C8 or cannabicyclohexanol is a variant of CP47,497 with an extension of the dimethylheptyl sidechain to a dimethyloctyl [308]. CP47,497 and their n-alkyl homologues belong to the cyclohexylphenol (CP) series and were developed by Pfizer in the 1970s [80]. In the scientific literature these chemical classes are referred as 'non-classical' cannabinoids, since CP compounds are more similar to the structure of Δ9-THC with regard to the alkyl chain attached to the central phenol moiety of the compound [10].

Cannabicyclohexanol has four enantiomers, being the 3-epi CP47,497-C8 one of them. By analogy with other related cannabinoid compounds, it can be expected that all isomers have widely varying affinity for cannabinoid receptors, and consequently will show considerable variation in potency. According to Uchiyama *et al.* [309], the (-)-cis enantiomer, discovered in the original Pfizer research, is expected to be the most potent; however all four enantiomers have been isolated from illicit samples and the properties of the other three enantiomers have not been studied in detail. Functionally, CP47,497-C8 is a bicyclic cannabinoid analog that avidly binds the CB_2 receptor and is ten-fold more potent than Δ9-THC, while 3-epi CP47,497-C8 is a by-product generated in the synthesis of CP47,497-C8 [310].

Regarding the EI mass spectra, since these two compounds are isomers, the fragmentation pattern is useful for interpreting the elemental composition but do not differentiate isomers. Despite the identification by MS libraries, it is not possible to confirm the exact molecule for each peak detected in the GC-MS chromatogram. The only difference that was observed was the base peak, in the CP47,497-C8 m/z 215 was main ion and for the enantiomer the fragment m/z 233 presented the highest abundance.

Currently, a large variety of 'herbal incenses' with many different brands is available. In many of these brands, the same product was found to vary, not only in the amount, but also in the type of added SCs, as well as, the presence of synthetic additives and/or adulterants, which may represent a great challenge for the analytical laboratories in the identification of the substances [60, 65]. In the present study, oleamide, vitamin E and vitamin E acetate were identified, despite the low abundance. According to the United Nations Office on Drugs and Crime (UNODC) [81], adulterants such as tocopherols or oleamide are frequently added to herbal products. It was possible to identify oleamide in 10 of the analysed samples. This compound is an endogenous sleep-inducing cannabinoid and exhibits cannabis-like behavioural responses when ingested and may have been added to modify the psychotropic effects [81, 186]. In Figure 42 the EI-MS, as well as the molecular structure of oleamide is presented.

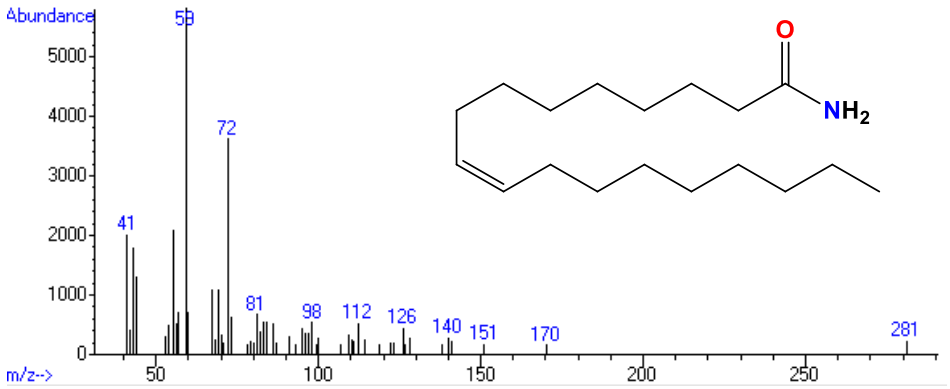

Figure 42. EI-MS of oleamide.

Vitamin E was detected in samples H2 and H3, while in sample H1, vitamin E acetate was the identified compound. These results were confirmed by comparing the EI mass spectra from the MS libraries with standard solutions analysed under the same conditions by GC-MS. Vitamin E is often added to these products as a masking agent with the intention to difficult forensic chemical detection of the compounds [10].

Vitamin E acetate is a synthetic form of vitamin E (Figure 43) and after extensive research, no study has been found to date reporting the detection of this compound in herbal incense products. However, very recently vitamin E acetate was found as a diluent in the cannabinoid containing fluids for vaporizer cartridges (e-cigarette) [311]. According to the authors, there was a sudden increase in reported cases of severe lung injury associated with vaping and, based on the analysis of 38 samples, a strong association of vitamin E acetate with reported lung injury was found. Despite these interesting findings, the present study could be the first work to report the detection and identification of vitamin E acetate in a seized herbal product.

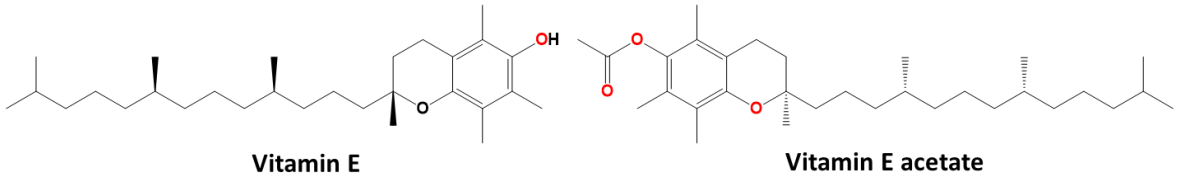

Figure 43. Molecular structures of vitamin E and vitamin E acetate.

Regarding the 2 samples referenced with the compounds JWH-018 and XLR-11 provided by LPC-PJ, the methanolic extracts (1 mg/ml) were injected into the GC-MS system and analysed.

According to chromatographic profiles (Figure 44), one peak is present in one of the samples and was identified as JWH-018, whereas in the other sample two peaks (one clearly in higher abundance) are present, being identified as XLR-11 and XLR-11 cyclopropyl rearrangement product when compared the EI-MS with the databases.

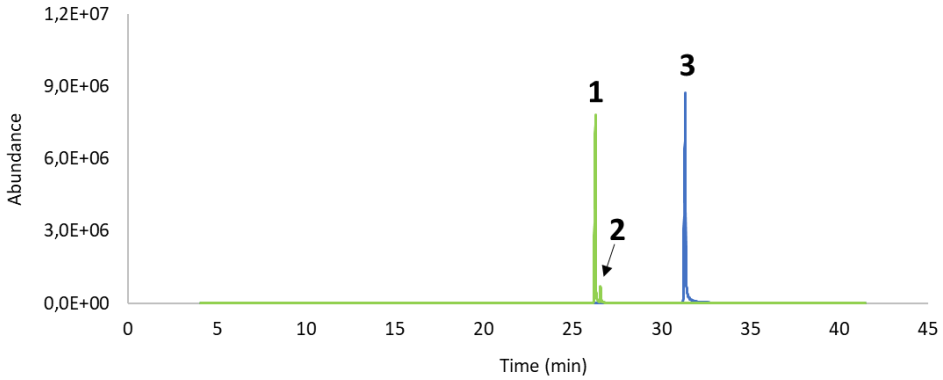

Figure 44. Overlay of the chromatograms obtained for the two reference samples (1 – XLR-11, 2 – XLR-11 degradant product and 3 – JWH-018).

This analysis allowed us to confirm the presence of these two compounds in the seized samples.

Regarding damiana sample, the obtained chromatogram of the extract is relatively free of interfering peaks when compared to RT of the identified synthetic compounds (Figure 45). Several chemical classes, such as flavonoids, terpenoids, saccharides, phenolics, among others were

identified. Interestingly, a small peak at 16.20 min was identified as oplopanone by the databases and is also present in samples H5-H8, B43, B63, C60, C61 and C66. Oplopanone is one of the abundant compounds that can be found in Damiana plant [312]. The presence of this compound in some of the samples may indicate that the damiana plant may have been used as the base herb for the mixture. However additional studies should be performed in order to conclude this finding.

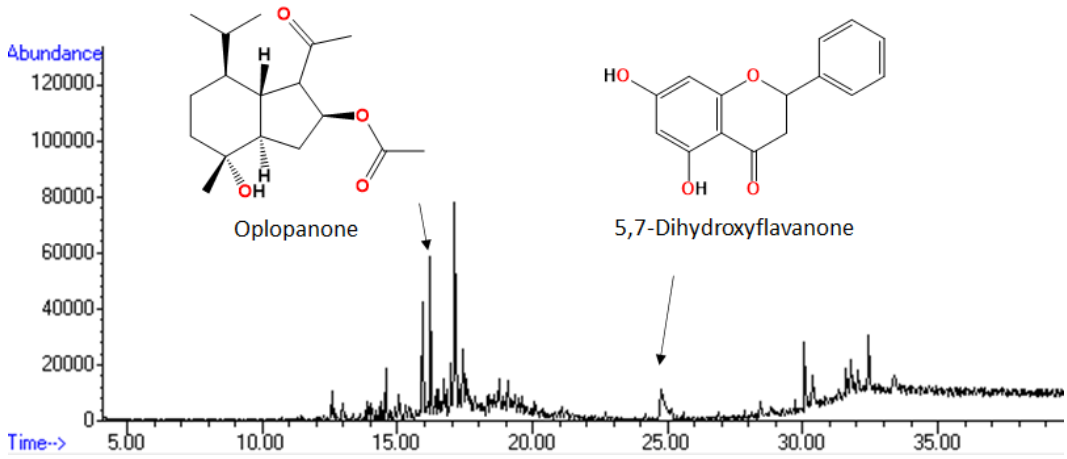

Figure 45. Chromatographic profile of damiana extract, highlighting two of the identified compounds.

3.1.2. NMR analysis

After the preliminary identification of the 19 seized 'herbal incenses' by GC-MS analysis, the samples were subjected to NMR analysis to confirm the GC-MS results and in some cases, search for possible structural isomerism.

Complete signals assignments are reported in Tables 13 and 14, being based on chemical shifts (δ, ppm) of ^{1}H and ^{13}C, on the multiplicity patterns of proton resonances depicted by the *J* couplings (Hz), and on the analysis of NMR spectra obtained by 2D (including the COSY, HMBC and HSQC experiments) techniques. For samples identified with fluorinated compounds (H2, H4, B54, C54, C56, and C58), a ^{19}F NMR spectrum was also recorded, and the respective signal assignment is presented in Table 14. The ^{1}H and ^{13}C NMR spectra of the seized herbal products are shown in Figures S3-S6 (see Supplementary Material I).

The extraction procedure was performed according to Naqi *et al* [313], Amato *et al.* [314] and Fowler *et al.* [315], using CD_3OD as extraction solvent and MA as internal standard for semi-quantitative reference. The chemical shifts were referenced to the signal of MA at 6.37 and 167 ppm for proton

and carbon NMR respectively, and two signals at 3.37 and 4.96 ppm detected in ^{1}H NMR are characteristic of solvent.

According to the results, eight SCs were found in the nineteen analysed samples by NMR, namely JWH-018, JWH-073, JWH-122, JWH-210, MAM-2201, APINACA, UR-144 and XLR-11. As seen in the MS analysis, JWH-018 was present in 13 of the samples. In samples H8, H9, C60, C61 and C66, JWH-018 and JWH-073 were the only SCs identified by NMR. Cannabicyclohexanol and its enantiomer were not identified by NMR methodology, probably due to their low concentrations in the sample and the presence of two other SCs with higher concentrations can mask the identification of the minor compounds.

The ^{1}H NMR spectrum of samples H6-H9 and C60, C61 and C66 were very similar, being in accordance with the results obtained by GC-MS. Since JWH-018 only differ structurally from JWH-073 by the presence of one more methylene group in the alkyl chain, two triplets were observed at 0.89 ppm (3 H from H-5''' in JWH-018) and 0.94 ppm (3H from H-4''' in JWH-073). These characteristic signals of each compound were considered for quantification since the rest of the spectrum is the same for both compounds. The obtained results are in agreement with those reported by Marino *et al.*[316] and Assemat *et al.* [317].

Table 13. NMR assignments of 'JWH' synthetic compounds identified in the herbal incenses analysed in this study.

Position	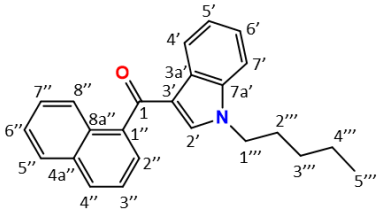				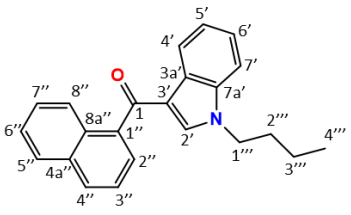				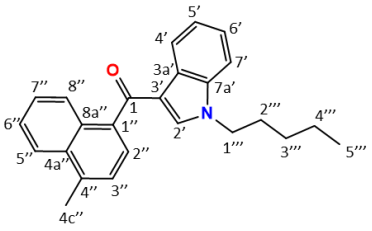				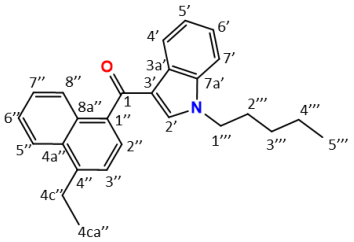			
	JWH-018				**JWH-073**				**JWH-122**				**JWH-210**			
	^{13}C (δ/ppm)	^{1}H δ (ppm)	^{1}H M[a]	^{1}H *J* (Hz)	^{13}C (δ/ppm)	^{1}H δ (ppm)	^{1}H M[a]	^{1}H *J* (Hz)	^{13}C (δ/ppm)	^{1}H δ (ppm)	^{1}H M[a]	^{1}H *J* (Hz)	^{13}C (δ/ppm)	^{1}H δ (ppm)	^{1}H M[a]	^{1}H *J* (Hz)
1	192.7	-	-	-	194.7	-	-	-	192.7	-	-	-	192.9	-	-	-
2'	138.6	7.44	s	-	141.0	7.44	s	-	138.6	7.42	s	-	138.8	7.44	brs	-
3'	116.1	-	-	-	118.2	-	-	-	116.1	-	-	-	116.1	-	-	-
3a'	126.0	-	-	-	128.2	-	-	-	126.0	-	-	-	126.0	-	-	-
4'	121.1	8.41-8.39	m	-	123.4	8.41	d	7.52	121.1	8.41-8.39	m	-	121.2	8.41	d	7.12
5'	121.6	7.38-7.36	m	-	123.9	7.41-7.37	m	-	121.6	7.38-7.36	m	-	121.7	7.38-7.36	m	-
6'	122.6	7.38-7.36	m	-	124.8	7.41-7.37	m	-	122.6	7.38-7.36	m	-	122.6	7.38-7.36	m	-
7'	109.4	7.42-7.39	m	-	111.7	7.42-7.40	m	-	109.4	7.42-7.39	m	-	1095	7.42-7.42	m	-
7a'	136.5	-	-	-	140.2	-	-	-	135.8	-	-	-	1364	-	-	-
1''	135.8	-	-	-	138.7	-	-	-	136.5	-	-	-	136.5	-	-	-
2''	124.2	7.64	dd	11.84, 4.38	126.5	7.69	dd	6.96, 1.88	122.9	7.64	dd	11.84, 4.38	122.9	7.64	brd	6.36
3''	123.2	7.40	brd	1.68	125.8	7.66	brd	7.88	122.6	7.40	brd	1.68	122.7	7.40	brd	1.68
4''	129.9	-	-	-	131.2	8.09	dd	7.76, 2.16	141.9	-	-	-	141.9	-	-	-
4a''	131.9	-	-	-	135.3	-	-	-	131.9	-	-	-	131.1	-	-	-
5''	124.6	8.13	d	8.44	126.9	8.03	d	7.92	123.2	8.13	d	8.44	122.9	8.14	d	8.48
6''	124.7	7.56-7.54	m	-	127.8	7.61	td	7.18	124.7	7.56-7.54	m	-	124.8	7.60	m	-
7''	125.2	7.56-7.54	m	-	127.4	7.54	td	7.18	125.2	7.52-7.49	m	-	125.2	7.53	t	7.08
8''	125.1	8.2	d	8.56	129.4	8.09	dd	7.76, 2.16	125.1	8.20	d	8.56	125.1	8.26	d	8.52
8a''	131.0	-	-	-	132.0	-	-	-	131.0	-	-	-	130.2	-	-	-
1'''	45.7	4.23	t	7.08	47.9	4.24	t	7.06	45.7	4.23	t	7.08	45.7	4.24	t	7.10
2'''	28.3	1.85	qt	7.27	32.9	1.891.79	quint	-	28.3	1.87	qt	7.30	28.4	1.87	qt	7.30
3'''	27.3	1.29-1.25	m	-	20.8	1.38-1.34	m	-	27.6	1.28-1.25	m	-	27.7	1.33-1.26	m	-

4’’’	20.9	1.38-1.31	m	-	14.2	0.94	t	7.36	20.9	1.38-1.31	m	-	21.0	1.38-1.33	m	-
5’’’	11.9	0.89	t	7.14					11.9	0.89	t	7.14	12.0	0.90	t	7.12
4c’’	-	-	-	-					17.5	2.84	s	-	24.9	3.26	qd	7.51
4ca’’	-	-	-	-					-	-	-	-	13.3	1.49	t	7.52

Table 14. NMR assignments of MAM-2201, APINACA, XLR-11 and UR-144 compounds identified in the herbal products.

Position	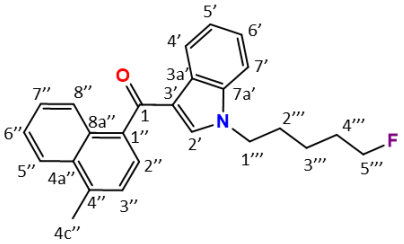					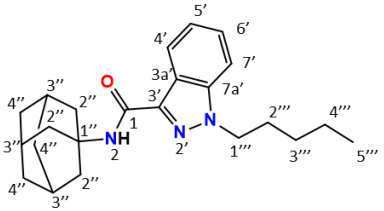				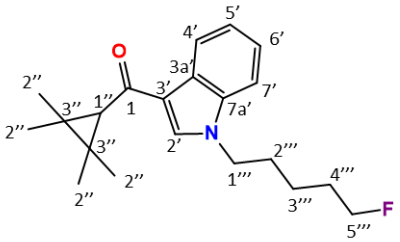				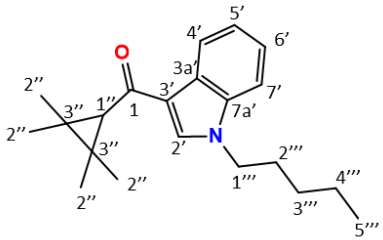			
	MAM-2201					**APINACA**				**XLR-11**				**UR-144**			
	^{13}C (δ/ppm)	^{19}F	^{1}H δ (ppm)	M[a]	*J* (Hz)	^{13}C (δ/ppm)	^{1}H δ (ppm)	M[a]	*J* (Hz)	^{13}C (δ/ppm)	^{19}F	^{1}H δ (ppm)	M[a]	*J* (Hz)	^{13}C (δ/ppm)	^{1}H δ (ppm)	M[a]	*J* (Hz)
1	192.8		-	-	-	161.8	-	-	-	195.1		-	-	-	196.0	-	-	-
2’	138.7		7.43	s	-	-	-	-	-	134.5		8.13	s	-	135.1	8.12	s	-
3’	116.3		-	-	-	136.5	-	-	-	118.3		-	-	-	118.7	-	-	-
3a’	127.3		-	-	-	125.7	-	-	-	125.7		-	-	-	126.2	-	-	-
4’	121.8		8.41-8.40	m	-	121.8	8.25	d	8.20	121.5		8.25	d	8.20	121.9	8.33	d	7.72
5’	121.2		7.38-7.36	m	-	125.4	7.54-7.48	m	-	120.9		7.54-7.48	m	-	121.4	7.53-7.51	m	-
6’	122.6		7.38-7.36	m	-	129.5	7.54-7.48	m	-	121.0		7.54-7.48	m	-	121.5	7.53-7.51	m	-
7’	109.5		7.38-7.36	m	-	109.0	7.34-7.24	m	-	108.7		7.34-7.24	m	-	109.3	7.35-7.26	m	-
7a’	136.2		-	-	-	140.2	-	-	-	136.0		-	-	-	136.5	-	-	-
1’’	136.6		-	-	-	48.0	-	-	-	40.5		1.85	s	-	41.0	1.87	s	-
2’’	124.7		7.64	d	6.36	35.2	2.27	s	-	15.2 22.0		1.39 1.35	s s	-	15.8 22.5	1.40 1.36	s s	-
3’’	124.3		7.38-7.36	m	-	27.8	2.21	s	-	28.8		-	-	-	29.4	-	-	-
4’’	136.0		-	-	-	29.0	1.80-1.71	m	-	-		-	-	-	-	-	-	-
4a’’	132.0		-	-	-	-	-	-	-	-		-	-	-	-	-	-	-

5''	123.3		8.13	d	8.44	-	-	-	-	-	-	-	-	-	-	-	-
6''	125.0		7.54-7.49	m	-	-	-	-	-	-	-	-	-	-	-	-	-
7''	125.6		7.54-7.49	m	-	-	-	-	-	-	-	-	-	-	-	-	-
8''	126.0		8.20	d	8.56	-	-	-	-	-	-	-	-	-	-	-	-
8a''	129.1		-	-	-	-	-	-	-	-	-	-	-	-	-	-	-
1'''	45.8		4.23	t	7.08	50.9	4.51	t	5.94	45.4	4.51	t	7.14	46.1	4.33	t	7.10
2'''	28.6		1.85	qt	7.52	30.7	1.99	qt	7.35	28.4	1.99	qt	7.35	28.4	2.01	qt	7.35
3'''	21.0		1.31-1.25	m	-	29.0	1.47-1.42	m	-	21.1	1.54-1.48	m	-	21.6	1.49-1.44	m	-
4'''	28.9		1.38-1.32	m	-	21.6	1.79-1.71	m	-	28.5	1.79-1.71	m	-	28.9	1.95-1.90	m	-
5'''	71.6		4.39	dt	47.44, 5.98	12.1	0.95	t	7.18	83.3	4.37	dt	47.32, 5.94	12.6	0.94	t	7.02
4c''	17.6		2.84	s	-	-	-	-	-	-	-	-	-	-	-	-	-
5'''F	-	-220.6				-	-	-			-220.1			-	-	-	-

Regarding to ^{13}C NMR spectra, the signals of the methylene groups of the alkyl chain (C-1’’’, C-2’’’, C-3’’’, C-4’’’ and C-5’’’’ in JWH-018) presented different shifts between the two compounds. The absence of one methyl group in JWH-073 leads to a downfield shift when compared to JWH-018, allowing a good characterization of these two compounds. COSY correlation made the distinction between the peaks produced by the aliphatic groups, so the identities of the SCs present in these herbal products could be confirmed (Figure 46). Regarding sample B23 JWH-018 was the only synthetic cannabinoid identified by GC-MS. By NMR analysis it was possible to distinguish the characteristic peaks of this compound. Moreover, the sample referenced as JWH-018 standard was also analysed by NMR, being possible to match the spectra of both samples (Figure 47). The 2D NMR spectrum (COSY and HSQC) obtained for sample B23 is shown in supplementary material (Figure S7).

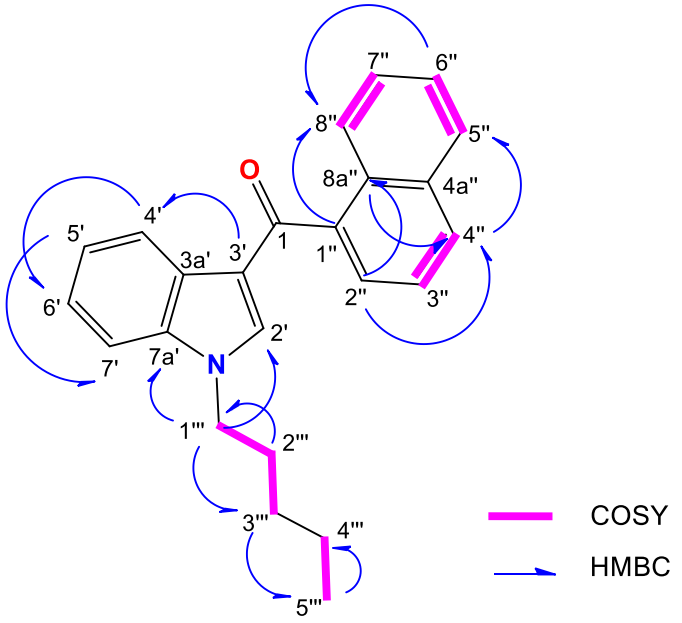

Figure 46. Key COSY and HMBC correlations in JWH-018 (adapted from [303]).

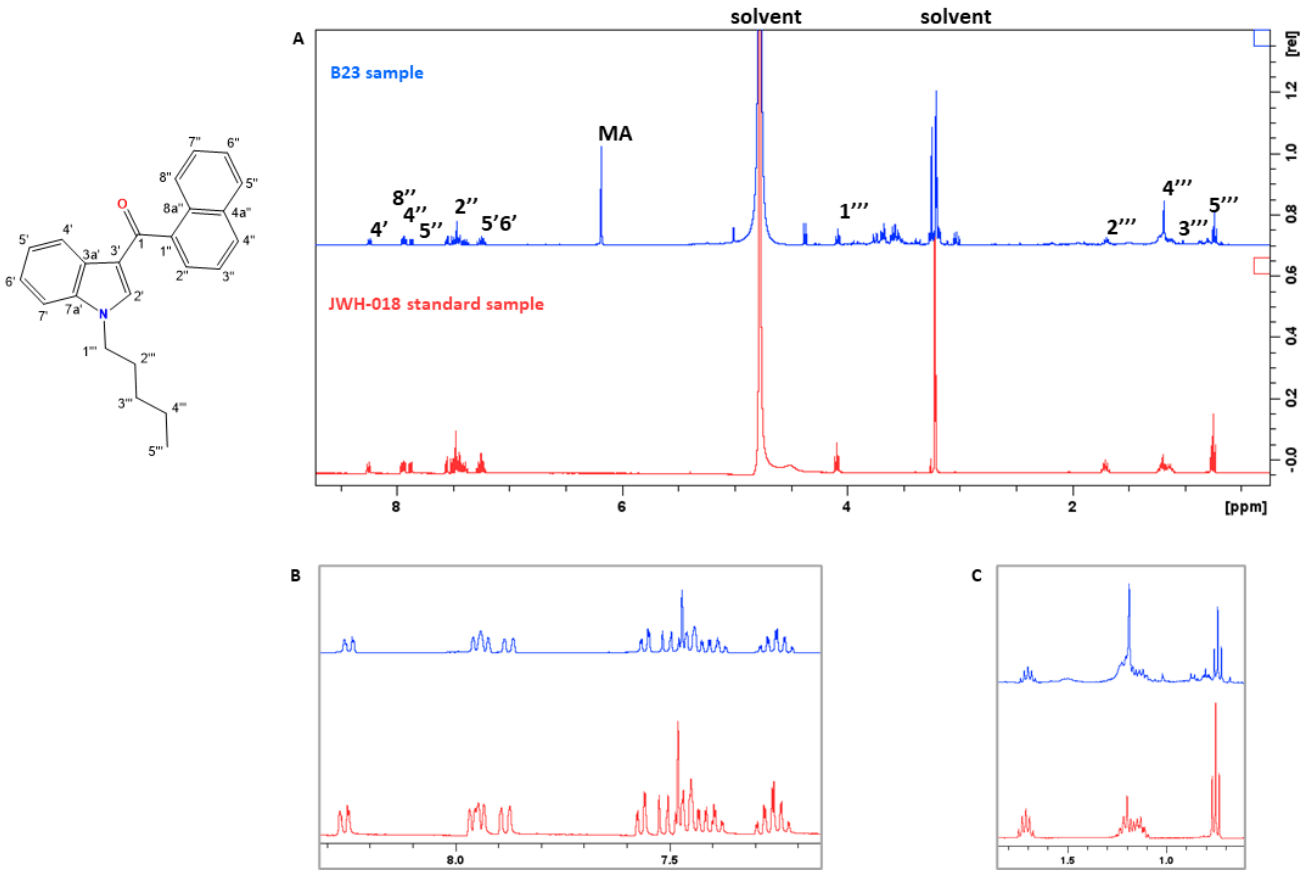

Figure 47. A - Comparison of ^{1}H NMR spectra of sample B23 (blue) and JWH-018 standard sample (red). B and C - Comparison in low and high fields, respectively.

An interesting fact reported by Assemat *et al*. [317] is that protons from aromatic, naphthyl, indole and indazole rings resonate in the range of 7.2-8.5 ppm. This fact was observed in all the identified SCs, since they present a similar structure. The naphthoyl alkylindoles show a singlet for H-2'of the indole group at 7.4 ppm and characteristic multiplets for the α-protons of the indole moiety around 7.3 ppm. On the other hand, a quintuplet produced by H-2''' from the alkyl chain is present in all SCs identified in this study.

JWH-122 and JWH-210 compounds were the only compounds identified in sample H5. The methyl and an ethyl substitution in H-4'' is easily identified, since the methyl group (3H from H-4c'') from JWH-122 produces a characteristic singlet at 2.84 ppm and JWH-210 a typical quadruplet (2H from H-4c'') with coupling constant of 7.51 Hz and a triplet at 1.49 ppm (3H from H-4ca'') with coupling constant of 7.52 Hz. These characteristic signals of each compound were considered for semi-quantification. JWH-122 was also identified in samples H1-H3 and JWH-210 in samples H1, H2 and B63 as in the results obtained by GC-MS.

In sample B63, according to GC-MS results, JWH-210 is the main synthetic cannabinoid having also been detected two very small peaks identified as JWH-018 and JWH-122 compounds. Regarding NMR analysis, the characteristic singlet at 2.84 ppm produced by H-4c'' is not present, which means that JWH-122 is present in this sample in trace amounts.

As in the proton, the ^{13}C-NMR spectra of JWH-122 and JWH-210 showed distinct signals at 17.5 ppm (C-c'' in JWH-122), 24.9 and 13.3 ppm (C-c'' and C-ca'' in JWH-210, respectively).

Relative to MAM-2201 and XLR-11, a characteristic signal of a double of triplets around 4.3 ppm (H-5''') was observed in these two fluorinated compounds (Table 14). A common fact very characteristic of a 5-fluoropentyl group due to spin coupling with ^{19}F and usually appear deshielded at approx. 4 ppm from methylene groups adjacent to a fluorine atom or to the nitrogen atom of the indole ring (H-1''') [317, 318]. These results are in accordance with previous published data [284, 307, 317]. In addition, the analysis of sample referenced as XLR-11 standard allowed to identify this compound in this samples, being the spectrum of sample C56 very similar to XLR-11 standard sample (Figure 48). The 2D NMR experiments (COSY and HSQC) obtained for sample C56 is shown in Figure S8.

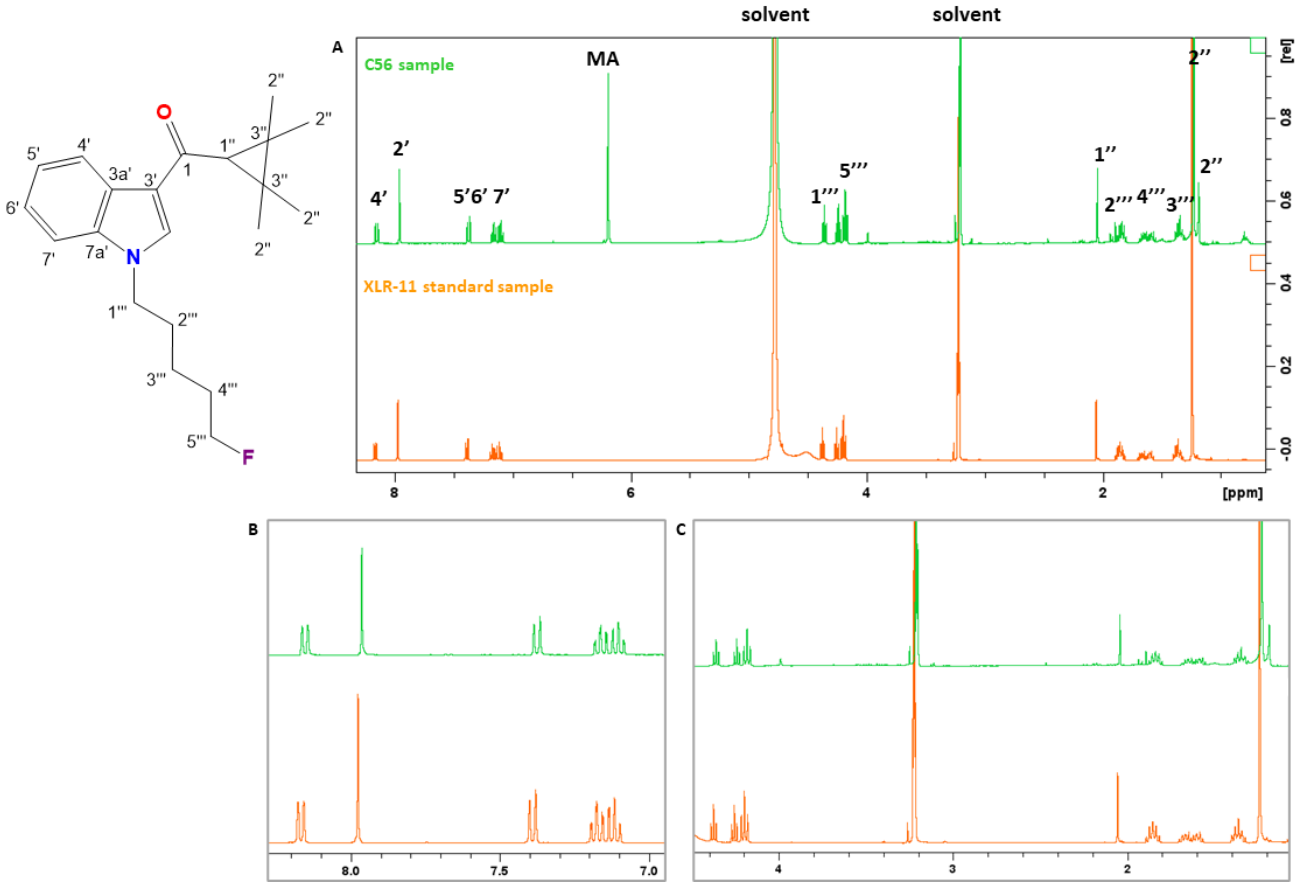

Figure 48. A – Overview of the comparison of ^{1}H NMR spectra of sample C56 (green) and XLR-11 standard sample (orange). B and C - Comparison in low and high fields, respectively.

In order to complete de analysis, the ^{19}F NMR chemical shift value for both compounds was -220 ppm, which is similar to the one reported in the literature [284, 319]. In Figure 49 the ^{19}F NMR signals at −220 ppm of samples with fluoride synthetic compounds is shown.

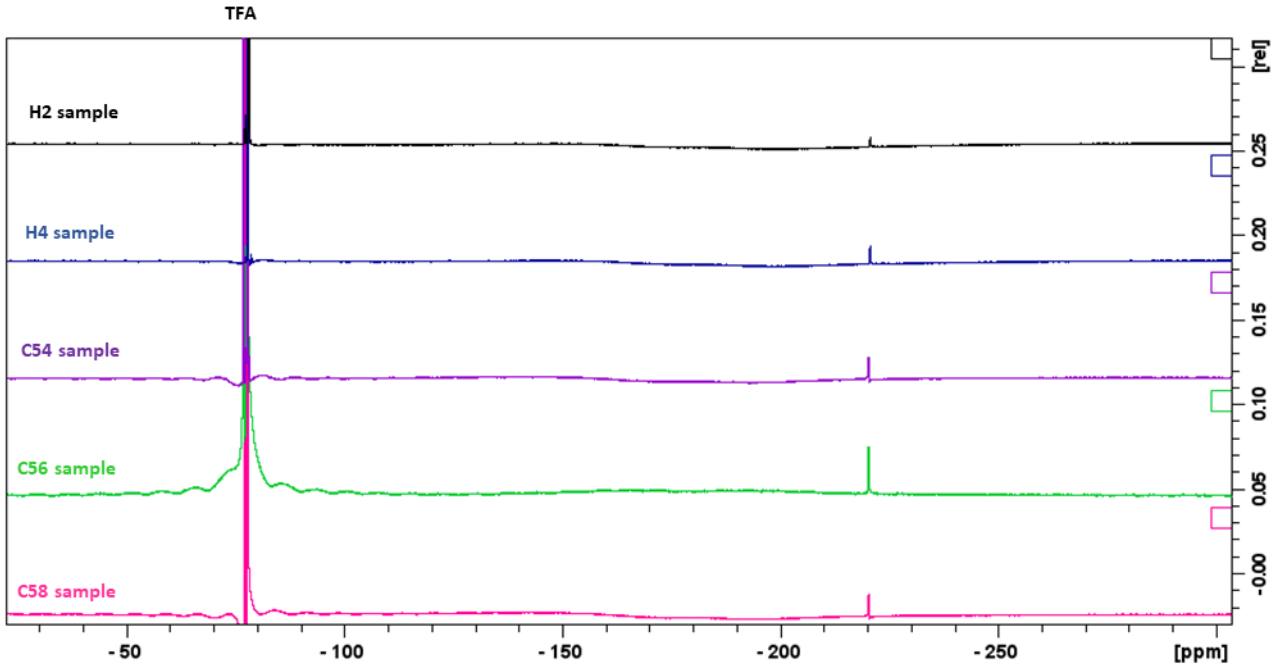

Figure 49. ^{19}F NMR signals at -220 ppm of seized samples with fluoride compounds.

Two singlets at 1.35 and 1.39 ppm were assigned, corresponding to methyl signals of the cis- and trans-methyl groups of H-2'' in the tetramethylcyclopropyl group. These two characteristic signals were also observed in B54 sample due to the presence of UR-144. Since UR-144 has a very similar structure to XLR-11, differing only in the absence of the fluoride group, the singlets of the methyl groups linked to the cyclopropyl ring should be expected. However, a triplet produced by H-5''' from the alkyl chain at 0.94 ppm differentiates the NMR analysis of these two compounds.

APINACA was confirmed in samples H4 and B54. As previously mentioned, this compound is structurally different when compared to other SCs, due to the presence of an adamantyl and an indazole group. The proton spectrum is not immediately interpretable and the absence of the signal of H-2 from NH group raised some doubts in the identification of the compound, since NH typically won´t be observed in solvents with exchangeable 2H, like CD_3OD, fact also observed by Amato *et al.* [314]. On the other hand, the ^{13}C-NMR spectrum provided important information with the assignment of 17 carbon signals. The signals produced by C-2'', C-3'' and C-4'' from the adamantyl group are consistent with the structure of APINACA. The COSY and HSQC experiments provided essential information for the characterization of this compound (see Figure S9).

Damiana extract was also analysed by NMR. As in the GC-MS results, ^{1}H NMR spectra obtained is relatively free of interfering peaks. This fact was also reported by Fowler *et al.* [315] whose study was the screening and quantification of SCs in herbal products using NMR.

The amount of synthetic cannabinoid measured in each herbal product sample by semi-quantitative ^{1}H NMR is reported in Table 15. The results are expressed in mg per gram of sample and a characteristic signal of each compound was considered for the measurement. This approach was based on the studies of Fowler *et al.* [315] and Assemat *et al.*[317].

All samples have, at least, 2 active compounds except for sample B23. Regarding to sample B43, no characteristic signal was observed for each synthetic cannabinoid previously identified by GC-MS, therefore the measurement was not possible.

Table 15. Amount of SCs measured by semi-quantitative ^{1}H NMR in each seized herbal product.

	Amount (mg/g ± SD)							
Samples	**JWH-018**	**JWH-073**	**JWH-122**	**JWH-210**	**MAM-2201**	**APINACA**	**XLR-11**	**UR-144**
H1	40.7 ± 1.1		60.9 ± 5.8	58.5 ± 7.4				
H2	12.5 ± 0.3		18.2 ± 4.4	13.5 ± 0.3	29.8 ± 0.8			
H3	86.6 ± 0.8		87.7 ± 4.3					
H4						183.1 ± 12.2	61.9 ± 2.2	
H5			19.1 ± 0.1	123.1 ± 0.7				
H6	57.5 ± 6.4	56.8 ± 7.2						
H7	55.5 ± 3.3	49.9 ± 2.8						
H8	48.4 ± 6.8	100.3 ± 17.3						
H9	28.6 ± 5.3	63.2 ± 8.9						
C54					8.0 ± 0.8		11.7 ± 1.5	
C56							10.1 ± 2.6	
C58					7.9 ± 3.5		10.7 ± 0.8	
C60	14.1 ± 4.8	12.7 ± 3.9						
C61	7.3 ± 3.9	6.4 ± 1.3						
C66	11.6 ± 3.1	10.1 ± 1.6						
B23	17.1 ± 3.7							
B43*								
B54						31.6 ± 6.0		5.5 ± 1.0
B63				17.8 ± 3.7				

*No characteristic signal was observed for the measurement of SCs. SD – standard deviation.

As can be seen in the previous Table, the values ranged from 6 to 183 mg/g between all seized samples, with APINACA with the highest amount and UR-144 with the lowest one.

Moreover, it was possible to verify that the content of each cannabinoid varies between samples. JWH-018 was detected in 11 of the analysed samples and the values ranged from 7 to 87 mg/g. Thus, it is possible to verify inconsistency between samples with the same brand name, e.g. H6 and H7, H8 and H9, C60 and C61. The same conclusion was obtained by Fowler *et al.* [315], with relative standard

deviation ranging from 7 to 68%. This indicates that there is lack of quality control in their production, increasing the danger for its consumption. Ingestion of even small amounts may result in pronounced effects because of inconstancies in the dosage, significantly increasing the risk of these substances.

The abundance of each compound in each seized sample is in accordance with those obtained by GC-MS analysis.

The three non-cannabinoid compounds identified by GC-MS, namely oleamide, vitamin E and vitamin E acetate were not detected by NMR, probably due to their low concentrations in the sample and the presence of other compounds with higher concentrations.

3.2. "Herbal incenses" extraction studies

Due to the fact SCs are frequently found on the surface of the plant material, an efficient and quick extraction is crucial to successfully analyse these compounds in this kind of matrix. The efficiency of an extraction is determined by two factors; the amount of synthetic cannabinoid extracted (signal strength) and the purity of the extract (level of the intrinsic plant compounds in the extract). However, the amount of the sample is often reduced making quantitative analysis difficult [182, 183, 320]. In this sense a quick, easy sample preparation with little sampling is essential.

Typically, ethanol, MeOH, chloroform, DCM, or acid/base extraction are used as the primary method for extracting SCs from herbal products. For even greater extraction efficiency, sonication is then used. In this study, we determined the optimal solvent and extraction time to develop a facile synthetic cannabinoid extraction method that could be easily analysed by GC-MS as primary screening technique. Sample B54 was chosen to carry out these extraction studies, since it had a greater quantity compared to the other seized samples.

Five common solvents (chloroform, MeOH, ethanol, acetone and DCM) were assessed for overall extraction efficiency. The optimization of solvent extraction studies was performed with 50 mg of sample B54 sonicated with 2 mL of solvent during 10 min.

In Figure 50 is graphically presented the extraction efficiency of the tested solvents.

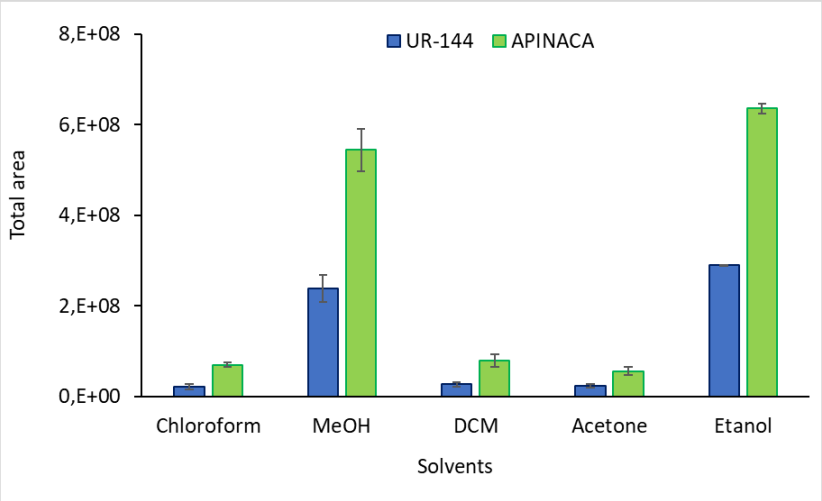

Figure 50. Solvent extraction efficiency.

Among the analysed solvents, it was observed that ethanol allowed the best extraction efficiency of UR-144 and APINACA compounds, since it gave a greater response in terms of total area, as well as less interference was observed; whereas acetone showed the lowest response.

After selecting the best extraction solvent, the shortest extraction time was determined. Four extraction times, namely 1, 5, 10 and 15 min, were analysed. The influence of extraction time is illustrated in the following Figure.

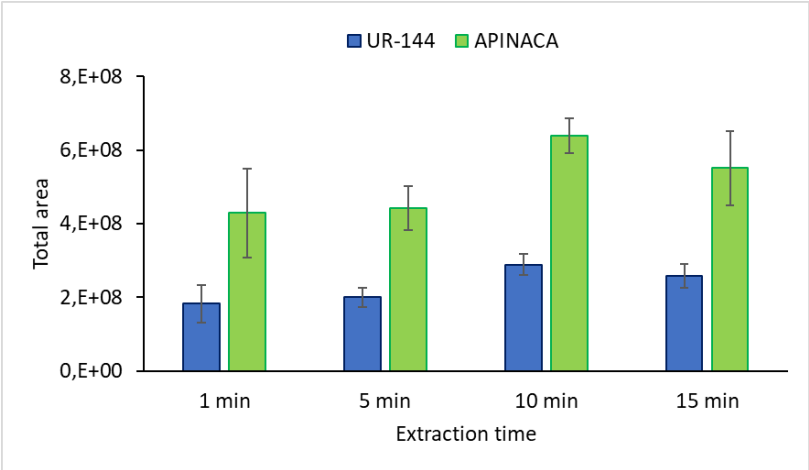

Figure 51. Extraction time efficiency.

According to the results, 10 min was the best extraction time efficiency for both compounds.

In West *et al.* [184] work a rapid and facile method to extract SCs from leafy substrates was determined. Win 55, 212-2 was used as the model synthetic cannabinoid while damiana leaf cuttings were used as a representative substrate material. Four solvents (dimethyl sulfoxide, chloroform, MeOH, and ethanol) at two different concentrations (2% and 100%) were studied and 30s and 1min periods were used to determine the shortest timeframe necessary to extract the most synthetic

cannabinoid. 100% ethanol and 30s of shaking were the best extraction parameters reported by the authors. However, it was also concluded that further studies are needed to determine if these extraction parameters are compatible with both real-world "spice" samples and a wide range of synthetic cannabinoid compounds.

4. Conclusions

The combination of GC-MS and NMR data demonstrated to be a powerful tool for SCs identification. In this study, nineteen seized herbal products suspected to contain SCs were analysed by GC-MS and NMR techniques. Without information about the chemical composition, the content of these so called 'herbal incenses' is not always the same between brands, and even from batch to batch.

Thus, based on GC-MS results, it was possible to identify 10 SCs: JWH-018, JWH-073, JWH-122, JWH-210, MAM-2201, APINACA, XLR-11, UR-144, CP47,497-C8 and its enantiomer.

Moreover, three adulterants, oleamide, vitamin E and vitamin E acetate were identified. Vitamin E acetate was an interesting finding in this work, since, to our knowledge, there is no report in the literature about the detection of this compound in a seized herbal product.

The applied methodology proved to be useful, allowing the preliminary identification of the different SCs in the different herbal products. Furthermore, the examination of mass spectral fragment ions, as well as the study of both 1D and 2D NMR experiments enabled the characterization of the molecular structure of SCs.

GC-MS can be regarded as the gold standard, as it provides not only excellent chromatographic resolution, but also allows the identification of active ingredients by their EI mass spectra [81]. The EI technique is very useful for the study of spectrometric and fragmentation behaviour of these compounds, being a huge aid in the discovery of novel synthetic compounds as well as, in the continuous monitoring of already existing substances. However, it is insufficient, when used alone, to discriminate structurally similar SCs and thus, the combination with NMR technique was crucial, since it allowed a positional isomer distinction.

According to the screening results it is possible to conclude that there is inconsistency between samples regarding to the type of synthetic cannabinoid, the amount of compound and the presence of adulterant agents.

Concerning to extraction studies, it is essential to perform an efficient and fast extraction of SCs from herbal matrices. Based on the results we concluded that ethanol provided the best extraction

of the SCs, UR-144 and APINACA, with 10 min of sonication. Although, additional studies would be interesting to complete these results.

CHAPTER II – Analytical determination of Synthetic Cannabinoids in biological samples

1. Introduction

HPLC is a well-established separation technique, being used to solve numerous analytical problems in several areas, including chemical, forensic, toxicological, clinical, and environmental. During the last years, many improvements have been incorporated into this technique, such as the development of new stationary phases and chromatographic supports, advances in instrumentation, among others, allowing faster and more efficient analysis, corroborating the current need to increase the number of analyses and throughput and reduce costs [321].

At the beginning of this century, the science of analytical separation was revolutionized with the introduction of Ultra High Performance Liquid Chromatography (UHPLC). Based on the same HPLC separation principles, UHPLC instrumentation has greater operating capacity with a maximal pressure of 1000 bar (15000 psi). In UHPLC, shorter length columns, as well as stationary phases packed with smaller particles (less than 2 µm of diameter) are used, providing a new level of chromatographic performance [321, 322]. In addition, the solvent consumption is relatively lower, and the flow can be higher. The combination of the particle size with the high linear velocities of the mobile phase allows an increase in resolution and a greater sensitivity of detection of the analytes present in the sample. All these advantages have contributed to a reduction in analysis time and eluents volume, one of the main difficulties in HPLC, being an asset for the determination of synthetic drugs in biological samples.

As previously mentioned, the difficulty in acquiring reference material due to legal issues, high costs, or even the lack of available chemical standards poses a great challenge to clinical and forensic toxicology laboratories. In this sense to overcome these drawbacks, the isolation of the SCs identified in the seized herbal samples (described in Chapter I) was carried out using a UHPLC with a PDA detector, and the development of two analytical approaches for the determination of SCs in oral fluid samples.

2. Materials and Methods

2.1. Reagents, materials, and standards

MeOH, acetonitrile (ACN), 2-propanol, and ethanol of HPLC gradient grade (>99% purity) were purchased from Fisher Chemicals (Loures, Portugal) and formic acid (FA) from Panreac (Barcelona, Spain). 3-Indole acetic acid (IAA) was acquired from Sigma Aldrich (Steinheim, Germany). Ultrapure water (18 MΩ cm at 23 °C) was obtained by means of a Milli-Q water purification system (Millipore,

Milford, MA, USA). The digiVOL® digital syringe driver, µSPEed® syringe (250µL) and µSPEed® cartridges were kindly provided by ePrep® company (Victoria, Australia). The eVol® XR hand-held automated analytical syringe (500µL) and the BIN (Barrel Insert and Needle) containing the sorbent material used for MEPS extraction were purchased from SGE Analytical Science (SGE Europe Ltd., Kiln Farm Milton Keynes, United Kingdom).

2.2. Biological samples

Drug-free oral fluid samples were provided by healthy volunteers and by laboratory staff with ages ranging from 19 to 59 years old. Authentic oral fluid samples were provided by recreational drug users. All samples were collected in sterile flasks and stored at −20 °C until analysis.

All the participants were correctly and fully informed of the purpose, methods and means of the study. All indicated their agreement to participate and signed an informed consent.

2.3. Seized herbal products preparation

An aliquot (1 ml) of herbal extract (see chapter I, section 2.3.1.) was evaporated to dryness, under a gentle stream of nitrogen and the extract mass was weighed. Finally, the residue was dissolved in pure MeOH, and working solutions at 10 µg/mL were prepared for all samples by proper dilution of stock solution with MeOH. All solutions were filtered through a 0.22 µm PTFE filter.

2.4. UHPLC-PDA analysis

The separation and identification of SCs were performed on a Waters Ultra Pressure Liquid Chromatographic Acquity system (UPLC, Acquity H-Class) (Milford, MA, USA) combined with a Waters Acquity quaternary solvent manager (QSM), an Acquity sample manager (SM), a column manager, a 2996 PDA detector, and a degassing system.

Data acquisition and processing were carried out using the Empower software v2.0 from Waters Corporation. The best separation conditions of the analytes were obtained with an Acquity UPLC™ high strength silica HSS T3 analytical column (2.1 mm × 100 mm, 1.8 µm particle size), packed with a trifunctional C_{18} alkyl phase and an Acquity UPLC™ HSS T3 Van Guard™ Pre-column (Waters; Milford, MA, USA), at 35°C. The elution of the compounds was performed by a binary mobile phase, which consisted of water with 0.1% FA (solvent A) and ACN as the organic phase (solvent B) with a constant flow rate of 0.350 mL/min.

The gradient was programmed as follows: 40% B at 0 min and linearly increased to 70% over the first half minute, held at 70% for 1.5 min followed by an increase of 20% over the next 6.5 min, isocratic during 2 min and finally decreased to the initial conditions for 0.5 min and equilibration time for 1 min, which resulted in a total run time of 12 min. In Figure 52 is graphically presented the gradient elution used for the separation of SCs.

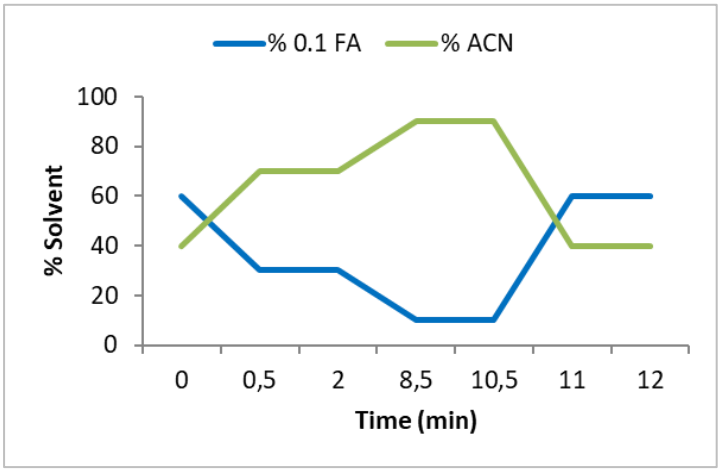

Figure 52. Gradient elution used for the separation of SCs.

The samples were kept at 20°C in the sample manager, and 2 µL were injected into the UHPLC system. The UV detection wavelength was set to the maximum range of absorbance for the target compounds: 210-400 nm.

The identification of the SCs was based on the comparison of PDA spectra of their peaks in the herbal samples, with those previously reported in the literature.

2.4.1. Optimization of UHPLC conditions

The optimal separation conditions for UHPLC analysis were chosen through a factorial design 4^2 x 3 (see Table 16). Different factors were combined and studied, namely different column flows (300, 350, 400 and 450 µL/min) and temperature (30, 35 and 40 °C). All the conditions were tested in the four available columns namely, CORTECS (2.1 mm × 100 mm, 1.6 µm particle size), Bridged Ethylene Hybrid (BEH, 2.1 mm × 50 mm, 1.7 µm particle size), HSS T3 (2.1 mm × 100 mm, 1.8 µm particle size), and Charged Surface Hybrid (CSH, 2.1 mm × 150 mm, 1.7 µm particle size) using the same binary mobile phase (H_2O with 0.1% FA and ACN). All columns were acquired from Waters (Milford, MA, USA).

Table 16. Instrumental UHPLC conditions tested.

Column	Flow (µL/min)	Temperature (°C)
CORTECS	300	30
BEH	350	35
HSS T3	400	40
CSH	450	

The quality of the chromatographic separation was quantified by looking at the retention time between the peaks of each chromatogram obtained with the best gradient program.

Resolution (*Rs*) was calculated according to the following Equation [323]:

$$R_s = 2\left(\frac{t_{R2} - t_{R1}}{w_{b1} + w_{b2}}\right) \qquad \textit{Equation 3}$$

where t_R is the retention time and w_b is the peak width at baseline of each component. European Pharmacopoeia recommend a *Rs* value greater than 1.5 to acquire a good resolution [324].

The efficiency of each column was measured by the number of theoretical plates (*N*) and was expressed by the following formula:

$$N = 16\left(\frac{t_R}{w_b}\right)^2 \qquad \textit{Equation 4}$$

The higher the plate number *N*, the greater the efficiency of the column.

2.5. Isolation of synthetic cannabinoids from seized herbal samples

The samples H1, B54, B63, C58 and C60 were chosen according to the contents previously identified by GC-MS analysis for the isolation of the SCs by UHPLC.

The extraction procedure for all samples was carried out using the best extraction conditions described in Chapter I, namely 50 mg of ground herbal material was extracted in 2 mL of ethanol, followed by vortexing 1 min and ultrasonication for 10 min. The extracts were evaporated to dryness, under a gentle stream of nitrogen and the extract mass was weighed. Finally, the residue was resuspended in 1 mL of MeOH and working solutions at 500 µg/mL were prepared for all samples by proper dilution of stock solution with MeOH. All solutions were filtered through a 0.22 µm PTFE filter.

Each sample extract was injected and fractions containing the target substances were collected, evaporated to dryness, dissolved in MeOH and re-injected in the UHPLC to verify its purity. The fractions of each compound were pooled, the solvent was evaporated, and the mass of each

compound isolated was weighed until at least 1 mg was obtained. The purity of each isolated substance was calculated based on the Duranovic *et al.* work [276], namely by the ratio between the isolated substance's peak area and the total peak area of the chromatogram. In addition, the pooled fractions were injected in GC-MS using the conditions described in Chapter I and analysed in TLC aluminium sheets with silica gel 60 and fluorescence indicator UV_{254}, purchased from Macherey-Nagel (Düren, Germany), using a *n*-hexane/diethylether (80:20, v/v) developing solvent system were also used to verify the isolation and purity of each compound.

2.6. Analytical determination of SCs in oral fluid samples

Two different microextraction techniques, MEPS and µSPEed, were tested and compared in order to evaluate their ability to extract SCs from oral fluid samples. Different parameters such as the chemical nature of the sorbent material, the sample volume, the number of extraction cycles, the elution solvent and the elution volume were optimized in both techniques to obtain the best conditions for the SCs extraction (see sections 2.6.2. and 2.6.3.). The optimization process was performed in triplicate and the optimal conditions were selected by the peak areas of each synthetic cannabinoid, obtained in each parameter.

2.6.1. Oral fluid sample pre-treatment

Before the extraction procedure, the samples were brought to room temperature and pre-treated to remove potential interferents such as proteins, food debris and air bubbles. The pre-treatment procedure was adapted from Bianchi *et al.* [247], Ares *et al.* [325] and Sergi *et al.* [326] works. Briefly, 100 µL of oral fluid spiked with the analytes (200 ng/mL) and IAA as IS (100 ng/mL) was mixed with 100 µL of MeOH and vortexed for 1 min. The mixed solution was, then, sonicated for 6 min and centrifuged at 12000 rpm for 5 min to promote protein precipitation. The supernatant was promptly separated from the pellet, to avoid protein resolubilization and used for optimization and analytical method validation of both microextraction techniques.

2.6.2. MEPS procedure

The MEPS procedure was carried out with an eVol® XR hand-held automated analytical syringe (500 µL) fitted with a BIN (Barrel Insert and Needle), containing 4 mg of the C_{18} sorbent, previously

selected as the best sorbent to extract the target analytes in the optimization step. Figure 53 shows the optimised MEPS procedure.

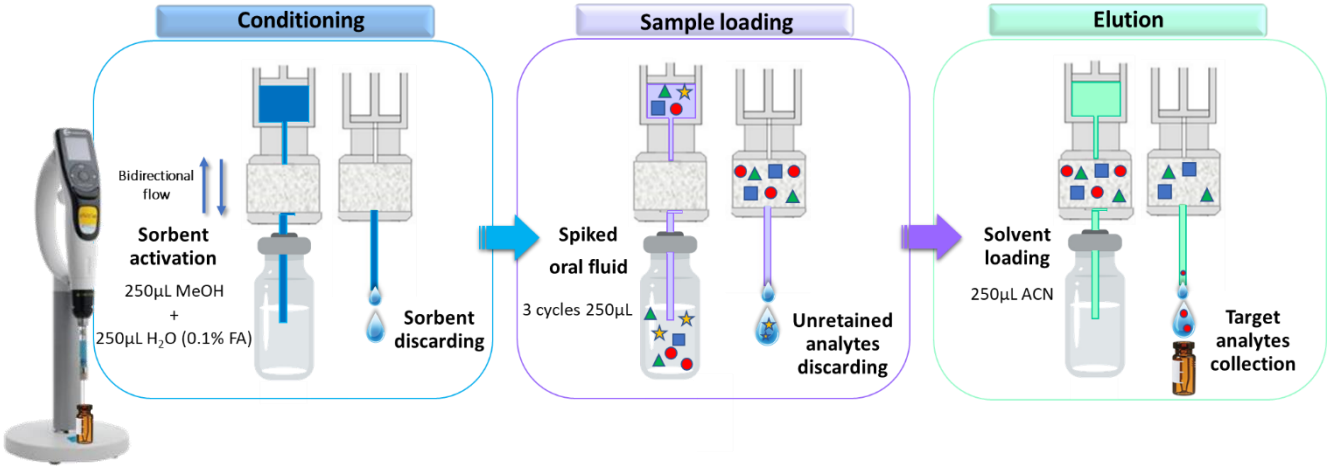

Figure 53. Schematic representation of MEPS with the optimised experimental parameters (adapted from [238]).

Prior to each sample extraction, the sorbent was conditioned with 250 µL MeOH, followed by 250 µL of acidified water (0.1% FA). This step activates the sorbent and ensures reproducible retention of the analytes. After the activation and conditioning steps, 250 µL sample was loaded using 3 charge/discharge cycles at a flow rate of about 20 µL/s. Endogenous interferences were removed with 100 µL of water containing 0.1% formic acid and the analytes were eluted with 250 µL ACN directly into a vial. The eluate was dried under gentle nitrogen stream, at room temperature, and the residue was dissolved in 100 µL of the mobile phase and injected, in triplicate, into the UHPLC-PDA system.

Between each extraction, the sorbent was rinsed with 250 µL MeOH followed by 250 µL of the washing solution. This step decreased memory effects (carry-over), but also functioned as conditioning step before the next extraction. All solvents and standards used during the extraction procedure were previously filtered.

2.6.3. µSPEed procedure

The µSPEed extraction of SCs from oral fluid samples was performed with digiVOL®, a digital syringe driver with stand fitted with a 250 µL digiVOL Syringe and a µSPEed cartridge. The experimental layout with optimized conditions is described schematically in Figure 54.

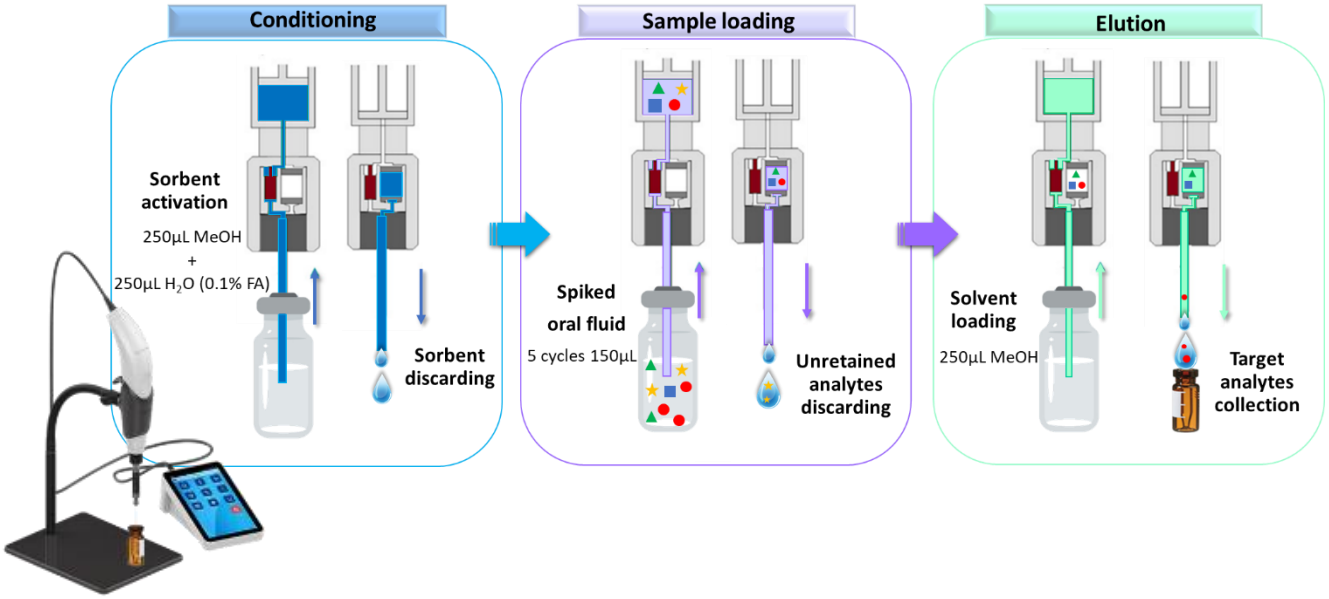

Figure 54. Representation of the optimized sample treatment procedures using µSPEed technique (adapted from [238, 327]).

Prior to each µSPEed experiment, the cartridge was conditioned with 250 µL MeOH and equilibrated with 250 µL acidified water (0.1% FA). Then, 150 µL of spiked oral fluid sample was drawn through the syringe up and down 5 times at a flow rate of 500 µL/min. The washing step was performed the same way as for the MEPS methodology, followed by the elution of the analytes with 250 µL MeOH. Between each extraction, the cartridge was rinsed with 250 µL MeOH followed by 250 µL of acidified water to avoid carry-over and to act as conditioning step for the next extraction.

2.6.4. Methods Validation

The analytical validation of both methodologies, MEPS and µSPEed followed by UHPLC–PDA, was carried out with drug-free oral samples spiked with standard solutions of the isolated compounds.

The methodology compliance must have some mandatory parameters, such as selectivity, precision, accuracy, linearity/calibration curve, detection and quantification limits, recovery and matrix effect. The validation followed the standards of the Associação de Laboratórios Acreditados de Portugal (Relacre) [328] and Eurachem guide [329].

2.6.4.1. Selectivity

To evaluate the method selectivity, the absence of interfering signals has to be demonstrated. The study involved a total of twenty drug-free oral fluid samples, which were named blank samples. These samples were randomly mixed in groups of 4, constituting 5 mixtures or pools. Each pool was

divided into two aliquots of oral fluid (2.5 mL). To one of the aliquots, only IS was added at a concentration of 100 ng/mL, while the second aliquot was spiked with a standard mixture of the SCs under study, including IS, at a concentration of 200 ng/mL. Both aliquots were applied to MEPS and µSPEed microextraction techniques prior to UHPLC-PDA analysis. The chromatograms were then compared, evaluating the existence or absence of interferences in the retention times of the different analytes.

2.6.4.2. Linearity and working range

Linearity was assessed by constructing eight calibration curves, one for each analyte, at a working range from 40 to 180 ng/mL using eight calibration points, in triplicate. Each concentration was prepared by spiking drug-free oral fluid samples with the SCs and IS (100 ng/mL). Calibration curves were constructed by plotting the peak area ratio between each analyte and the IS *versus* analyte concentration (peak area analyte/peak area IS *vs.* concentration).

The line that best fits the set of experimental results was carried out by using the least squares method. It is assumed that the residuals (errors) that present a normal distribution and null value, are independent and have a homogeneity of variances along the working range (homoscedasticity) [330]. Values greater than 0.99 are required for the linear correlation coefficient (*r*) and determination (R^2) of the calibration curves, to guarantee a better fit of the results (less dispersion of the set of experimental points and less uncertainty of the estimated regression coefficients). However, the estimates obtained in the regression and the graphical representation of the function, by themselves, are not enough to establish linearity and for this reason, some statistical tests were performed to complement the linearity of the method, such as the Mandel test or the Fisher/Snedecor test (*F-test*) and residual analysis.

Mandel's fitting test allows the comparison of two methods through least squares modelling – one linear and the other non-linear (polynomial) – to test the linearity of the data set that provides a better fit of the points of the calibration curve [221, 328, 331]. The difference in the variance (DS^2) is calculated by Equation 5 and then, DS^2 and the variance of the non-linear calibration function are submitted to *F-test* to examine for significant differences. The test value (*TV*) is calculated by Equation 6.

$$DS^2 = (N-2) \times S^2_{y/x} - (N-3) \times S^2_{y^2} \qquad \textit{Equation 5}$$

Where:

N is the number of measurement points (calibration points);

$S^2_{y/x}$ is the linear residual variance

$S^2_{y^2}$ is the non-linear residual variance

$$TV = \frac{DS^2}{S^2_{y^2}} \qquad \textit{Equation 6}$$

F tabulated or critical value (N-1; N-1;α) is obtained at 95% confidence level.

If TV<F: non-linear calibration function does not lead to significantly better adjustment, i.e., the calibration function is linear;

If TV>F: non-linear calibration function should be used. In this case, reducing the working range, or another adjustable function e.g. non-linear regression (e.g. quadratic, cubic) or weighted linear regression may solve the problem [328].

Linear and non-linear regression analysis was performed using a Windows Excel spreadsheet. Finally, a residual analysis was performed, which was based on the evaluation of the distance between the experimental *y* values and the ideal *y'* values of the calibration curve. A graphic representation of the residual values as a function of concentrations was made to verify the linearity of the model previously chosen by the Mandel test (see Supplementary Material III).

2.6.4.3. Limit of detection and limit of quantification

There are several methods for determining the limit of detection (LOD) and limit of quantification (LOQ) [332]. In this work, the study of these parameters was based on the calibration method, whose methodology is more logical and linear, theoretically obtaining the true values of the limits. The limits calculation was performed using the data from the calibration curves obtained in the linearity for each compound, and applying the following mathematical Equations:

$$LOD = \frac{(3{,}3 \times S_{y/x})}{b} \qquad \textit{Equation 7}$$

$$LOQ = \frac{(10 \times S_{y/x})}{b} \qquad \textit{Equation 8}$$

Where, $S_{y/x}$ represents the residual standard deviation and b the slope of the calibration curve.

2.6.4.4. Precision studies

The precision expresses the degree of variation (dispersion) between several measurements obtained from multiple samplings of the same sample, under the same conditions. This parameter can be measured by repeatability, intermediate precision and reproducibility [333].

Repeatability, also called intra-day precision was studied at the same time as intermediate precision. To study these parameters, precision was expressed as the percentage of the relative standard deviation (*RSD*) or coefficient of variation (*CV*), and three concentration levels 40, 100 and 180 ng/mL, which characterize the working range (low, medium and high level respectively), were prepared in triplicated by spiked samples from a pool of oral fluid, free from the analytes under study. All replicates were performed in the same day to obtain repeatability. Intermediate precision evaluation was obtained by analysing three times over during five non-consecutive days (n=15).

The replicates were extracted and analysed using the two extractive procedures (MEPS and µSPEed) and the experimental conditions used in the validation of the developed methods were analysed concomitantly, in the same period, using the same reagents and equipment, performed by a single operator, and analysed independently.

The relative areas for each substance were obtained, and the mean, standard deviation (*SD*), and *RSD* were calculated (Equation 9 and 10).

$$SD = \sqrt{\frac{\sum_{i=1}^{n}(x_i - \bar{X})^2}{(n-1)}} \qquad \textit{Equation 9}$$

$$RSD\ or\ CV\ (\%) = \left(\frac{SD}{\bar{X}}\right) \times 100 \qquad \textit{Equation 10}$$

Where, $\bar{X}$ is the mean of a small number of measurements; x_i the individual value of a measurement and n the number of measurements.

Subsequently, the results were treated by applying the One-way ANOVA test, through which repeatability and intermediate precision can be estimated, according to the international standard ISO 5725 [221, 336]. In Tables 17 and 18 are presented the expressions used.

Table 17. Analysis of variance - one-way Table (adapted from [221, 334, 335]).

Source	Sum of Squares (*SS*)	Mean Squares (*MS*)	Degrees of Freedom
Between	$SSrun = n\sum_{i=1}^{p}(\bar{X}_\iota - \bar{\bar{X}})^2$	$MSrun = \frac{n\sum_{i=1}^{p}(\bar{X}_\iota - \bar{\bar{X}})^2}{p-1}$	$p-1$
Within	$SSr = \sum_{i=1}^{p}\sum_{j=1}^{n}(X_{ij} - \bar{X}_\iota)^2$	$MSr = \frac{\sum_{i=1}^{p}\sum_{j=1}^{n}(X_{ij} - \bar{X}_\iota)^2}{p(n-1)}$	$p(n-1)$
Total	SS_T	$MS_T = \frac{SS_T}{n-1}$	$pn-1$

Table 18. Calculation of variance for the experimental model used in the study of repeatability and intermediate precision (adapted from [221, 334, 335]).

Variance	Expression
Repeatability Variance ($\boldsymbol{S_r^2}$)	$S_r^2 = MS_r$
Precision Variance ($\boldsymbol{S_{run}^2}$)	$S_{run}^2 = \frac{MS_{run} - MS_r}{n}$
Intermediate Precision Variance ($\boldsymbol{S_i^2}$)	$S_i^2 = (S_r^2) + (S_{run}^2)$

Where p is the number of analysis sequences for each concentration level (one sequence per day); n is the number of replicates performed in each sequence; X_{ij} represents an individual replicated (replicated j) obtained in sequence i; $\overline{X}_i$ represents the average of n replicates obtained in sequence i; $\overline{\overline{X}}$ is the average of the averages of p sequences.

The calculation of the coefficient of repeatability variation (CV_r), expressed in percentage and defined as the ratio of the standard deviation of repeatability (S_r) in relation to the mean value ($\overline{X}$), allowed to estimate the repeatability of the analytical method, for each concentration range (Equation 11) and the coefficient of intermediate precision (CV_{si}), also expressed in percentage, was calculated by Equation 12, where S_i is the standard deviation of intermediate precision.

$$CV_r = \frac{S_r}{\overline{\overline{X}}} \times 100 \qquad \textit{Equation 11}$$

$$CV_{si} = \frac{S_i}{\overline{\overline{X}}} \times 100 \qquad \textit{Equation 12}$$

The experimental procedure was repeated on different days, over a period of two months. Also, different drug-free oral fluid samples and different extraction sorbents/cartridges were tested to study the causes of variability. Many authors also recommend changing equipment, which was not possible in this project, as well as inter-laboratory tests for the study of reproducibility.

2.6.4.5. Accuracy

The experimental methodology used for the study of this parameter was the one described for the intermediate precision.

The accuracy of a method is affected by both, systematic and random errors (precision), but it is commonly used only to evaluate systematic errors. The processes normally used to evaluate this parameter are the use of certified reference materials (CRM), with the participation in inter-laboratory comparisons and the performance of recovery assays [328]. In the absence of CRM, the

impossibility of inter-laboratory tests and the absence of a reference method, the veracity of the analytical method can be evaluated through the absolute recovery values obtained from the analysis of fortified samples with a known concentration [337]. This procedure may have some limitations, since the estimate of recovery obtained in fortified samples may be different from what would be obtained in a real sample [213]. However, it is considered that fortification of liquid samples may constitute a reasonable representation of the analytes in real samples [221, 338].

Accuracy, in percentage, can be expressed as the mean relative error of the estimated concentration (*Bias*) (Equation 13) for each concentration level or as percent recovery [332].

$$Bias = \frac{(\bar{x} - x_{ref})}{x_{ref}} \times 100 \qquad \textit{Equation 13}$$

Where, $\bar{x}$ is the mean of obtained concentration, and x_{ref} is the expected concentration.

As previously mentioned, when using spiked samples, the obtained estimate recovery may present differences in relation to the real samples. In this case, the analytical results must be corrected for these systematic errors so that the final value is traceable. In addition, the uncertainty of the results must be calculated as a measure of confidence [221, 334].

In this work, the uncertainty associated with the recovery of both methodologies developed, MEPS/UHPLC-PDA and µSPEed/UHPLC-PDA, was estimated. The recovery of the method was determined in percentage (R_i) by the ratio between the observed value (C_{obs}) and the expected value (C_{fort}) (Equation 14) in order to investigate the existence of systematic errors, define correction factors and estimate the uncertainty associated with the recovery of the analytical method [221]. Subsequently, the average recovery ($\bar{R}$) was calculated according to Equation 15, for each concentration range.

$$R_i = \frac{C_{obs}}{C_{fort}} \qquad \textit{Equation 14}$$

$$\bar{R} = \frac{\sum_{i=1}^{p} R_i}{p} \qquad \textit{Equation 15}$$

Where:
p represents the number of groups (days);
R_i is the average recovery of n replicates obtained under repeatability conditions.

Using the *Student's t-test*, the test value (t_{exp}) was calculated by Equation 16, in order to ascertain whether the average percentage recovery was statistically different from the unit (which corresponds to 100%) for each concentration range [221, 338].

$$t_{exp} = \frac{|1 - \bar{R}|}{U_{\%\bar{R}}} \qquad \textit{Equation 16}$$

$$U_{\%\bar{R}} = \frac{S_{obs}}{\sqrt{p}} \qquad \textit{Equation 17}$$

Wherein:
$U_{\%\bar{R}}$ represents the uncertainty in average recovery;
S_{obs} is the standard deviation of p values of R_i obtained under intermediate conditions

The test value is compared against the value obtained from the two-tailed critical value (t_{crit}), for $p - 1$ degrees of freedom and 95% of confidence level.

If $t_{exp} \leq t_{crit}$, then $\bar{R}$ is not significantly different from 100% [334] and $U_{\bar{R}}$ is calculated according to Equation 18. However, if $t_{exp} > t_{crit}$, then $\bar{R}$ is significantly different from 100%. When no correction factors are introduced, $U_{\bar{R}}$ is calculated according to Equation 19. In this case, the uncertainty is increased in order to adjust this additional uncertainty factor [339].

$$U_{\bar{R}} = \frac{U_{\%\bar{R}}}{\bar{R}} \qquad \textit{Equation 18}$$

$$U_{\bar{R}} = \frac{\sqrt{(U_{\%\bar{R}})^2 + \left(\frac{1 - \bar{R}}{k}\right)^2}}{\bar{R}} \qquad \textit{Equation 19}$$

Where:
k is the coverage factor, which was used to calculate the expanded uncertainty.

2.6.4.6. Analyte recovery and matrix effect

The integration of an extractive step into an assay procedure entails an unavoidable loss of analyte. The analyte recovery can indicate the effectiveness of an analytical method by the comparison of the response obtained by the detector from a sample with an amount of analyte, previously extracted, and the response of that detector to the same amount of analyte theoretically present (no extraction) [340]. The recovery does not need to be 100%, but should be as close as possible to it, as long as it is reproducible and the method has adequate accuracy [341].

The extraction recovery study was performed by comparing 2 sets of blank oral fluid samples in triplicate. In one of the sets, the samples were fortified with the analytes under study in the three concentration levels used for precision (40, 100 and 180 ng/mL), being later subjected to extraction

with both methodologies (MEPS and µSPEed). In the second set, the oral fluid samples were subjected to extraction by both methods, the extracts being subsequently fortified with the same analytes, in the three concentration ranges mentioned above.

The extraction recovery (R%) and extraction efficiency (EE%) were calculated according to the following Equations:

$$R\ (\%) = \frac{Area\ A}{Area\ B} \times 100 \qquad \textit{Equation 20}$$

$$EE\ (\%) = \frac{Area\ A}{Area\ C} \times 100 \qquad \textit{Equation 21}$$

Where:

$Area\ A$ is the relative area obtained with extraction (spiked samples before extraction); $Area\ B$ is the relative area of the analyte peak obtained without extraction (eluate fortified after extraction; and $Area\ C$ is the relative area of a standard solution at the same concentration.

These parameters also allows investigating the existence of systematic errors, defining correction factors and, if relevant, estimating the uncertainty associated with the method recovery as input data for the uncertainty calculation procedure [221]. In the current work, this statistical part of the recovery was not investigated since the evaluation of this parameter was previously calculated when optimizing the extraction techniques.

Regarding matrix effect, this parameter is equally important in the validation of an analytical method, as it is one of the main causes of errors in bioanalytical analysis. Matrix effects are often caused by the alteration of ionization efficiency of target analytes in the presence of co-eluting compounds in the same matrix and can be observed either as a loss in response (ion suppression) or as an increase in response (ion enhancement) [342].

Since the matrix effect is related to the change in the ionization of a compound, this parameter becomes more relevant when the analytical method involves MS, not being considered for most method validations if they do not influence reproducibility or assay linearity [343]. However, even with conventional detectors (i.e., UV/VIS, FID) it became evident that different sample matrices present peculiar interfering compounds, and the importance of using appropriate spiked matrix calibrators in order to get reliable quantitative results was recognized [344].

In this sense, the evaluation of matrix effect (ME %) was established at the same concentrations used on the recovery studies. The relative area obtained by fortifying post-extraction ($Area\ B$) was compared with those obtained by the standard solution at the same concentration ($Area\ C$) (see Equation 21).

$$ME\ (\%) = \frac{Area\ B}{Area\ C} \times 100 \qquad \textit{Equation 22}$$

2.6.4.7. Stability studies

Stability can be defined as the lowering of the analyte content in the sample over a period of time. Analyte stability must be ensured during the sample collection, processing, storage, handling, extraction, and duration of the analysis in order to generate reliable (bio)analytical data. Therefore, the stability tests can be among the most time-consuming tests in the validation procedure.
In Aldlgan *et al.* [177] review, it is reported that due to the stability issue of SCs, it is recommended to keep samples frozen whenever possible and sample extracts should be analysed shortly after extraction.

In this work, stability tests were conducted in triplicate at the same concentration levels used in the previous parameters. The spiked samples were storage at three different temperatures (4, -20 and -80°C) and for three time periods, namely 1, 15 and 30 days. On the day of each analysis, the samples were brought to room temperature and the extraction procedures with both methodologies (MEPS and µSPEed) were carried out.

3. Results and Discussion

3.1. Optimization of UHPLC conditions

Chromatographic conditions were optimized to achieve a suitable compromise between separation, resolution, and analysis time. After selecting the best gradient program for each column, a factorial design was applied being evaluated the following parameters: column flow (300, 350, 400 and 450 µL/min) and column temperature (30, 35 and 40°C) for each column under study, namely the CORTECS, BEH, HSS T3, and CSH.

From the general point of view and according to the chromatographic profiles, HSS T3 column presented the best separation of the analytes when compared to the other columns (see Figure S10). The best separation conditions obtained for CORTECS column were 40°C with a flow of 300 µL/min and using the following gradient program: 50% during half minute, then an increase to 70% ACN during 2 min, following an increase of 20% during 2 min and finally decreased to the initial conditions with a total run time of 12 min.

With BEH column it was not possible to obtain a good separation of the analytes, however the best conditions were obtained at 35°C and 350 µL/min of flow. The best gradient program was obtained using the same initial conditions used with CORTECS column, namely 50% of solvent, then an increase of organic solvent of 10% during half minute, followed by a second increase to 80% until 9 min and finally decreased to initial conditions to a total run time of 11 min.

The CSH column presented the worst chromatographic profile not being possible to achieve the separation of all analytes, even with changes in gradient, temperature, and flow.

Finally, with HSS T3 column, an excellent separation of all analytes was achieved using 35°C as column temperature and a flow rate of 350 µL/min. The best gradient program is described in the section 2.4.

Comparing the specifications of all columns tested, chemically all the four stationary phases are C_{18} and the separation mode is reverse phase. The main difference between them is the particle size, being HSS T3 column the one with the largest particle size (1.8 µm). Moreover, HSS T3 column presents medium silanol activity, while the remaining columns show low silanol activity [345]. These differences may justify the obtained results.

To measure the separation of analyte peaks, the *Rs* between consecutive peaks was calculated. In Table 19 is shown the comparison of *Rs* and *N* values for the tested columns with the best separation conditions described above.

Table 19. Resolution values (Rs) and number of theoretical plates (N) for the four tested columns.

	Column							
	CORTECS		**BEH**		**CSH**		**HSS T3**	
Peak no.	*Rs*	*N*	*Rs*	*N*	*Rs*	*N*	*Rs*	*N*
1	1.2	4648	1.0	3325	1.1	2679	1.4	4131
2	0.9	6539	0.9	4244	0.6	3620	1.3	7010
3	2.3	4919	1.9	2427	2.1	4464	2.5	6383
4	3.3	5138	2.5	2361	2.2	3045	3.0	4990
5	3.1	8288	3.0	4589	2.0	4386	3.4	10041
6	4.4	9770	3.3	5738	2.6	4562	5.5	10003
7	-	12547	-	3909	-	4786	-	12511

The goal in chromatography is to obtain the highest resolution possible, avoiding coelution. This is an issue because two coeluting peaks will mix together in the detector. This is the reason why it is important to achieve baseline resolution ($RS \geq 1.5$) [346]. As can be seen in Table 19, although the first two peaks present values below 1.5, the greater *Rs* values were achieved for HSS T3 column. Regarding the number of plates, the higher *N* value, the greater the efficiency of the column and the

better the potential for separation [346]. In general BEH and CSH columns presented the lowest number of plates being the columns with the lowest efficiency, whereas CORTECS and HSS T3 the most efficient columns.

Given the results, the column HSS T3 was chosen for the following analysis.

3.2. Identification and isolation of SCs from seized herbal samples by UHPLC-PDA

To complement the results obtained by GC-MS and NMR (described in Chapter I), the methanolic extracts of herbal samples were analysed by UHPLC-PDA (see Figure S11).

The scanning of the absorption spectrum between 200 and 400 nm, allowed to acquire the maximum wavelength for each analyte and compare the PDA spectra with those previously reported in the literature. In Figure 55 the UV spectra of each synthetic cannabinoid identified in the herbal samples is presented.

Due to the absence of analytical standards, one of the aims of this work was the isolation of the SCs identified in the seized herbal samples using UHPLC. Based on the results presented in Chapter I, samples H1, B54, B63, C58 and C60 were chosen according to the contents previously identified by GC-MS analysis. In Table 20 is presented the total extract volume injected in the UHPLC system and the mass obtained for each isolated compound.

To verify the success of the isolation of each compound, the collected fractions were re-injected in the UHPLC system and analysed by GC-MS. The UHPLC and GC-MS chromatographic profiles of each isolated compound are shown in Figures S12 and S13 (supplementary material).

The UHPLC chromatograms confirmed the purity of the isolated substances and provided an estimate of purity of 100% calculated using the ratio of the peak area to the total area under the chromatogram for all the compounds at their maximum wavelength, except for MAM-2201 whose purity was estimated at 98.8%. In addition, a spectrum scan was carried out between 220 and 400 nm to verify the presence of any impurity. The GC-MS data also confirmed the isolation of the compounds, giving a positive match with existing libraries.

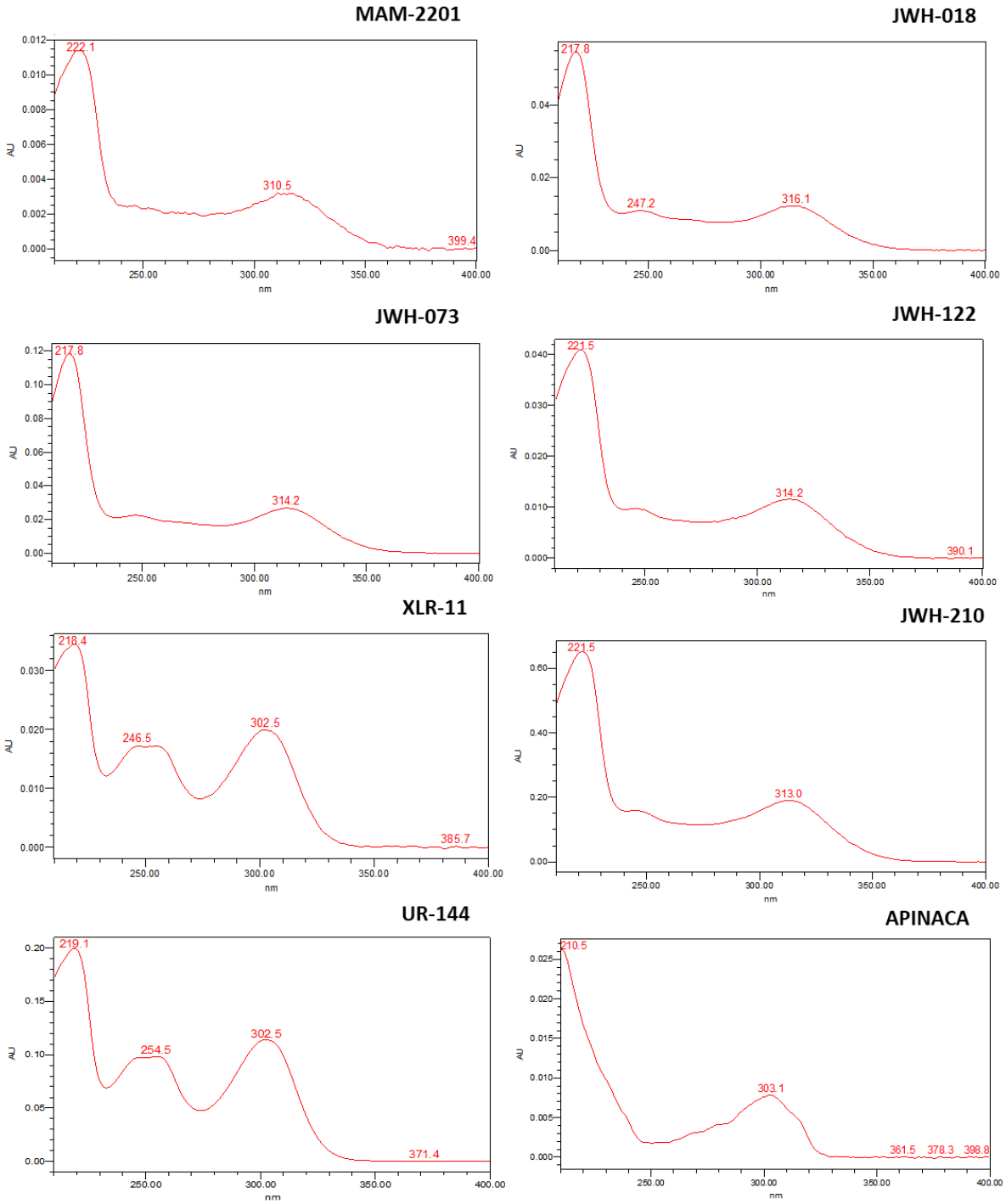

Figure 55. UV Spectra of SCs identified in the seized herbal samples.

Table 20. Total extract volume and final mass of each isolated compound.

Sample extract	Total extract volume (µL)	Isolated Compound	Mass (mg)
B54	700	APINACA	1.3
		UR-144	1.3
C58	940	XLR-11	1.7
		MAM-2201	1.7
H1	690	JWH-122	2.5
B63	450	JWH-210	3.6
C60	650	JWH-073	1.0
		JWH-018	1.2

In order to complement the UHPLC and GC-MS data, TLC was performed with the fractions of the isolated compounds, as well as with the sample extracts (see Figure S14).

Figure 56 represents the UHPLC-PDA chromatogram with the mixture of SCs previously isolated. Peak number and Rt of each compound are described in Table 21.

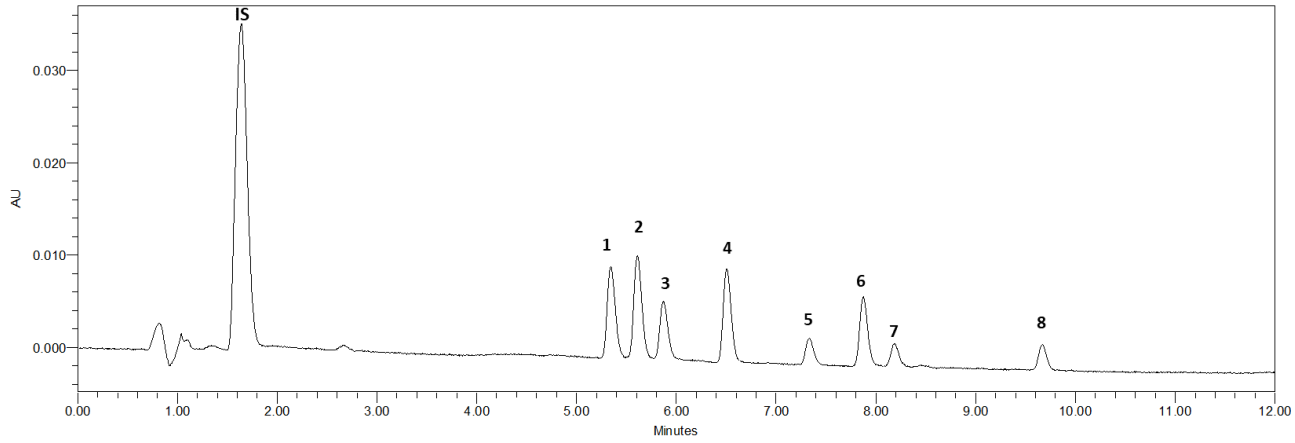

Figure 56. UHPLC-PDA chromatogram of a mixture of the isolated SCs with a concentration of 200 ng/mL at 254 nm. (IS – internal standard, 1-MAM-2201, 2- JWH-073, 3- XLR-11, 4- JWH-018, 5- JWH-122, 6- UR-144, 7- JWH-210, and 8- APINACA).

Table 21. Identification of the peaks, Rt and maximum wavelength of each compound.

Peak	Compound	Rt (min)	Wavelength (nm)
IS	IAA	1.630	279
1	MAM-2201	5.221	310
2	JWH-073	5.492	314
3	XLR-11	5.737	302
4	JWH-018	6.395	316
5	JWH-122	7.224	314
6	UR-144	7.784	302
7	JWH-210	8.085	313
8	APINACA	9.618	303

3.3. Optimization of MEPS extraction parameters

In order to maximize MEPS extraction efficiency, several experimental parameters such as sorbent selection, sample volume, number of extraction cycles, and elution conditions were optimized using a univariate experimental design to establish analyte partition equilibrium in shorter analysis time and obtain adequate sensitivity for the analysis by UHPLC-PDA.

The initial MEPS procedure was performed using 250 µL of MeOH followed by 250 µL of H_2O 0.1% FA for conditioning step. An aliquot of 150 µL of spiked oral fluid sample was passed three times through the sorbent, then washed with 100 µL of H_2O 0.1% FA and finally eluted with 250 µL of MeOH.

The entire optimization process was performed in triplicate, using blank oral fluid samples spiked with the isolated SCs from herbal samples, at a concentration of 200 ng/mL. The extraction efficiency was determined by the average total peak area response observed on UHPLC-PDA and %RSD.

3.3.1. Sorbent selection

The selection of the appropriate sorbent is an important factor, as it is directly related to the chemical nature of the analyte of interest and the matrix in which it is found. Therefore, five different MEPS sorbents, namely C_8, C_{18}, HDVB, Sil, and M_1, were tested under the same extraction conditions. Figure 57 shows the UHPLC-PDA response of the analytes under study for the different sorbents studied.

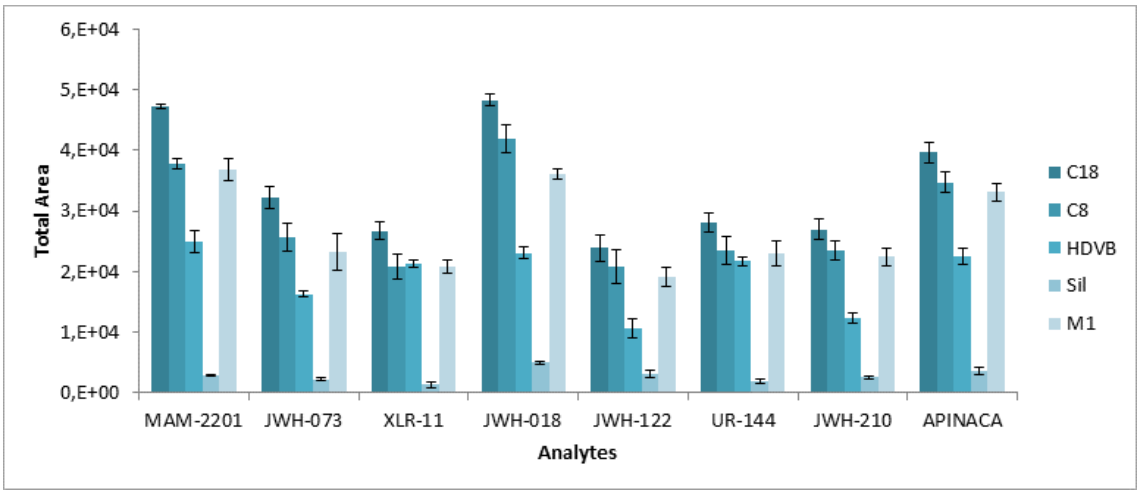

Figure 57. Comparison of extraction efficiency of the different MEPS sorbents tested for each synthetic cannabinoid. Values expressed as mean ± SD (n=3).

The performance of each MEPS sorbent was evaluated in terms of intensity of the response observed (peak area) and reproducibility. According to the results, C_{18} provided the best extraction efficiency for all the analytes, followed by C_8 and M_1 sorbents. In turn, HDVB and Silica sorbents presented lower or even unsatisfactory retention of the SCs under study. As mentioned in Table 6 (Part 1 – Chapter II), C_2-C_{18} sorbents are more suitable for non-polar analytes, while silica or polymeric phases like HDVB are better for polar analytes such as acidic and basic compounds. The fact that the analytes under study are non-polar, allowed a high affinity towards the silica sorbent functionalized with an octadecyl group, through *van der Waals* or dispersion interactions. Analytes are strongly retained due to attractive forces between carbon-hydrogen bonds on the analyte molecules and non-polar functional groups on the sorbent surface [214].

After choosing the best sorbent, the number of extraction cycles and sample volume were optimised.

3.3.2. Sample volume and extraction cycles

The number of extraction cycles is an important parameter, since it influences the retention of analytes in the solid phase of the sorbent [347]. The sample can be drawn up and down through the needle into the syringe, once or several times (cycles). There are two ways to performed the multiple extraction cycles: draw-eject (discard in the same vial of the sample) or extract-discard (discard in a waste vial) [348]. The first option was selected for this study.

Generically, MEPS procedures use one or more extraction cycles, providing an opportunity for optimization. When the sample passes several times through the sorbent the interaction of the analytes with the solid phase is greater, enabling a higher extraction efficiency [349].

Since MEPS is a technique that aims to decrease the sample volume used, it is also necessary to optimize this parameter. In this regard, the number of extraction cycles and sample volume were optimised by testing 1, 3 and 5 cycles on aliquots of 50, 100, 150, 200 and 250 µL of spiked oral fluid samples. The influence of the number of extraction cycles and sample volume on MEPS performance is illustrated in Figure 58.

The flow rate during aspiration, is equally important as it prevents cavitation phenomena, and increases the interaction time of the analyte with the sorbent, thus increasing the extraction efficiency. Thereby, the flow rate was limited to 20 µL/s.

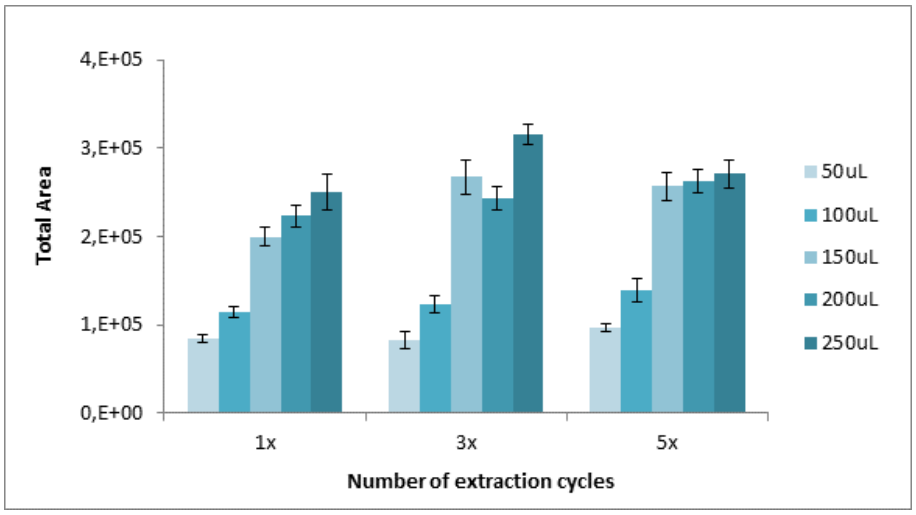

Figure 58. Influence of the number of extraction cycles and sample volume in MEPS procedure. Values expressed as average total peak areas ± SD (n=3).

According to the results, it can be observed that the competition for the active adsorption sites of the C_{18} sorbent increases with the number of cycles. On the other hand, a biological sample, such as oral fluid, can saturate the stationary phase and prevent the access of the analytes to the adsorption sites already blocked by interferences. For this reason, 3 cycles of extraction were selected due to the good efficiency and the possibility of extending the lifetime of the sorbent.

Regarding the sample volume, there is a gradual increase of the areas as the sample volume increases. The results showed that a volume of 250 µL and 3 cycles are sufficient to obtain a good extraction efficiency.

3.3.3. Solvent effect and elution volume

In relation to the desorbing conditions, the solvent and its volume were investigated to ensure effective elution of the analytes from the sorbent. A good elution solvent should overcome the primary and possibly secondary interactions in which the analyte may be subjected. It is recommended that the elution solution should be pure and have a high solvent percentage (≥60 %) and/or mixed with acid or basic solutions (0.1–3%). In addition, it should elute the analyte using the smallest possible volume [348]. In this work, three different solvents (MeOH, ACN and 2-propanol) were assayed and compared (Figure 59).

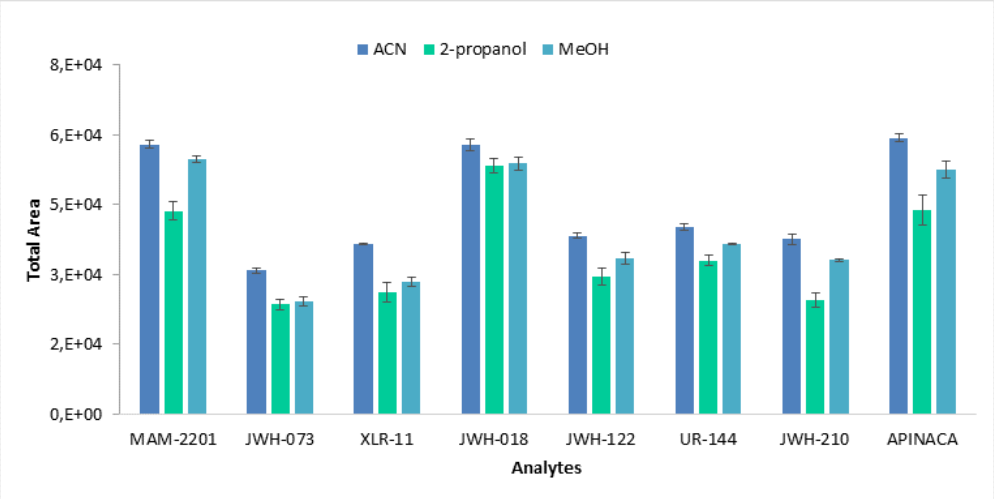

Figure 59. Influence of the elution solvent for each analyte in MEPS procedure. Values expressed as mean ± SD (n=3).

As can be seen in Figure 59, the results indicate that the best extraction efficiency was obtained using ACN as elution solvent for all the SCs, while 2-propanol presented the lowest extraction efficiency and higher SD values.

After selecting the best elution solvent, different volumes (50, 150, 250, 350 and 500 µL) were studied (Figure 60). The analyte response was observed to increase up to 250 µL elution volume, then decreased with higher volumes. This can be justified by a possible dilution effect with higher volumes. Therefore, a volume of 250 µL was selected for desorption of analytes.

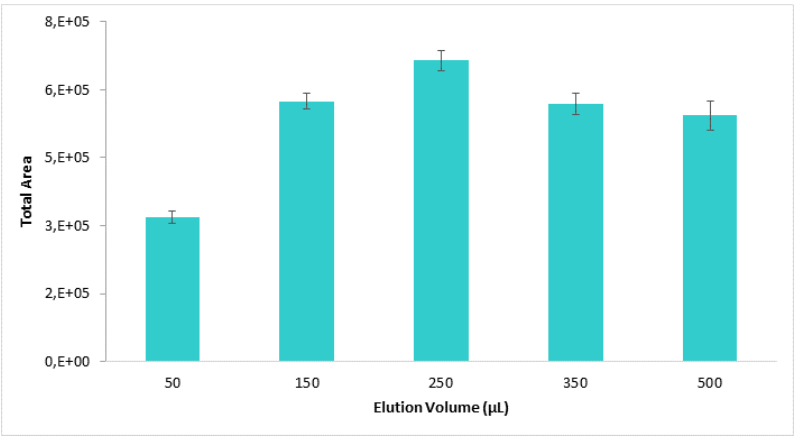

Figure 60. Influence of elution volume in MEPS procedure. Values expressed as average total peak areas ± SD (n=3).

Overall, the best MEPS conditions were obtained by loading three times 250 µL of spiked oral fluid samples through the C_{18} sorbent and elution of the SCs with 250 µL of ACN. These results contrast with those obtained by Sorribes-Soriano *et al.* [241], whose work was the development of a procedure for the determination of third generations SCs in oral fluid samples using MEPS followed by GC-MS as methodology. Some of extraction parameters were evaluated, such as number of

loading cycles, elution solvent, elution volume and sample pH. According to the authors, the best extraction conditions were obtained using a C_{18} sorbent, with five charge/discharge cycles of 100 µL of spiked oral fluid sample and desorbing the analytes with 5 cycles of 50 µL of 2-propanol. The main difference is found in the elution solvent, where MeOH, 2-propanol and chloroform were evaluated as elution solvents. Although MeOH was suitable for the extraction of most of the SCs analysed, 2-propanol was selected by the authors because of the best RSD values.

Regarding to the sample pH, this parameter was not evaluated in the present work since SCs do not show any protonation/deprotonation at physiological pH and no pKa values are reported for these compounds [241]. The same authors evaluated pH of the loading step (5.0, 7.0, and 9.0) and as they already expected, no significant changes in the obtained recovery values were observed.

3.4. Validation of the analytical method for the analysis of SCs by MEPS/UHPLC-PDA

3.4.1. Selectivity

Method selectivity was evaluated considering the peak shape, Rt and chromatographic purity of the spectrum, in order to detect possible interferences. The analytes were identified by comparing the Rt and maximum wavelength (λ_{max}) previously determined by injecting individual solutions of the isolated compounds (see Table 21).

All oral fluid samples were analysed under the same conditions and were free of interference peaks from endogenous matrix substances at the Rt of each analyte and the IS, demonstrating the selectivity of the assay. Representative chromatograms of blank oral fluid sample and spiked oral fluid samples with SCs are shown in Figure S15.

3.4.2. Linearity and working range

The linearity of the MEPS/UHPLC-PDA method was studied by constructing eight calibration curves (one for each substance), with 8 concentration points ranging from 40 to 180 ng/mL, in triplicate.

Each calibration curve was graphically constructed by relating the ratio of the areas (analyte area/IS area) to the concentrations of the analyte by applying the ANOVA tool (Figure S16).

The linearity results are summarised in Table 22 and the statistical regression studies are presented in the Supplementary Material III. The linear regression analysis by least squares method

showed values of *R* and R^2 higher than 0.99 for all compounds under study and the intercept was close to zero, considering a 95% confidence interval.

Regarding the evaluation of the residuals along the concentration values, no trends were observed, i.e., all residuals showed a deviation of less than 10%.

Table 22. Summary of linear regression model results for the SCs under study by MEPS/UHPLC-PDA.

Synthetic Cannabinoid	Equation	*R*	R^2	$S_{y/x}$	Intercept 95% confidence interval	
					Lower	Upper
MAM-2201	$y = 0.1397x - 1.9052$	0.998	0.996	0.486	-3.769	-1.063
JWH-073	$y = 0.0813x - 1.1152$	0.998	0.996	0.266	-2.118	-0.771
XLR-11	$y = 0.0775x - 0.7514$	0.997	0.994	0.309	-1.935	-0.242
JWH-018	$y = 0.1395x - 2.4355$	0.998	0.997	0.431	-3.931	-2.255
JWH-122	$y = 0.0558x - 0.2059$	0.998	0.996	0.196	-0.042	0.943
UR-144	$y = 0.0840x - 1.0148$	0.998	0.996	0.279	-2.057	-0.241
JWH-210	$y = 0.0760x - 0.2256$	0.999	0.997	0.219	-0.934	-0.239
APINACA	$y = 0.1202x - 1.9956$	0.998	0.996	0.412	-3.465	-1.727

As previously mentioned, the estimates obtained in the regression and the graphical representation are not sufficient to establish the linearity. Thus, two regression models: linear and non-linear (polynomial) were assessed. Through the Mandel test, it was possible to evaluate which of the models provided the best fit to the calibration points. Table 23 presents the *TV* values calculated according to Equation 6 (section 2.6.4.2.), and the Snedecor's F distribution values (F_{crit}).

According to the previously established criteria, as the *TV* values were lower than the F_{crit} values (0.95;1;N-3) for all SCs, the results showed that the linear model is the one that best fits the points of each calibration curve, within the working range.

Table 23. Results of the Mandel test for the SCs under study by MEPS/UHPLC-PDA.

Synthetic Cannabinoid	*TV*	F_{crit} (0.95;1;N-3)
MAM-2201	0.480	
JWH-073	0.313	
XLR-11	0.148	
JWH-018	1.114	6.608 *F* (0.95;1;4)
JWH-122	0.504	
UR-144	0.003	
JWH-210	0.311	
APINACA	0.808	

3.4.3. Limit of detection and limit of quantification

As previously mentioned, there are several methods for the determination of LODs and LOQs. In this work, these two parameters were studied using the calibration method. The calculation was performed using Equations 7 and 8 (section 2.6.4.3.), based on the data of the calibration curves obtained in the linearity for each compound under study. The calculated LOD and LOQ values are shown in Table 24.

Table 24. LOD and LOQ values calculated for each synthetic cannabinoid by MEPS/UHPLC-PDA.

Synthetic Cannabinoid	LOD (ng/mL)	LOQ (ng/mL)
MAM-2201	11.5	34.8
JWH-073	10.8	32.8
XLR-11	13.2	39.9
JWH-018	10.2	30.9
JWH-122	11.6	35.2
UR-144	11.0	33.2
JWH-210	9.50	28.8
APINACA	11.3	34.3

The obtained LOD and LOQ values ranged from 9.5 to 13.2 ng/mL and from 28.8 to 39.9 ng/mL, respectively, being satisfactory, taking into account the small sample volume (250 µL) and using UHPLC-PDA as analytical methodology. Comparing these results with other works it can be considered that they are acceptable.

Rocchi *et al.* [248], developed a rapid sample preparation based on protein precipitation and MEPS techniques followed by UHPLC-MS/MS for quantitative analysis of several NPS classes including SCs in oral fluid samples. The authors reported lower LOD (0.005 to 0.275 ng/mL) and LOQ values (0.015 to 0.820 ng/mL) for the SCs analysed. These results were expected considering the type of detector used in the study. However, in Sorribes-Soriano *et al.* [241] work the LOD and LOQ values ranged from 10 to 20 µg/L and from 30 to 60 µg/L, respectively using a GC-MS, with our results being in agreement with those obtained by this study.

3.4.4. Precision studies and accuracy

Precision was assessed in terms of repeatability and intermediate precision. For this purpose, three different concentration levels, low (LL), medium (ML), and high level (HL) of the calibration curve (40, 100 and 180 ng/mL, respectively) were prepared by fortification of blank oral fluid samples.

Repeatability was assessed simultaneously with the first day of the intermediate precision study, with three replicates being analysed on the same day. After applying the method, the relative areas were obtained for each substance and the mean, *SD* and *CV* or *RSD* were calculated, according to Equations 9 and 10.

To evaluate the intermediate precision, three replicates of each level were also analysed during five non-consecutive days (n = 15) and a calibration curve for each day was determined. Once the test procedure was applied, the results of this study were treated by applying single factor ANOVA using the expressions in Table 17 and Table 18. The results obtained from these expressions are summarized in Table 25. The detailed Tables, with the data of the calibration curves obtained for intermediate precision, as well as the statistical treatment of these results, for each synthetic cannabinoid, are presented in Supplementary Material III.

The experimental methodology used for the study of accuracy was the same as that described for intermediate precision. This was expressed as *Bias* for the three concentration levels and calculated according to Equation 13. The *Bias* results are also shown in Table 25.

Table 25. Summary of the results obtained for the study of precision and accuracy of the method, for each synthetic cannabinoid by MEPS/UHPLC-PDA.

Synthetic Cannabinoid	Concentration (ng/mL)		Repeatability (S_r)	Precision between groups (S_{run})	Intermediate precision (S_1)	*CV* (%)	*Bias* (%)
	theoretical	measured					
MAM-2201	40	39.9	0.75	2.81	2.91	7.30	-0.35
	100	100.2	4.48	4.26	6.18	6.16	0.25
	180	179.9	3.51	0.67	3.57	1.99	-0.06
JWH-073	40	40.3	2.48	0.97	2.66	6.61	0.67
	100	99.5	3.35	2.33	4.08	4.10	-0.47
	180	180.2	1.94	0.49	2.00	1.11	0.11
XLR-11	40	41.8	0.89	1.44	1.70	4.07	4.47
	100	96.9	1.10	2.62	2.84	2.93	-3.13
	180	181.4	1.76	0.59	1.85	1.02	0.75
JWH-018	40	39.2	0.67	1.19	1.36	3.45	-1.06
	100	100.7	1.93	1.89	2.70	2.68	0.74
	180	179.7	1.30	0.50	1.40	0.78	-0.18
JWH-122	40	39.2	0.48	1.92	1.98	5.04	-2.02
	100	101.4	2.22	3.14	3.84	3.79	1.41
	180	179.4	0.42	1.43	1.49	0.83	-0.34
UR-144	40	40.8	0.22	1.75	1.76	4.32	1.92
	100	98.7	2.27	2.77	3.58	3.63	-1.34
	180	180.6	1.38	1.04	1.73	0.96	0.32
JWH-210	40	39.9	0.62	0.89	1.08	2.72	-0.35
	100	100.2	2.49	0.87	2.63	2.63	-0.01
	180	179.9	1.18	0.21	1.20	0.67	0.00

	40	41.2	0.29	0.99	1.03	2.50	2.98
APINACA	100	97.9	0.66	1.69	1.81	1.85	-2.01
	180	180.9	0.53	0.67	0.86	0.47	1.12

It is possible to verify that the *CV* values obtained for intermediate precision are equal or lower than 7.3%, being in accordance with the criteria of Relacre and Eurachem guides.

Regarding accuracy, the absolute values vary between 0.002 and 4.5%, which are within the limits considered acceptable: ±20% near the LOQ and ±15% in the other concentrations. However, the presence of systematic errors (trends) was also investigated for this parameter, for each concentration level. For this purpose, a statistical test was used to infer whether the mean recovery (%) was statistically different from unity. The results obtained are described in the following Table.

Table 26. Summary of the results of the hypothesis test (t-Student test) for the study of systematic errors associated with the method recovery by MEPS/UHPLC-PDA.

Synthetic Cannabinoid	**Concentration (ng/mL)**	$\bar{R}$	t_{exp}	t_{crit} **(N-1;0,95)**
MAM-2201	LL	99.6	0.11	2.78
	ML	100.2		
	HL	99.9		
JWH-073	LL	100.7	0.35	
	ML	99.5		
	HL	99.5		
XLR-11	LL	104.5	2.61	
	ML	96.9		
	HL	100.7		
JWH-018	LL	98.9	0.75	
	ML	100.7		
	HL	99.8		
JWH-122	LL	98.0	0.93	
	ML	101.4		
	HL	99.7		
UR-144	LL	101.9	0.98	
	ML	98.7		
	HL	100.3		
JWH-210	LL	99.7	0.32	
	ML	100.0		
	HL	100.0		
APINACA	LL	103.0	1.64	
	ML	98.0		
	HL	101.1		

The results revealed that t_{exp} is lower than t_{crit} for a 95% confidence interval for all SCs, concluding absence of systematic errors, thus proving the accuracy of the method. Furthermore, the recovery rate values are within the range, defined by a 20% margin of error (ranging between 80 and 120%) [350].

3.4.5. Analyte recovery and matrix effect

Recovery and extraction efficiency studies were carried out according to the procedure described in section 2.6.4.6. Table 27 shows the values obtained from the evaluation of these two parameters through Equations 20 and 21, by MEPS for the compounds under study. The calculated values of the matrix effect can also be found in the following Table for the same concentration levels.

Table 27. Results of the determination of recovery, extraction efficiency and matrix effect by MEPS for three concentration levels.

Synthetic cannabinoid	LL			ML			HL		
	R (%)	EE (%)	ME (%)	R (%)	EE (%)	ME (%)	R (%)	EE (%)	ME (%)
MAM-2201	73.5	76.7	104.3	82.2	72.5	88.2	92.6	86.1	93.0
JWH-073	76.8	77.1	100.4	73.7	70.8	96.1	75.1	90.8	84.5
XLR-11	86.4	89.8	103.9	74.0	71.9	97.1	73.6	70.8	96.2
JWH-018	87.8	79.2	90.1	78.1	71.6	91.8	72.8	71.8	98.7
JWH-122	85.6	89.0	104.0	85.7	75.0	87.4	74.8	72.4	96.9
UR-144	78.0	85.3	109.4	89.3	87.8	98.3	90.4	98.8	109.3
JWH-210	86.1	91.3	106.1	89.9	80.3	89.3	78.6	73.4	93.3
APINACA	79.3	81.5	102.8	73.8	70.4	95.4	75.0	71.5	95.3

The recovery values ranged from 73 and 93% and from 70 and 99% for extraction efficiency for all SCs. These results are acceptable with no significant loss of each analyte in the extraction process. Thus, we can consider that the proposed MEPS/UHPLC-PDA procedure is suitable for the extraction of SCs in oral fluid samples. In Rocchi *et al.* [248] work, the recovery values obtained for the SCs ranged from 49 and 96%, using the same extraction technique followed by UHPLC/MS-MS, with our results being higher than those obtained by this study.

Regarding matrix effect results, the values ranged from 85 and 109%. It is considered absence of matrix effect when ratio value is in the range of 85–110% [348]. Based on the obtained results no matrix effect was observed.

3.4.6. Stability studies

Stability tests were conducted with spiked oral fluid samples processed by MEPS. Storage solutions at -20°C did not change significantly for any of the compounds in short and long term (Figure S17). However, regardless of whether the analysis is carried out within a short period of time, it is recommended that oral fluid samples should be analysed as soon as possible after collection and be kept stored frozen [248].

3.5. Optimization of µSPEed extraction parameters

After literature search, to the date of this work, no application of µSPEed in the extraction of SCs in oral fluid samples was found. Therefore, as in MEPS procedure, some experimental parameters were optimized (cartridge selection, sample volume, number of extraction cycles, and elution conditions).

The initial µSPEed procedure was performed using 250 µL of MeOH followed by 250 µL of H_2O 0.1% FA for conditioning step. An aliquot of 100 µL of spiked oral fluid sample was passed five times through the sorbent, then washed with 100 µL of H_2O 0.1% FA and finally eluted with 250 µL of MeOH.

As in MEPS, the entire optimization process was performed in triplicate, using spike oral fluid samples concentration of 200 ng/mL and the best conditions were selected by the total peak areas of each analyte, obtained in each parameter.

3.5.1. Sorbent selection

For the selection of the appropriate sorbent, seven available µSPEed cartridges, namely C_8, C_{18}, Sil, PS/DVB, SAX, SCX and Mix, were tested under the same extraction conditions. The UHPLC-PDA response of for the different sorbents is shown in Figure 61.

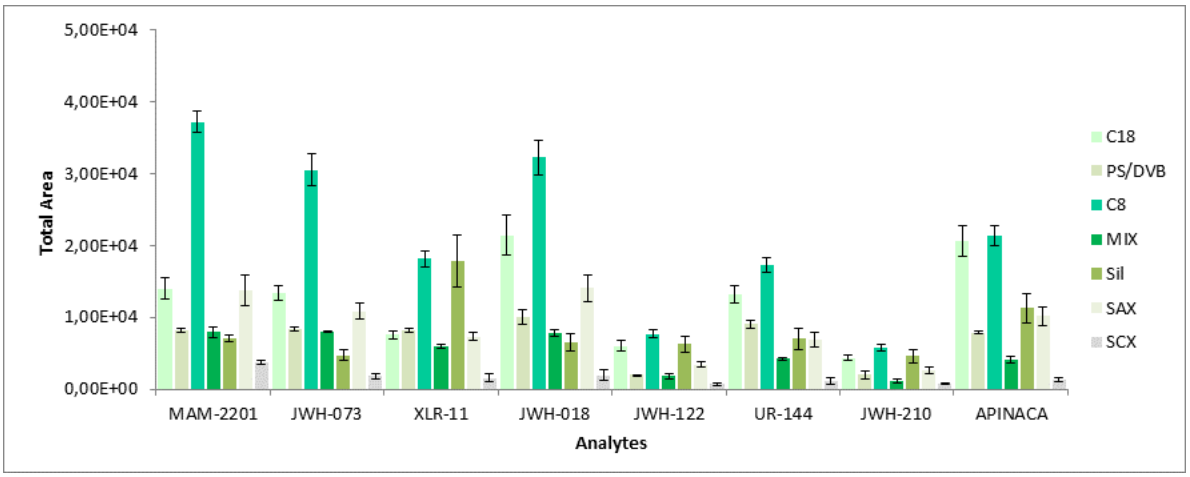

Figure 61. Comparison of extraction efficiency of the different µSPEed sorbents tested for each synthetic cannabinoid. Values expressed as mean ± SD (n=3).

The performance of each µSPEed sorbent was evaluated in terms of peak area and reproducibility. According to the results, C_8 provided the best extraction efficiency for all the analytes, followed by C_{18} sorbent. These results contrast with those obtained by MEPS. One possible reason could be the smaller sorbent particles in µSPEed cartridges which allows greater interaction between the analytes and the silica sorbent functionalized with an octyl group. The worst results were obtained with silica and ionic change sorbents which was already expected.

3.5.2. Sample volume and extraction cycles

The retention of the analytes in µSPEed is also influenced by the number of extraction cycles. Like MEPS, the multiple extraction cycles can be carried out in draw-eject or extract-discard mode and as in MEPS procedure the first option was selected.

The number of extraction cycles and sample volume were evaluated under the same conditions as those tested in MEPS procedure, namely 1, 3 and 5 cycles on aliquots of 50, 100, 150, 200 and 250 µL of spiked oral fluid samples. The flow rate was limited to 500 µL/min.

The influence of the number of extraction cycles and sample volume on µSPEed performance is illustrated in Figure 62.

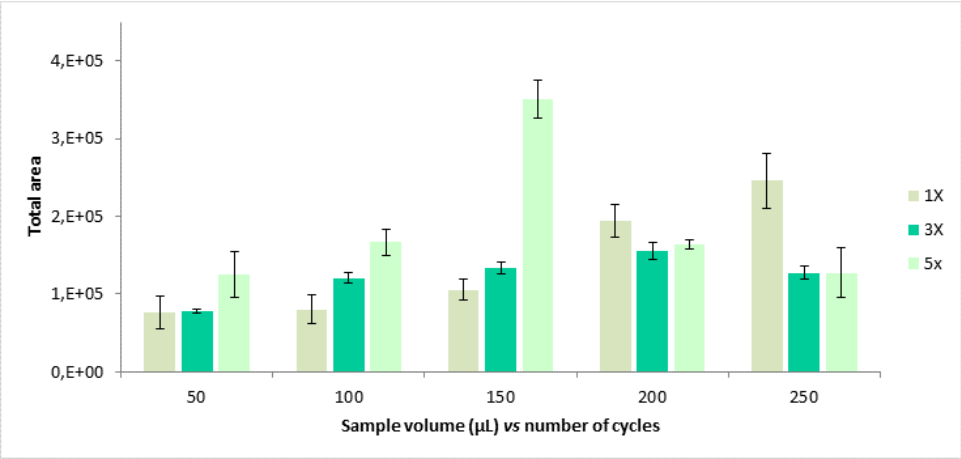

Figure 62. Influence of the number of extraction cycles and sample volume in µSPEed procedure. Values expressed as average total peak areas ± SD (n=3).

According to the results, the best extraction conditions were obtained by passing 5 times 150 µL of sample volume through C_8 sorbent. The competition for the active adsorption sites of the sorbent increases with the number of cycles until 150 µL. However, for higher volumes there is a decrease in analyte retention with increasing number of cycles. This can be explained by the saturation of the stationary phase.

3.5.3. Solvent effect and elution volume

The desorption conditions were the same as those evaluated in MEPS, namely MeOH, ACN and 2-propanol were tested as elution solvents and 50, 150, 250, 350 and 500 µL as elution volumes.

The following Figures (63 and 64) show the results obtained for these optimisation parameters.

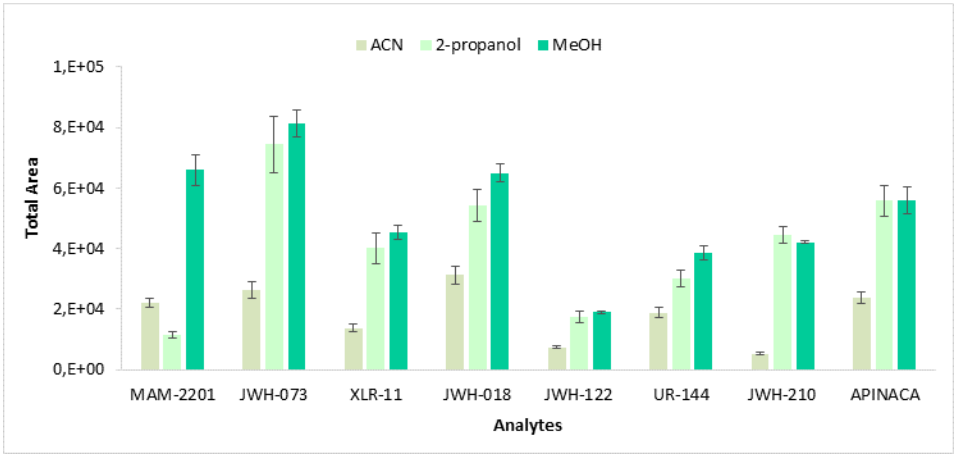

Figure 63. Influence of the elution solvent for each analyte in µSPEed procedure. Values expressed as mean ± SD (n=3).

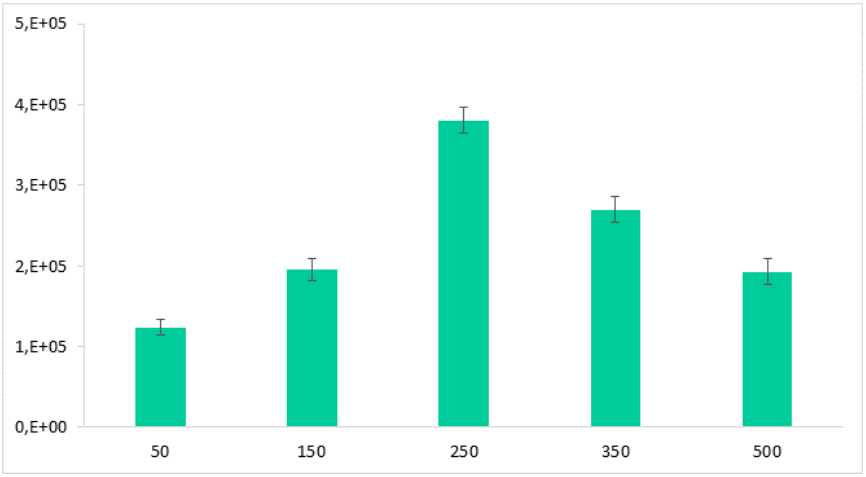

Figure 64. Influence of elution volume in µSPEed procedure. Values expressed as average total peak areas ± SD (n=3).

The results showed that the best extraction efficiency was obtained using MeOH as elution solvent for all the SCs, while ACN presented the lowest extraction efficiency. These results were different from those obtained by MEPS and a possible explanation is that ACN may be reacting with the µSPEed cartridge material, being one of the limitations of this extraction technique.

Regarding elution volume, the analyte response was observed to increase up to 250 µL elution volume, then decreased with higher volumes. Thus, a volume of 250 µL was selected for desorption of analytes.

3.6. Validation of the analytical method for the analysis of SCs by µSPEed/UHPLC-PDA

3.6.1. Selectivity

The selectivity of the µSPEed method was also defined by evaluating the chromatographic purity of the spectrum, taking into account the peak shape, the Rt and the UV absorption spectrum, for the detection of possible matrix interferents. Representative chromatograms of blank oral fluid sample and spiked oral fluid samples with SCs are shown in Figure S18.

All oral fluid samples were analysed under the same conditions and by comparing the chromatograms it was found that no interference of matrix constituents at the Rt of each analyte and maximum wavelength was detected, demonstrating the selectivity of the assay.

3.6.2. Linearity and working range

The linearity of the µSPEed/UHPLC-PDA method was also studied by constructing eight calibration curves, with 8 concentration levels (40 to 180 ng/mL), in triplicate. As in MEPS, each

calibration curve was constructed by relating the ratio of the areas (analyte area/IS area) to the analyte concentrations, by applying the ANOVA tool (Figure S18).

Table 28 summarises the results of this study and the statistical regression studies are summarised in Supplementary Material III.

Table 28 .Summary of linear regression model results for the SCs under study by µSPEed/UHPLC-PDA.

Synthetic Cannabinoid	Equation	*R*	R^2	$S_{y/x}$	Intercept 95% confidence interval	
					Lower	Upper
MAM-2201	$y = 0.1476x - 3.7034$	0.999	0.997	0.411	-4.628	-2.778
JWH-073	$y = 0.0979x - 2.3743$	0.999	0.998	0.224	-2.879	-1.870
XLR-11	$y = 0.0896x - 2.2887$	1.000	0.999	0.120	-2.558	-2.017
JWH-018	$y = 0.1280x - 2.6295$	0.999	0.999	0.240	-3.169	-2.090
JWH-122	$y = 0.0578x - 1.4164$	0.998	0.997	0.177	-1.814	1.019
UR-144	$y = 0.0756x - 2.1335$	0.998	0.997	0.235	-2.663	-1.604
JWH-210	$y = 0.0716x - 1.8584$	0.999	0.998	0.163	-2.224	-1.493
APINACA	$y = 0.0762x - 1.6285$	0.998	0.997	0.226	-2.137	-1.120

The linear regression analysis by least squares method showed values of *R* and R^2 higher than 0.99 for all compounds under study and the intercept was close to zero, considering a 95% confidence interval. Through the evaluation of the residuals, no trends were observed, with a deviation of less than 10%.

Linearity of the µSPEed/UHPLC-PDA methodology was also assessed using Mandel's test in order to verify which of the two regression models, linear and non-linear (polynomial) best fitted the calibration points. The *TV* and F_{crit} values are presented in the following Table.

Table 29. Results of the Mandel test for the SCs under study by µSPEed/UHPLC-PDA.

Synthetic Cannabinoid	*TV*	F_{crit} (0.95;1;N-3)
MAM-2201	0.621	
JWH-073	1.168	
XLR-11	0.006	
JWH-018	0.016	6.608 *F* (0.95;1;4)
JWH-122	0.047	
UR-144	0.048	
JWH-210	0.558	
APINACA	0.050	

As the *TV* values were lower than the F_{crit} values (0.95;1;N-3) for all SCs, the results showed that the linear model is the one that best fits the points of each calibration curve, within the working range, instead of the polynomial function.

3.6.3. Limit of detection and Limit of quantification

These two parameters were studied as in the methodology by MEPS/UHPLC-PDA, i.e., using the calibration method. The calculation of the limits was also performed using Equations 7 and 8, based on the data of the calibration curves obtained in the linearity, for each compound under study. The calculated LOD and LOQ values are shown in Table 30.

Table 30. LOD and LOQ values calculated for each synthetic cannabinoid by µSPEed/UHPLC-PDA.

Synthetic Cannabinoid	LOD (ng/mL)	LOQ (ng/mL)
MAM-2201	9.2	27.9
JWH-073	7.6	22.9
XLR-11	4.4	13.9
JWH-018	6.2	18.7
JWH-122	10.1	30.6
UR-144	10.3	31.1
JWH-210	7.5	22.7
APINACA	9.8	29.7

Since no studies with the application of µSPEed in the extraction of these synthetic compounds in oral fluid samples were found in the literature, we compared the LOD and LOQ values with other microextraction techniques in the same biological sample. The obtained LOD and LOQ values ranged

from 4.4 to 10.3 ng/mL and from 13.9 to 31.1 ng/mL, respectively, being very satisfactory when compared to our MEPS results. Bianchi *et al.* [247] developed and validated a screening and non-invasive method based on the use of MEPS coupled with desorption electrospray ionization-high resolution mass spectrometry for the detection of NPS in oral fluid. The authors obtained LLOQ values in the 0.05 – 0.25 mg/mL range for several SCs, including UR-144 and JWH-122 compounds. Another work [351] used a dispersive liquid-liquid microextraction (DLLME) to extract six SCs (JWH-018, JWH-019, JWH-073, JWH-200, or WIN 55,225, JWH-250, and AM-694) from oral fluids and a HPLC-MS for analyte quantitative determination. The validated method presented LODs an LLOQs in the range of 0.002 - 0.021 ng/mL and 0.004 – 0.035 ng/mL respectively. These values are better than those obtained in this work since MS has the ability to detect/quantify much lower levels.
However, it was found that the technique has great potential, since the LOD and LOQ values are slightly lower than those obtained by MEPS.

3.6.4. Precision studies and accuracy

The precision was evaluated in terms of repeatability and intermediate precision with the same concentration levels (40, 100 and 180 ng/mL) and procedure applied in MEPS. The relative areas for each substance were acquired in replicate and the mean, *SD* and *CV* were calculated.

Accuracy, expressed by *Bias,* was studied using the same experimental methodology described for intermediate precision. The precision and accuracy results are shown in Table 31. The detailed Tables, with the data of the calibration curves obtained for intermediate precision, as well as the statistical treatment of these results, for each synthetic cannabinoid, are presented in Supplementary Material III.

Table 31. Summary of the results obtained for the study of precision and accuracy of the method, for each synthetic cannabinoid by µSPEed/UHPLC-PDA.

Synthetic Cannabinoid	Concentration (ng/mL)		Repeatability (S_r)	Precision between groups (S_{run})	Intermediate precision (S_1)	*CV* (%)	*Bias* (%)
	theoretical	measured					
MAM-2201	40	38.8	0.97	1.75	2.00	5.15	-3.04
	100	102.1	2.74	2.74	3.88	3.80	2.13
	180	179.1	2.22	0.50	2.27	1.27	-0.51
JWH-073	40	40.6	0.79	1.31	1.53	3.76	1.42
	100	99.0	1.75	2.14	2.77	2.80	-0.99
	180	180.4	1.74	0.09	1.74	0.96	0.24
XLR-11	40	39.1	0.92	1.15	1.48	3.78	-2.16
	100	101.5	1.69	2.01	2.63	2.59	1.51
	180	179.3	1.58	0.25	1.60	0.89	-0.36
JWH-018	40	41.0	1.07	1.61	1.93	4.71	2.39
	100	98.3	1.31	2.99	3.27	3.32	-1.67
	180	180.7	2.08	0.53	2.15	1.19	0.40
JWH-122	40	40.1	0.39	1.82	1.86	4.64	0.29
	100	99.8	4.36	1.91	4.76	4.77	-0.21
	180	180.1	1.89	0.75	2.03	1.13	0.05
UR-144	40	39.3	0.62	1.46	1.59	4.04	-1.85
	100	101.3	4.17	1.06	4.30	4.25	1.29
	180	179.4	1.78	0.44	1.83	1.02	-0.31
JWH-210	40	39.4	0.37	0.44	0.58	1.47	-1.44
	100	100.7	1.51	0.83	1.73	1.71	0.76
	180	179.5	0.47	0.26	0.54	0.30	-0.18
APINACA	40	40.2	0.29	1.61	1.63	4.06	0.51
	100	99.6	0.78	2.89	2.90	2.91	-0.68
	180	180.0	1.38	0.83	1.61	0.89	-0.24

Based on the data obtained in the previous Table, the *CVs* were lower than 5.2%. Regarding accuracy, the absolute values vary between 0.05 and 3.0%, which are within the limits considered acceptable.

The presence of systematic errors was investigated, for each concentration level, through a statistical test. The results obtained are described in the following Table.

Table 32. Summary of the results of the hypothesis test (t-Student test) for the study of systematic errors associated with the method recovery by µSPEed/UHPLC-PDA.

Synthetic Cannabinoid	Concentration (ng/mL)	$\bar{R}$	t_{exp}	t_{crit} (N-1;0.95)
MAM-2201	LL	97.0	1.50	2.78
	ML	102.1		
	HL	99.5		
JWH-073	LL	101.4	0.93	
	ML	99.0		
	HL	99.0		
XLR-11	LL	97.8	1.51	
	ML	101.5		
	HL	99.6		
JWH-018	LL	102.4	1.22	
	ML	98.3		
	HL	100.4		
JWH-122	LL	100.3	0.15	
	ML	99.8		
	HL	100.0		
UR-144	LL	98.2	1.10	
	ML	101.3		
	HL	99.7		
JWH-210	LL	98.6	2.61	
	ML	101.0		
	HL	99.8		
APINACA	LL	100.5	0.27	
	ML	99.3	0.48	
	HL	99.8	0.72	

The results showed that t_{exp} is lower than t_{crit} for all SCs within a 95% confidence interval, indicating the absence of systematic errors and demonstrating the accuracy of the method. The recovery rate values are also within the range defined by a 20% margin of error.

3.6.5. Analyte recovery and matrix effect

Recovery and extraction efficiency studies were carried out with the same procedure applied in MEPS. Table 33 presents the values obtained from the evaluation of recovery, extraction efficiency and matrix effect with the three concentration levels using µSPEed as extraction technique.

Table 33. Results of the determination of recovery, extraction efficiency and matrix effect by µSPEed for three concentration levels.

Synthetic cannabinoid	LL			ML			HL		
	R (%)	EE (%)	ME (%)	R (%)	EE (%)	ME (%)	R (%)	EE (%)	ME (%)
MAM-2201	80.9	67.3	83.2	87.8	76.6	87.2	79.1	73.5	92.9
JWH-073	80.8	73.8	91.4	86.6	63.9	73.8	80.8	90.8	78.0
XLR-11	78.2	76.8	98.2	93.7	72.3	77.2	81.0	70.8	87.4
JWH-018	81.5	76.2	93.4	85.3	80.5	94.4	78.2	70.2	89.8
JWH-122	89.4	68.5	76.7	77.5	63.9	82.5	98.7	68.6	69.5
UR-144	92.7	66.5	71.8	86.1	73.0	84.8	87.3	65.8	75.4
JWH-210	91.0	62.5	68.7	81.2	70.4	86.6	84.1	67.1	79.7
APINACA	95.3	67.9	71.3	83.9	67.8	80.8	93.4	77.1	82.5

The recovery values ranged from 78 and 99% and from 63 and 91% for extraction efficiency. Although these results were lower than those obtained by MEPS, they were higher than those reported by Rocchi *et al.* [248].

Regarding matrix effect results, the values ranged from 69 and 98%. Since some values are below the defined parameters (85–110%), it is possible to conclude that some matrix effect was observed.

3.6.6. Stability studies

The µSPEed stability tests were performed on the same days and under the same conditions as MEPS. The results (see Figure S20) revealed that for the LL concentration, the temperature of 4°C obtained the best results from short to long term. While for ML and HL concentration, -20°C was the storage temperature with the best results for the analysed time. According to these results, we conclude that -20°C is the most suitable temperature to store this type of samples.

3.7. Application of MEPS/UHPLC-PDA and µSPEed/UHPLC-PDA methodologies to real samples

After validation of the two analytical methodologies developed for the determination of eight SCs in oral fluid samples, the two methods were applied to real samples provided from recreational drug users. Each donor was orally informed on the whole project and its analytical purposes. Only the age and gender of the donors were requested, and an internal code was applied to each sample.

Two male subjects, aged 22 and 27, agreed to participate in the study. The specimens were collected, just after smoking an herbal mixture (apparently cannabis plant), in sterile flasks and then stored at −20 °C until analysis.

Figure 65 shows the chromatographic profile obtained for both methodologies for each real sample.

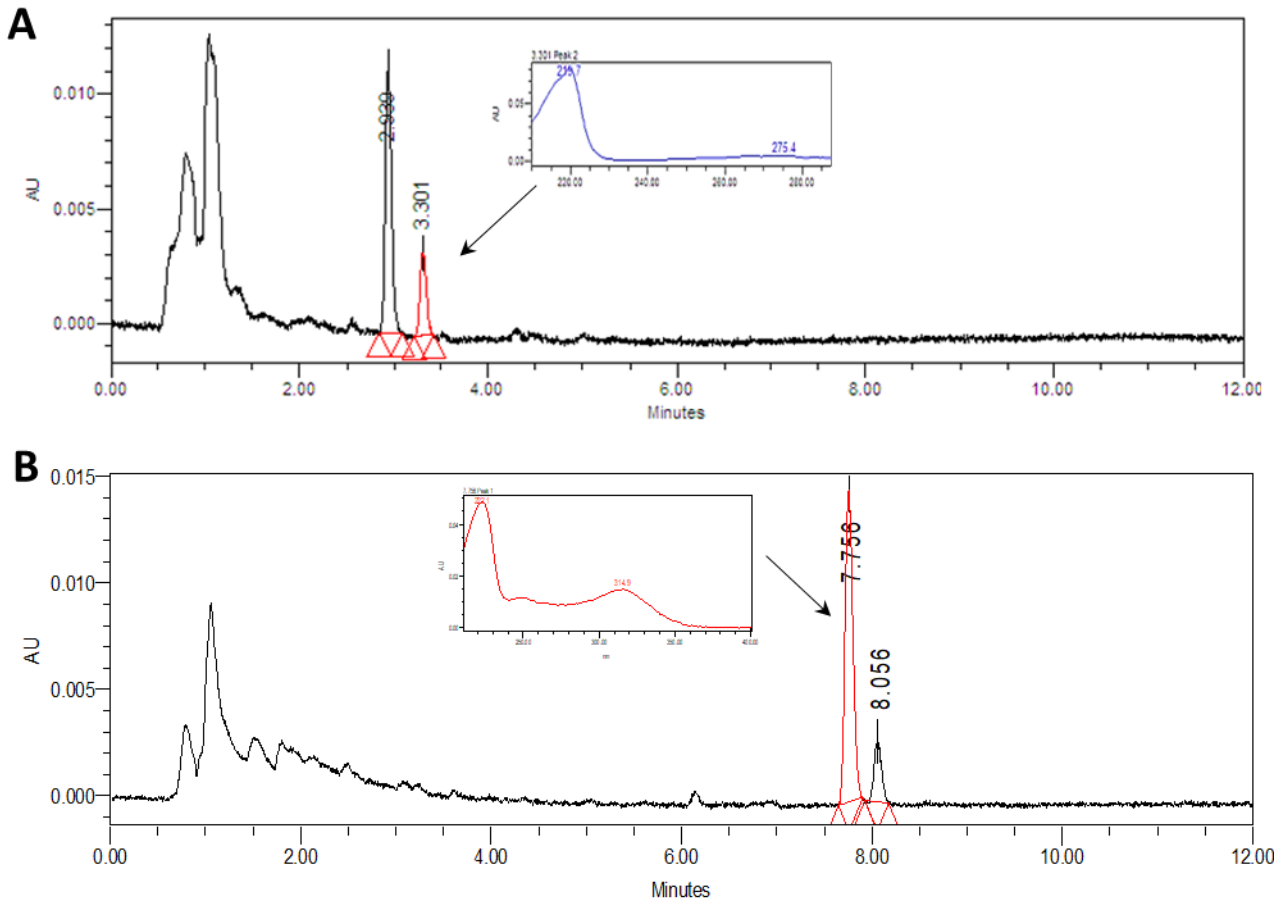

Figure 65. Chromatographic profiles of real samples with UV spectrum of the selected peaks. A – Sample RS1 at 254 nm obtained by µSPEed/UHPLC-PDA and B – Sample RS2 at 314 nm obtained by MEPS/UHPLC-PDA.

For sample RS1, no peaks were identified at the Rt and wavelengths for the compounds under study. However, two peaks were observed at 2.9 and 3.3 min. After a literature search it was found that the UV spectrum of the second peak shows some similarities with the Δ9-tetrahydrocannabinolic UV spectrum. Nonetheless, the reference standard of this compound could confirm such finding.

Regarding RS2, two peaks were detected at 7.8 and 8.1 min. The UV spectrum of the first peak is very similar to that of the JWH-210 compound, in addition the Rt corresponds to this synthetic cannabinoid. The concentration obtained with MEPS technique was 6.67 ± 0.63 ng/mL and 4.06 ± 1.29 ng/mL with µSPEed.

This was an interesting finding since the consumer allegedly smoked cannabis. Thus, we can conclude that either the herbal mix was contaminated with SCs or the consumer had omitted the real nature of the sample.

4. Conclusions

The main objective of this chapter was the development of two microextraction techniques, MEPS and µSPEed, combined with UHPLC-PDA analysis for the simultaneous determination of SCs in oral fluid samples. Since it was not possible to acquire reference standards, the first step was to isolate the SCs identified in the seized herbal samples. Eight SCs were successfully isolated, and its purity verified by UHPLC-PDA, GC-MS, and TLC.

In the next step, two analytical methodologies, MEPS/UHPLC-PDA and µSPEed/UHPLC-PDA, were developed and validated, for the simultaneous determination of MAM-2201, JWH-073, JWH-018, JWH-122, JWH-210, UR-144, XLR-11 and APINACA, in human oral fluid samples.

The chromatographic separation of the analytes was achieved within 12 min, using a gradient elution and HSS T3 as analytical column. The analyses were carried out using small sample volumes (250 µL in MEPS and 150 µL in µSPEed) and in a short time period (between 5 to 8 min for the entire sample preparation step). The C_{18} sorbent was found to be the most suitable coating for the extraction of these compounds in MEPS, whereas in µSPEed the C_8 sorbent provided the best extraction efficiency. Other parameters influencing the adsorption and desorption of analytes were also studied, with the main difference between these two techniques being in the elution solvent, namely ACN was selected for MEPS and MeOH for µSPEed.

Results of the validation studies indicated that the developed methods are precise and accurate in extracting the target compounds in oral fluid samples. Both methodologies have shown good recovery values (above 73% for MEPS and above 78% for µSPEed) for all SCs. µSPEed presented lower LOD and LOQ values comparing to MEPS, however lower extraction efficiency values were obtained and some matrix effect was observed.

Since it was not possible to obtain a good sampling of real samples, the applicability of the developed methodologies needs more testing. However, several works using MEPS as extraction technique are reported showing the potential of this miniaturised technique. Regarding µSPEed, due to be very recent, no studies were found for the extraction of synthetic drugs in biological samples. Despite that, both approaches offer simplicity, decreased sample preparation and analysis time, low-

cost and minimum extraction solvent consumption (environmentally friendly) as compared to traditional methodologies.

The methodologies can be applied, as an attractive and very promising approaches, to the analysis of SCs in other biological matrices, as well as other drugs in forensic toxicology and clinical investigations.

CHAPTER III – Cytotoxicity study of Synthetic Cannabinoids

1. Introduction

In recent years, more and more new consumers have been attracted to the use of SCs. The fact that these compounds are cheaper, novel and provide stronger effects when compared to cannabis, are some of the points that have led to an increase in the consumption of these substances [352].

The identification and quantification of SCs and their corresponding derivatives in herbal products as adulterants have been the subject of various studies over the past few years. Despite being the focus of numerous investigations, the secondary and toxic effects hidden behind these products is still unclear [178]. Several hospitalizations with synthetic cannabinoid use have been reported, with some patients exhibiting respiratory failure, pulmonary infiltrates, alveolar damage or haemorrhage and histopathological features similar to the organising pneumonia. It is yet unclear how SCs damage pulmonary tissue, whether by binding to CB_1, CB_2, or another receptor, and what subsequent effects such binding causes [352].

Although many of these compounds are already considered illegal, there is a lack of studies assessing their toxicity when combined with other derived substances. Several studies have shown that many samples contained various combinations of different SCs, raising the possibility of serious health problems since these substances have not been thoroughly studied and their toxicity as well as pharmacological effects are unknown [178, 353].

Multiple SCs have frequently been found in herbal blends, and the studies described in Chapters I and II of part 3 were able to confirm this finding. However few studies have been reported on the assessment of the toxicity inherent in the co-existence of more than one compound. In this sense, due to the scarce information available regarding SCs toxicological profiles and considering smoking as the main route of consumption, this chapter presents the study of the toxicity induced on lung cells (A549 cell line) using seized herbal products extracts.

2. Materials and Methods

2.1. Chemicals and supplies

F-12K medium was purchased from Quimigen (Alverca, Portugal). Trypan blue solution, Triton X-100 and 3-(4,5-Dimethylthiazol)-2,5-diphenyltetrazolium (MTT), bicinchoninic acid solution (BCA), bovine serum albumin solution (BSA), 2',7'-dichlorofluorescin diacetate (DCFH-DA), and copper (II) sulfate solution 4% (w/v) were purchased from Sigma-Aldrich (St. Louis, MO, USA). Antibiotic mixture

of penicillin/streptomycin, fetal bovine serum (FBS), phosphate buffered saline (PBS), and trypsin were obtained from Gibco Invitrogen (Barcelona, Spain).

Hank's balanced salts solution (HBSS) from Biowest and dimethyl sulfoxide (DMSO) from Fisher Scientific were acquired from VWR (Carnaxide, Portugal). ATP determination kit was obtained from Invitrogen by Thermo Fisher Scientific (Waltham, Massachusetts, USA), and Amplite™ Fluorimetric Glutathione GSH/GSSG Ratio Assay Kit from AAT Bioquest was purchased from Deltaclon (Madrid, Spain).

2.2. Cell line

For cell culture and *in vitro* assays A549 cells (human lung cell line) was purchased from Quimigen (Alverca, Portugal).

2.3. Herbal samples

Eight seized herbal samples, namely B23, B54, B63, H1, H3, H4, H6 and H8 were selected for the cytotoxicity studies. Dried damiana leaves (*Turnera aphrodisiaca*) were purchased online at chasdomundo.pt.

Methanolic extract samples were evaporated under nitrogen and the mass extract weighed. Then, the extract was redissolved in DMSO at a concentration of 200 mg/mL.

2.4. Cytotoxicity assays

2.4.1. Cell culture

A549 cells were cultured in Ham´s F-12 medium (Kaighn's modification), supplemented with 10% (v/v) of FBS, 1% (v/v) antibiotic mixture (10,000 units/mL of penicillin and 10,000 µg/mL of streptomycin) in petri dishes. Cells were maintained in a humidified incubator at 37°C and 5% CO_2. Growth medium was changed 2 times per week.

2.4.2. Cell viability (MTT assay)

The cytotoxic effect of herbal extracts was evaluated in A549 cells, as a model of lung cells, by the MTT assay.

MTT is one of the most widely used cell viability test due to its reliability and the ease to implementation [354]. This assay is used to measure cellular metabolic activity as an indicator of cell viability, proliferation, and cytotoxicity. This colorimetric assay is based on the reduction of a yellow tetrazolium salt (3-(4,5-dimethylthiazol-2-yl)-2,5-diphenyltetrazolium bromide or MTT) to water insoluble purple formazan crystals by dehydrogenases occurring in the mitochondria of viable cells (Figure 66) [56, 355]. The insoluble formazan crystals are dissolved using a solubilization solution, usually DMSO and the resulting-coloured solution is quantified by measuring absorbance at 500-600 nm using a multi-well spectrophotometer. The darker the solution, the greater the number of viable, metabolically active cells [354, 355].

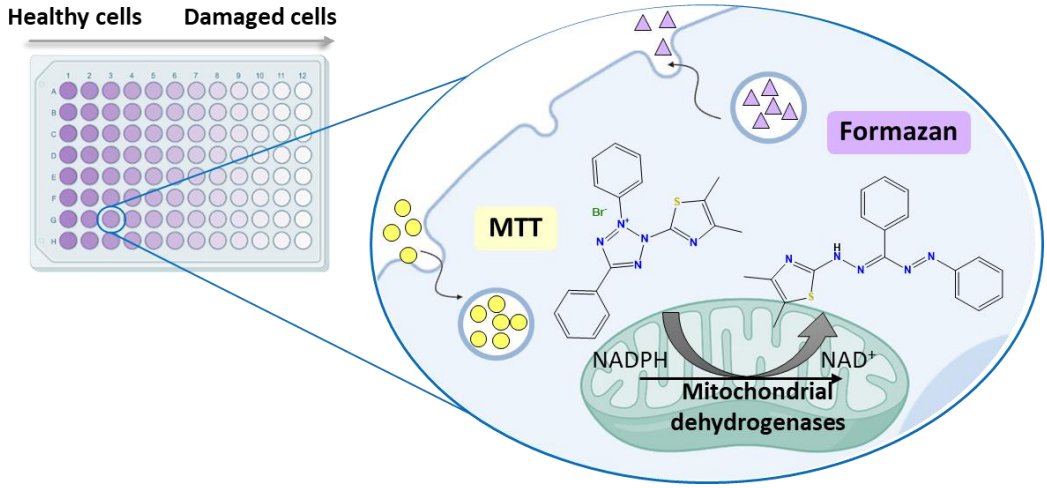

Figure 66. Principle of MTT reaction (adapted from [355, 356]).

A549 cells were seeded on 96-well plates at a concentration of 1×10^4 cells/well. After 24 h of cell grown, the cells were exposed to different concentrations (ranging from 50 to 1750 µg/mL) of extract solutions with 1% DMSO and incubated at 37°C and 5% CO_2 for 48h and 72h. After these periods, the medium was removed and 200 µL of MTT at a concentration of 0.5 mg/mL in culture medium was added to each well. After 2.5 h of incubation under the same standard conditions, the MTT solution was removed, 100 µL of DMSO solution was added to each well to dissolve the formazan crystals formed and the absorbance was measured at 550 nm using a multilabel plate counter (Victor^3 1420, Perkin-Elmer). In Figure 67 is graphically represented the MTT procedure.

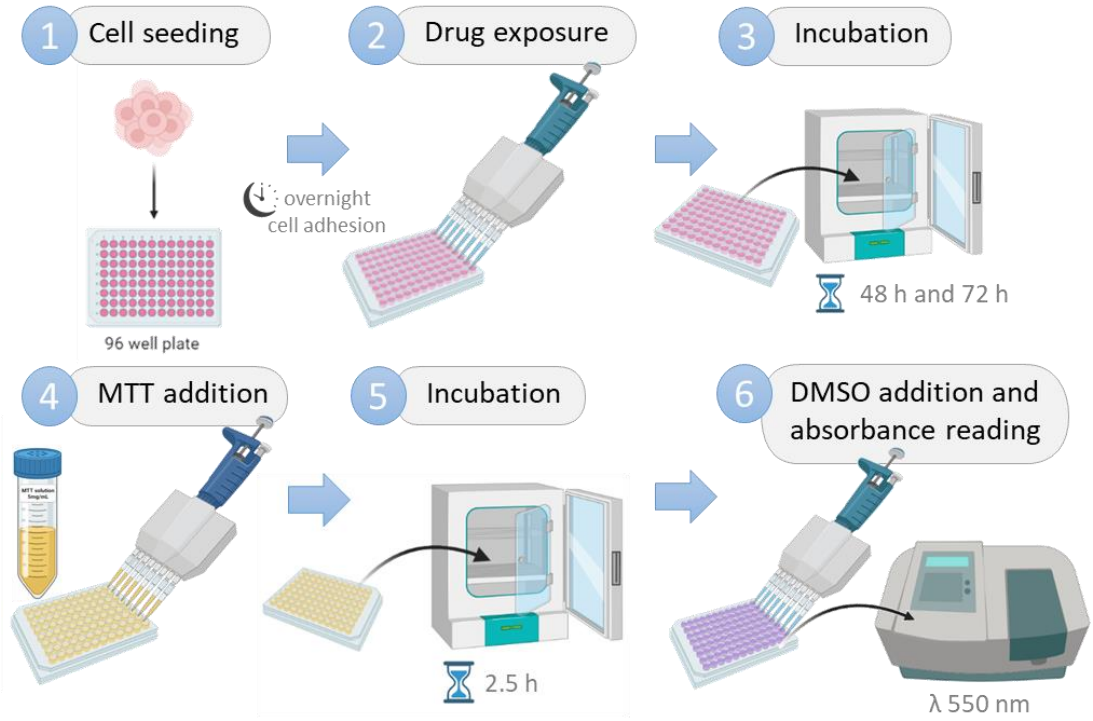

Figure 67. Schematic representation of MTT procedure.

All experiments were performed in triplicate. In each experiment, a control culture (cells, medium and an equivalent amount of DMSO, *n* = 6), a negative control (cells and medium, *n* = 5) and a positive control (cells, medium and 1% Triton X-100, *n* = 5) were performed. Results were graphically presented as percentage of cell death versus log concentration (µg/mL). The control culture was set to 100% cell viability and the percentage of cell death was determined as follows [357]:

$$Cytotoxicity\ (\%) = \frac{A_{sample} - A_{negative\ control}}{A_{positive\ control} - A_{negative\ control}} \times 100 \qquad \textit{Equation 23}$$

Where A_{sample} is the average of the absorbance measured for the test sample, $A_{negative\ control}$ is the average of the absorbance measured for the negative control, and $A_{positive\ control}$ is the average of the absorbance measured for the positive control.

2.4.3. Intracellular reactive oxygen and nitrogen species (ROS/RNS)

The formation of reactive oxygen species (ROS) and/or reactive nitrogen species (RNS) and the resulting oxidative and/or nitrosative stress is a common toxicological pathway of cytotoxicity for drugs of abuse, and pharmaceuticals [358]. ROS are formed as a natural by-product of the normal metabolism of oxygen and have significant roles in cell signalling and homeostasis. Normal cellular homeostasis therefore involves a delicate balance between the rate and amount of ROS production

and the rate of oxidant elimination. Oxidative stress can be defined as the pathogenic outcome of the over production of ROS that overwhelms the cellular antioxidant capacity. Under conditions of oxidative stress, ROS production is dramatically increased, resulting in subsequent alteration of membrane lipids, proteins, and nucleic acids [359-361].

Oxygen molecules including free oxygen radicals, such as superoxide ($O_2^{\cdot}$-), hydroxyl (·OH), peroxyl ($RO_2^{\cdot}$), and alkoxyl (RO-) as well as hypochlorous acid (HOCl), ozone (O_3), singlet oxygen ($^1O_2$), and hydrogen peroxide (H_2O_2), which are non-radicals, are some ROS examples. These non-radicals are either oxidizing agents or easily converted into radicals. Nitrogen-containing oxidants, such as nitric oxide ($NO^{\cdot}$) peroxynitrite ($ONOO^{\cdot}$), nitrogen dioxide (NO_2) are called RNS [361].

At a molecular level, ROS and RNS exhibit signalling and cell-function-modifying roles. They are not single entities but represent a broad range of chemically distinct reactive species with diverse biological reactivities. To clearly attribute a particular cell signalling event to a specific reactive oxygen or nitrogen species, it is essential to detect and characterize these species accurately [359].

In the present work, the intracellular ROS and RNS production was monitored via DCFH-DA fluorescence assay. DCFH-DA is a cell-permeable fluorogenic probe that readily diffuses into the cells, where it is deacetylated by cellular esterases, and the resultant non-fluorescent dichlorofluorescein (DCFH) is further oxidized by ROS and RNS to the highly fluorescent 2',7'-dichlorofluorescein (DCF) [362, 363] (Figure 68).

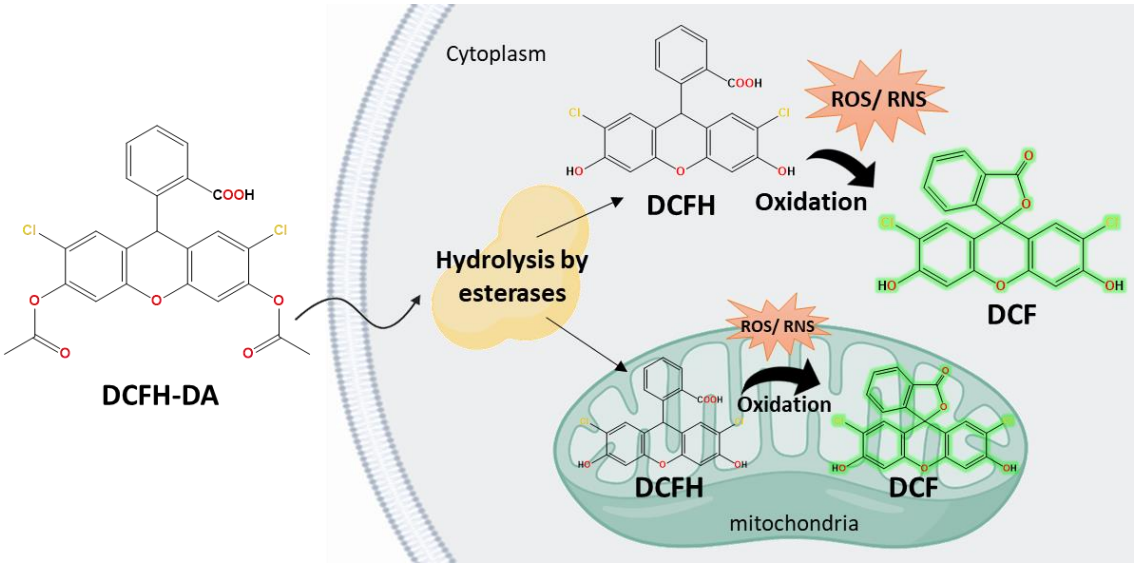

Figure 68. Formation of fluorescent compound DCF by ROS/RNS (adapted from [364, 365]).

The intracellular ROS and RNS production was monitored via DCFH-DA fluorescence assay according to Dias da Silva *et al*. [358] and Valente *et al.* [363] works with minor modifications. For this

assay, after overnight cell adhesion in 96-well black plates, cells were incubated with 10 µM DCFH-DA for 30 min at 37°C, protected from light. As DCFH-DA is a non-water-soluble powder, it was initially prepared as a 20 mM stock solution in DMSO and made up to the final concentration in fresh culture medium (ensuring that the final concentration of DMSO did not exceed 0.05%) immediately before each experiment. After 30 min, cells were rinsed with HBSS and incubated with IC_{25} and IC_{50} determined by the MTT concentration–response curves for each herbal extract, at 37 °C during 72 h. Fluorescence was then recorded on a microplate reader (Victor^3 1420, Perkin-Elmer) set to 485 nm excitation and 530 nm emission (Figure 69). Cells were also incubated with hydrogen peroxide which was used as a positive control. Results were normalized to negative controls (no treatment) and calculated as fold-increase over control.

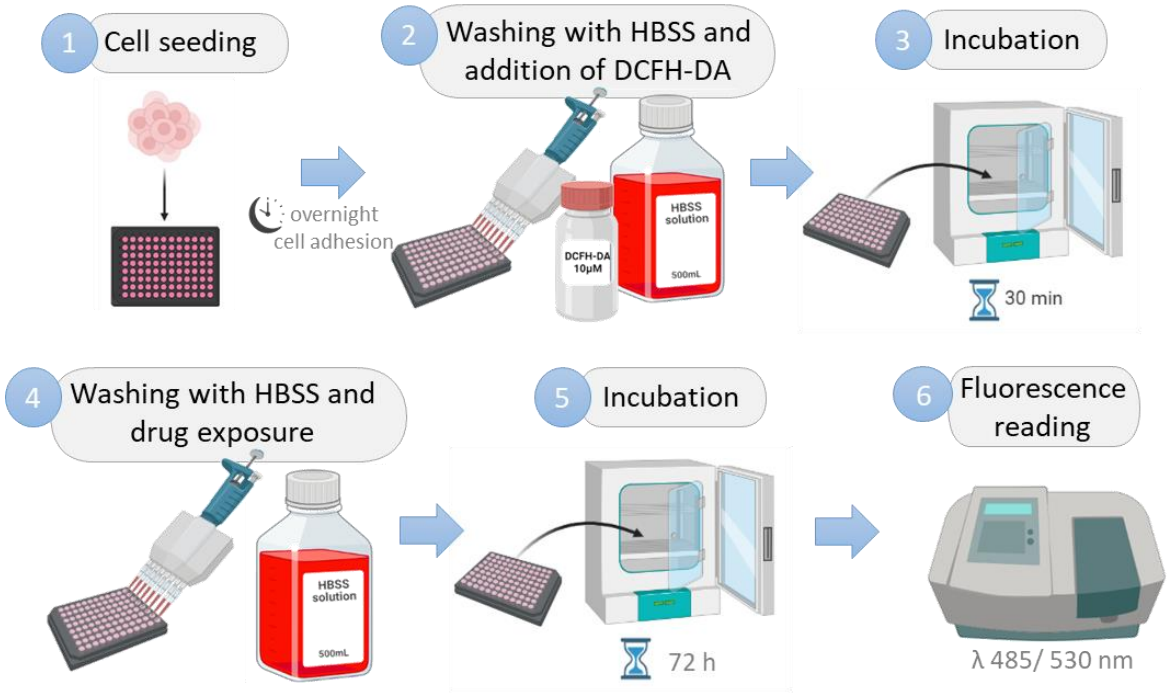

Figure 69. Schematic representation of ROS/RNS

2.4.4. Intracellular ATP levels

Adenosine triphosphate (ATP) is involved in a variety of enzymatic reactions to maintain normal life activities. When normal cells undergo apoptosis and necrosis, ATP content will be characteristic changed. Thus, ATP has been widely accepted as a valid marker of viable cells. The measurement of ATP using firefly luciferase is the most, commonly, applied method for estimating the number of viable cells [366].

The method is based on the luciferase-catalysed bioluminescence formation obtained through the reaction between luciferin and intracellular ATP [367, 368]. Bioluminescent ATP assays take advantage of the firefly luciferase enzymatic reaction, which uses ATP from viable cells to generate photons of light. Viable cells are lysed to release the ATP for detection, and reagents containing firefly luciferase enzyme and substrate are added to catalyse a two-step reaction [366].

Luciferin is initially activated by ATP to produce luciferyl-adenylate and pyrophosphate. The second phase involves the reaction of luciferyl-adenylate with molecular oxygen, producing CO_2 and oxyluciferin in an electronically excited state (Figure 70). Following a release of green to yellow luminescent light, oxyluciferin returns from its excited state to its ground state (550–570nm). The intensity of bioluminescence is detected using a luminometer and is proportional to the ATP levels in the sample [366, 367].

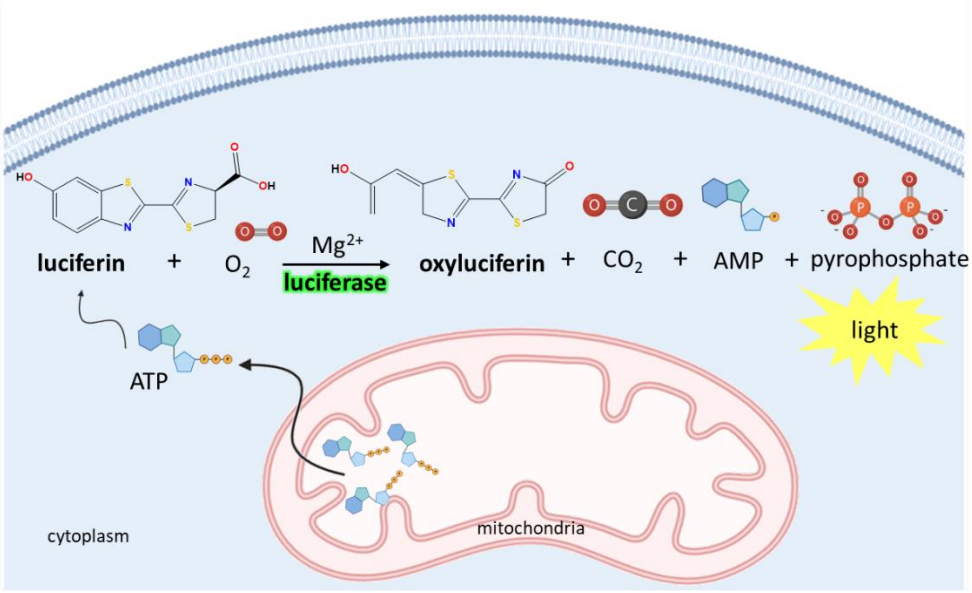

Figure 70. Principle of ATP bioluminescent reaction (adapted from [366, 369].

Evaluation of energy metabolism was performed according to the procedure described by Silva *et al.* [368] and Alexandre *et al.* [367] with minor adaptations. Briefly, cells were seeded at 1 × 10^5 cells/well in 24-well plates and incubated with IC_{25} and IC_{50} determined by the MTT concentration–response curves for each herbal extract for 72h. Following cell exposure, cells were washed with HBSS and precipitated with 200 µL of 5% perchloric acid and further incubated for 20 min at 4 °C. Cells were then scrapped and collected into 1.5 mL tubes, which were then centrifuged at 10,000 g for 5 min at 4 °C. The supernatants were collected into new 1.5 mL tubes and neutralized with 200 µL of 0.76 M $KHCO_3$, while the pellets were resuspended in 0.3 M NaOH and used to determine the total amount of protein through the Bicinchoninic Acid protein method. The solutions containing the

neutralized supernatants were centrifuged for 5 min at 10,000 g, at 4 °C. The reaction was then initiated by adding 10 µL of each supernatant to 96-well opaque plates with 90 µL of luciferin-luciferase reagent (dH_2O, 20X reaction buffer (500mM tricine buffer, pH 7.8, 100 mM $MgSO_4$, 2mM EDTA, 2 mM sodium azide), 0.1 M dithiothreitol (DTT), 10 mM D-luciferin and 5mg/mL of firefly luciferase) and immediately the luminescence was measured. Figure 71 shows a schematic diagram of ATP procedure.

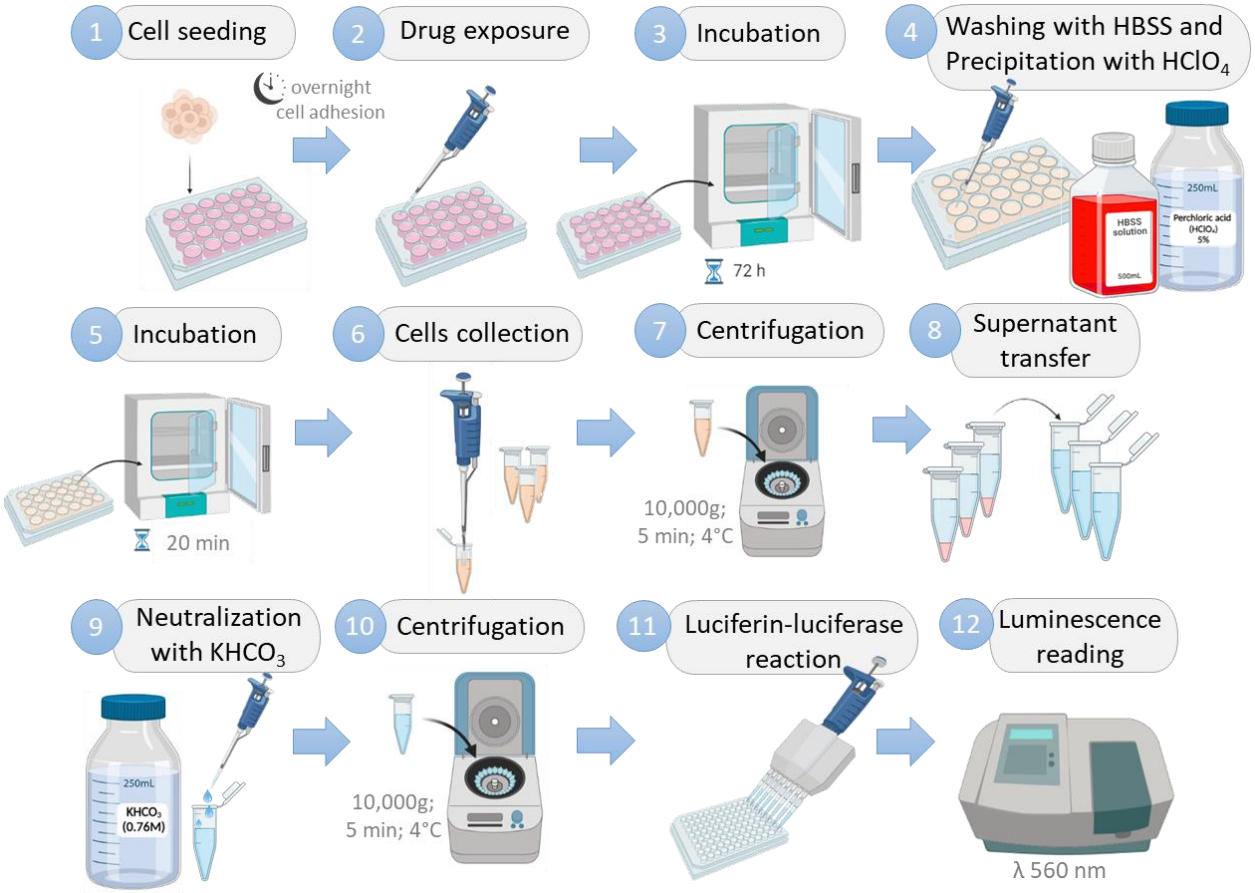

Figure 71. Schematic representation of ATP procedure.

The amount of ATP was determined by interpolation from an ATP standard calibration curve (0 to 1000 nM), normalized by the total protein amount. Results were then expressed in terms of fold-change relatively to the control.

2.4.5. Intracellular reduced glutathione (GSH) and oxidized glutathione (GSSG) levels

Glutathione is a tripeptide that contains L-cysteine, L-glutamic acid, and glycine. It is the smallest intracellular protein thiol molecule in the cells, which prevents cell damage caused by ROS such as free radicals and peroxides. There are reduced and oxidized forms of glutathione. Reduced

glutathione (GSH) is a major tissue antioxidant that provides reducing equivalents for the glutathione peroxidase (GP) catalysed reduction of lipid hydroperoxides to their corresponding alcohols and hydrogen peroxide to water. In the GP catalysed reaction, the formation of a disulfide bond between two GSH molecules generates oxidized glutathione (GSSG). The enzyme glutathione reductase (GR) recycles GSSG to GSH with the simultaneous oxidation of β-nicotinamide adenine dinucleotide phosphate (β-NADPH2) (Figure 72). In healthy cells, more than 90% of the total glutathione pool is in the reduced form (GSH). When cells are exposed to increased levels of oxidative stress, GSSG accumulates and the ratio of GSSG to GSH increases. An increased ratio of GSSG-to-GSH is an indication of oxidative stress. The monitoring of reduced and oxidized GSH in biological samples is essential for evaluating the redox and detoxification status of the cells and tissues against oxidative and free radicals mediated cell injury [370].

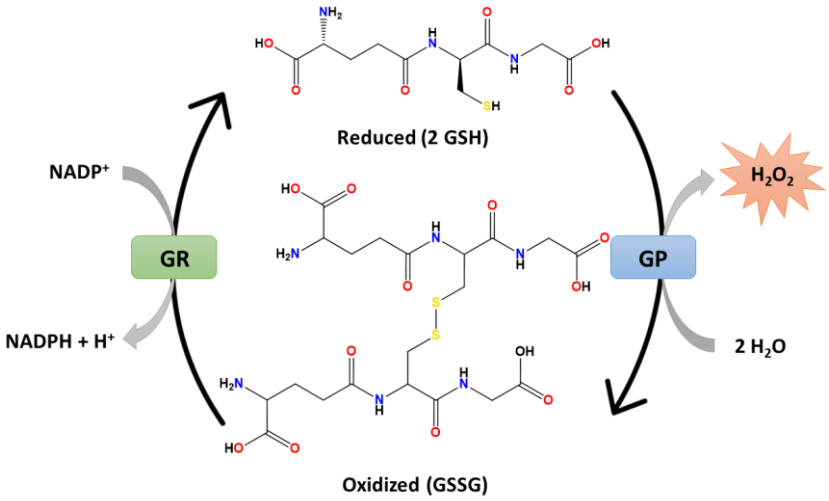

Figure 72. Glutathione oxidation reduction cycle (adapted from [371]).

GSH and GSSG contents were determined using a fluorimetric glutathione assay kit. This kit provides an ultrasensitive assay to quantitate GSH in the sample, in which it employs a proprietary non-fluorescent and pH-dependent glutathione sensor that becomes strongly fluorescent upon reacting with thiol [372].

After exposure to the IC_{25} and IC_{50} of the tested herbal extracts, cells were rinsed and treated as described above for ATP measurement. After neutralization, 50 µL of the supernatants were added to 96-well black plates with 50 µL of GSH working solution (1 mM) or GSSG working solution (1 mM). Plates were then incubated for 10 to 60 minutes at room temperature, protected from light and fluorescence increase was monitored at Ex/Em = 485/535 nm, every 10 min. Figure 73 demonstrates a flowchart of the GSH and GSSG assay procedure.

Serially diluted GSH and GSSG standards (0 to 10 µM) were prepared to construct the standard calibration curves. Serially diluted GSSG standard solutions were performed 1:2 from the GSH standard solutions, since for each redox of GSSG, two moles of GSH are produced.

The concentration of GSH and GSSG were calculated by interpolation from the GSH and GSSG standard calibration curves, respectively and normalized by the total protein amount.

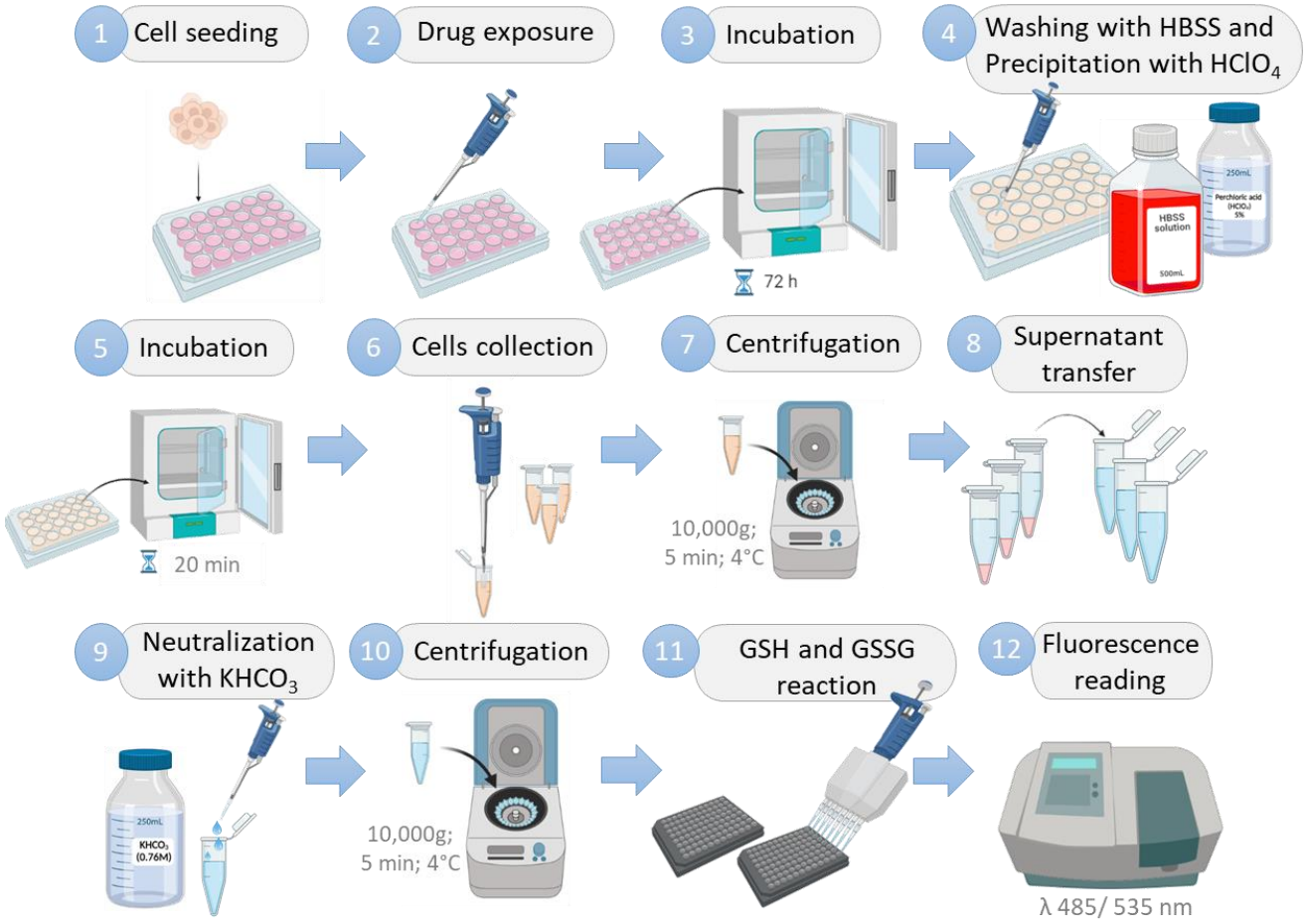

Figure 73. Schematic representation of GSH and GSSG procedure.

2.4.6. Total protein extraction

Quantification of total protein in the cell extracts was determined using the Bicinchoninic Acid (BCA) Protein Assay and was performed according to the procedure described by Thermo Scientific [373] and previously reported studies [374, 375] with minor adaptations.

The pellets obtained in the measurement of ATP procedure were resuspended in 100 of 0.3 M NaOH. 10 µL were added to 96-well plates with 190 µL of BCA working reagent (50 parts of BCA solution with 1 part of 4% (w/v) copper (II) sulfate solution). Plates were, then, incubated at 37°C during 1 h and absorbance was recorded on a microplate reader at 550 nm.

Serially diluted BSA standard solutions (0 to 5 µg/µL) were prepared to construct the standard calibration curve. The protein content was calculated using the linear Equation obtained from the calibration curve.

Figure 74 shows the schematised procedure for the determination of the total protein.

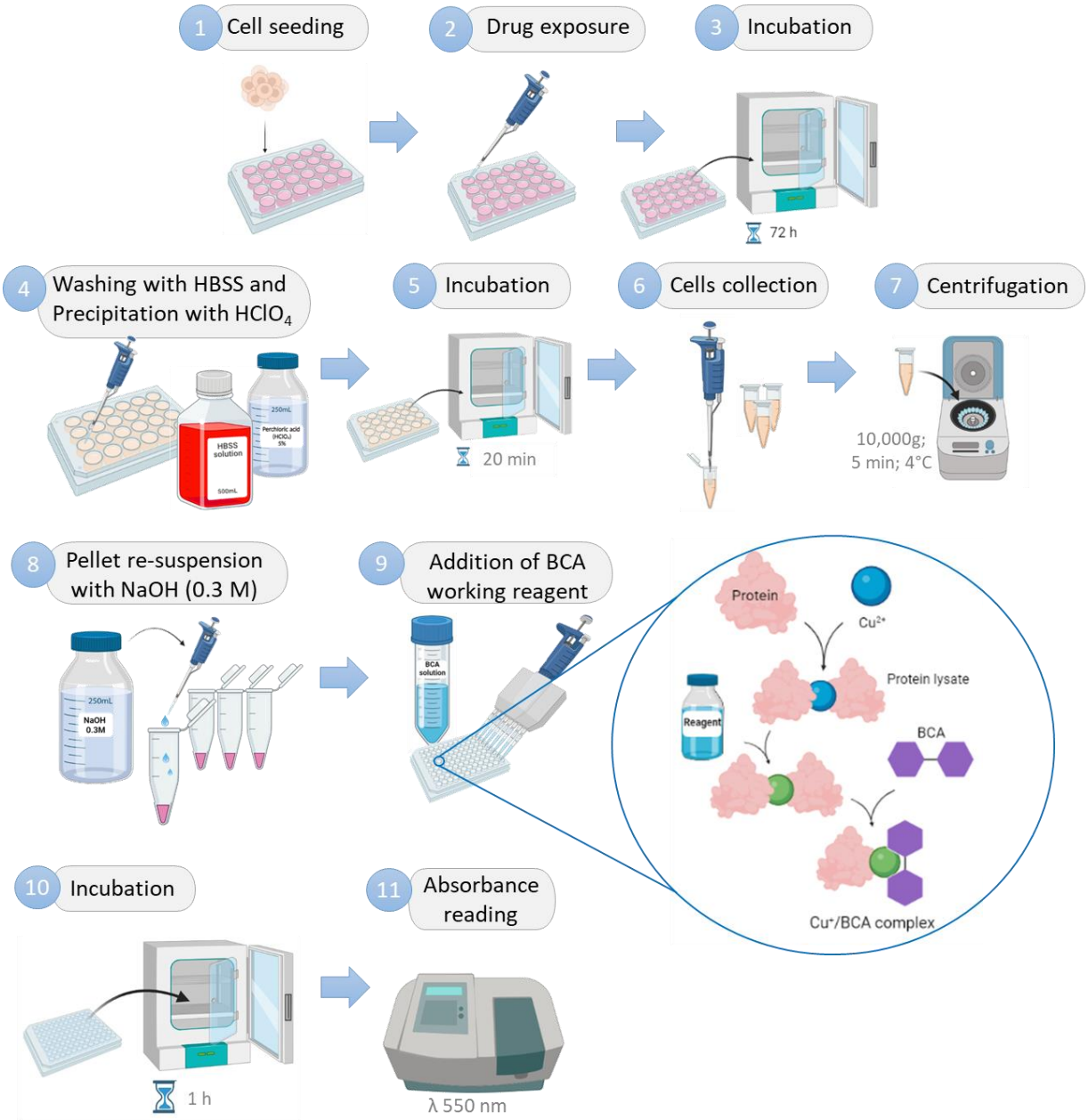

Figure 74. Graphic representation of total protein determination procedure.

2.5. Statistical analysis

Curves of normalized MTT data were constructed and analysed using the best-fit approach. In the present study the logit function (*Equation 24*) was employed as described by Araújo *et al.* [56]:

$$Y = \theta_{min} + (\theta_{max-}\theta_{min})/(1 + \exp(-\theta_1 - \theta_2 \times \log(x))) \quad \textit{Equation 24}$$

Where θ_{min} and θ_{max} are the minimal and maximal observed effects, respectively; x is the concentration of the test drug; θ_1 is the parameter for the location, and θ_2 is the slope parameter [56]. The nonlinear regression models were constructed using the GraphPad Prism 8 (version 8.4.3). MTT data are presented as mean ± 95 % confidence interval (CI). The half-maximal response (IC_{50}) values were determined for each sample extract.

For further assays, results are presented as mean ± standard error of the mean (SEM). Multiple comparisons between each herbal extract and control or between each seized sample and damiana extract were performed through one-way ANOVA, followed by a Dunnett's comparison post-test. *P*-values lower than 0.05 were considered statistically significant.

3. Results and Discussion

3.1. Features of A549 cell line

As previously mentioned, acute intoxications with SCs use have been reported. Among the adverse events, several pulmonary problems, such as respiratory failure, alveolar damage or haemorrhage have been verified in emergency services [352].

Considering smoking the main route of administration, the lung cell line (A549) was chosen to test the cytotoxicity of herbal extracts.

A549 cells are lung carcinoma epithelial cells and have been used to model the alveolar type II pulmonary epithelium. Studies have shown that this can be particularly useful in research for studying the metabolic processing of lung tissue and for identifying mechanisms of drug delivery to the tissue [376]. Since this cell line is known to express cannabinoid receptors, it has been used in the cytotoxic investigations of cannabinoids, such as Δ9-THC or CBD [377, 378], as well as few studies with SCs [379, 380].

The fact that it is a cancer cell line, therefore, they are immortalised, which may result in differences from primary cell lines. However, the use of cytotoxicity assays on cancer cell lines is a fair measure of the overall cytotoxicity potential [379]. Figure 75 shows A549 cells in culture medium and in Figure S21 is presented the microscopic images of A549 after exposure with the different herbal extracts.

Figure 75. Microscopic appearance of A549 in a magnification of 40x.

3.2. Evaluation of cytotoxicity by the MTT reduction assay

In the present study the evaluation of the effects of herbal extracts containing different SCs in the viability of the A549 cell line was performed using concentrations ranging from 50 to 1750 µg/mL and treatments of 48 and 72 h.

Figure 76 presents the concentration-response curves of A549 cells exposed for 48 and 72 h to eight seized herbal extracts (B23, B54, B63, H1, H3, H4, H6 and H8) and to damiana extract, obtained through the MTT reduction assay. A summary of the estimated IC_{25} and IC_{50} of each extract is presented in Table 34 and other parameters from the nonlinear regression fit are provided in Supplementary Material IV.

All the nonlinear regression models describe sigmoidal concentration–response relationships. According to the results, significant differences were observed between 48 h and 72 h of exposure. For samples B63, H1, H3, H6 and damiana it was not possible to calculate a complete CI (95% confidence level) regarding to 48 h of extract exposure, and 72 h was selected for the following assays.

In general, a significant concentration dependent decrease in cell viability was observed for all the herbal extracts tested. Regarding IC_{50} values, sample B54 composed by APINACA and UR-144 compounds (according to the results described in Chapter I of Part 3), showed the lowest value (123 µg/mL) when compared with other extracts, thus concluding that this sample presents higher cytotoxicity. On the other hand, sample B63 presented the highest IC_{50} value (2338 µg/mL), being this the sample with the lowest cytotoxicity among the extracts tested.

Interestingly, samples B63 and H1 have the same SCs, namely JWH-210, JWH-122 and JWH-018. Despite the herbal mixture's components being the same, sample H1 showed more cytotoxicity at lower concentrations (see Figure 76). These results allowed to conclude that although the

composition is the same among the samples the concentration of the compounds varies and has different cytotoxic effects.

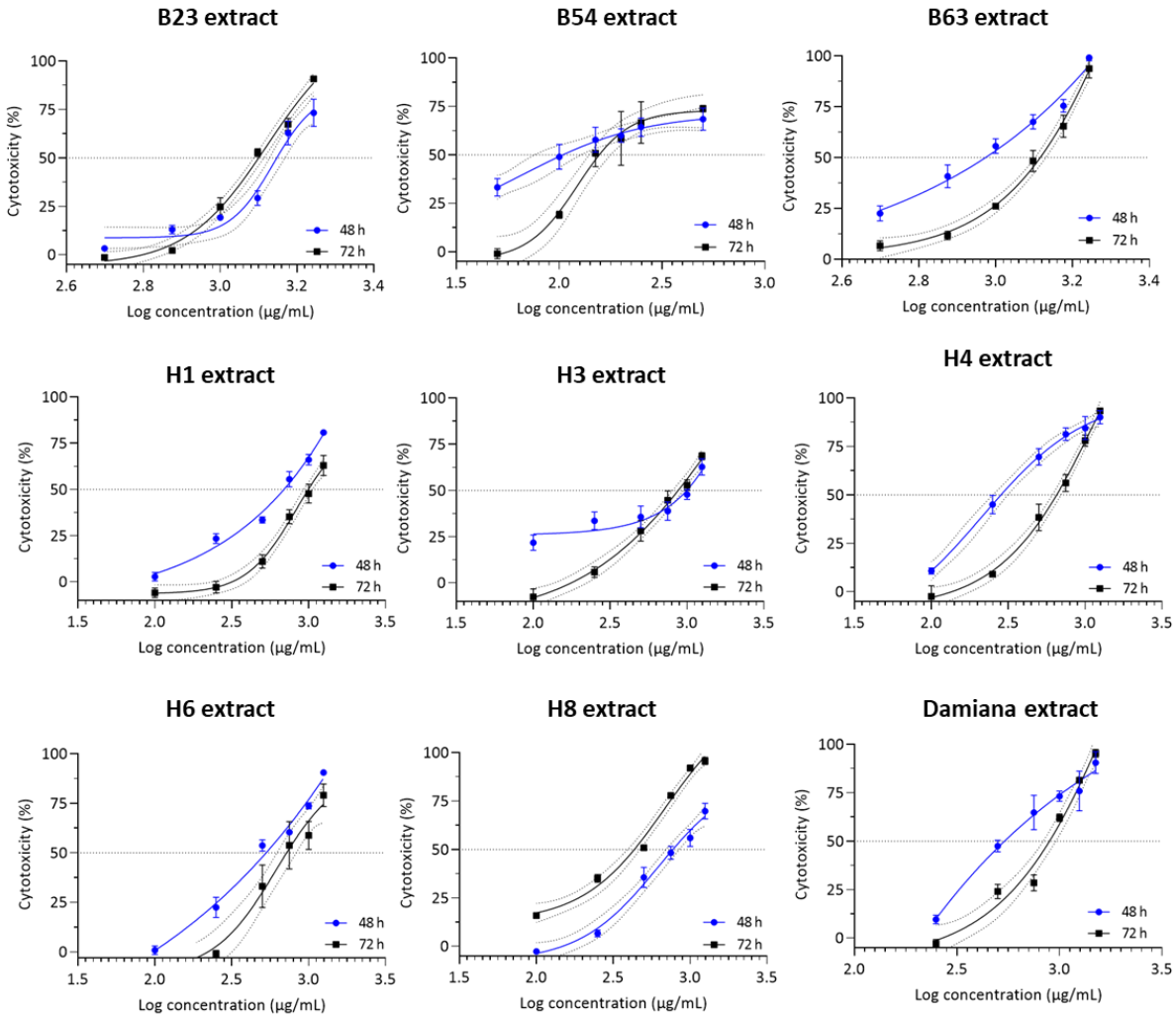

Figure 76. Nonlinear regression models for the cytotoxicity effects of herbal extracts in A549 cells, as evaluated by the MTT reduction assay after 48 h (blue line) and 72 h (black line). The grey line shows IC_{50} for each response curve and dashed lines show the 95% confidence band of each fit. Data were normalized to negative (untreated) and positive (1% Triton X-100) controls. Results were obtained ate least four independent experiments, performed in triplicate.

Table 34. IC_{25} and IC_{50} values of herbal extracts in the MTT assay, after 72 h of exposure at 37°C.

Sample extract	IC_{25} (µg/mL) ($\rho<0.05$)	IC_{50} (µg/mL) ($\rho<0.05$)	SCs previously identified*
B23	1015	1326	JWH-018
B54	90	123	APINACA; UR-144
B63	1584	2338	JWH-210; JWH-122; JWH-018
H1	553	833	JWH-210; JWH-122; JWH-018
H3	603	1888	JWH-122; JWH-018
H4	572	1265	APINACA; XLR-11
H6	369	615	JWH-018; JWH-073
H8	354	689	JWH-018; JWH-073
Damiana	1044	2147	-

**Chapter I of Part 3*

In relation to samples H6 and H8, no significant differences were found between mean IC_{50} values (615 and 689 µg/mL, respectively), meaning that these two samples have similar cytotoxic potencies. These results were expected since these samples have the same SCs (JWH-018 and JWH-073) and in similar percentages.

Sample B23, which has only the synthetic cannabinoid JWH-018 and with an IC_{50} of 1326 µg/mL, shares a similar potency of cytotoxic effects with sample H3 (IC_{50} of 1888 µg/mL) featuring not only JWH-018 but also JWH-122.

Recently, Almada *et al.* [381] explored the impact of the SCs, JWH-018, JWH-122 and UR-144 and the phytocannabinoid Δ9-THC, in human placental cytotrophoblast cell model. MTT and lactate dehydrogenase (LDH) assays were performed in 24, 48 and 72 h of treatment. According to the authors, no effects on cell viability were detected after 24 h; however, at 48 h all the SCs significantly decreased cell viability at 10 µM in the MTT assay accompanied by alterations in cell morphology. On the other hand, Δ9-THC did not alter cell viability at the same concentrations and time of treatment.

Regarding sample H4 with compounds XLR-11 and APINACA, it showed less cytotoxic effect when compared with sample B54, which has APINACA compound in common and the defluorinated form of XLR-11, i.e., UR-144. Although APINACA is the majority compound in both samples, UR-144 compound may have greater potency than XLR-11 compound, however further studies would be necessary to conclude these results.

The damiana leaf extract was further studied in the A549 cell line to consider the contribution of the damiana leaves regarding cell viability. Damiana extract with an IC_{50} of 2147 µg/mL, shared a similar potency with sample B63, with these two samples showing the lowest cytotoxicity.

After a literature search, only one study was found with the application of herbal extracts to the same cell line. Grafinger *et al.* [379] investigated the cytotoxicity of reference standards, herbal blend extracts and smoke condensates of five SCs. Since the herbal extracts and the tested SCs were not the same as the present study, it was not possible to compare our results with Grafinger´s *et al.* study. However, damiana leaf extracts were also evaluated, reporting an IC_{50} of 1222 µg/mL. According to the authors, the data showed that the presence of damiana plant contributed to enhancing the cytotoxicity of 5C-AKB48, 5F-MDMB-PINACA, and MDMB-CHMICA, with plant effects being generally more marked for smoke condensates.

Another interesting work by Willer *et al.* [382], reported the cytotoxic properties of damiana extracts and constituents. Several compounds revealed significant cytotoxic effects against myeloma

cell lines, in which naringenin and apigenin were identified as two components with the greatest responsibility in the observed activity.

According to some online forums and blogs, damiana is smoked by some users due to its flavour being similar to cannabis when smoked and produce a mild euphoria gently similar to marijuana. In addition, this plant is considered as a potent aphrodisiac, heightening sexual rejuvenation and virility [383]. Since damiana leaves are one of the most common substrates used in the preparation of smoking mixtures, the cytotoxicity of SCs could be increased as reported in Grafinger *et al.* [379] work. However, further studies are needed to confirm this finding.

3.3. Evaluation of oxidative stress

Oxidative stress can be considered as an important underlying cause of cannabinoid toxicity. ROS accumulation leads to oxidative stress due to the pro-oxidant–antioxidant balance gets disturbed.

The disturbance in this redox equilibrium causes severe irreversible interruption to the normal functions of cells, thereby affecting the entire system [384].

The levels of reactive species following 72 h exposure with herbal extracts are shown in Figure 77. Almost all herbal samples induced the production of reactive species after 72 h exposure. This effect was significant ($p < 0.05$, ANOVA/ Dunnett's) and concentration-dependent for all the tested samples. Interestingly, among the same concentration levels, sample B23 and damiana significantly ($p < 0.001$ vs. control) induced more reactive species formation than the other extracts at IC_{25} (3.51 ± 0.31 and 3.45 ± 0.39, respectively) and IC_{50} concentration levels (4.12 ± 0.33 and 3.90 ± 0.23, respectively). On the other hand, at equipotent cytotoxic concentrations, no significant differences were observed among B54, H4, H6 and H8 compared with control (1.06 ± 0.11, 1.56 ± 0.21, 1.83 ± 0.07 and 1.19 ± 0.07, respectively).

Comparing the seized sample extracts with damiana extract, significant differences were observed in almost all samples ($p < 0.001$), with exception of sample B23. This result may be due to the fact sample B23 induced more the formation of reactive species among the seized herbal extracts.

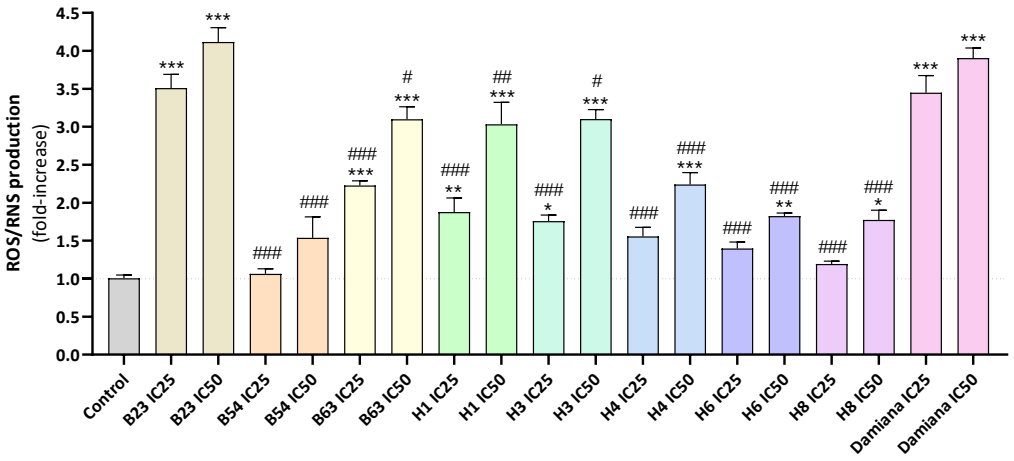

*Figure 77. Reactive species (ROS/RNS) production, measured through the DCFH-DA assay, in A549 cells after 72 h exposure of herbal extracts at IC25 and IC50 concentrations. Results are presented as mean ± SEM from three independent experiments, performed with eight replicates within each experiment. *p < 0.01, ** p < 0.005, *** p < 0.001 mixture versus control; # p < 0.01, ## p < 0.005, ### p < 0.001 mixture versus damiana at the same cytotoxicity levels (IC_{25} and IC_{50}).*

According to our research, no *in vitro* studies were found with the assessment of oxidative stress by measuring the generation of ROS and RNS in herbal extracts. Silva *et al.* [368] reported the assessment of XLR-11's nephrotoxicity, as a first approach to identify its cellular targets and how they may account for this compound induced kidney damage. According to the authors, XLR-11 did not significantly alter intracellular ROS/RNS production. In comparison with our sample H4, in which XLR-11 is present, significant differences were observed at the highest concentration, which may be due to the presence of another synthetic cannabinoid in the same sample, namely APINACA. Further studies would be needed to confirm and/or complement these results.

Other studies concluded that an important underlying cause of cannabinoid toxicity can be oxidative stress, and this can be attributed to the effect of Δ9-THC, which may induce oxidative stress (*in vitro* and *in vivo*) [385]. Given that SCs act in a similar way to Δ9-THC, binding to the same receptors, we can conclude that they may contribute to oxidative stress causing a relevant toxic effect among users.

Almada *et al.* [381] also evaluated the impact of JWH-018, JWH-122, UR-144 and Δ9-THC on ROS/RNS generation. The results revealed that JWH-018 and JWH-122 treatment resulted in a significant ($p < 0.05$) ROS production, while UR-144 and Δ9-THC did not affect the redox state, suggesting that the activated mechanisms of cell death may vary for the different cannabinoids. In addition, Δ9-THC, UR-144 and JWH-122 caused loss of mitochondrial membrane potential. According to the authors, the work demonstrated the ability of Δ9-THC and SCs to induce apoptotic cell death, although they can act through different mechanisms and potencies.

The intracellular content of GSH and GSSG was measure after exposure of lung cell line (A549) to herbal extracts (IC_{25} and IC_{50}) at 37°C. As shown in Figure 78A, a significant GSH depletion ($p < 0.001$) was noted for samples B23, H4 and damiana extract at IC_{50}. The same results were observed for GSSG levels (Figure 78B). Interestingly, these results agree with the generation of reactive species (ROS/RNS), since the highest GSH depletion was observed at IC_{50}, which also induced the highest formation of ROS/RNS.

In biological systems, GSH is the most important antioxidant, being the first line of defence against reactive species formation and ensuing oxidative damage. Its biosynthesis, which occurs in the cytosol, involves two enzymes: γ-glutamylcysteine ligase and GSH synthase, the first catalyzing the rate-limiting step of this biosynthetic pathway [358, 362, 363]. Since one of the functions of this antioxidant is the direct elimination of superoxide anion and hydroxyl radical, GSH depletion is a predictable result of increased ROS and RNS production. It is also, acknowledged that oxidative stress arises from the disruption of the mitochondrial respiratory chain, contributing to an increase in intracellular ROS and RNS formation [386].

Regarding other extracts, a general increased was observed in both reduced and oxidized forms in an apparent concentration-dependent manner. However, the increase in intracellular GSSG levels was not accompanied by a decrease in intracellular GSH contents. One possible reason may be due to the efflux of GSSG. The formed GSSG is extruded via an ATP-dependent export for the extracellular medium as a protective response of the cells against oxidative stress [358, 386].

The influence of JWH-122, UR-144 and WIN55,212-2 in human endometrial stromal cells was studied by Fonseca *et al.* [387]. The authors reported that JWH-122 and UR-144 (0.01–25 µM) induce prompt ROS/RNS formation and endoplasmic reticulum stress without reduction in cell viability. To further investigate the modifications induced by the tested SCs on the cell redox state, the levels of total, oxidized and reduced glutathione were also determined. The results revealed an increase in the GSH and GSSG ratio of JWH-122 and UR-144 compounds.

In comparison with our results, a significant increase in GSH/GSSG levels ($p < 0.001$ *vs* control) was observed in sample B54 at IC_{50}, in which the compound UR-144 is present, in the same way that no increase in ROS/RNS levels was observed. Oxidative stress would be expected to underlie the cytotoxicity observed for sample B54 compared to other extracts. The absence of GSH depletion and/ or a significant increase in ROS/RNS production could be related to an adaptive mechanism by the cell that involves alterations in the redox status. However, the adaptive mechanisms fail and a pro-apoptotic program to eliminate the injured cell is initiated in B54 extract-treated cells [387]. Further

studies are required to ascertain the contribution of redox properties of these synthetic compounds to the respective toxicological effects [384].

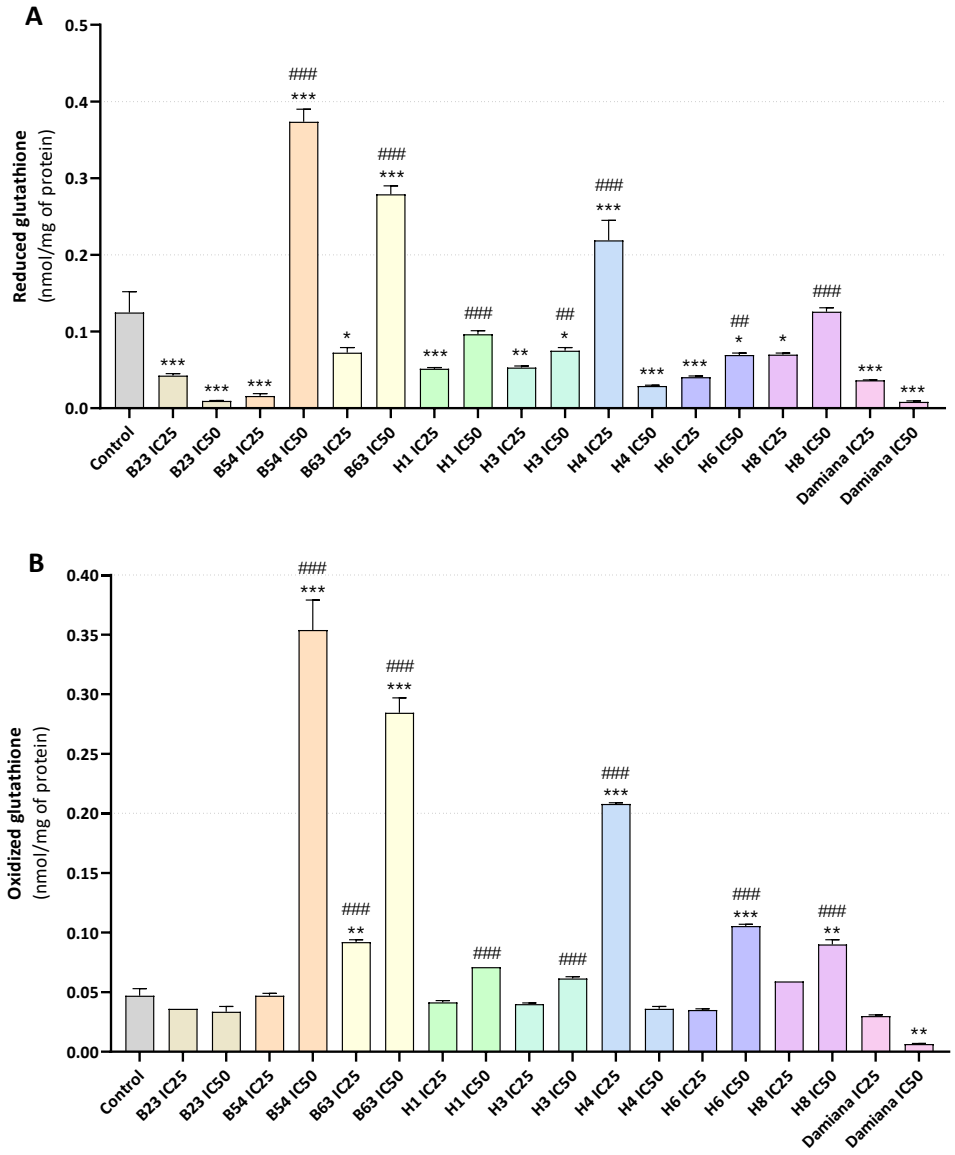

*Figure 78. Intracellular levels of (A) GSH and (B) GSSG in A549 cells after 72 h exposure of herbal extracts at IC25 and IC50 concentrations. Results were normalized by the amount of protein and then expressed as mean ± SEM (n =2). *p < 0.01, ** p < 0.005, *** p < 0.001 mixture versus control; # p < 0.01, ## p < 0.005, ### p < 0.001 mixture versus damiana at the same cytotoxicity levels (IC_{25} and IC_{50}).*

3.4. Evaluation of energetic status

To better understand the potential mechanisms involved in cytotoxicity induced by herbal extracts containing SCs, the bioenergetic function was investigated in the A549 cell line.

ATP is the key intermediate for energy exchange, it is related with cellular energetics, metabolic regulation, and signalling. ATP is fundamental for all cells to maintain their viability and perform their

specific functions. Since ATP is momentarily suppressed by many types of cellular stress, its levels reflect the functional integrity of viable cells [358].

As depicted in Figure 79, after 72 h of exposure, an increase in ATP production was observed in samples B54 and H6 at the highest concentration and H8 for both concentrations tested ($p < 0.001$ vs. control), whereas a significant reduction of ATP intracellular levels at IC_{50} was observed in samples B63, H4 and damiana extract. H4 and damiana samples were the most effective extracts, inducing a decrease of over 90% on ATP levels (0.03 ± 0.02 and 0.02 ± 0.01 nmol/mg of protein, respectively).

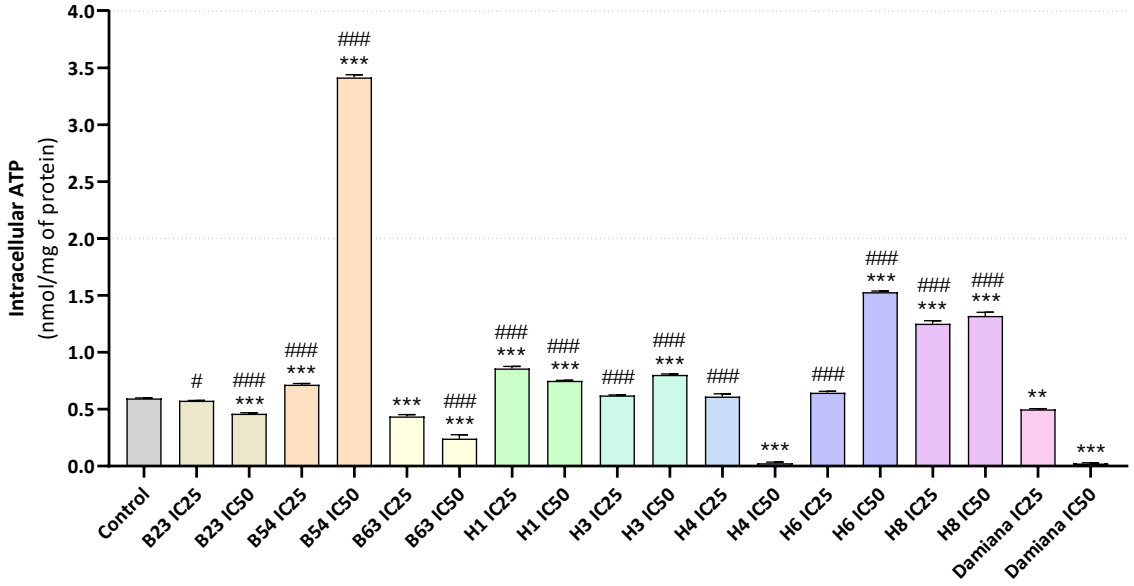

*Figure 79. Intracellular ATP levels determined using luciferin-luciferase-based assay in A549 cells after 72 h exposure of herbal extracts at IC25 and IC50 concentrations. Results were normalized by the amount of protein and then expressed as mean ± SEM (n =3). *p < 0.01, ** p < 0.005, *** p < 0.001 mixture versus control; # p < 0.01, ## p < 0.005, ### p < 0.001 mixture versus damiana at the same cytotoxicity levels (IC_{25} and IC_{50}).*

In comparison with damiana extract, significant differences were observed in almost all seized herbal extracts ($p < 0.001$) at IC_{50}, with exception of sample H4.

In Silva *et al.* [368] work, the results revealed that XLR-11 induced the hyperpolarization of the mitochondrial membrane, increased ATP production and promoted the translocation of a pro-apoptotic protein from the cytosol into mitochondria, concluding that this synthetic cannabinoid leads to the activation of apoptotic cell death pathways by the deregulation of mitochondrial function. As with the ROS/RNS results, the ATP results of sample H4 contrast with those reported by Silva *et al.* [368] concluding that the behaviour of the isolated compound is different when in the presence of another cannabinoid. These results prove the need to study the toxicity evaluation inherent to the coexistence of more than one compound in the same sample.

Another work from the same authors [388], assessed the in vitro nephrotoxicity of three SCs (AB-FUBINACA, JWH-122, and THJ-2201) in human proximal tubule cells (HK-2), to ascertain potential similarities and/or differences regarding their nephrotoxicity signatures. JWH-122 and THJ-2201 compounds increased intracellular ATP levels, whereas AB-FUBINACA stood out among the tested SCs by producing no clear effect on ATP levels. According to the authors, this synthetic cannabinoid mainly differs from the other SCs tested by a missing pentyl side chain in its tail structure, hypothesizing that AB-FUBINACA might follow a different catabolic pathway, which could account for not observing any molecular signatures of nephrotoxicity mechanism.

Regarding to our results, JWH-122 was previously identified in samples B63, H1 and H3. Although samples B63 and H1 have the same SCs, the intracellular ATP levels were slightly different, namely 0.44 ± 0.03 and 0.86 ± 0.03 nmol/mg of protein for the lower concentration and 0.24 ± 0.06 and 0.75 ± 0.004 nmol/mg of protein for the higher concentration tested, respectively. These results allow us to conclude that although the composition is the same for the two samples, the interaction of the compounds is different possibly due to the difference in percentage of each compound in the two samples. According to the results described in Chapter I, JWH-210 is the majority compound in sample B63, while in sample H1 it is JWH-122.

Increased intracellular ATP levels are commonly associated with the triggering of energy-dependent processes leading to apoptotic cell death. High intracellular ATP levels induced by SCs could be possibly attributed to the inhibition of adenylate cyclase activity by these substances. The activation of the cannabinoid receptors is known to inhibit the activity of this enzyme, which is responsible for the synthesis of cyclic adenosine monophosphate (cAMP) from ATP and a decreased in ATP consumption derived from reduced cAMP synthesis could thus result in increased ATP levels [388].

On the other hand, depletion of ATP is a typical feature of hypoxic and toxic injury [358]. A decrease in ATP synthesis and an increase in ROS are the result of the inhibition of complex I and/or II of the electron transport chain, with subsequent accumulation of dysfunctional proteins, which impairs mitochondrial function [358]. H4 and damiana samples elicited a significant decline in ATP synthesis after 72 h of extract exposure. This decreased occurred at a concentration where the GSH depletion and the formation of ROS and RNS were significantly increased, suggesting that oxidative stress may be involved in mitochondrial dysfunction [386].

To explore the mechanisms underlying cell death, further studies would be interesting, such as the involvement of the intrinsic apoptotic pathway by assessing caspase activity and mitochondrial membrane potential.

4. Conclusions

This chapter presents interesting and promising data towards understanding the role of SCs present in seized herbal extracts. Nevertheless, it is still at an early stage and further research is thus required to explore the underlying mechanisms involved in the observed effects. To the best of our knowledge, only one study was found with the evaluation of the cytotoxicity of SCs in herbal extracts. However, the tested SCs were not the same as the present study and only one compound was present in each herbal extract, being this study the first to evaluate the cytotoxicity of mixture of SCs in herbal extracts.

Considering smoking the main route of administration, A549 lung cell line was chosen to evaluate the cytotoxicity of the herbal extracts. Since damiana leaves are one of the most common substrates used in the preparation of smoking mixtures, damiana extract was also evaluated at the same conditions as the seized herbal extracts.

For all the herbal extracts tested, a significant concentration-dependent decrease in cell viability was observed. Sample B54 composed by APINACA and UR-144 compounds, revealed higher cytotoxicity among other samples, while sample B63, which has the SCs JWH-210, JWH-018 and JWH-122, showed lower cytotoxicity as did damiana extract.

Regarding oxidative stress in lung cells, sample B23, which has JWH-018, and damiana significantly induced more reactive species formation than the other extracts at the lowest concentration, whereas a significant depletion of GSH/GSSG levels was observed, reflecting a possible oxidative stress from the disruption of the mitochondrial respiratory chain. A decrease in ATP levels was also observed in damiana extract and sample H4, which has XLR-11 and APINACA compounds. This depletion occurred at a concentration where GSH depletion was also observed, with overproduction of ROS and RNS, suggesting that the disruption of mitochondrial functioning may be caused by oxidative stress. Interestingly, damiana extract showed less cytotoxic effect on cell viability among the seized herbal extracts, however it seems to induce more oxidative stress and disturb the energetic status of A549 lung cells.

Overall, our results support the harmful potential of SCs use, especially considering its potentially adverse outcomes among different herbal samples. The increasing use of SCs and the development

of new, more powerful ones, poses a serious scientific and social challenge. Further research is needed to fully understand the mechanisms of action and physiological consequences of these substances[387].

Part 4 – FINAL CONCLUSIONS

1. Final Conclusions and Future Perspectives

In recent years, there has been a dramatic increase in the consumption, as well as the availability and spread of synthetic drugs in Portugal, especially in the Autonomous Regions of Madeira and the Azores. The variety of modifications in molecules and the speed which they arrive on the market are both challenges for laboratories in the development of analytical methods capable of a rapid identification and quantitative determination of new substances. Several studies have reported the presence of various combinations of different SCs in herbal samples, raising the possibility of serious health problems, since the side effects and toxicity of these products have not yet been properly studied. In this context, the current study aimed to identify the chemical composition of seized herbal products, to develop analytical methodologies for the determination of SCs in oral fluid samples and to study the cytotoxicity of the herbal extracts in human lung cells (A549). Overall, the data obtained in this thesis allowed the following achievements and conclusions:

- The combination of complementary analytical techniques, such as GC-MS, and NMR proved to be a powerful tool in the identification of active principles found in seized herbal products;
- Ten SCs (JWH-018, JWH-073, JWH-122, JWH-210, MAM-2201, APINACA, XLR-11, UR-144, CP47,497-C8 and its enantiomer), and three adulterants (oleamide, vitamin E and vitamin E acetate) were identified by GC-MS in nineteen seized herbal products;
- JWH-018 was the most compound detected among the seized herbal samples, while UR-144 was only identified in one sample;
- Inconsistency in both qualitative and quantitative compositions was verified among the analysed samples. As has been shown, products with the same 'commercial' name have a different content and the same mixture is sold under different brand names. This diversity in composition could lead to serious consequences, since consumers are unaware of dose, durability and even the type of effects triggered;
- Due to the absence of reference materials, the isolation of eight SCs (MAM-2201, JWH-073, JWH-018, JWH-122, JWH-210, UR-144, XLR-11 and APINACA) from seized herbal samples was performed using an UHPLC with a PDA detector;
- The isolation of each compound was achieved, and the purity of the isolated substances verified by UHPLC-PDA, GC-MS and TLC. The estimate purity was 100% for all the compounds at their maximum wavelength, except for MAM-2201 whose purity was estimated at 98.8%. The methodology used proved to be efficient and easy to obtain isolated compounds in a

relative short time, showing to be a good alternative. The isolation of the compounds facilitates the timely development or enhancement of analytical methods in forensic toxicology. It is particularly helpful when new synthetic compounds with yet unknown structures emerge[389];

- The number of SCs, their chemical diversity and variability on the drug market, as well as low concentrations in biological specimens cause many analytical problems. For that reason, two microextraction techniques, MEPS and µSPEed, combined with UHPLC-PDA analysis were developed and validated for the simultaneous determination of SCs in oral fluid samples;
- The chromatographic separation of the eight SCs was achieved with a reduced run time (12 min). The proposed microextraction techniques (MEPS and µSPEed) combined with UHPLC-PDA, provided simplicity, reduced sample preparation and analysis, low-cost and minimal extraction solvent use;
- MEPS best extractions conditions were obtained using a C_{18} sorbent, 3 charge/discharge cycles of 250 µL of sample, and 250 µL of ACN for elution. While for µSPEed, the best extraction conditions were obtained using a C_8 sorbent, 5 loading/unloading cycles of 150 µL of sample, and 250 µL of MeOH for elution;
- Both methodologies showed satisfactory results in terms of linearity ($R^2 \geq 0.994$) within the studied concentration ranges and proved to be precise and accurate in extracting the target compounds in oral fluid samples. Adequate sensitivity and good recovery values (above 73% for MEPS and above 78% for µSPEed) were also obtained;
- Compared to MEPS, µSPEed presented lower LOD and LOQ values ranged from 4.4 – 10.3 ng/mL and 13.9 – 31.1 ng/mL, respectively against to 9.5 – 13.2 ng/mL and 28.8 – 39.9 ng/mL of MEPS. However lower extraction efficiency values were obtained, and some matrix effect was observed for µSPEed;
- No studies have been found to date with the extraction of synthetic drugs in biological samples using µSPEed as extraction technique, being the present study the first to report the extraction of SCs in oral fluid samples;
- Despite the low sampling of real samples, both methodologies showed potential to be applied, as an attractive and very promising approaches, to the analysis of SCs in biological matrices, as well as other drugs in forensic toxicology and clinical investigations;
- Finally, in the last chapter of this work the cytotoxicity of seized herbal extracts containing several SCs was assessed. To the best of our knowledge, this study was the first to evaluate

the cytotoxicity of mixture of SCs in herbal extracts in human lung cells (A549). Damiana extract was also evaluated at the same conditions as the seized herbal extracts since this plant is commonly used in the preparation of smoking mixtures;

- *In vitro* results showed that after 72 h exposure period, all herbal extracts induced cytotoxicity in a concentration-dependent manner, highlighting the potential harmful effects of SCs, especially when more than one substance is present in the sample;
- The herbal extract B54 composed by APINACA and UR-144 compounds, revealed higher cytotoxicity among other samples, while herbal extract B63, which has the SCs JWH-210, JWH-018 and JWH-122, showed lower cytotoxicity as did damiana extract;
- Oxidative stress was also observed, with JWH-018 (in herbal extract B23) and damiana extract inducing significantly more reactive species formation than the other extracts at the lowest concentration, as well as significant depletion of GSH/GSSG levels;
- Damiana extract showed less cytotoxic effect on cell viability among the seized herbal extracts, however it seems to induce more oxidative stress and disturb the energetic status of A549 lung cells.

Despite these promising results, is extremely important to conduct further studies to fully understand the combination effects of SCs from a toxicological point of view, as consumers are totally unaware of their content and psychoactive effects.

Understanding the impact of drug interactions can provide valuable information to explore the causes of sudden lethal intoxications, as well as facilitate the diagnosis and treatment of non-fatal cases. A better knowledge of these combined effects may have a significant impact on public health, by increasing public awareness of the potential severe toxicity and influence behaviour changes globally[56]. In addition, the identification of new substances that rapid emerge on the drug market, as well as the development of analytical methods capable of determining these synthetic drugs in biological samples is fundamental to provide interdisciplinary information and help, particularly among researchers, public health officials, and police forces working in this field.

As main future perspectives we can highlight:

- Improvement of the developed analytical methodology to include other SCs or other synthetic drugs, as well as to apply it to other biological samples, such as blood or urine;

- Explore the mechanisms underlying cell death pathways and investigate the potential toxic effects of the SCs in other cell lines such as neuronal and renal, since SCs are referred to as substances with structural features which exhibit higher binding affinity at both CB_1 and CB_2 receptors and renal as the main route of elimination of these substances as metabolites.

REFERENCES

1. WHO. World Health Organization. Management of substance abuse: cannabis. 2016. https://www.who.int/substance_abuse/facts/cannabis/en.2016. Accessed 3 March 2020.
2. depositphotos. Cannabis. https://pt.depositphotos.com/stock-photos/weed.html. Accessed 5th March 2022.
3. Thomas BF, ElSohly M. The Analytical Chemistry of Cannabis: Quality Assessment, Assurance, and Regulation of Medicinal Marijuana and Cannabinoid Preparations. Amsterdam, NL: Elsevier Science; 2016.
4. Maroon J, Bost J. Review of the neurological benefits of phytocannabinoids. Surg Neurol Int. 2018;9:91-. doi:10.4103/sni.sni_45_18.
5. Shevyrin VA, Morzherin YY. Cannabinoids: structures, effects, and classification. Russ Chem Bull. 2015;64(6):1249-66. doi:10.1007/s11172-015-1008-1.
6. Lambert DM. Cannabinoids in Nature and Medicine. Cham, CH: Wiley; 2009.
7. Mander L, Liu HW. Comprehensive Natural Products II: Chemistry and Biology. Oxford, UK: Elsevier Science; 2010.
8. Halawa OI, Furnish TJ, Wallace MS. Chapter 56 - Role of Cannabinoids in Pain Management. In: Benzon HT, Raja SN, Liu SS, Fishman SM, Cohen SP, editors. Essentials of Pain Medicine (Fourth Edition). Philadelphia, USA: Elsevier; 2018. p. 509-20.
9. Chakravarti B, Ravi J, Ganju RK. Cannabinoids as therapeutic agents in cancer: current status and future implications. Oncotarget. 2014;5(15):5852-72. doi:10.18632/oncotarget.2233.
10. Alves VL, Gonçalves JL, Aguiar J, Teixeira HM, Câmara JS. The synthetic cannabinoids phenomenon: from structure to toxicological properties. A review. Crit Rev Toxicol. 2020;50(5):1-24. doi:10.1080/10408444.2020.1762539.
11. Lu H-C, Mackie K. An Introduction to the Endogenous Cannabinoid System. Biol Psychiatry. 2016;79(7):516-25. doi:10.1016/j.biopsych.2015.07.028.
12. Hourani W, Alexander SPH. Cannabinoid ligands, receptors and enzymes: Pharmacological tools and therapeutic potential. Brain and Neuroscience Advances. 2018;2:1-8. doi:10.1177/2398212818783908.
13. Nicolussi S, Gertsch J. Endocannabinoid transport revisited. Vitam Horm. 2015;98:441-85. doi:10.1016/bs.vh.2014.12.011.
14. Zou S, Kumar U. Cannabinoid Receptors and the Endocannabinoid System: Signaling and Function in the Central Nervous System. Int J Mol Sci. 2018;19(3):833. doi:10.3390/ijms19030833.
15. Aizpurua-Olaizola O, Elezgarai I, Rico-Barrio I, Zarandona I, Etxebarria N, Usobiaga A. Targeting the endocannabinoid system: future therapeutic strategies. Drug Discov Today. 2017;22(1):105-10. doi:10.1016/j.drudis.2016.08.005.
16. Niaz K, Khan F, Maqbool F, Momtaz S, Ismail Hassan F, Nobakht-Haghighi N et al. Endo-cannabinoids system and the toxicity of cannabinoids with a biotechnological approach. EXCLI journal. 2017;16:688-711. doi:10.17179/excli2017-257.
17. Cooper ZD. Adverse Effects of Synthetic Cannabinoids: Management of Acute Toxicity and Withdrawal. Curr Psychiatry Rep. 2016;18(5):52. doi:10.1007/s11920-016-0694-1.
18. Shivangi Bajpai AS. Cannabis Sativa: Therapeutic Chemistry and Classification. Journal of Pharmaceutial Analysis. 2016;5(3):126-35.
19. Wang M, Wang Y-H, Avula B, Radwan MM, Wanas AS, Mehmedic Z et al. Quantitative Determination of Cannabinoids in Cannabis and Cannabis Products Using Ultra-High-Performance Supercritical Fluid Chromatography and Diode Array/Mass Spectrometric Detection. J Forensic Sci. 2017;62(3):602-11. doi:10.1111/1556-4029.13341.
20. Andre CM, Hausman J-F, Guerriero G. Cannabis sativa: The Plant of the Thousand and One Molecules. Front Plant Science. 2016;7:19-. doi:10.3389/fpls.2016.00019.
21. Messina F, Rosati O, Curini M, Marcotullio MC. Chapter 2 - Cannabis and Bioactive Cannabinoids. In: Atta ur R, editor. Studies in Natural Products Chemistry. Oxford, UK: Elsevier; 2015. p. 17-57.
22. Cohen K, Weinstein AM. Synthetic and Non-synthetic Cannabinoid Drugs and Their Adverse Effects-A Review From Public Health Prospective. Frontiers in public health. 2018;6:162. doi:10.3389/fpubh.2018.00162.

23. Feng L-Y, Battulga A, Han E, Chung H, Li J-H. New psychoactive substances of natural origin: A brief review. J Food Drug Anal. 2017;25(3):461-71. doi:10.1016/j.jfda.2017.04.001.
24. Montesano C, Vannutelli G, Piccirilli V, Sergi M, Compagnone D, Curini R. Application of a rapid µ-SPE clean-up for multiclass quantitative analysis of sixteen new psychoactive substances in whole blood by LC–MS/MS. Talanta. 2017;167:260-7. doi:10.1016/j.talanta.2017.02.019.
25. Gonçalves JL, Alves VL, Aguiar J, Teixeira HM, Câmara JS. Synthetic cathinones: an evolving class of new psychoactive substances. Crit Rev Toxicol. 2019;49(7):549-66. doi:10.1080/10408444.2019.1679087.
26. Lafaye G, Karila L, Blecha L, Benyamina A. Cannabis, cannabinoids, and health. Dialogues Clin Neurosci. 2017;19(3):309-16. doi:10.31887/DCNS.2017.19.3/glafaye.
27. Papaseit E, Pérez-Mañá C, Pérez-Acevedo AP, Hladun O, Torres-Moreno MC, Muga R et al. Cannabinoids: from pot to lab. Int J Med Sci. 2018;15(12):1286-95. doi:10.7150/ijms.27087.
28. De Luca MA, Fattore L. Therapeutic Use of Synthetic Cannabinoids: Still an Open Issue? Clin Ther. 2018;40(9):1457-66. doi:10.1016/j.clinthera.2018.08.002.
29. Wiley JL, Marusich JA, Huffman JW, Balster RL, Thomas BF. Hijacking of Basic Research: The Case of Synthetic Cannabinoids. Methods report (RTI Press). 2011;2011:17971. doi:10.3768/rtipress.2011.op.0007.1111.
30. Linda W. John W. Huffman. Chemical & Engineering News. 2010. https://cen.acs.org/articles/88/i26/John-W-Huffman.html. Accessed 3rd March 2022.
31. Nagarkatti P, Pandey R, Rieder SA, Hegde VL, Nagarkatti M. Cannabinoids as novel anti-inflammatory drugs. Future Med Chem. 2009;1(7):1333-49. doi:10.4155/fmc.09.93.
32. Preedy VR. Handbook of Cannabis and Related Pathologies: Biology, Pharmacology, Diagnosis, and Treatment. London, UK: Elsevier Science; 2016.
33. Parker LA. Cannabinoids and the Brain. Cambridge, UK: MIT Press; 2017.
34. EMCDDA. Perspectives On Drugs: Synthetic cannabinoids in Europe. 2017. http://www.emcdda.europa.eu/publications/pods/synthetic-cannabinoids_en. Accessed 12 April 2019.
35. EMCDDA. European Drug Report 2021: Trends and Developments. 2021. https://www.emcdda.europa.eu/system/files/publications/13838/TDAT21001ENN.pdf. Accessed 02 May 2022.
36. Barratt M, Seear K, Lancaster K. A critical examination of the definition of 'psychoactive effect' in Australian drug legislation. Int J Drug Policy. 2016;40:16-25. doi:10.1016/j.drugpo.2016.10.002.
37. Caviness CM, Tzilos G, Anderson BJ, Stein MD. Synthetic Cannabinoids: Use and Predictors in a Community Sample of Young Adults. Subst Abus. 2015;36(3):368-73. doi:10.1080/08897077.2014.959151.
38. Zimmermann US, Winkelmann PR, Pilhatsch M, Nees JA, Spanagel R, Schulz K. Withdrawal phenomena and dependence syndrome after the consumption of "spice gold". Dtsch Arztebl Int. 2009;106(27):464-7. doi:10.3238/arztebl.2009.0464.
39. Seyit M, Ozen M, Oskay A, Kadioglu E. Effectiveness of the synthetic cannabinoids seminar. Turk J Emerg Med. 2016;16(2):57-9. doi:10.1016/j.tjem.2016.03.001.
40. Waugh J, Najafi J, Hawkins L, Hill SL, Eddleston M, Vale JA et al. Epidemiology and clinical features of toxicity following recreational use of synthetic cannabinoid receptor agonists: a report from the United Kingdom National Poisons Information Service. Clin Toxicol. 2016;54(6):512-8. doi:10.3109/15563650.2016.1171329.
41. Advisory Council on the Misuse of Drugs. 'Third generation' synthetic Cannabinoids. 2014. https://assets.publishing.service.gov.uk/government/uploads/system/uploads/attachment_data/file/380161/CannabinoidsReport.pdf. Accessed 16 July 2019.
42. Home Office. Review of the Psychoactive Substances Act 2016. 2018. https://assets.publishing.service.gov.uk/government/uploads/system/uploads/attachment_data/file/756896/Review_of_the_Psychoactive_Substances_Act__2016___web_.pdf. Accessed 17 July 2019.
43. Henriques S, Silva JP, Hsu K. Overview on new psychoactive substances in Portugal. Centro de Investigação e Estudos de Sociologia Instituto Universitário de Lisboa 2018.
44. Saúde Md. Decreto-Lei n.º 54/2013, de 17 de abril. Diário da República n.º 75/2013, Série I de 2013-04-172013. p. 2250 - 4.

45. Drug Enforcement Administration (DEA). Schedules of Controlled Substances: Temporary Placement of Five Synthetic Cannabinoids Into Schedule I. 2011. p. 11075–11078. [accessed 2019 15 March]. https://www.deadiversion.usdoj.gov/fed_regs/rules/2011/fr0301.htm, (2011).
46. Musah RA, Domin MA, Cody RB, Lesiak AD, John Dane A, Shepard JRE. Direct analysis in real time mass spectrometry with collision-induced dissociation for structural analysis of synthetic cannabinoids. Rapid Commun Mass Spectrom. 2012;26(19):2335-42. doi:10.1002/rcm.6354.
47. Brents LK, Prather PL. The K2/Spice phenomenon: emergence, identification, legislation and metabolic characterization of synthetic cannabinoids in herbal incense products. Drug Metab Rev. 2014;46(1):72-85. doi:10.3109/03602532.2013.839700.
48. Tettey JN, Levissianos S. The Global Emergence of NPS: An Analysis of a New Drug Trend. In: Corazza O, Roman-Urrestarazu A, editors. Novel Psychoactive Substances: Policy, Economics and Drug Regulation. Cham, CH: Springer International Publishing; 2017. p. 1-12.
49. Spaderna M, Addy PH, D'Souza DC. Spicing things up: synthetic cannabinoids. Psychopharmacol. 2013;228(4):525-40. doi:10.1007/s00213-013-3188-4.
50. Chopra N. “Fake Marijuana”: A Real Problem. The American Journal of Psychiatry Residents’ Journal. 2015;10(6):2-3.
51. Sanders AN, Stogner JM. A Profile of Synthetic Cannabinoid Users. In: Preedy VR, editor. Handbook of Cannabis and Related Pathologies: Biology, Pharmacology, Diagnosis, and Treatment. London, UK: Elsevier Science; 2016. p. 53-60.
52. Mills B, Yepes A, Nugent K. Synthetic Cannabinoids. The American Journal of the Medical Sciences. 2015;350(1):59-62. doi:10.1097/MAJ.0000000000000466.
53. Duccio P, Fabrizio S, Laura O. Synthetic Cannabinoids and Synthetic Cannabinoid-Induced Psychotic Disorders. In: Compton MT, Manseau MW, editors. The Complex Connection Between Cannabis and Schizophrenia. San Diego: Academic Press; 2018. p. 199-220.
54. Britannica E. Cannabis. Encyclopædia Britannica, inc. 2018. https://www.britannica.com/plant/cannabis-plant. Accessed 17 April 2019.
55. Musah RA, Domin MA, Walling MA, Shepard JRE. Rapid identification of synthetic cannabinoids in herbal samples via direct analysis in real time mass spectrometry. Rapid Commun Mass Spectrom. 2012;26(9):1109-14. doi:10.1002/rcm.6205.
56. Araújo AM, Valente MJ, Carvalho M, Dias da Silva D, Gaspar H, Carvalho F et al. Raising awareness of new psychoactive substances: chemical analysis and in vitro toxicity screening of ‘legal high’ packages containing synthetic cathinones. Arch Toxicol. 2015;89(5):757-71. doi:10.1007/s00204-014-1278-7.
57. Scourfield A, Flick C, Ross J, Wood DM, Thurtle N, Stellmach D et al. Synthetic cannabinoid availability on darknet drug markets—changes during 2016–2017. Toxicol Commun. 2019;3(1):7-15. doi:10.1080/24734306.2018.1563739.
58. Debruyne D, Le Boisselier R. Emerging drugs of abuse: current perspectives on synthetic cannabinoids. Subst Abuse Rehabil. 2015;6:113-29. doi:10.2147/sar.S73586.
59. EMCDDA. New report highlights public health and social risks posed by synthetic cannabinoids in Europe. 2021. https://www.emcdda.europa.eu/news/2021/new-report-highlights-public-health-and-social-risks-posed-synthetic-cannabinoids-europe_en. Accessed 20 April 2022.
60. Zawilska JB, Wojcieszak J. Spice/K2 drugs – more than innocent substitutes for marijuana. Int J Neuropsychopharmacol. 2014;17(3):509-25. doi:10.1017/S1461145713001247.
61. John CA. Synthetic Cannabinoids as Drugs of Abuse. Current Drug Abuse Reviews. 2012;5(2):158-68. doi:10.2174/1874473711205020158.
62. Manseau MW. Synthetic Cannabinoids - Emergence, Epidemiology, Clinical Effects, and Management. In: Compton MT, editor. Marijuana and Mental Health. Arlington, VA: American Psychiatric Publishing; 2016. p. 149-69.
63. EMCDDA. Fentanils and synthetic cannabinoids: driving greater complexity into the drug situation. 2018. http://www.emcdda.europa.eu/system/files/publications/8870/2018-2489-td0118414enn.pdf. Accessed 23 February 2019.
64. Auwärter V, Dresen S, Weinmann W, Müller M, Pütz M, Ferreirós N. ‘Spice’ and other herbal blends: harmless incense or cannabinoid designer drugs? Journal of Mass Spectrometry. 2009;44(5):832-7. doi:10.1002/jms.1558.

65. UNODC. Synthetic Cannabinoids in Herbal Products. 2011. https://www.unodc.org/documents/scientific/Synthetic_Cannabinoids.pdf. Accessed 10th March 2019.
66. Lefever TW, Marusich JA, Thomas BF, Barrus DG, Peiper NC, Kevin RC et al. Vaping Synthetic Cannabinoids: A Novel Preclinical Model of E-Cigarette Use in Mice. Substance abuse: research and treatment. 2017;11:1178221817701739-. doi:10.1177/1178221817701739.
67. Blundell MS, Dargan PI, Wood DM. The dark cloud of recreational drugs and vaping. QJM: An International Journal of Medicine. 2017;111(3):145-8. doi:10.1093/qjmed/hcx049.
68. Breitbarth AK, Morgan J, Jones AL. E-cigarettes—An unintended illicit drug delivery system. Drug Alcohol Depend. 2018;192:98-111. doi:10.1016/j.drugalcdep.2018.07.031.
69. Obafemi AI, Kleinschmidt K, Goto C, Fout D. Cluster of Acute Toxicity from Ingestion of Synthetic Cannabinoid-Laced Brownies. J Med Toxicol. 2015;11(4):426-9. doi:10.1007/s13181-015-0482-z.
70. Phillips J, Lim F, Hsu R. The emerging threat of synthetic cannabinoids. Nurs Manage. 2017;48(3):22-30. doi:10.1097/01.NUMA.0000512504.16830.b6.
71. EMCDDA. Synthetic cannabinoids and "Spice" drug profile. 2015. http://www.emcdda.europa.eu/publications/drug-profile/synthetic-cannabinoids-drug-profile_en. Accessed 15 April 2019.
72. Salomone A. Chapter 11 - Detection of New Psychoactive Substances. In: Kintz P, Salomone A, Vincenti M, editors. Hair Analysis in Clinical and Forensic Toxicology. Boston, USA: Academic Press; 2015. p. 301-36.
73. Alves VL, Gonçalves JL, Aguiar J, Caldeira MJ, Teixeira HM, Câmara JS. Highly sensitive screening and analytical characterization of synthetic cannabinoids in nine different herbal mixtures. Anal Bioanal Chem. 2021;413(8):2257-73. doi:10.1007/s00216-021-03199-6.
74. Carlsson A. Synthesis and spectroscopic characterization of emerging synthetic cannabinoids and cathinones [Dissertation]. Sweden: Linköping University; 2016.
75. Hess C, Schoeder CT, Pillaiyar T, Madea B, Müller CE. Pharmacological evaluation of synthetic cannabinoids identified as constituents of spice. Forensic Toxicol. 2016;34:329-43. doi:10.1007/s11419-016-0320-2.
76. ElSohly MA, Ahmed S, Gul SW, Gul W. Chapter 22 - Review of Synthetic Cannabinoids on the Illicit Drug Market. In: Dasgupta A, editor. Critical Issues in Alcohol and Drugs of Abuse Testing (Second Edition). San Diego, USA: Academic Press; 2019. p. 273-319.
77. Presley B, Varnum S, Logan B. Analysis of Synthetic Cannabinoids in Botanical Material: A Review of Analytical Methods and Findings. Forensic Sci Rev. 2013;25(1-2):27-46.
78. Malfitano AM, Basu S, Maresz K, Bifulco M, Dittel BN. What we know and do not know about the cannabinoid receptor 2 (CB2). Semin Immunol. 2014;26(5):369-79. doi:10.1016/j.smim.2014.04.002.
79. Robinson L, Goonawardena AV, Pertwee RG, Hampson RE, Riedel G. The synthetic cannabinoid HU210 induces spatial memory deficits and suppresses hippocampal firing rate in rats. Br J Pharmacol. 2007;151(5):688-700. doi:10.1038/sj.bjp.0707273.
80. EMCDDA. EMCDDA, Understanding the 'Spice' phenomenon. 2009. http://www.emcdda.europa.eu/publications/thematic-papers/understanding-spice-phenomenon_en. Accessed 23 February 2019.
81. UNODC. Recommended methods for the Identification and Analysis of Synthetic Cannabinoid Receptor Agonists in Seized Materials. United Nations. 2013. https://www.unodc.org/unodc/en/scientists/recommended-methods-for-the-identification-and-analysis-of-synthetic-cannabinoid-receptor-agonists-in-seized-materials.html. Accessed 16th April 2019.
82. Diao X, Huestis MA. Approaches, Challenges, and Advances in Metabolism of New Synthetic Cannabinoids and Identification of Optimal Urinary Marker Metabolites. Clin Pharmacol Ther. 2017;101(2):239-53. doi:10.1002/cpt.534.
83. Shevyrin V, Melkozerov V, Endres GW, Shafran Y, Morzherin Y. On a New Cannabinoid Classification System: A Sight on the Illegal Market of Novel Psychoactive Substances. Cannabis Cannabinoid Res. 2016;1.1:186-94. doi:10.1089/can.2016.0004.
84. Gamage TF, Farquhar CE, Lefever TW, Marusich JA, Kevin RC, McGregor IS et al. Molecular and Behavioral Pharmacological Characterization of Abused Synthetic Cannabinoids MMB- and MDMB-FUBINACA, MN-18, NNEI, CUMYL-PICA, and 5-Fluoro-CUMYL-PICA. J Pharmacol Exp Ther. 2018;365(2):437-46. doi:10.1124/jpet.117.246983.

85. Tai S, Fantegrossi WE. Pharmacological and Toxicological Effects of Synthetic Cannabinoids and Their Metabolites. Curr Top Behav Neurosci. 2017;32:249-62. doi:10.1007/7854_2016_60.
86. Carlier J, Wohlfarth A, Salmeron BD, Scheidweiler KB, Huestis MA, Baumann MH. Pharmacodynamic Effects, Pharmacokinetics, and Metabolism of the Synthetic Cannabinoid AM-2201 in Male Rats. J Pharmacol Exp Ther. 2018;367(3):543-50. doi:10.1124/jpet.118.250530.
87. Huffman JW, Zengin G, Wu M-J, Lu J, Hynd G, Bushell K et al. Structure–activity relationships for 1-alkyl-3-(1-naphthoyl)indoles at the cannabinoid CB1 and CB2 receptors: steric and electronic effects of naphthoyl substituents. New highly selective CB2 receptor agonists. Bioorg Med Chem. 2005;13(1):89-112. doi:10.1016/j.bmc.2004.09.050.
88. Castaneto MS, Gorelick DA, Desrosiers NA, Hartman RL, Pirard S, Huestis MA. Synthetic cannabinoids: Epidemiology, pharmacodynamics, and clinical implications. Drug Alcohol Depend. 2014;144:12-41. doi:10.1016/j.drugalcdep.2014.08.005.
89. Gertsch J, Pertwee RG, Di Marzo V. Phytocannabinoids beyond the Cannabis plant - do they exist? Br J Pharmacol. 2010;160(3):523-9. doi:10.1111/j.1476-5381.2010.00745.x.
90. Carvalho Â, Hansen EH, Kayser O, Carlsen S, Stehle F. Designing microorganisms for heterologous biosynthesis of cannabinoids. FEMS yeast research. 2017;17(4):fox037. doi:10.1093/femsyr/fox037.
91. Altintas M, Inanc L, Oruc GA, Arpacioglu S, Gulec H. Clinical characteristics of synthetic cannabinoid-induced psychosis in relation to schizophrenia: a single-center cross-sectional analysis of concurrently hospitalized patients. Neuropsychiatr Dis Treat. 2016;12:1893-900. doi:10.2147/ndt.S107622.
92. Schoeder CT, Hess C, Madea B, Meiler J, Müller CE. Pharmacological evaluation of new constituents of "Spice": synthetic cannabinoids based on indole, indazole, benzimidazole and carbazole scaffolds. Forensic Toxicol. 2018;36(2):385-403. doi:10.1007/s11419-018-0415-z.
93. Deng H, Verrico CD, Kosten TR, Nielsen DA. Psychosis and synthetic cannabinoids. Psychiatry Res. 2018;268:400-12. doi:10.1016/j.psychres.2018.08.012.
94. Pertwee RG. Cannabinoids. Handbook of experimental Pharmacology. Heidelberg, DE: Springer Science & Business Media; 2006.
95. Aung MM, Griffin G, Huffman JW, Wu M-J, Keel C, Yang B et al. Influence of the N-1 alkyl chain length of cannabimimetic indoles upon CB1 and CB2 receptor binding. Drug Alcohol Depend. 2000;60(2):133-40. doi:10.1016/S0376-8716(99)00152-0.
96. Brents LK, Reichard EE, Zimmerman SM, Moran JH, Fantegrossi WE, Prather PL. Phase I hydroxylated metabolites of the K2 synthetic cannabinoid JWH-018 retain in vitro and in vivo cannabinoid 1 receptor affinity and activity. PLoS One. 2011;6(7):e21917. doi:10.1371/journal.pone.0021917.
97. Tarzia G, Duranti A, Tontini A, Spadoni G, Mor M, Rivara S et al. Synthesis and structure–activity relationships of a series of pyrrole cannabinoid receptor agonists. Bioorg Med Chem. 2003;11(18):3965-73. doi:10.1016/S0968-0896(03)00413-9.
98. Huffman JW, Padgett LW. Recent developments in the medicinal chemistry of cannabimimetic indoles, pyrroles and indenes. Curr Med Chem Anti-Cancer Agents. 2005;12(12):1395-411. doi:10.2174/0929867054020864.
99. Maurer H, Brandt SD, Nature S. New Psychoactive Substances: Pharmacology, Clinical, Forensic and Analytical Toxicology. Cham, CH: Springer International Publishing; 2018.
100. Technologies B. AM2233. 2022. https://www.bertin-bioreagent.com/pr75780/am2233. Accessed 10th February 2022.
101. Marusich JA, Wiley JL, Lefever TW, Patel PR, Thomas BF. Finding order in chemical chaos - Continuing characterization of synthetic cannabinoid receptor agonists. Neuropharmacology. 2018;134:73-81. doi:10.1016/j.neuropharm.2017.10.041.
102. Huffman JW, Szklennik PV, Almond A, Bushell K, Selley DE, He H et al. 1-Pentyl-3-phenylacetylindoles, a new class of cannabimimetic indoles. Bioorg Med Chem Lett. 2005;15(18):4110-3. doi:10.1016/j.bmcl.2005.06.008.
103. Huffman JW, Padgett LW, Isherwood ML, Wiley JL, Martin BR. 1-Alkyl-2-aryl-4-(1-naphthoyl)pyrroles: new high affinity ligands for the cannabinoid CB1 and CB2 receptors. Bioorg Med Chem Lett. 2006;16(20):5432-5. doi:10.1016/j.bmcl.2006.07.051.

104. Banister SD, Stuart J, Kevin RC, Edington A, Longworth M, Wilkinson SM et al. Effects of bioisosteric fluorine in synthetic cannabinoid designer drugs JWH-018, AM-2201, UR-144, XLR-11, PB-22, 5F-PB-22, APICA, and STS-135. ACS Chem Neurosci. 2015;6(8):1445-58. doi:10.1021/acschemneuro.5b00107.
105. Baumann MH, Glennon RA, Wiley JL. Neuropharmacology of New Psychoactive Substances (NPS): The Science Behind the Headlines. Cham, CH: Springer International Publishing; 2017.
106. Banister SD, Moir M, Stuart J, Kevin RC, Wood KE, Longworth M et al. Pharmacology of Indole and Indazole Synthetic Cannabinoid Designer Drugs AB-FUBINACA, ADB-FUBINACA, AB-PINACA, ADB-PINACA, 5F-AB-PINACA, 5F-ADB-PINACA, ADBICA, and 5F-ADBICA. ACS Chem Neurosci. 2015;6(9):1546-59. doi:10.1021/acschemneuro.5b00112.
107. Wiley JL, Marusich JA, Lefever TW, Antonazzo KR, Wallgren MT, Cortes RA et al. AB-CHMINACA, AB-PINACA, and FUBIMINA: Affinity and Potency of Novel Synthetic Cannabinoids in Producing Δ9-Tetrahydrocannabinol-Like Effects in Mice. J Pharmacol Exp Ther. 2015;354(3):328-39. doi:10.1124/jpet.115.225326.
108. Seely KA, Brents LK, Franks LN, Rajasekaran M, Zimmerman SM, Fantegrossi WE et al. AM-251 and rimonabant act as direct antagonists at mu-opioid receptors: implications for opioid/cannabinoid interaction studies. Neuropharmacology. 2012;63(5):905-15. doi:10.1016/j.neuropharm.2012.06.046.
109. Nakajima Ji, Takahashi M, Nonaka R, Seto T, Suzuki J, Yoshida M et al. Identification and quantitation of a benzoylindole (2-methoxyphenyl)(1-pentyl-1H-indol-3-yl)methanone and a naphthoylindole 1-(5-fluoropentyl-1H-indol-3-yl)-(naphthalene-1-yl)methanone (AM-2201) found in illegal products obtained via the Internet and their cannabimimetic effects evaluated by in vitro [35S]GTPγS binding assays. Forensic Toxicol. 2011;29(2):132-41. doi:10.1007/s11419-011-0114-5.
110. Shim JY, Welsh WJ, Howlett AC. Homology model of the CB1 cannabinoid receptor: sites critical for nonclassical cannabinoid agonist interaction. Biopolymers. 2003;71(2):169-89. doi:10.1002/bip.10424.
111. Evren C, Bozkurt M. Synthetic Cannabinoids: Crisis of The Decade The Journal of Psychiatry and Neurological Sciences. 2013;26:1-11. doi:10.5350/DAJPN20132601001.
112. Fattore L, Fratta W. Beyond THC: The New Generation of Cannabinoid Designer Drugs. Front Behav Neurosci. 2011;5(60):1-12. doi:10.3389/fnbeh.2011.00060.
113. Verty ANA, Stefanidis A, McAinch AJ, Hryciw DH, Oldfield B. Anti-Obesity Effect of the CB2 Receptor Agonist JWH-015 in Diet-Induced Obese Mice. PloS one. 2015;10(11):1-19. doi:10.1371/journal.pone.0140592.
114. Cohen K, Weinstein A. The Effects of Cannabinoids on Executive Functions: Evidence from Cannabis and Synthetic Cannabinoids—A Systematic Review. Brain Sciences. 2018;8(3):40. doi:10.3390/brainsci8030040.
115. Preedy VR. Neuropathology of Drug Addictions and Substance Misuse Volume 1: Foundations of Understanding, Tobacco, Alcohol, Cannabinoids and Opioids. London, UK: Elsevier Science; 2016.
116. Aso E, Ferrer I. CB2 Cannabinoid Receptor As Potential Target against Alzheimer's Disease. Front Neurosci. 2016;10:243-. doi:10.3389/fnins.2016.00243.
117. Manera C, Arena C, Chicca A. Synthetic Cannabinoid Receptor Agonists and Antagonists: Implication in CNS Disorders. Recent Pat CNS Drug Discovery. 2016;10(2):142-56. doi:10.2174/1574889810666160519113853.
118. Meyer MR. New psychoactive substances: an overview on recent publications on their toxicodynamics and toxicokinetics. Arch Toxicol. 2016;90(10):2421-44. doi:10.1007/s00204-016-1812-x.
119. Hruba L, McMahon LR. The cannabinoid agonist HU-210: pseudo-irreversible discriminative stimulus effects in rhesus monkeys. Eur J Pharmacol. 2014;727:35-42. doi:10.1016/j.ejphar.2014.01.041.
120. Schaefer N, Kettner M, Laschke MW, Schlote J, Ewald AH, Menger MD et al. Distribution of Synthetic Cannabinoids JWH-210, RCS-4 and Δ 9-Tetrahydrocannabinol After Intravenous Administration to Pigs. Curr Neuropharmacol. 2017;15(5):713-23. doi:10.2174/1570159X15666161111114214.
121. Castaneto MS, Wohlfarth A, Desrosiers NA, Hartman RL, Gorelick DA, Huestis MA. Synthetic cannabinoids pharmacokinetics and detection methods in biological matrices. Drug Metab Rev. 2015;47(2):124-74. doi:10.3109/03602532.2015.1029635.
122. Teske J, Weller JP, Fieguth A, Rothamel T, Schulz Y, Troger HD. Sensitive and rapid quantification of the cannabinoid receptor agonist naphthalen-1-yl-(1-pentylindol-3-yl)methanone (JWH-018) in human serum by liquid chromatography-tandem mass spectrometry. Journal of Chromatography B: Analytical Technologies in the Biomedical and Life Sciences. 2010;878(27):2659-63. doi:10.1016/j.jchromb.2010.03.016.

123. Kacinko SL, Xu A, Homan JW, McMullin MM, Warrington DM, Logan BK. Development and validation of a liquid chromatography-tandem mass spectrometry method for the identification and quantification of JWH-018, JWH-073, JWH-019, and JWH-250 in human whole blood. J Anal Toxicol. 2011;35(7):386-93. doi:10.1093/anatox/35.7.386.
124. Hutter M, Moosmann B, Kneisel S, Auwarter V. Characteristics of the designer drug and synthetic cannabinoid receptor agonist AM-2201 regarding its chemistry and metabolism. Journal of Mass Spectrometry. 2013;48(7):885-94. doi:10.1002/jms.3229.
125. Kneisel S, Speck M, Moosmann B, Corneillie TM, Butlin NG, Auwarter V. LC/ESI-MS/MS method for quantification of 28 synthetic cannabinoids in neat oral fluid and its application to preliminary studies on their detection windows. Anal Bioanal Chem. 2013;405(14):4691-706. doi:10.1007/s00216-013-6887-0.
126. Diao X, Huestis MA. New Synthetic Cannabinoids Metabolism and Strategies to Best Identify Optimal Marker Metabolites. Front Chem. 2019;7:109-. doi:10.3389/fchem.2019.00109.
127. Fantegrossi WE, Moran JH, Radominska-Pandya A, Prather PL. Distinct pharmacology and metabolism of K2 synthetic cannabinoids compared to Δ(9)-THC: mechanism underlying greater toxicity? Life Sci. 2014;97(1):45-54. doi:10.1016/j.lfs.2013.09.017.
128. Patton AL, Seely KA, Yarbrough AL, Fantegrossi W, James LP, McCain KR et al. Altered metabolism of synthetic cannabinoid JWH-018 by human cytochrome P450 2C9 and variants. Biochem Biophys Res Commun. 2018;498(3):597-602. doi:10.1016/j.bbrc.2018.03.028.
129. Auwärter V, Dargan PI, Wood DM. Chapter 13 - Synthetic Cannabinoid Receptor Agonists. In: Dargan PI, Wood DM, editors. Novel Psychoactive Substances. Boston, USA: Academic Press; 2013. p. 317-43.
130. Zhang Q, Ma P, Iszard M, Cole RB, Wang W, Wang G. In Vitro Metabolism of R(+)-[2,3-Dihydro-5-methyl-3-[(morpholinyl)methyl]pyrrolo [1,2,3-de]1,4-benzoxazinyl]-(1-naphthalenyl) methanone mesylate, a Cannabinoid Receptor Agonist. Drug Metab Dispos. 2002;30(10):1077. doi:10.1124/dmd.30.10.1077.
131. Zhang Q, Ma P, Wang W, Cole RB, Wang G. Characterization of rat liver microsomal metabolites of AM-630, a potent cannabinoid receptor antagonist, by high-performance liquid chromatography/electrospray ionization tandem mass spectrometry. Journal of Mass Spectrometry. 2004;39(6):672-81. doi:10.1002/jms.640.
132. Zhang Q, Ma P, Cole R, Wang G. Identification of in vitro metabolites of JWH-015, an aminoalkylindole agonist for the peripheral cannabinoid receptor (CB2) by HPLC-MS/MS. Anal Bioanal Chem. 2006;386:1345-55. doi:10.1007/s00216-006-0717-6.
133. Sobolevsky T, Prasolov I, Rodchenkov G. Detection of JWH-018 metabolites in smoking mixture post-administration urine. Forensic Sci Int. 2010;200(1-3):141-7. doi:10.1016/j.forsciint.2010.04.003.
134. Chimalakonda KC, Seely KA, Bratton SM, Brents LK, Moran CL, Endres GW et al. Cytochrome P450-mediated oxidative metabolism of abused synthetic cannabinoids found in K2/Spice: identification of novel cannabinoid receptor ligands. Drug Metab Dispos. 2012;40(11):2174-84. doi:10.1124/dmd.112.047530.
135. Toennes SW, Geraths A, Pogoda W, Paulke A, Wunder C, Theunissen EL et al. Pharmacokinetic properties of the synthetic cannabinoid JWH-018 and of its metabolites in serum after inhalation. J Pharm Biomed Anal. 2017;140:215-22. doi:10.1016/j.jpba.2017.03.043.
136. Patton AL, Seely KA, Chimalakonda KC, Tran JP, Trass M, Miranda A et al. Targeted Metabolomic Approach for Assessing Human Synthetic Cannabinoid Exposure and Pharmacology. Anal Chem. 2013;85(19):9390-9. doi:10.1021/ac4024704.
137. Nielsen LM, Holm NB, Olsen L, Linnet K. Cytochrome P450-mediated metabolism of the synthetic cannabinoids UR-144 and XLR-11. Drug Testing and Analysis. 2016;8(8):792-800. doi:10.1002/dta.1860.
138. Kong TY, Kim J-H, Kim DK, Lee HS. Synthetic cannabinoids are substrates and inhibitors of multiple drug-metabolizing enzymes. Arch Pharmacal Res. 2018;41(7):691-710. doi:10.1007/s12272-018-1055-x.
139. Brock TG. The Metabolism of JWH-type Synthetic Cannabinoids. 2012. https://www.caymanchem.com/news/metabolism-of-jwh-type-synthetic-cannabinoids. Accessed 22 April 2019.
140. Abbate V, Schwenk M, Presley Brandon C, Uchiyama N. The ongoing challenge of novel psychoactive drugs of abuse. Part I. Synthetic cannabinoids (IUPAC Technical Report). Pure Appl Chem. 2018;90(8):1255. doi:10.1515/pac-2017-0605.

141. Strano-Rossi S, Anzillotti L, Dragoni S, Pellegrino RM, Goracci L, Pascali VL et al. Metabolism of JWH-015, JWH-098, JWH-251, and JWH-307 in silico and in vitro: a pilot study for the detection of unknown synthetic cannabinoids metabolites. Anal Bioanal Chem. 2014;406(15):3621-36. doi:10.1007/s00216-014-7793-9.
142. Moran CL, Le VH, Chimalakonda KC, Smedley AL, Lackey FD, Owen SN et al. Quantitative measurement of JWH-018 and JWH-073 metabolites excreted in human urine. Anal Chem. 2011;83(11):4228-36. doi:10.1021/ac2005636.
143. Hutter M, Broecker S, Kneisel S, Auwärter V. Identification of the major urinary metabolites in man of seven synthetic cannabinoids of the aminoalkylindole type present as adulterants in 'herbal mixtures' using LC-MS/MS techniques. Journal of Mass Spectrometry. 2012;47(1):54-65. doi:10.1002/jms.2026.
144. De Brabanter N, Esposito S, Tudela E, Lootens L, Meuleman P, Leroux-Roels G et al. In vivo and in vitro metabolism of the synthetic cannabinoid JWH-200. Rapid Commun Mass Spectrom. 2013;27(18):2115-26. doi:10.1002/rcm.6673.
145. Kavanagh P, Grigoryev A, Melnik A, Savchuk S, Simonov A, Rozhanets V. Detection and tentative identification of urinary phase I metabolites of phenylacetylindole cannabimimetics JWH-203 and JWH-251, by GC-MS and LC-MS/MS. Journal of Chromatography B: Analytical Technologies in the Biomedical and Life Sciences. 2013;934:102-8. doi:10.1016/j.jchromb.2013.07.005.
146. Grigoryev A, Melnik A, Savchuk S, Simonov A, Rozhanets V. Gas and liquid chromatography-mass spectrometry studies on the metabolism of the synthetic phenylacetylindole cannabimimetic JWH-250, the psychoactive component of smoking mixtures. Journal of Chromatography B: Analytical Technologies in the Biomedical and Life Sciences. 2011;879(25):2519-26. doi:10.1016/j.jchromb.2011.07.004.
147. Cannaert A, Storme J, Franz F, Auwärter V, Stove C. Detection and activity profiling of synthetic cannabinoids and metabolites with a newly developed bio-assay. Anal Chem. 2016;88(23):11476-85. doi:10.1021/acs.analchem.6b02600.
148. Holm NB, Nielsen LM, Linnet K. CYP3A4 Mediates Oxidative Metabolism of the Synthetic Cannabinoid AKB-48. The AAPS journal. 2015;17(5):1237-45. doi:10.1208/s12248-015-9788-7.
149. Sobolevsky T, Prasolov I, Rodchenkov G. Study on the phase I metabolism of novel synthetic cannabinoids, APICA and its fluorinated analogue. Drug Testing and Analysis. 2015;7(2):131-42. doi:10.1002/dta.1756.
150. Kavanagh P, Grigoryev A, Savchuk S, Mikhura I, Formanovsky A. UR-144 in products sold via the Internet: identification of related compounds and characterization of pyrolysis products. Drug Testing and Analysis. 2013;5(8):683-92. doi:10.1002/dta.1456.
151. Kanamori T, Kanda K, Yamamuro T, Kuwayama K, Tsujikawa K, Iwata YT et al. Detection of main metabolites of XLR-11 and its thermal degradation product in human hepatoma HepaRG cells and human urine. Drug Testing and Analysis. 2015;7(4):341-5. doi:10.1002/dta.1765.
152. Jang M, Kim IS, Park YN, Kim J, Han I, Baeck S et al. Determination of urinary metabolites of XLR-11 by liquid chromatography-quadrupole time-of-flight mass spectrometry. Anal Bioanal Chem. 2016;408(2):503-16. doi:10.1007/s00216-015-9116-1.
153. Wurita A, Hasegawa K, Minakata K, Gonmori K, Nozawa H, Yamagishi I et al. Identification and quantification of metabolites of AB-CHMINACA in a urine specimen of an abuser. Leg Med. 2016;19:113-8. doi:10.1016/j.legalmed.2015.07.011.
154. Sim J, Cho HS, Lee J, In S, Kim E. Determination of AB-CHMINACA and its metabolites in human hair and their deposition in hair of abusers. J Pharm Biomed Anal. 2017;140:162-8. doi:10.1016/j.jpba.2017.03.041.
155. Castaneto M. Identification of AB-FUBINACA metabolites in human hepatocytes and urine using high-resolution mass spectrometry. Forensic Toxicol. 2015;33:295-310. doi:10.1007/s11419-015-0275-8.
156. Ashino T, Hakukawa K, Itoh Y, Numazawa S. Inhibitory effect of synthetic cannabinoids on CYP1A activity in mouse liver microsomes. The Journal of toxicological sciences. 2014;39(6):815-20. doi:10.2131/jts.39.815.
157. Hudson S, Ramsey J, King L, Timbers S, Maynard S, Dargan PI et al. Use of high-resolution accurate mass spectrometry to detect reported and previously unreported cannabinomimetics in "herbal high" products. J Anal Toxicol. 2010;34(5):252-60. doi:10.1093/jat/34.5.252.
158. Tournebize J, Gibaja V, Kahn JP. Acute effects of synthetic cannabinoids: Update 2015. Substance abuse : research and treatment. 2017;38(3):344-66. doi:10.1080/08897077.2016.1219438.

159. Alipour A, Patel PB, Shabbir Z, Gabrielson S. Review of the many faces of synthetic cannabinoid toxicities. Ment Health Clin. 2019;9(2):93-9. doi:10.9740/mhc.2019.03.093.
160. Lam RPK, Tang MHY, Leung SC, Chong YK, Tsui MSH, Mak TWL. Supraventricular tachycardia and acute confusion following ingestion of e-cigarette fluid containing AB-FUBINACA and ADB-FUBINACA: a case report with quantitative analysis of serum drug concentrations. Clin Toxicol. 2017;55(7):662-7. doi:10.1080/15563650.2017.1307385.
161. Patton AL, Chimalakonda KC, Moran CL, McCain KR, Radominska-Pandya A, James LP et al. K2 toxicity: fatal case of psychiatric complications following AM2201 exposure. J Forensic Sci. 2013;58(6):1676-80. doi:10.1111/1556-4029.12216.
162. Shanks KG, Dahn T, Terrell AR. Detection of JWH-018 and JWH-073 by UPLC-MS-MS in postmortem whole blood casework. J Anal Toxicol. 2012;36(3):145-52. doi:10.1093/jat/bks013.
163. van Amsterdam J, Brunt T, van den Brink W. The adverse health effects of synthetic cannabinoids with emphasis on psychosis-like effects. J Psychopharmacol (Oxf). 2015;29(3):254-63. doi:10.1177/0269881114565142.
164. Moeller S, Lucke C, Struffert T, Schwarze B, Gerner ST, Schwab S et al. Ischemic stroke associated with the use of a synthetic cannabinoid (spice). Asian J Psychiatr. 2017;25:127-30. doi:10.1016/j.ajp.2016.10.019.
165. CDC. Centers for Disease Control and Prevention. Acute kidney injury associated with synthetic cannabinoid use--multiple states, 2012. MMWR Morbidity and mortality weekly report. 2013;62(6):93-8.
166. Buser GL, Gerona RR, Horowitz BZ, Vian KP, Troxell ML, Hendrickson RG et al. Acute kidney injury associated with smoking synthetic cannabinoid. Clin Toxicol. 2014;52(7):664-73. doi:10.3109/15563650.2014.932365.
167. Williams J. Sample Preservation – urine. http://www.birmingham.ac.uk/Documents/college-mds/facilities/crf/scientists/sample-preservation-urine.pdf. Accessed 30.08.14.
168. Moritz E, Austin C, Wahl M, DesLauriers C, Navon L, Walblay K et al. Notes from the Field: Outbreak of Severe Illness Linked to the Vitamin K Antagonist Brodifacoum and Use of Synthetic Cannabinoids - Illinois, March-April 2018. MMWR Morbidity and mortality weekly report. 2018;67(21):607-8. doi:10.15585/mmwr.mm6721a4.
169. Cohen K, Kapitány-Fövény M, Mama Y, Arieli M, Rosca P, Demetrovics Z et al. The effects of synthetic cannabinoids on executive function. Psychopharmacology. 2017;234(7):1121-34. doi:10.1007/s00213-017-4546-4.
170. Livny A, Cohen K, Tik N, Tsarfaty G, Rosca P, Weinstein A. The effects of synthetic cannabinoids (SCs) on brain structure and function. European Neuropsychopharmacology. 2018;28(9):1047-57. doi:10.1016/j.euroneuro.2018.07.095.
171. Hakimian D, Tomer O, Hiller N, Heyman SN, Israel S. Fatal Mesenteric Ischemia Induced by Synthetic Cannabinoids: A Case Report and Literature Review. Case Rep Emerg Med. 2017;2017:6964078-. doi:10.1155/2017/6964078.
172. Emery DW, Iceman CR, Hayes SM. Geographic Variability of Active Ingredients in Spice as an Indicator of Mechanisms of Distribution and Manufacture Within Alaska. J Young Investig. 2018;34(4):7-16. doi:10.22186/jyi.34.4.7-16.
173. Tai S, Fantegrossi WE. Synthetic Cannabinoids: Pharmacology, Behavioral Effects, and Abuse Potential. Curr Addict Rep. 2014;1(2):129-36. doi:10.1007/s40429-014-0014-y.
174. Miliano C, Serpelloni G, Rimondo C, Mereu M, Marti M, De Luca MA. Neuropharmacology of New Psychoactive Substances (NPS): Focus on the Rewarding and Reinforcing Properties of Cannabimimetics and Amphetamine-Like Stimulants. Front Neurosci. 2016;10:153. doi:10.3389/fnins.2016.00153.
175. Hervás ES. Synthetic cannabinoids: characteristics, use and clinical implications. Arch Psychiatry Psychother. 2017;19(2):42-8. doi:10.12740/APP/71073.
176. Bruni AT, Rodrigues CHP, dos Santos C, de Castro JS, Mariotoo LS, Sinhorini LFC. Analytical Challenges for Identification of New Psychoactive Substances - A Literature-Based Study for Seized Drugs. Brazilian Journal of Analytical Chemistry. 2022;9(34):52-78. doi:10.30744/brjac.2179-3425.RV-41-2021.
177. Aldlgan AA, Torrance HJ. Bioanalytical methods for the determination of synthetic cannabinoids and metabolites in biological specimens. TrAC Trends in Analytical Chemistry. 2016;80:444-57. doi:10.1016/j.trac.2016.03.025.

178. Lopes IC. A Comprehensive Study of Herbal Blends from Portuguese Smart Shops: Isolation, Analysis and Toxicological Impact.: Instituto Superior de Ciências da Saúde Egas Moniz; 2014.
179. Couto RAS, Gonçalves LM, Carvalho F, Rodrigues JA, Rodrigues CMP, Quinaz MB. The Analytical Challenge in the Determination of Cathinones, Key-Players in the Worldwide Phenomenon of Novel Psychoactive Substances. Crit Rev Anal Chem. 2018;48(5):372-90. doi:10.1080/10408347.2018.1439724.
180. Rosado T, Gonçalves J, Luís Â, Malaca S, Soares S, Vieira DN et al. Synthetic cannabinoids in biological specimens: a review of current analytical methods and sample preparation techniques. Bioanalysis. 2018;10(19):1609-23. doi:10.4155/bio-2018-0150.
181. Kumar S, Baggi TR. Analytical Methods for Herbal Products Containing Synthetic Cannabinoids: A Review. Forensic Chemistry. 2022;27:100396. doi:10.1016/j.forc.2021.100396.
182. UNODC. Recommended methods for the Identification and Analysis of Synthetic Cannabinoid Receptor Agonists in Seized Materials (Revised and Updated). United Nations. 2020. https://www.unodc.org/documents/scientific/STNAR48_Rev.1_ebook.pdf. Accessed 4th May 2022.
183. Znaleziona J, Ginterová P, Petr J, Ondra P, Válka I, Ševčík J et al. Determination and identification of synthetic cannabinoids and their metabolites in different matrices by modern analytical techniques – a review. Anal Chim Acta. 2015;874:11-25. doi:10.1016/j.aca.2014.12.055.
184. West A, Hoque N, Griep M. Extraction Efficacy of Synthetic Cannabinoids From Damania Leaf Substrates Utilizing Electrolytic Solvents. Oak Ridge Association of Universities (ORAU), Oak Ridge, TN 2015.
185. Hudson S, Ramsey J, King L, Timbers S, Maynard S, Dargan P et al. Use of High-Resolution Accurate Mass Spectrometry to Detect Reported and Previously Unreported Cannabinomimetics in "Herbal High" Products. J Anal Toxicol. 2010;34:252-60. doi:10.1093/jat/34.5.252.
186. Uchiyama N, Kikura-Hanajiri R, Ogata J, Goda Y. Chemical analysis of synthetic cannabinoids as designer drugs in herbal products. Forensic Sci Int. 2010;198(1):31-8. doi:10.1016/j.forsciint.2010.01.004.
187. Uchiyama N, Kawamura M, Kikura-Hanajiri R, Goda Y. Identification of two new-type synthetic cannabinoids, N-(1-adamantyl)-1-pentyl-1H-indole-3-carboxamide (APICA) and N-(1-adamantyl)-1-pentyl-1H-indazole-3-carboxamide (APINACA), and detection of five synthetic cannabinoids, AM-1220, AM-2233, AM-1241, CB-13 (CRA-13), and AM-1248, as designer drugs in illegal products. Forensic Toxicol. 2012;30(2):114-25. doi:10.1007/s11419-012-0136-7.
188. Martijn D, Blanckaert P, Coopman V, Van Quekelberghe S, Calenbergh S, Cordonnier J. Identification of a new tert-leucinate class synthetic cannabinoid in powder and "spice-like" herbal incenses: Methyl 2-[[1-(5-fluoropentyl)indole-3-carbonyl]amino]-3,3-dimethyl-butanoate (5F-MDMB-PICA). Forensic Sci Int. 2017;273. doi:10.1016/j.forsciint.2017.01.023.
189. Wu N, Danoun S, Balayssac S, Malet-Martino M, Lamoureux C, Gilard V. Synthetic cannabinoids in e-liquids: A proton and fluorine NMR analysis from a conventional spectrometer to a compact one. Forensic Sci Int. 2021;324:110813. doi:10.1016/j.forsciint.2021.110813.
190. Angerer V, Franz F, Moosmann B, Bisel P, Auwärter V. 5F-Cumyl-PINACA in 'e-liquids' for electronic cigarettes: comprehensive characterization of a new type of synthetic cannabinoid in a trendy product including investigations on the in vitro and in vivo phase I metabolism of 5F-Cumyl-PINACA and its non-fluorinated analog Cumyl-PINACA. Forensic Toxicol. 2019;37(1):186-96. doi:10.1007/s11419-018-0451-8.
191. Norman C, Walker G, McKirdy B, McDonald C, Fletcher D, Antonides LH et al. Detection and quantitation of synthetic cannabinoid receptor agonists in infused papers from prisons in a constantly evolving illicit market. Drug Testing and Analysis. 2020;12(4):538-54. doi:10.1002/dta.2767.
192. Lavado E, Leonardo J, Carapinha L, Torrado M, Frango P, Calado V. Novas Substâncias Psicoativas em Portugal. Serviço de Intervenção nos Comportamentos Aditivos e nas Dependências (SICAD) 2018.
193. Rodrigues TB, Souza MP, de Melo Barbosa L, de Carvalho Ponce J, Júnior LFN, Yonamine M et al. Synthetic cannabinoid receptor agonists profile in infused papers seized in Brazilian prisons. Forensic Toxicol. 2022;40(1):119-24. doi:10.1007/s11419-021-00586-7.
194. Esteve-Turrillas FA, Armenta S, de la Guardia M. Sample preparation strategies for the determination of psychoactive substances in biological fluids. J Chromatogr A. 2020;1633:461615. doi:10.1016/j.chroma.2020.461615.
195. Kneisel S, Auwärter V. Analysis of 30 synthetic cannabinoids in serum by liquid chromatography-electrospray ionization tandem mass spectrometry after liquid-liquid extraction. Journal of Mass Spectrometry. 2012;47(7):825-35. doi:10.1002/jms.3020.

196. Ji J, Wang J, Zhang Y. Rapid screening of 23 synthetic cannabinoids in blood by direct analysis in real time - Tandem mass spectrometry. Int J Mass Spectrom. 2021;469:116667. doi:10.1016/j.ijms.2021.116667.
197. Ong RS, Kappatos DC, Russell SGG, Poulsen HA, Banister SD, Gerona RR et al. Simultaneous analysis of 29 synthetic cannabinoids and metabolites, amphetamines, and cannabinoids in human whole blood by liquid chromatography–tandem mass spectrometry – A New Zealand perspective of use in 2018. Drug Testing and Analysis. 2020;12(2):195-214. doi:10.1002/dta.2697.
198. Knittel JL, Holler JM, Chmiel JD, Vorce SP, Magluilo J, Jr., Levine B et al. Analysis of Parent Synthetic Cannabinoids in Blood and Urinary Metabolites by Liquid Chromatography Tandem Mass Spectrometry. J Anal Toxicol. 2016;40(3):173-86. doi:10.1093/jat/bkv137.
199. Castaneto MS, Scheidweiler KB, Gandhi A, Wohlfarth A, Klette KL, Martin TM et al. Quantitative urine confirmatory testing for synthetic cannabinoids in randomly collected urine specimens. Drug Testing and Analysis. 2015;7(6):483-93. doi:10.1002/dta.1709.
200. Blandino V, Wetzel J, Kim J, Haxhi P, Curtis R, Concheiro M. Oral Fluid vs. Urine Analysis to Monitor Synthetic Cannabinoids and Classic Drugs Recent Exposure. Curr Pharm Biotechnol. 2017;18(10):796-805. doi:10.2174/1389201018666171122113934.
201. Khurshid Z, Zohaib S, Najeeb S, Zafar MS, Slowey PD, Almas K. Human Saliva Collection Devices for Proteomics: An Update. Int J Mol Sci. 2016;17(6):846. doi:10.3390/ijms17060846.
202. Wille SMR, Eliaerts J, Di Fazio V, Samyn N. Challenges concerning new psychoactive substance detection in oral fluid. Toxicologie Analytique et Clinique. 2017;29(1):11-7. doi:10.1016/j.toxac.2016.12.004.
203. Kneisel S, Auwärter V, Kempf J. Analysis of 30 synthetic cannabinoids in oral fluid using liquid chromatography-electrospray ionization tandem mass spectrometry. Drug Testing and Analysis. 2013;5(8):657-69. doi:10.1002/dta.1429.
204. Desrosiers NA, Huestis MA. Oral Fluid Drug Testing: Analytical Approaches, Issues and Interpretation of Results. J Anal Toxicol. 2019;43(6):415-43. doi:10.1093/jat/bkz048.
205. Williams M, Martin J, Galettis P. A Validated Method for the Detection of Synthetic Cannabinoids in Oral Fluid. J Anal Toxicol. 2018;43(1):10-7. doi:10.1093/jat/bky043.
206. Hutter M, Kneisel S, Auwärter V, Neukamm MA. Determination of 22 synthetic cannabinoids in human hair by liquid chromatography–tandem mass spectrometry. J Chromatogr B. 2012;903:95-101. doi:10.1016/j.jchromb.2012.07.002.
207. Salomone A, Luciano C, Di Corcia D, Gerace E, Vincenti M. Hair analysis as a tool to evaluate the prevalence of synthetic cannabinoids in different populations of drug consumers. Drug Testing and Analysis. 2014;6(1-2):126-34. doi:10.1002/dta.1556.
208. Gottardo R, Sorio D, Musile G, Trapani E, Seri C, Serpelloni G et al. Screening for synthetic cannabinoids in hair by using LC-QTOF MS: A new and powerful approach to study the penetration of these new psychoactive substances in the population. Med Sci Law. 2014;54(1):22-7. doi:10.1177/0025802413477396.
209. Franz F, Jechle H, Angerer V, Pegoro M, Auwärter V, Neukamm MA. Synthetic cannabinoids in hair – Pragmatic approach for method updates, compound prevalences and concentration ranges in authentic hair samples. Anal Chim Acta. 2018;1006:61-73. doi:10.1016/j.aca.2017.12.029.
210. Jones G. Postmortem toxicology. In: Moffat AC, Osselton MD, Widdop B, editors. Clarke's Analysis of Drugs and Poisons. 3ª ed. London: Pharmaceutical Press; 2003. p. 94-108.
211. Queiroz SCN, Collins CH, Jardim ICSF. Métodos de extração e/ou concentração de compostos encontrados em fluidos biológicos para posterior determinação cromatográfica. Química Nova. 2001;24:68-76.
212. Wohlfarth A, Scheidweiler KB, Chen X, Liu H-f, Huestis MA. Qualitative Confirmation of 9 Synthetic Cannabinoids and 20 Metabolites in Human Urine Using LC–MS/MS and Library Search. Anal Chem. 2013;85(7):3730-8. doi:10.1021/ac3037365.
213. Escada MSdS. Métodos de análise de piperazinas em fluidos biológicos. Aveiro: Universidade de Aveiro; 2007.
214. Pinto MMM, Almeida AP, Palmeira A, Fernandes CS, Afonso CM, Adriano G et al. Manual de Trabalhos Laboratorais de Química Orgância e Farmacêutica. Lisboa: Lidel - Edições Técnicas Lda. ; 2011.
215. Arntson A, Ofsa B, Lancaster D, Simon JR, McMullin M, Logan B. Validation of a novel immunoassay for the detection of synthetic cannabinoids and metabolites in urine specimens. J Anal Toxicol. 2013;37(5):284-90. doi:10.1093/jat/bkt024.

216. Grigoryev A, Kavanagh P, Melnik A. The detection of the urinary metabolites of 3-[(adamantan-1-yl)carbonyl]-1-pentylindole (AB-001), a novel cannabimimetic, by gas chromatography-mass spectrometry. Drug Testing and Analysis. 2012;4(6):519-24. doi:10.1002/dta.350.
217. Kavanagh P, Grigoryev A, Melnik A, Simonov A. The identification of the urinary metabolites of 3-(4-methoxybenzoyl)-1-pentylindole (RCS-4), a novel cannabimimetic, by gas chromatography-mass spectrometry. J Anal Toxicol. 2012;36(5):303-11. doi:10.1093/jat/bks032.
218. Sobolevsky T, Prasolov I, Rodchenkov G. Detection of urinary metabolites of AM-2201 and UR-144, two novel synthetic cannabinoids. Drug Testing and Analysis. 2012;4(10):745-53. doi:10.1002/dta.1418.
219. de Jager AD, Warner JV, Henman M, Ferguson W, Hall A. LC-MS/MS method for the quantitation of metabolites of eight commonly-used synthetic cannabinoids in human urine--an Australian perspective. Journal of Chromatography B: Analytical Technologies in the Biomedical and Life Sciences. 2012;897:22-31. doi:10.1016/j.jchromb.2012.04.002.
220. Płotka-Wasylka J, Szczepańska N, de la Guardia M, Namieśnik J. Miniaturized solid-phase extraction techniques. TrAC Trends in Analytical Chemistry. 2015;73:19-38. doi:10.1016/j.trac.2015.04.026.
221. Alves VLG. Desenvolvimento e Validação de Novas Metodologias Analíticas Baseadas na MEPS/UHPLC-PDA e QuEChERS/UHPLC-PDA para a Determinação de Antidepressivos em Amostras de Urina: Universidade de Coimbra; 2015.
222. Stone J. Chapter 3 - Sample preparation techniques for mass spectrometry in the clinical laboratory. In: Nair H, Clarke W, editors. Mass Spectrometry for the Clinical Laboratory. San Diego: Academic Press; 2017. p. 37-62.
223. Solid-Phase Extraction. Chemistry Libre texts. 2020. https://chem.libretexts.org/@go/page/155906. Accessed 10 May 2022.
224. Guale F, Shahreza S, Walterscheid JP, Chen H-H, Arndt C, Kelly AT et al. Validation of LC–TOF-MS Screening for Drugs, Metabolites, and Collateral Compounds in Forensic Toxicology Specimens. J Anal Toxicol. 2012;37(1):17-24. doi:10.1093/jat/bks084.
225. Simões SS, Silva I, Ajenjo AC, Dias MJ. Validation and application of an UPLC–MS/MS method for the quantification of synthetic cannabinoids in urine samples and analysis of seized materials from the Portuguese market. Forensic Sci Int. 2014;243:117-25. doi:10.1016/j.forsciint.2014.07.022.
226. de Castro A, Piñeiro B, Lendoiro E, Cruz A, López-Rivadulla M. Quantification of selected synthetic cannabinoids and Δ9-tetrahydrocannabinol in oral fluid by liquid chromatography–tandem mass spectrometry. J Chromatogr A. 2013;1295:99-106. doi:10.1016/j.chroma.2013.04.035.
227. Anastassiades M, Lehotay SJ, tajnbaher D, Schenck FJ. Fast and easy multiresidue method employing acetonitrile extraction/partitioning and "dispersive solid-phase extraction" for the determination of pesticide residues in produce. J AOAC Int. 2003;86(2):412-31.
228. Hasegawa K, Minakata K, Gonmori K, Nozawa H, Yamagishi I, Watanabe K et al. Identification and quantification of predominant metabolites of synthetic cannabinoid MAB-CHMINACA in an authentic human urine specimen. Drug Testing and Analysis. 2018;10(2):365-71. doi:10.1002/dta.2220.
229. Pereira J, Câmara JS, Colmsjö A, Abdel-Rehim M. Microextraction by packed sorbent: an emerging, selective and high-throughput extraction technique in bioanalysis. Biomedical Chromatography. 2014;28(6):839-47. doi:10.1002/bmc.3156.
230. Pereira J, Silva CL, Perestrelo R, Gonçalves J, Alves V, Câmara JS. Re-exploring the high-throughput potential of microextraction techniques, SPME and MEPS, as powerful strategies for medical diagnostic purposes. Innovative approaches, recent applications and future trends. Anal Bioanal Chem. 2014;406(8):2101-22. doi:10.1007/s00216-013-7527-4.
231. Arthur CL, Pawliszyn J. Solid phase microextraction with thermal desorption using fused silica optical fibers. Anal Chem. 1990;62(19):2145-8. doi:10.1021/ac00218a019.
232. Shirey RE. 4 - SPME Commercial Devices and Fibre Coatings. In: Pawliszyn J, editor. Handbook of Solid Phase Microextraction. Oxford: Elsevier; 2012. p. 99-133.
233. Anzillotti L, Marezza F, Calò L, Andreoli R, Agazzi S, Bianchi F et al. Determination of synthetic and natural cannabinoids in oral fluid by solid-phase microextraction coupled to gas chromatography/mass spectrometry: A pilot study. Talanta. 2019;201:335-41. doi:10.1016/j.talanta.2019.04.029.

234. Cox AO, Daw RC, Mason MD, Grabenauer M, Pande PG, Davis KH et al. Use of SPME-HS-GC-MS for the analysis of herbal products containing synthetic cannabinoids. J Anal Toxicol. 2012;36(5):293-302. doi:10.1093/jat/bks025.
235. Falcó IPR, Moya MN. Determination of Volatile Organic Compounds in Water. In: Nollet LML, De Gelder LSP, editors. Handbook of Water Analysis, Third Edition. Flórida: CRC Press; 2013. p. 549-610.
236. Queiroz MEC. Microextração em fase sólida para análise de fármacos em fluidos biológicos. Scientia Chromatographica. 2009;1(3):11-9.
237. Sánchez-González J, Odoardi S, Bermejo AM, Bermejo-Barrera P, Romolo FS, Moreda-Piñeiro A et al. Development of a micro-solid-phase extraction molecularly imprinted polymer technique for synthetic cannabinoids assessment in urine followed by liquid chromatography–tandem mass spectrometry. J Chromatogr A. 2018;1550:8-20. doi:10.1016/j.chroma.2018.03.049.
238. Pereira JAM, Gonçalves J, Porto-Figueira P, Figueira JA, Alves V, Perestrelo R et al. Current trends on microextraction by packed sorbent – fundamentals, application fields, innovative improvements and future applications. Analyst. 2019;144(17):5048-74. doi:10.1039/C8AN02464B.
239. Dawes P. It's A Small World. The Column. 2007;3(7):26-9.
240. Stefanello ST, Dobrachinski F, de Carvalho NR, Amaral GP, Barcelos RP, Oliveira VA et al. Free radical scavenging in vitro and biological activity of diphenyl diselenide-loaded nanocapsules: DPDS-NCS antioxidant and toxicological effects. Int J Nanomedicine. 2015;10:5663-70. doi:10.2147/IJN.S87190.
241. Sorribes-Soriano A, Verdeguer J, Pastor A, Armenta S, Esteve-Turrillas FA. Determination of Third-Generation Synthetic Cannabinoids in Oral Fluids. J Anal Toxicol. 2021;45(4):331-6. doi:10.1093/jat/bkaa091.
242. Casado N, Perestrelo R, Silva CL, Sierra I, Câmara JS. Comparison of high-throughput microextraction techniques, MEPS and µ-SPEed, for the determination of polyphenols in baby food by ultrahigh pressure liquid chromatography. Food Chemistry. 2019;292:14-23. doi:10.1016/j.foodchem.2019.04.038.
243. Ivanov ID, Stoykova S, Ivanova E, Vlahova A, Burdzhiev N, Pantcheva I et al. A case of 5F-ADB / FUB-AMB abuse: Drug-induced or drug-related death? Forensic Sci Int. 2019;297:372-7. doi:10.1016/j.forsciint.2019.02.005.
244. Gjerde H, Nordfjærn T, Bretteville-Jensen AL, Edland-Gryt M, Furuhaugen H, Karinen R et al. Comparison of drugs used by nightclub patrons and criminal offenders in Oslo, Norway. Forensic Sci Int. 2016;265:1-5. doi:10.1016/j.forsciint.2015.12.029.
245. Cooman T, Santos H, Cox J, Filho JFA, Borges KB, Romão W et al. Development, validation and evaluation of a quantitative method for the analysis of twenty-four new psychoactive substances in oral fluid by LC–MS/MS. Forensic Chemistry. 2020;19:100231. doi:10.1016/j.forc.2020.100231.
246. Bertol E, Vaiano F, Milia MGD, Mari F. In vivo detection of the new psychoactive substance AM-694 and its metabolites. Forensic Sci Int. 2015;256:21-7. doi:10.1016/j.forsciint.2015.07.018.
247. Bianchi F, Agazzi S, Riboni N, Erdal N, Hakkarainen M, Ilag LL et al. Novel sample-substrates for the determination of new psychoactive substances in oral fluid by desorption electrospray ionization-high resolution mass spectrometry. Talanta. 2019;202:136-44. doi:10.1016/j.talanta.2019.04.057.
248. Rocchi R, Simeoni MC, Montesano C, Vannutelli G, Curini R, Sergi M et al. Analysis of new psychoactive substances in oral fluids by means of microextraction by packed sorbent followed by ultra-high-performance liquid chromatography–tandem mass spectrometry. Drug Testing and Analysis. 2018;10(5):865-73. doi:10.1002/dta.2330.
249. Durmus H, Durmazel S, Üzer A, Gökdere B, Erçag E, Apak R. Colorimetric Determination of (Aminoalkyl)indole-containing Synthetic Cannabimimetics. Analytical Sciences. 2018;34(12):1419-25. doi:10.2116/analsci.18P305.
250. Namera A, Kawamura M, Nakamoto A, Saito T, Nagao M. Comprehensive review of the detection methods for synthetic cannabinoids and cathinones. Forensic Toxicol. 2015;33(2):175-94. doi:10.1007/s11419-015-0270-0.
251. Isaacs RCA. A structure–reactivity relationship driven approach to the identification of a color test protocol for the presumptive indication of synthetic cannabimimetic drugs of abuse. Forensic Sci Int. 2014;242:135-41. doi:10.1016/j.forsciint.2014.06.027.
252. Slagle KM, Ghosn SJ. Immunoassays: Tools for Sensitive, Specific, and Accurate Test Re. Laboratory Medicine. 1996;27(3):177-83.

253. Hand C, Baldwin D. Immunoassays. In: Jickells S, Negrusz A, editors. Clarke's Analytical Forensic Toxicology. London: Pharmaceutical Press; 2008. p. 375-91.
254. Moser AC, Carlson TL. General principles of immunoassays. Novel Approaches in Immunoassays. Future Medicine; 2014. p. 6-19.
255. Barnes AJ, Young S, Spinelli E, Martin TM, Klette KL, Huestis MA. Evaluation of a homogenous enzyme immunoassay for the detection of synthetic cannabinoids in urine. Forensic Sci Int. 2014;241:27-34. doi:10.1016/j.forsciint.2014.04.020.
256. Rodrigues WC, Catbagan P, Rana S, Wang G, Moore C. Detection of Synthetic Cannabinoids in Oral Fluid Using ELISA and LC–MS-MS. J Anal Toxicol. 2013;37(8):526-33. doi:10.1093/jat/bkt067.
257. Merck. Thin Layer Chromatography. 2022. https://www.sigmaaldrich.com/PT/en/applications/analytical-chemistry/thin-layer-chromatography. Accessed 29 June 2022.
258. Thin Layer Chromatography. priyamstudycentre. 2021. https://www.priyamstudycentre.com/2021/11/thin-layer-chromatography.html. Accessed 6th july 2022.
259. Logan BK, Reinhold LE, Xu A, Diamond FX. Identification of Synthetic Cannabinoids in Herbal Incense Blends in the United States. J Forensic Sci. 2012;57(5):1168-80. doi:10.1111/j.1556-4029.2012.02207.x.
260. Kneisel S, Bisel P, Brecht V, Broecker S, Müller M, Auwärter V. Identification of the cannabimimetic AM-1220 and its azepane isomer (N-methylazepan-3-yl)-3-(1-naphthoyl)indole in a research chemical and several herbal mixtures. Forensic Toxicol. 2012;30(2):126-34. doi:10.1007/s11419-012-0137-6.
261. Ciura K, Dziomba S, Nowakowska J, Markuszewski MJ. Thin layer chromatography in drug discovery process. J Chromatogr A. 2017;1520:9-22. doi:10.1016/j.chroma.2017.09.015.
262. Niessen WMA. Current Practice of Gas Chromatography-Mass Spectrometry. CRC Press; 2001.
263. Brettell TA, Lum BJ. Analysis of Drugs of Abuse by Gas Chromatography–Mass Spectrometry (GC-MS). In: Musah RA, editor. Analysis of Drugs of Abuse. New York, NY: Springer New York; 2018. p. 29-42.
264. Ramoo B, Funke M, Frazee C, Garg U. Comprehensive Urine Drug Screen by Gas Chromatography/Mass Spectrometry (GC/MS). In: Garg U, editor. Clinical Applications of Mass Spectrometry in Drug Analysis: Methods and Protocols. New York, NY: Springer New York; 2016. p. 125-31.
265. de Aguiar JMV. Determinação de Compostos Bioativos em Frutas e Vegetais Consumidos na Região Autónoma da Madeira: Universidade da Madeira; 2017.
266. Murayama C, Kimura Y, Setou M. Imaging mass spectrometry: principle and application. Biophysical reviews. 2009;1(3):131. doi:10.1007/s12551-009-0015-6.
267. Rockwood AL, Kushnir MM, Clarke NJ. 2 - Mass Spectrometry. In: Rifai N, Horvath AR, Wittwer CT, editors. Principles and Applications of Clinical Mass Spectrometry. Elsevier; 2018. p. 33-65.
268. Choi H, Heo S, Choe S, Yang W, Park Y, Kim E et al. Simultaneous analysis of synthetic cannabinoids in the materials seized during drug trafficking using GC-MS. Anal Bioanal Chem. 2013;405(12):3937-44. doi:10.1007/s00216-012-6560-z.
269. Gomes SMdC. Determinação de Antioxidantes por Cromatografia Líquida de Alta Pressão com Detecção Electroquímica: Universidade de Coimbra; 2010.
270. Maldaner L, Jardim ICSF. O estado da arte da cromatografia líquida de ultra eficiência. Química Nova. 2009;32:214-22. doi:10.1590/S0100-40422009000100036
271. Aryal S. HPLC- Definition, Principle, Parts, Types, Uses, Diagram. Microbe Notes. 2022. https://microbenotes.com/high-performance-liquid-chromatography-hplc/. Accessed 8th july 2022.
272. Cass QB, Degani ALG. Desenvolvimento de métodos por HPLC: fundamentos, estratégias e validação. São Paulo: EdUFSCar; 2001.
273. Raimundo Jr. IM, Pasquini C. Espectrofotometria multicanal e arranjos de fotodiodos. Química Nova. 1997;20:83-8.
274. Skoog DA, Holler J, Nieman T. Princípios de Análise Instrumental. 5ª ed. Porto Alegre: Bookman; 2002.
275. Waters. *2998 Photodiode Array (PDA) Detector for Alliance HPLC Systems*. https://www.waters.com/. Accessed 19th april 2022.
276. Duranovic S, Elie M, Baron M. The isolation and characterisation of the synthetic cannabinoid AM-2201 from commercial products using purification by HPLC-DAD. Sample Preparation. 2015;2. doi:10.1515/sampre-2015-0004.

277. Singh MK, Singh A. Chapter 14 - Nuclear magnetic resonance spectroscopy. In: Singh MK, Singh A, editors. Characterization of Polymers and Fibres. Woodhead Publishing; 2022. p. 321-39.
278. Günther H. NMR Spectroscopy : Basic Principles, Concepts, and Applications in Chemistry. 3rd ed. Weinheim, Germany: Wiley VCH; 2013.
279. Rankin N, Preiss D, Welsh P, Burgess K, Nelson S, Lawlor D et al. The emergence of proton nuclear magnetic resonance metabolomics in the cardiovascular arena as viewed from a clinical perspective. Atherosclerosis. 2014;237:287–300. doi:10.1016/j.atherosclerosis.2014.09.024.
280. Komoroski EM, Komoroski RA, Valentine JL, Pearce JM, Kearns GL. The use of nuclear magnetic resonance spectroscopy in the detection of drug intoxication. J Anal Toxicol. 2000;24(3):180-7. doi:10.1093/jat/24.3.180.
281. Dawson B. Nuclear Magnetic Resonance Spectroscopy in Pharmaceutical Analysis. Encyclopedia of Analytical Chemistry.
282. Moosmann B, Kneisel S, Girreser U, Brecht V, Westphal F, Auwarter V. Separation and structural characterization of the synthetic cannabinoids JWH-412 and 1-[(5-fluoropentyl)-1H-indol-3yl]-(4-methylnaphthalen-1-yl)methanone using GC-MS, NMR analysis and a flash chromatography system. Forensic Sci Int. 2012;220(1-3):e17-22. doi:10.1016/j.forsciint.2011.12.010.
283. Ernst L, Krüger K, Lindigkeit R, Schiebel H-M, Beuerle T. Synthetic cannabinoids in “spice-like” herbal blends: First appearance of JWH-307 and recurrence of JWH-018 on the German market. Forensic Sci Int. 2012;222(1):216-22. doi:10.1016/j.forsciint.2012.05.027.
284. Simolka K, Lindigkeit R, Schiebel H-M, Papke U, Ernst L, Beuerle T. Analysis of synthetic cannabinoids in “spice-like” herbal highs: snapshot of the German market in summer 2011. Anal Bioanal Chem. 2012;404(1):157-71. doi:10.1007/s00216-012-6122-4.
285. Dickschat JS. Capturing volatile natural products by mass spectrometry. Nat Prod Rep. 2014;31(6):838-61. doi:10.1039/C3NP70080A.
286. Ogata J, Uchiyama N, Kikura-Hanajiri R, Goda Y. DNA sequence analyses of blended herbal products including synthetic cannabinoids as designer drugs. Forensic Sci Int. 2013;227(1):33-41. doi:10.1016/j.forsciint.2012.09.006.
287. Zacca JJ, Giudice GH, Souza MP, Caldas LNB, Vieira ML, Machado AHL. Development and validation of analytical method for identification of new psychoactive substances using linear retention indexes and gas chromatography-mass spectrometry. J Chromatogr A. 2021;1636:461783. doi:10.1016/j.chroma.2020.461783.
288. Zaitsu K, Katagi M, Nakanishi K, Shima N, Kamata HT, Kamata T et al. Comprehensive analytical methods of the synthetic cannabinoids appearing in the illicit drug market. Japanese Journal of Forensic Science and Technology. 2011;16:73-90.
289. Xing Y, Xu X, Liu X, Xu B, Ma Q, Lei H. Study on the mass fragmentation pathway of the synthetic cannabinoids JWH-018 and JWH-073. Int J Mass Spectrom. 2015;379:139-45. doi:10.1016/j.ijms.2015.01.007.
290. Dresen S, Ferreiros Bouzas N, Pütz M, Westphal F, Zimmermann R, Auwärter V. Monitoring of herbal mixtures potentially containing synthetic cannabinoids as psychoactive compounds. Journal of Mass Spectrometry. 2010;45:1186-94. doi:10.1002/jms.1811.
291. Akutsu M, Sugie K-i, Saito K. Analysis of 62 synthetic cannabinoids by gas chromatography–mass spectrometry with photoionization. Forensic Toxicol. 2017;35(1):94-103. doi:10.1007/s11419-016-0342-9.
292. Sekuła K, Zuba D, Stanaszek R. Identification of naphthoylindoles acting on cannabinoid receptors based on their fragmentation patterns under ESI-QTOFMS. Journal of Mass Spectrometry. 2012;47(5):632-43. doi:10.1002/jms.3004.
293. Thaxton A, Belal TS, Smith F, DeRuiter J, Abdel-Hay KM, Clark CR. GC–MS studies on the six naphthoyl-substituted 1-n-pentyl-indoles: JWH-018 and five regioisomeric equivalents. Forensic Sci Int. 2015;252:107-13. doi:10.1016/j.forsciint.2015.04.023.
294. Grabenauer M, Krol WL, Wiley JL, Thomas BF. Analysis of Synthetic Cannabinoids Using High-Resolution Mass Spectrometry and Mass Defect Filtering: Implications for Nontargeted Screening of Designer Drugs. Anal Chem. 2012;84(13):5574-81. doi:10.1021/ac300509h.

295. Thaxton A, Belal TS, Smith F, DeRuiter J, Abdel-Hay KM, Clark CR. Mass spectral studies on 1-n-pentyl-3-(1-naphthoyl)indole (JWH-018), three deuterium-labeled analogues and the inverse isomer 1-naphthoyl-3-n-pentylindole. Rapid Commun Mass Spectrom. 2015;29(9):871-7. doi:10.1002/rcm.7171.
296. Harris DN, Hokanson S, Miller V, Jackson GP. Fragmentation differences in the EI spectra of three synthetic cannabinoid positional isomers: JWH-250, JWH-302, and JWH-201. Int J Mass Spectrom. 2014;368:23-9. doi:10.1016/j.ijms.2014.05.005.
297. Ma Q, Bai H, Li W, Wang C, Cooks RG, Ouyang Z. Rapid analysis of synthetic cannabinoids using a miniature mass spectrometer with ambient ionization capability. Talanta. 2015;142:190-6. doi:10.1016/j.talanta.2015.04.044.
298. Asada A, Doi T, Tagami T, Takeda A, Sawabe Y. Isomeric discrimination of synthetic cannabinoids by GC-EI-MS: 1-adamantyl and 2-adamantyl isomers of N-adamantyl carboxamides. Drug Testing and Analysis. 2017;9(3):378-88. doi:10.1002/dta.2124.
299. Gandhi AS, Zhu M, Pang S, Wohlfarth A, Scheidweiler KB, Liu H-F et al. First characterization of AKB-48 metabolism, a novel synthetic cannabinoid, using human hepatocytes and high-resolution mass spectrometry. The AAPS journal. 2013;15(4):1091-8. doi:10.1208/s12248-013-9516-0.
300. Jia W, Meng X, Qian Z, Hua Z, Li T, Liu C. Identification of three cannabimimetic indazole and pyrazole derivatives, APINACA 2H-indazole analogue, AMPPPCA, and 5F-AMPPPCA. Drug Testing and Analysis. 2017;9(2):248-55. doi:10.1002/dta.1967.
301. Adamowicz P, Lechowicz W. The Influence of Synthetic Cannabinoid UR-144 on Human Psychomotor Performance--A Case Report Demonstrating Road Traffic Risks. Traffic Inj Prev. 2015;16(8):754-9. doi:10.1080/15389588.2015.1018990.
302. Heredia KFA. Chemical Identification of Synthetic Cannabinoids in Herbal Incenses Products: University of New York; 2017.
303. Leal CRQ. Mass Spectrometry Library of NPS: Isolation and Characterisation of Designer Drugs from Herbal Incenses and Plant Feeders: Faculdade de Ciências da Universidade de Lisboa; 2015.
304. Arar SH, ALSoufi H, Abu-Nameh E, Deeb A, Habahbeh A. Screening of (Aminoalkylindols) Cannabinoids in smoking products by GC-EI/MS in Jordan: Liquid-liquid extraction optimization. Egypt J Chem. 2020;63(2):373-87. doi:10.21608/ejchem.2019.11591.1737.
305. Thomas BF, Lefever TW, Cortes RA, Grabenauer M, Kovach AL, Cox AO et al. Thermolytic Degradation of Synthetic Cannabinoids: Chemical Exposures and Pharmacological Consequences. The Journal of pharmacology and experimental therapeutics. 2017;361(1):162-71. doi:10.1124/jpet.116.238717.
306. Hiang Ng C, Ani SAC, Mustafa K, Desa S, Sulaiman M. Identification of synthetic cannabinoids 5F-ADB and XLR-11 in seized sample in Penang, Malaysia. Malaysian Journal of Forensic Sciences. 2019;9(1):1-6.
307. Choi H, Heo S, Kim E, Hwang BY, Lee C, Lee J. Identification of (1-pentylindol-3-yl)-(2,2,3,3-tetramethylcyclopropyl)methanone and its 5-pentyl fluorinated analog in herbal incense seized for drug trafficking. Forensic Toxicol. 2013;31(1):86-92. doi:10.1007/s11419-012-0170-5.
308. Atwood B, Lee D, Straiker A, Widlanski T, Mackie K. CP47,497-C8 and JWH073, commonly found in 'Spice' herbal blends, are potent and efficacious CB1 cannabinoid receptor agonists. Eur J Pharmacol. 2011;659:139-45. doi:10.1016/j.ejphar.2011.01.066.
309. Uchiyama N, Kikura-Hanajiri R, Shoda T, Fukuhara K, Goda Y. Isomeric analysis of synthetic cannabinoids detected as designer drugs. Yakugaku Zasshi. 2011;131(7):1141-7. doi:10.1248/yakushi.131.1141.
310. Gwak S, Arroyo-Mora LE, Almirall JR. Qualitative analysis of seized synthetic cannabinoids and synthetic cathinones by gas chromatography triple quadrupole tandem mass spectrometry. Drug Testing and Analysis. 2015;7(2):121-30. doi:10.1002/dta.1667.
311. Duffy B, Li L, Lu S, Durocher L, Dittmar M, Delaney-Baldwin E et al. Analysis of Cannabinoid-Containing Fluids in Illicit Vaping Cartridges Recovered from Pulmonary Injury Patients: Identification of Vitamin E Acetate as a Major Diluent. Toxics. 2020;8(1):8. doi:10.3390/toxics8010008.
312. Reyes-Becerril M, Ruvalcaba F, Sanchez V, López MG, Silva-Jara J, Hernandez-Adame L et al. Green synthesis of gold nanoparticles using Turnera diffusa Willd enhanced antimicrobial properties and immune response in Longfin yellowtail leukocytes. Aquac Res. 2021;2021 v.52 no.7(no. 7):pp. 3391-402. doi:10.1111/are.15184.
313. Naqi H, Woodman T, Husbands S, Blagbrough I. 19F and 1H quantitative-NMR spectroscopic analysis of fluorinated third-generation synthetic cannabinoids. Analytical Methods. 2019. doi:10.1039/C9AY00814D.

314. Amato J, Iaccarino N, Pagano B, Compagnone V, Rosa F, Peluso G et al. NMR Assignment of N-(1-adamantyl)-1-pentyl-1H-indazole-3-carboxamide Seized as Herbal Incense for the First Time in Italy. Journal of Forensic Science & Criminology. 2014;2(1). doi:10.15744/2348-9804.1.403.
315. Fowler F, Voyer B, Marino M, Finzel J, Veltri M, Wachter N et al. Rapid screening and quantification of synthetic cannabinoids in herbal products with NMR spectroscopic methods. Analytical methods. 2015;7. doi:10.1039/C5AY01754H.
316. Marino MA, Voyer B, Cody RB, Dane AJ, Veltri M, Huang L. Rapid Identification of Synthetic Cannabinoids in Herbal Incenses with DART-MS and NMR. J Forensic Sci. 2016;61 Suppl 1:S82-91. doi:10.1111/1556-4029.12932.
317. Assemat G, Dubocq F, Balayssac S, Lamoureux C, Malet-Martino M, Gilard V. Screening of "spice" herbal mixtures: From high-field to low-field proton NMR. Forensic Sci Int. 2017;279:88-95. doi:10.1016/j.forsciint.2017.08.006.
318. Langer N, Lindigkeit R, Schiebel H-M, Ernst L, Beuerle T. Identification and quantification of synthetic cannabinoids in 'spice-like' herbal mixtures: A snapshot of the German situation in the autumn of 2012. Drug Testing and Analysis. 2014;6(1-2):59-71. doi:10.1002/dta.1499.
319. Shevyrin V, Melkozerov V, Nevero A, Eltsov O, Morzherin Y, Shafran Y. Identification and analytical properties of new synthetic cannabimimetics bearing 2,2,3,3-tetramethylcyclopropanecarbonyl moiety. Forensic Sci Int. 2013;226(1):62-73. doi:10.1016/j.forsciint.2012.12.009.
320. Burns NK, Ashton TD, Stevenson PG, Pearson JR, Fox IL, Pfeffer FM et al. Extraction, identification and detection of synthetic cannabinoids found pre-ban in herbal products in Victoria, Australia. Forensic Chemistry. 2018;7:19-25. doi:10.1016/j.forc.2017.12.003.
321. Maldaner L, Jardim ICSF. UHPLC – Uma abordagem atual: desenvolvimentos e desafios recentes. Scientia Chromatographica. 2012;4(3):197-207. doi:10.4322/sc.2012.014.
322. Waters. Beginners Guide to UPLC: Ultra-Performance Liquid Chromatography. 1st ed., vol Waters Series. Waters Corporation; 2014.
323. Ohannesian LSAJ. Handbook of pharmaceutical analysis. New York: Marcel Dekker; 2002.
324. European Pharmacopoeia. Chromatographic Separation Techniques. 9th ed. 2017.
325. Ares AM, Fernández P, Regenjo M, Fernández AM, Carro AM, Lorenzo RA. A fast bioanalytical method based on microextraction by packed sorbent and UPLC–MS/MS for determining new psychoactive substances in oral fluid. Talanta. 2017;174:454-61. doi:10.1016/j.talanta.2017.06.022.
326. Sergi M, Montesano C, Odoardi S, Mainero Rocca L, Fabrizi G, Compagnone D et al. Micro extraction by packed sorbent coupled to liquid chromatography tandem mass spectrometry for the rapid and sensitive determination of cannabinoids in oral fluids. J Chromatogr A. 2013;1301:139-46. doi:10.1016/j.chroma.2013.05.072.
327. Yang L, Said R, Abdel-Rehim M. Sorbent, device, matrix and application in microextraction by packed sorbent (MEPS): A review. J Chromatogr B. 2017;1043:33-43. doi:10.1016/j.jchromb.2016.10.044.
328. Relacre (Associação de Laboratórios Acreditados de Portugal). *Validação de métodos internos de ensaio em análise química— Guia Relacre nº 13*. Lisboa: Relacre 2000.
329. B. Magnusson and U. Örnemark (eds.) Eurachem Guide: The Fitness for Purpose of Analytical Methods – A Laboratory Guide to Method Validation and Related Topics (2nd Edition). 2014.
330. Ramachandran KM, Tsokos CP. Chapter 10 - Analysis of Variance. In: Ramachandran KM, Tsokos CP, editors. Mathematical Statistics with Applications in R (Second Edition). Boston: Academic Press; 2015. p. 495-547.
331. Andrade JM, Gómez-Carracedo MP. Notes on the use of Mandel's test to check for nonlinearity in laboratory calibrations. Analytical Methods. 2013;5(5):1145-9. doi:10.1039/C2AY26400E.
332. International Conference on Harmonization. *Validation of analytical methods – Methodology ICH Q2*. Disponível em: http://www.ich.org. Acedido a 17.10.2021.
333. Polettini A. Applications of LC-MS in Toxicology. London: Pharmaceutical Press; 2006.
334. Maroto A, Boqué R, Riu J, Xavier Rius F. Estimation of measurement uncertainty by using regression techniques and spiked samples. Anal Chim Acta. 2001;446(1–2):131-43. doi:10.1016/S0003-2670(01)00842-X.
335. Maroto A, Riu J, Boqué R, Xavier Rius F. Estimating uncertainties of analytical results using information from the validation process. Anal Chim Acta. 1999;391(2):173-85. doi:10.1016/S0003-2670(99)00111-7.

336. International Organization for Standardization. *Accuracy (trueness and precision) of measurement methods and results - Part 1: General principles and definitions. ISO 5725-1*. Genève 1994.
337. Marson B, Concentino V, Junkert A, Fachi M, Vilhena R. Validation of analytical methods in a pharmaceutical quality system: An overview focused on HPLC methods. Quimica Nova. 2020;43(8):1190-203. doi:10.21577/0100-4042.20170589
338. Maroto A, Boqué R, Riu J, Rius FX. Measurement uncertainty in analytical methods in which trueness is assessed from recovery assays. Anal Chim Acta. 2001;440(2):171-84. doi:10.1016/S0003-2670(01)01058-3.
339. J. Barwick V, L. R. Ellison S. Measurement uncertainty: Approaches to the evaluation of uncertainties associated with recovery[dagger]. Analyst. 1999;124(7):981-90. doi:10.1039/A901845J.
340. Zrostlikova J, Hajslova J, Godula M, Mastovska K. Performance of programmed temperature vaporizer, pulsed splitless and on-column injection techniques in analysis of pesticide residues in plant matrices. J Chromatogr A. 2001;937(1-2):73-86. doi:10.1016/s0021-9673(01)01308-5.
341. United Nations Office on Drugs and Crime. Guidance for the Validation of Analytical Methodology and Calibration of Equipment used for Testing of Illicit Drugs in Seized Materials and Biological Specimens. UNODC 2009.
342. Zhou W, Yang S, Wang PG. Matrix effects and application of matrix effect factor. Bioanalysis. 2017;9(23):1839-44. doi:10.4155/bio-2017-0214.
343. Rogatsky E, Stein D. Evaluation of Matrix Effect and Chromatography Efficiency: New Parameters for Validation of Method Development. J Am Soc Mass Spectrom. 2005;16(11):1757-9. doi:10.1016/j.jasms.2005.07.012.
344. Silvestro L, Tarcomnicu I, Savu SR. Matrix Effects in Mass Spectrometry Combined with Separation Methods — Comparison HPLC, GC and Discussion on Methods to Control these Effects. In: Coelho AV, de Matos Ferraz Franco C, editors. Tandem Mass Spectrometry - Molecular Characterization. London: IntechOpen; 2013.
345. Waters. Columns Specifications. Waters. www.waters.com. Accessed 6th july 2021.
346. Stauffer E, Dolan JA, Newman R. CHAPTER 8 - Gas Chromatography and Gas Chromatography—Mass Spectrometry. In: Stauffer E, Dolan JA, Newman R, editors. Fire Debris Analysis. Burlington: Academic Press; 2008. p. 235-93.
347. Abdel-Rehim M. Microextraction by packed sorbent (MEPS): A tutorial. Anal Chim Acta. 2011;701(2):119-28. doi:10.1016/j.aca.2011.05.037.
348. Alves V, Gonçalves J, Conceição C, Teixeira HM, Câmara JS. An improved analytical strategy combining microextraction by packed sorbent combined with ultra high pressure liquid chromatography for the determination of fluoxetine, clomipramine and their active metabolites in human urine. J Chromatogr A. 2015;1408:30-40. doi:10.1016/j.chroma.2015.07.021.
349. Abdel-Rehim M. Recent advances in microextraction by packed sorbent for bioanalysis. J Chromatogr A. 2010;1217(16):2569-80. doi:10.1016/j.chroma.2009.09.053.
350. Ribani M, Bottoli CBG, Collins CH, Jardim ICSF, Melo LFC. Validação em métodos cromatográficos e eletroforéticos. Química Nova. 2004;27:771-80.
351. Tomai P, Gentili A, Curini R, Gottardo R, Franco T, Fanali S. Dispersive liquid-liquid microextraction, an effective tool for the determination of synthetic cannabinoids in oral fluid by liquid chromatography–tandem mass spectrometry. Journal of Pharmaceutical Analysis. 2021;11(3):292-8. doi:10.1016/j.jpha.2020.11.004.
352. Zawatsky CN, Abdalla J, Cinar R. Synthetic cannabinoids induce acute lung inflammation via cannabinoid receptor 1 activation. ERJ open research. 2020;6(3). doi:10.1183/23120541.00121-2020.
353. UNODC. The challenge of new psychoactive substances. United Nations Publication. 2013. https://www.unodc.org/documents/scientific/NPS_Report.pdf. Accessed 24th May 2022.
354. Rocha A. Drug Delivery of Methyl-Carboxilated 5-Fluorouracil by means of Human serum albumin microcarriers: Faculdade de Ciências da Universidade de Lisboa; 2014.
355. Merck. MTT Assay Protocol for Cell Viability and Proliferation. Merck. 2022. https://www.sigmaaldrich.com/PT/en/technical-documents/protocol/cell-culture-and-cell-culture-analysis/cell-counting-and-health-analysis/cell-proliferation-kit-i-mtt. Accessed 9th September 2022.
356. Ali-Boucetta H, Al-Jamal K, Kostarelos K. Cytotoxic Assessment of Carbon Nanotube Interaction with Cell Cultures. Methods in molecular biology (Clifton, NJ). 2011;726:299-312. doi:10.1007/978-1-61779-052-2_19.

357. Soenen SJ, De Cuyper M, De Smedt SC, Braeckmans K. Chapter ten - Investigating the Toxic Effects of Iron Oxide Nanoparticles. In: Düzgüneş N, editor. Methods in Enzymology. Academic Press; 2012. p. 195-224.
358. Dias-da-Silva D, Arbo MD, Valente MJ, Bastos ML, Carmo H. Hepatotoxicity of piperazine designer drugs: Comparison of different in vitro models. Toxicol in Vitro. 2015;29(5):987-96. doi:10.1016/j.tiv.2015.04.001.
359. Kalyanaraman B, Darley-Usmar V, Davies KJ, Dennery PA, Forman HJ, Grisham MB et al. Measuring reactive oxygen and nitrogen species with fluorescent probes: challenges and limitations. Free Radic Biol Med. 2012;52(1):1-6. doi:10.1016/j.freeradbiomed.2011.09.030.
360. Kim H, Xue X. Detection of Total Reactive Oxygen Species in Adherent Cells by 2',7'-Dichlorodihydrofluorescein Diacetate Staining. Journal of Visualized Experiments. 2020(160). doi:10.3791/60682.
361. Ozcan A, Ogun M. Biochemistry of Reactive Oxygen and Nitrogen Species. In: Gowder SJT, editor. Basic Principles and Clinical Significance of Oxidative Stress. London: IntechOpen; 2015.
362. Barbosa DJ, Serrat R, Mirra S, Quevedo M, de Barreda EG, Àvila J et al. The mixture of "ecstasy" and its metabolites impairs mitochondrial fusion/fission equilibrium and trafficking in hippocampal neurons, at in vivo relevant concentrations. Toxicol Sci. 2014;139(2):407-20. doi:10.1093/toxsci/kfu042.
363. Valente MJ, Araújo AM, Silva R, Bastos Mde L, Carvalho F, Guedes de Pinho P et al. 3,4-Methylenedioxypyrovalerone (MDPV): in vitro mechanisms of hepatotoxicity under normothermic and hyperthermic conditions. Arch Toxicol. 2016;90(8):1959-73. doi:10.1007/s00204-015-1653-z.
364. Yu D, Zha Y, Zhong Z, Ruan Y, Li Z, Sun L et al. Improved detection of reactive oxygen species by DCFH-DA: New insight into self-amplification of fluorescence signal by light irradiation. Sensors Actuators B: Chem. 2021;339:129878. doi:10.1016/j.snb.2021.129878.
365. Held P, Newick K. Using BioTek's Synergy™ HT Reader to Measure Reactive Oxygen Species (ROS) Generation in Stimulated Cells. BioTechniques. 2009;46:61-2. doi:10.2144/000113081.
366. Bioarray C. ATP Cell Viability Assay. Creative Bioarray. 2022. https://www.creative-bioarray.com/support/atp-cell-viability-assay.htm. Accessed 14th september 2022.
367. Alexandre J, Malheiro R, Dias da Silva D, Carmo H, Carvalho F, Silva JP. The Synthetic Cannabinoids THJ-2201 and 5F-PB22 Enhance In Vitro CB1 Receptor-Mediated Neuronal Differentiation at Biologically Relevant Concentrations. 2020;21(17):6277. doi:10.3390/ijms21176277.
368. Silva JP, Carmo H, Carvalho F. The synthetic cannabinoid XLR-11 induces in vitro nephrotoxicity by impairment of endocannabinoid-mediated regulation of mitochondrial function homeostasis and triggering of apoptosis. Toxicology Letters. 2018;287:59-69. doi:10.1016/j.toxlet.2018.01.023.
369. Promega. ATP Assays. 2022. https://worldwide.promega.com/resources/guides/cell-biology/atp-assays/. Accessed 14th September 2022.
370. Abnova, GSH/GSSG Ratio Assay Kit (Fluorometric). Catalog No: KA2520.
371. Xiong Y, Uys J, Tew K, Townsend D. S-Glutathionylation: From Molecular Mechanisms to Health Outcomes. Antioxid Redox Signaling. 2011;15:233-70. doi:10.1089/ars.2010.3540.
372. Bioquest A, Amplite™ Fluorimetric Glutathione GSH/GSSG Ratio Assay Kit *Green Fluorescence*. 2011. Catalog No: 10056.
373. Scientific T, Pierce™ BCA Protein Assay Kit. 2020. Catalog No: 23225 and 23227.
374. Brown RE, Jarvis KL, Hyland KJ. Protein measurement using bicinchoninic acid: elimination of interfering substances. Anal Biochem. 1989;180(1):136-9. doi:10.1016/0003-2697(89)90101-2.
375. Smith PK, Krohn RI, Hermanson GT, Mallia AK, Gartner FH, Provenzano MD et al. Measurement of protein using bicinchoninic acid. Anal Biochem. 1985;150(1):76-85. doi:10.1016/0003-2697(85)90442-7.
376. Synthego. A549 Cells: An Overview. 2022. https://www.synthego.com/a549-cells. Accessed 17th September 2022.
377. Milian L, Mata M, Alcacer J, Oliver M, Sancho-Tello M, Martín de Llano JJ et al. Cannabinoid receptor expression in non-small cell lung cancer. Effectiveness of tetrahydrocannabinol and cannabidiol inhibiting cell proliferation and epithelial-mesenchymal transition in vitro. PLoS One. 2020;15(2):e0228909. doi:10.1371/journal.pone.0228909.
378. Turcotte C, Blanchet MR, Laviolette M, Flamand N. Impact of Cannabis, Cannabinoids, and Endocannabinoids in the Lungs. Front Pharmacol. 2016;7:317. doi:10.3389/fphar.2016.00317.

379. Grafinger KE, Mandhair HK, Broillet A, Gertsch J, Weinmann W. Cytotoxicity of the synthetic cannabinoids 5C-AKB48, 5F-MDMB-PINACA, ADB-CHMINACA, MDMB-CHMICA and NM-2201 in A549 and TR146 cell lines. Forensic Toxicol. 2019;37(2):398-411. doi:10.1007/s11419-019-00474-1.
380. Tomiyama K, Funada M. Cytotoxicity of synthetic cannabinoids found in “Spice” products: The role of cannabinoid receptors and the caspase cascade in the NG 108-15 cell line. Toxicology Letters. 2011;207(1):12-7. doi:10.1016/j.toxlet.2011.08.021.
381. Almada M, Alves P, Fonseca BM, Carvalho F, Queirós CR, Gaspar H et al. Synthetic cannabinoids JWH-018, JWH-122, UR-144 and the phytocannabinoid THC activate apoptosis in placental cells. Toxicology Letters. 2020;319:129-37. doi:10.1016/j.toxlet.2019.11.004.
382. Willer J, Jöhrer K, Greil R, Zidorn C, Çiçek SS. Cytotoxic Properties of Damiana (Turnera diffusa) Extracts and Constituents and A Validated Quantitative UHPLC-DAD Assay. Molecules. 2019;24(5). doi:10.3390/molecules24050855.
383. Damiana. 2011. https://www.smokableherbs.com/damiana/. Accessed 10th October 2022.
384. Esawy A, Eltablawy NAA, Abd El-Fattah A, Abdalwahab WA. Oxidative Stress, Inflammation and Apoptosis are the Main Mediators in AMB-FUBINACA Induced Brain Injury in Male Albino Rats International Journal of Pharmaceutical and Medical Sciences. 2022;2(1):82-95. doi:10.21608/aijpms.2021.210570.
385. Guler E, Bektay M, Akyildiz A, Sisman B, Izzettin F, Kocyigit A. Investigation of DNA damage, oxidative stress, and inflammation in synthetic cannabinoid users. Hum Exp Toxicol. 2020;39(11):1454-62. doi:10.1177/0960327120930057.
386. Valente MJ, Araújo AM, Bastos Mde L, Fernandes E, Carvalho F, Guedes de Pinho P et al. Characterization of Hepatotoxicity Mechanisms Triggered by Designer Cathinone Drugs (β-Keto Amphetamines). Toxicol Sci. 2016;153(1):89-102. doi:10.1093/toxsci/kfw105.
387. Fonseca BM, Fernandes R, Almada M, Santos M, Carvalho F, Teixeira NA et al. Synthetic cannabinoids and endometrial stromal cell fate: Dissimilar effects of JWH-122, UR-144 and WIN55,212-2. Toxicology. 2019;413:40-7. doi:10.1016/j.tox.2018.11.006.
388. Silva JP, Araújo AM, de Pinho PG, Carmo H, Carvalho F. Synthetic Cannabinoids JWH-122 and THJ-2201 Disrupt Endocannabinoid-Regulated Mitochondrial Function and Activate Apoptotic Pathways as a Primary Mechanism of In Vitro Nephrotoxicity at In Vivo Relevant Concentrations. Toxicol Sci. 2019;169(2):422-35. doi:10.1093/toxsci/kfz050.
389. Moosmann B, Kneisel S, Wohlfarth A, Brecht V, Auwärter V. A fast and inexpensive procedure for the isolation of synthetic cannabinoids from 'Spice' products using a flash chromatography system. Anal Bioanal Chem. 2013;405(12):3929-35. doi:10.1007/s00216-012-6462-0.

SUPPLEMENTARY MATERIAL

Supplementary Material I – Characterization studies

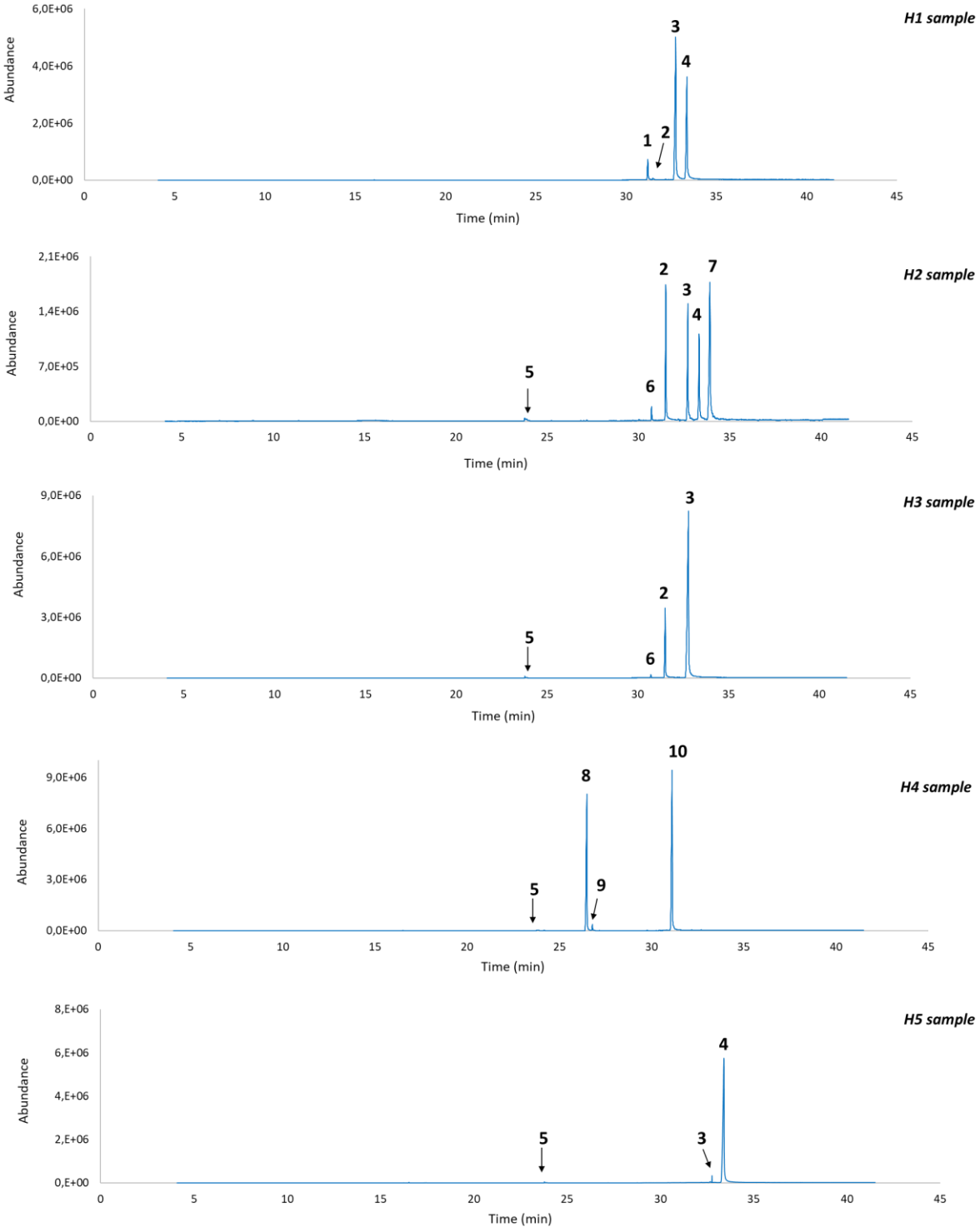

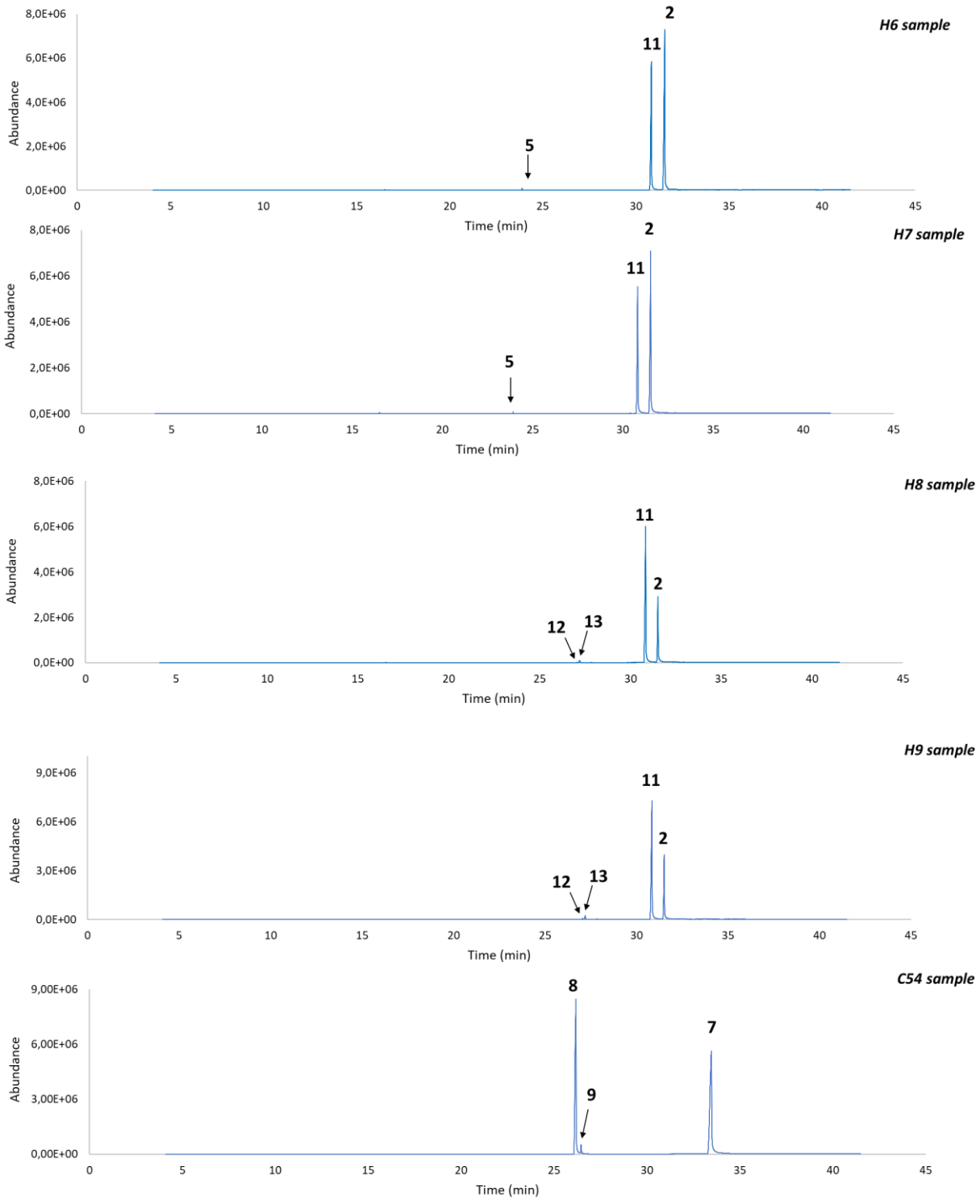
H6 sample
H7 sample
H8 sample
H9 sample
C54 sample
Abundance
Time (min)
2
11
5
12
13
8
9
7

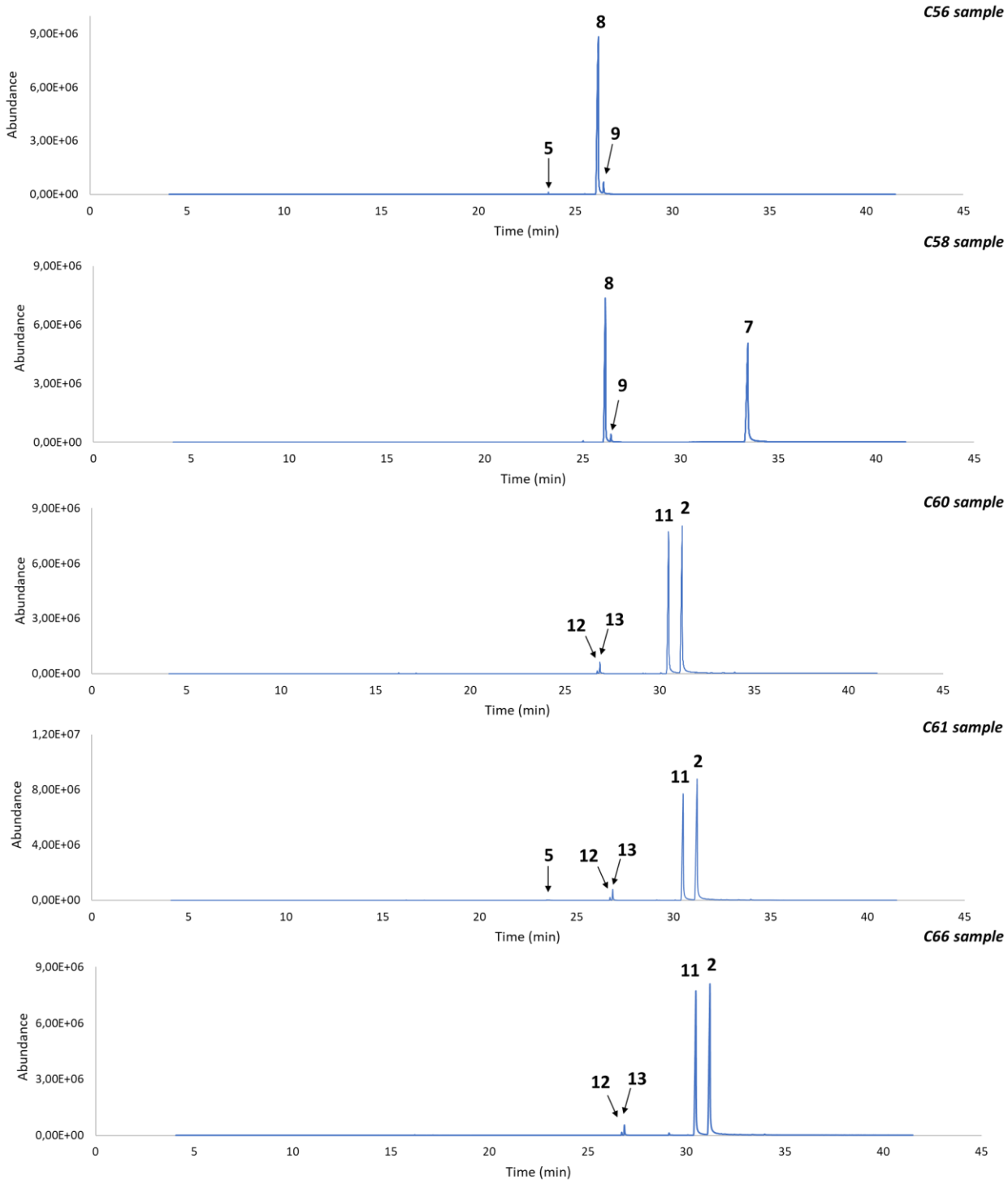
C56 sample
Abundance
9,00E+06
6,00E+06
3,00E+06
0,00E+00
8
5
9
0
5
10
15
20
25
30
35
40
45
Time (min)
C58 sample
Abundance
9,00E+06
6,00E+06
3,00E+06
0,00E+00
8
7
9
Time (min)
C60 sample
Abundance
9,00E+06
6,00E+06
3,00E+06
0,00E+00
11
2
12
13
Time (min)
C61 sample
Abundance
1,20E+07
8,00E+06
4,00E+06
0,00E+00
11
2
5
12
13
Time (min)
C66 sample
Abundance
9,00E+06
6,00E+06
3,00E+06
0,00E+00
11
2
12
13
Time (min)

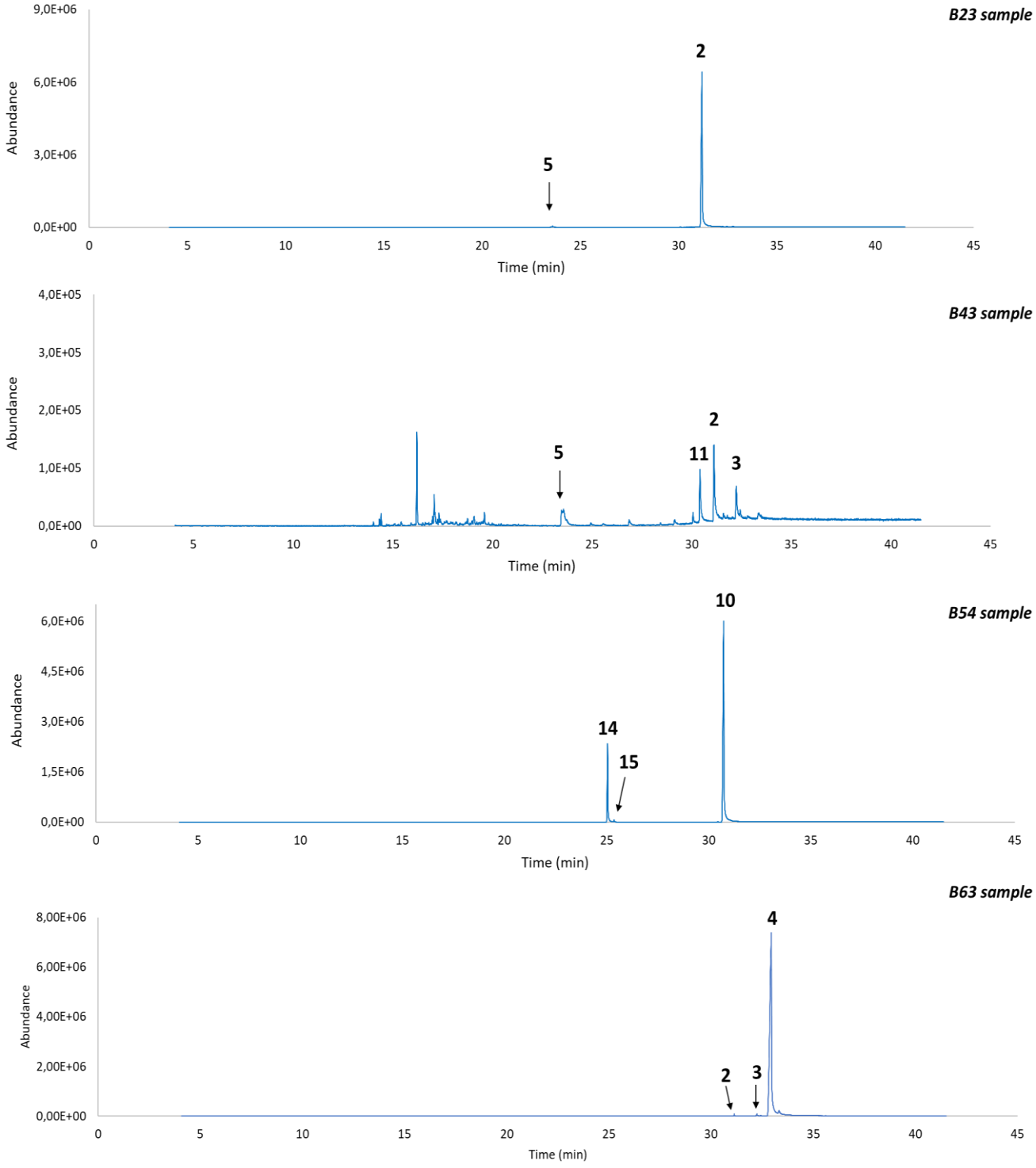

Figure S1. GC-MS analysis of seized herbal products suspected to contain SCs. Peak identification: 1 – vitamin E acetate, 2 – JWH-018, 3 – JWH-122, 4 - JWH-210, 5 – oleamide, 6 – vitamin E, 7 – MAM-2201, 8 – XLR-11, 9 – XLR-11 cyclopropyl rearrangement product, 10 – APINACA, 11 - JWH-073, 12 – 3-epi CP47, 497, C8, 13 – CP47, 497, C8, 14 – UR-144, 15 – UR-144 cyclopropyl rearrangement product.

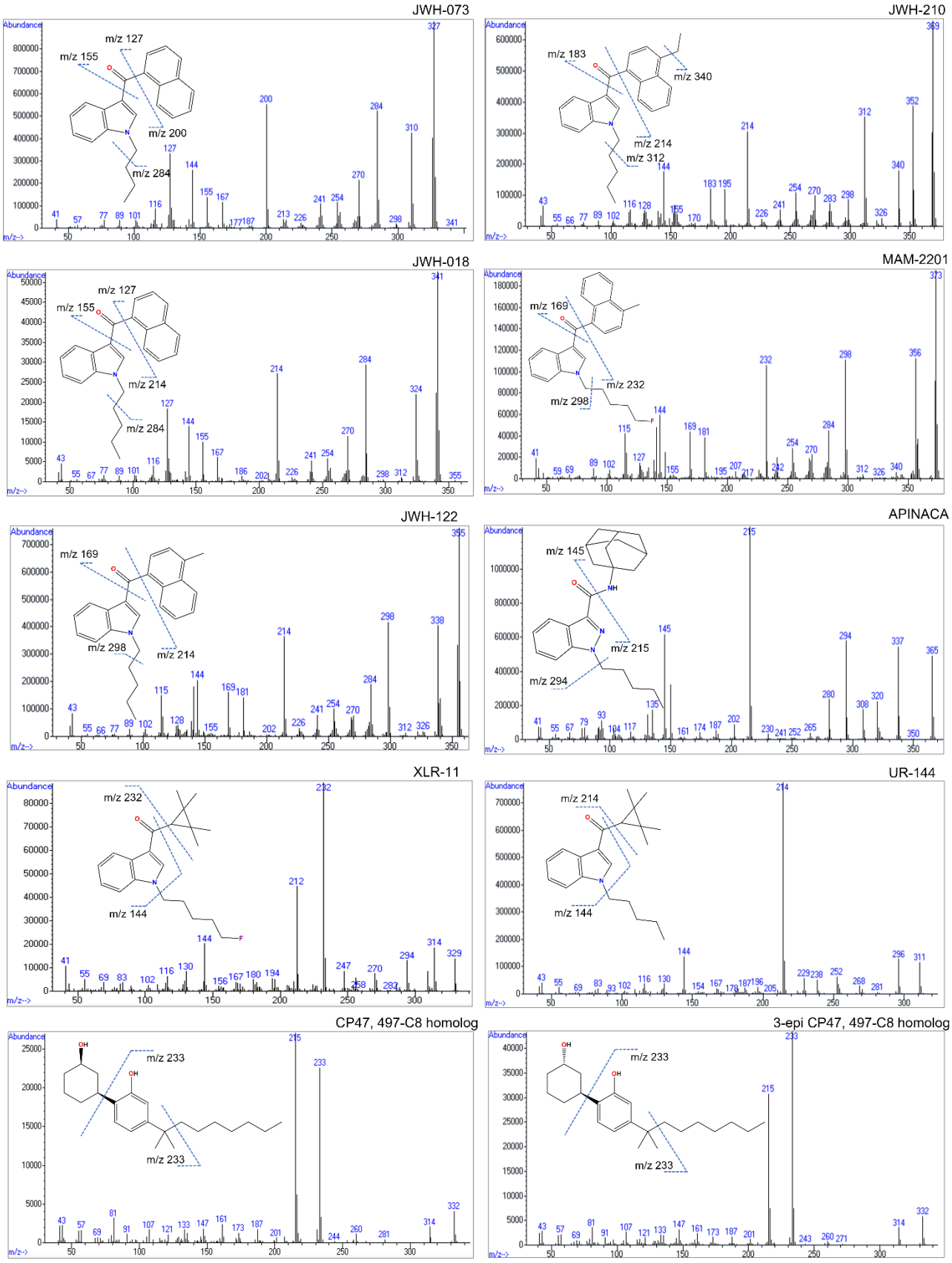

Figure S2. EI mass spectra of the SCs found in seized herbal products.

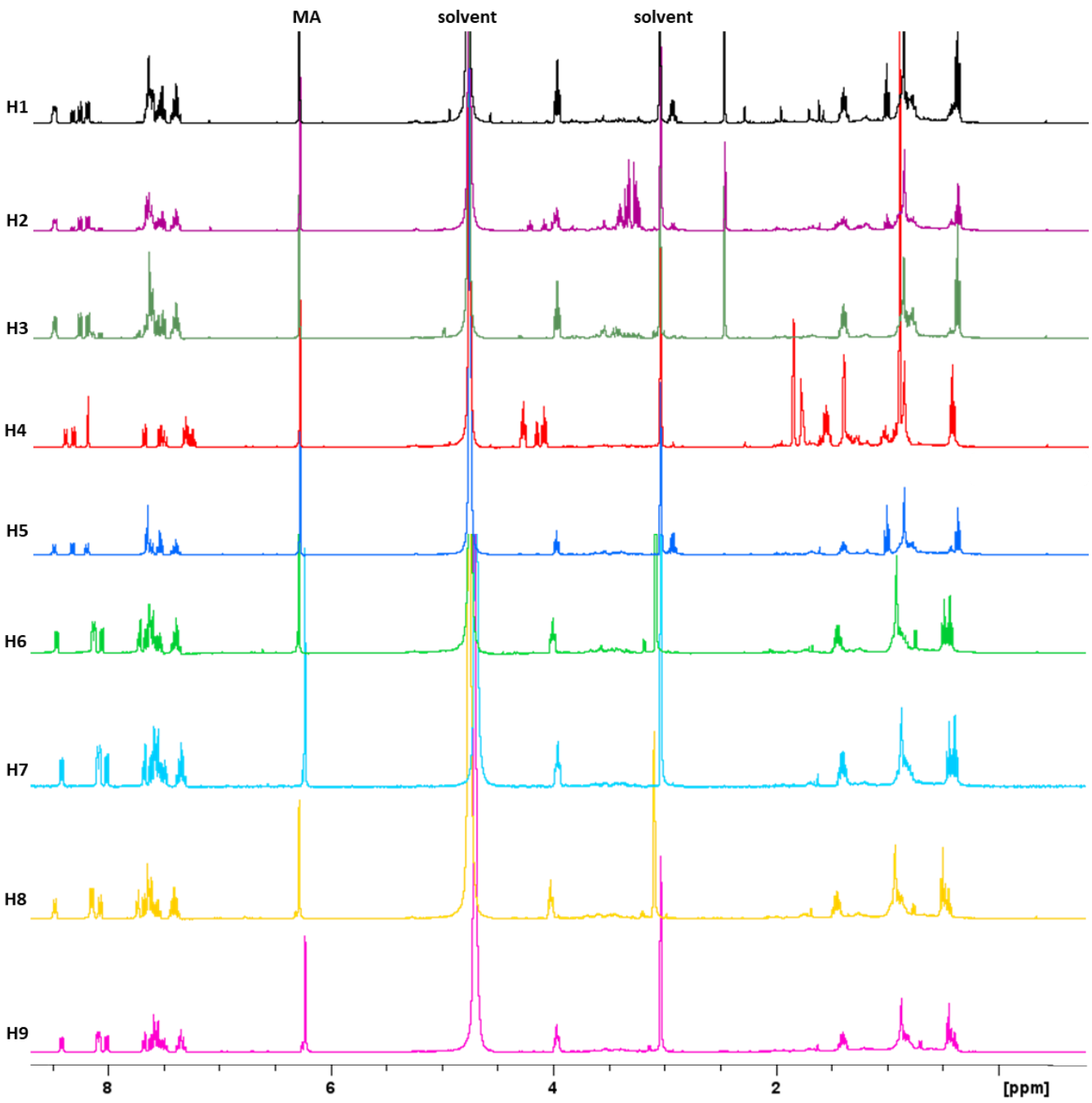

Figure S3. ^{1}H NMR spectra of seized herbal products (samples H1-H9).

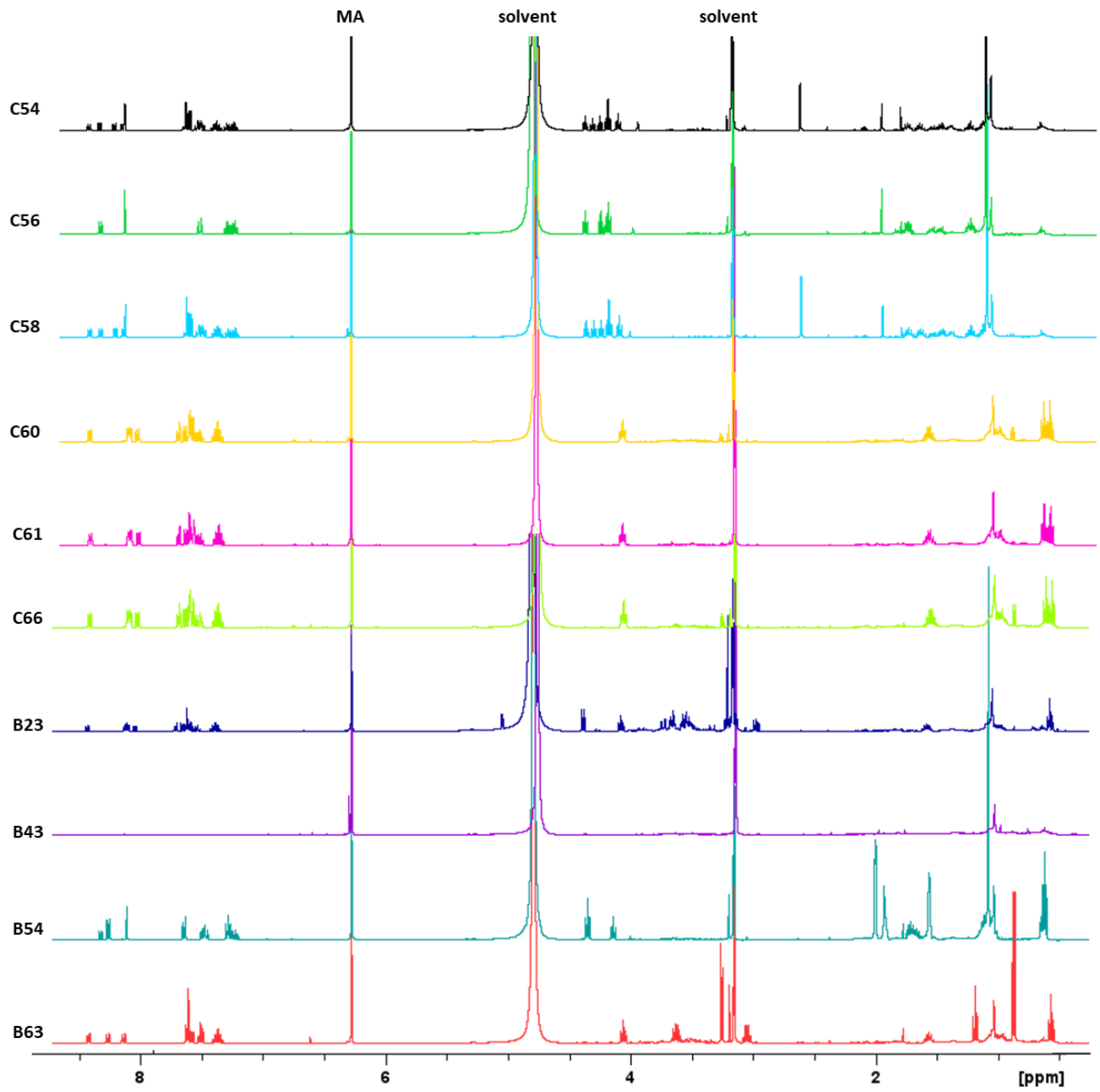

Figure S4. ^{1}H NMR spectra of seized herbal products (samples C54, C56, C58, C60, C61, C66, B23, B43, B54 and B63).

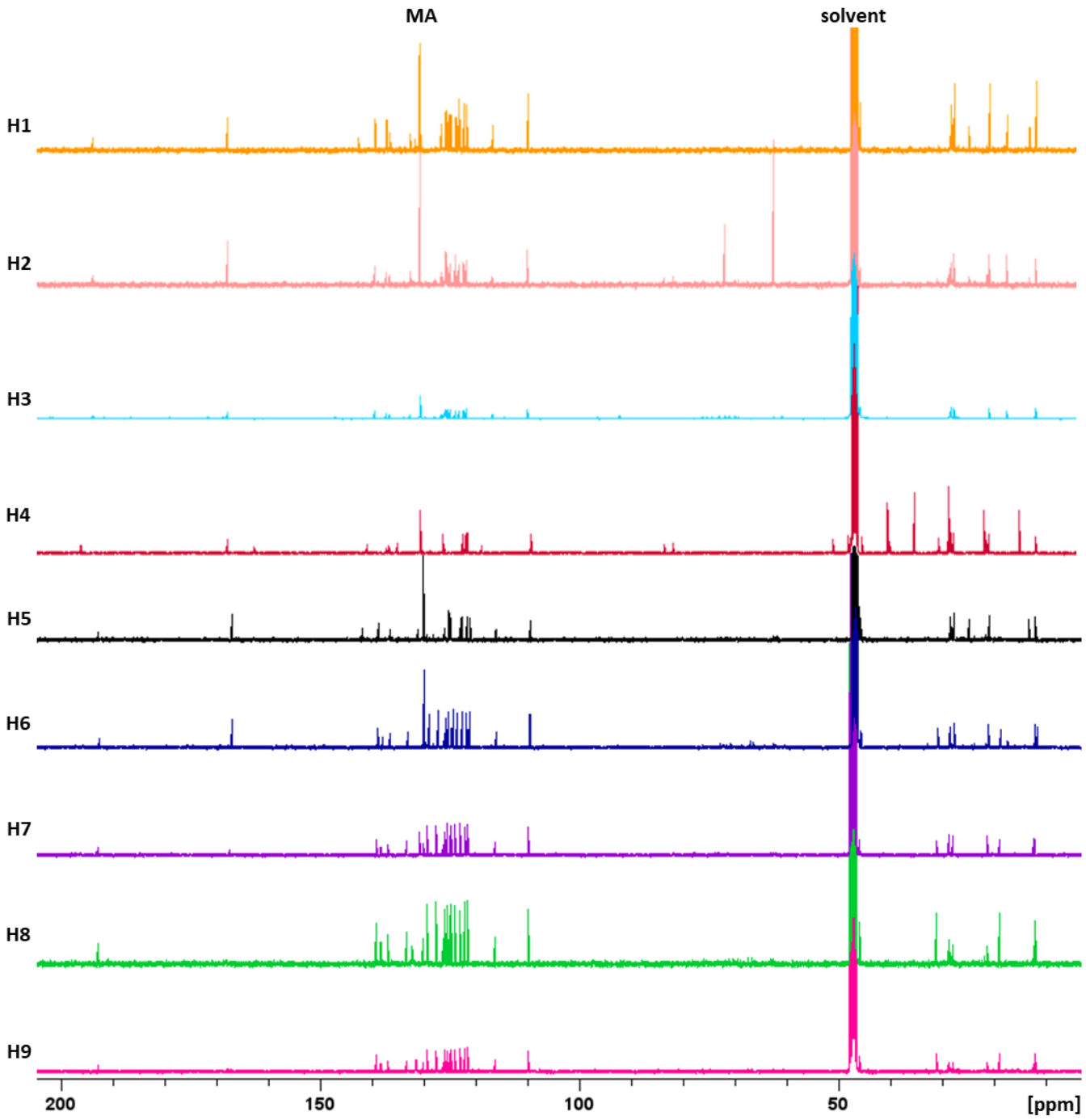

Figure S5. ^{13}C NMR spectra of seized herbal products (samples H1-H9).

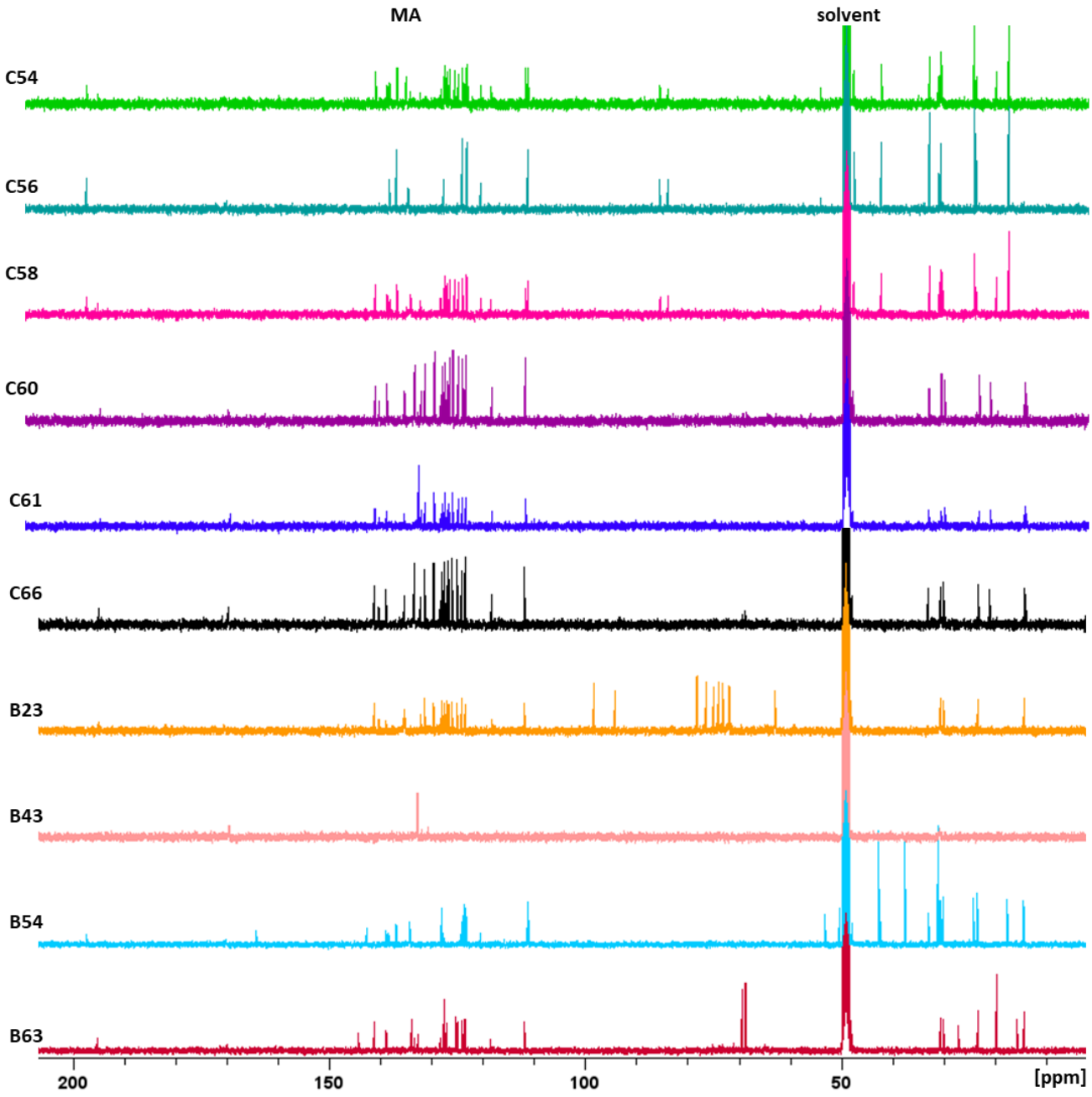

Figure S6. ^{13}C NMR spectra of seized herbal products (samples C54, C56, C58, C60, C61, C66, B23, B43, B54 and B63).

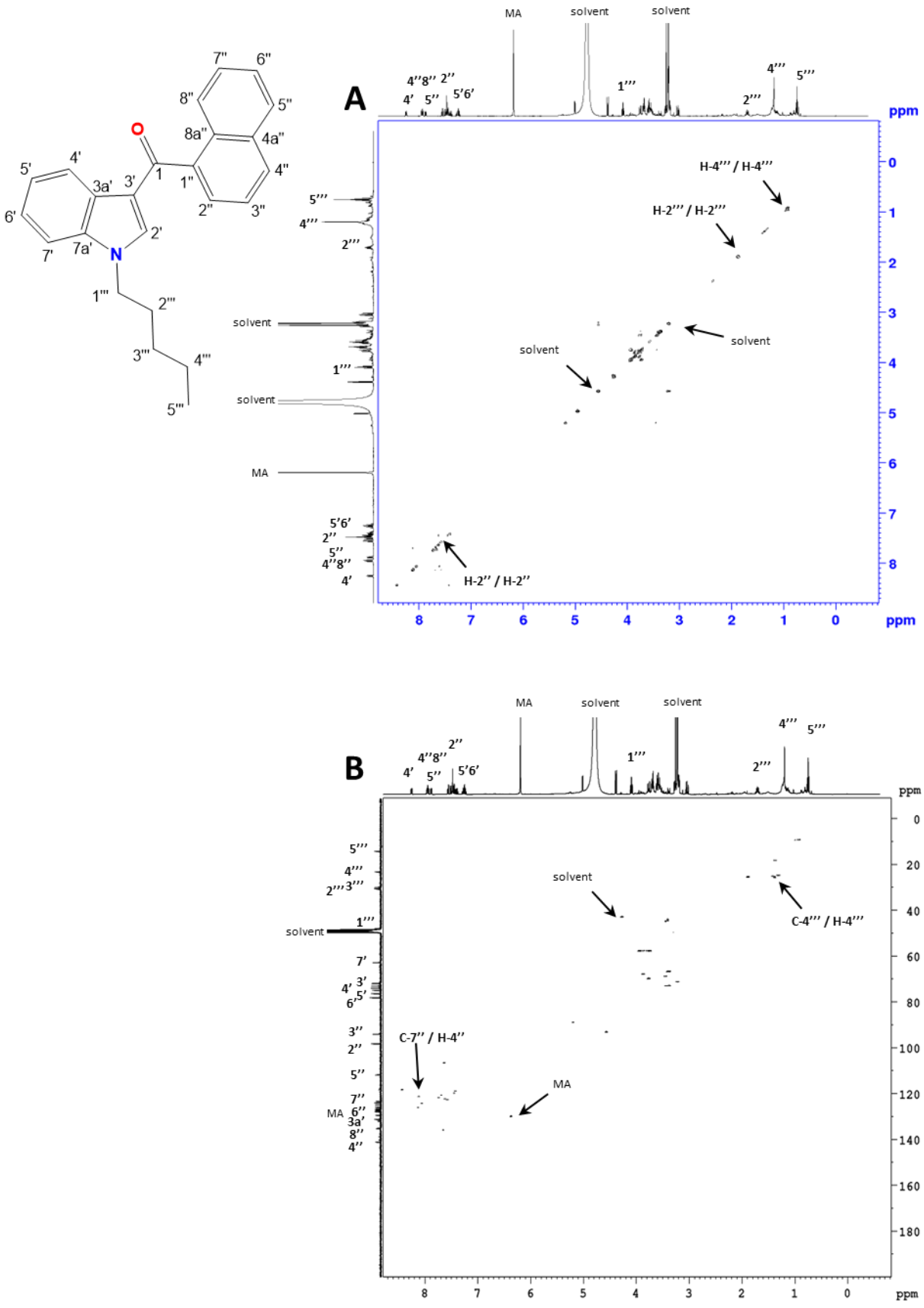

Figure S7. 2D NMR spectrum of JWH-018 found in sample B23. A- ^{1}H-^{1}H COSY NMR and B- ^{1}H-^{13}C HSQC NMR.

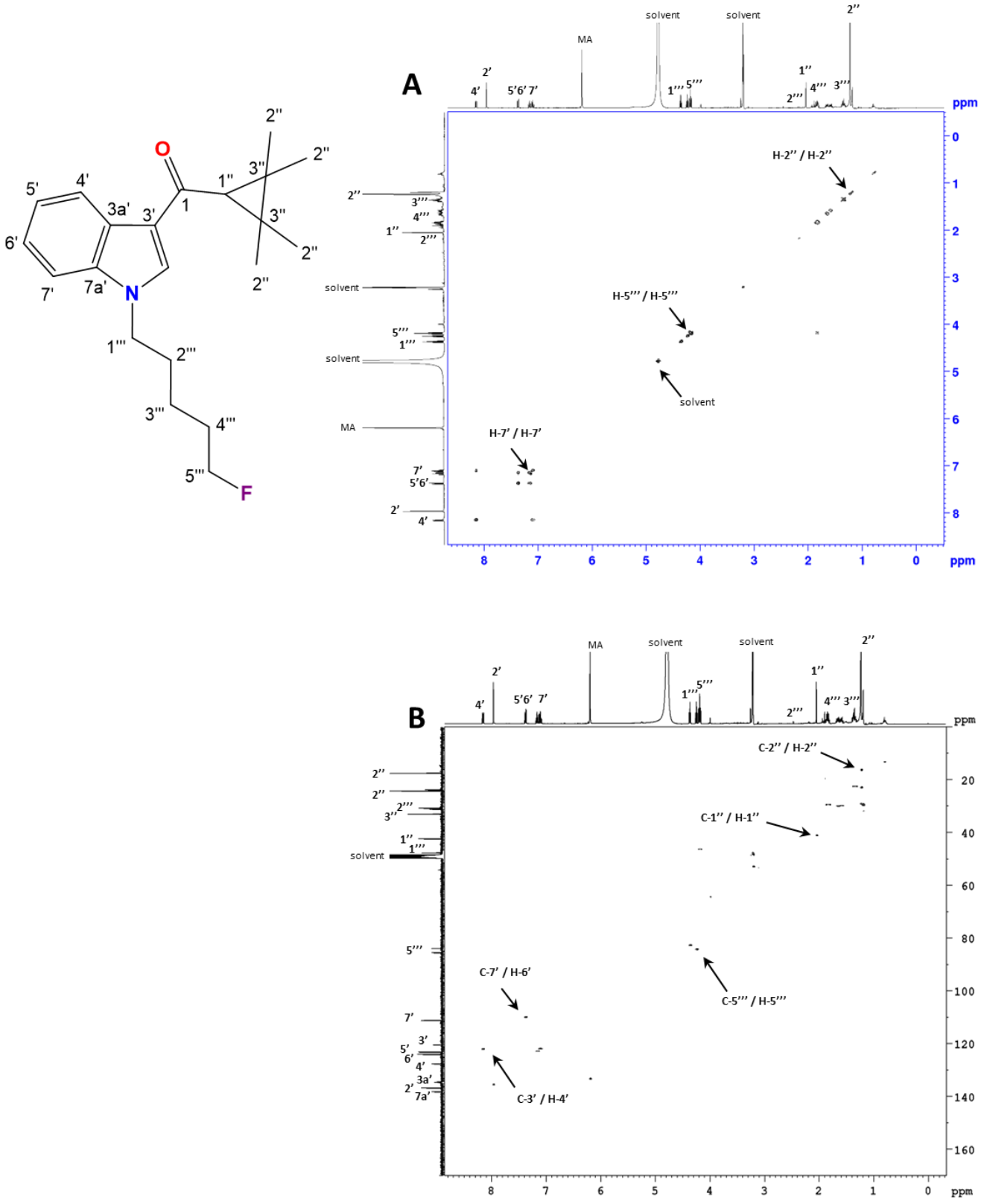

Figure S8. 2D NMR spectrum of XLR-11 found in sample C56. A- ^{1}H-^{1}H COSY NMR and B- ^{1}H-^{13}C HSQC NMR.

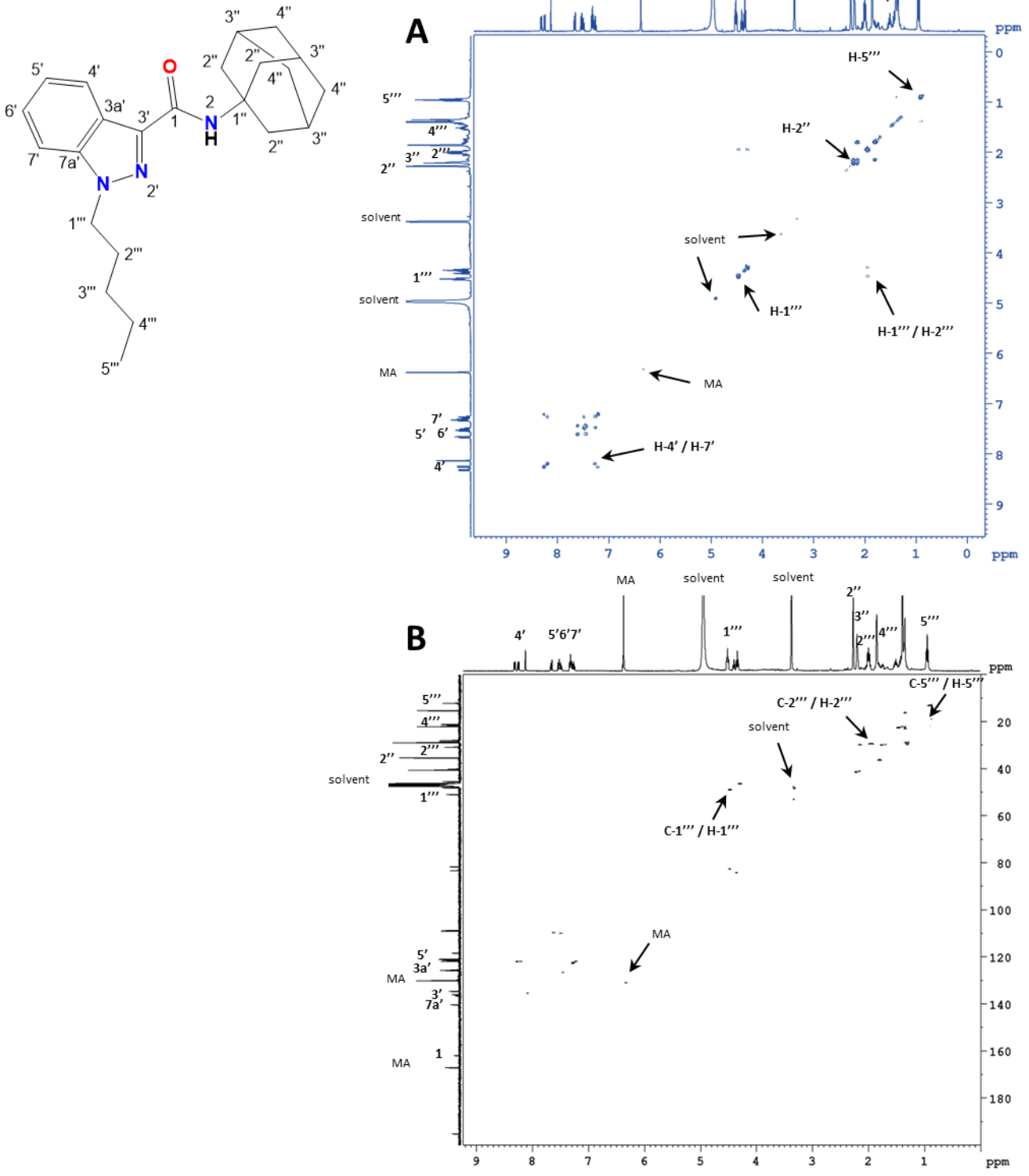

Figure S9. 2D NMR spectrum of APINACA found in sample H4. A- ^{1}H-^{1}H COSY NMR and B- ^{1}H-^{13}C HSQC NMR.

Supplementary Material II – Analytical determination studies

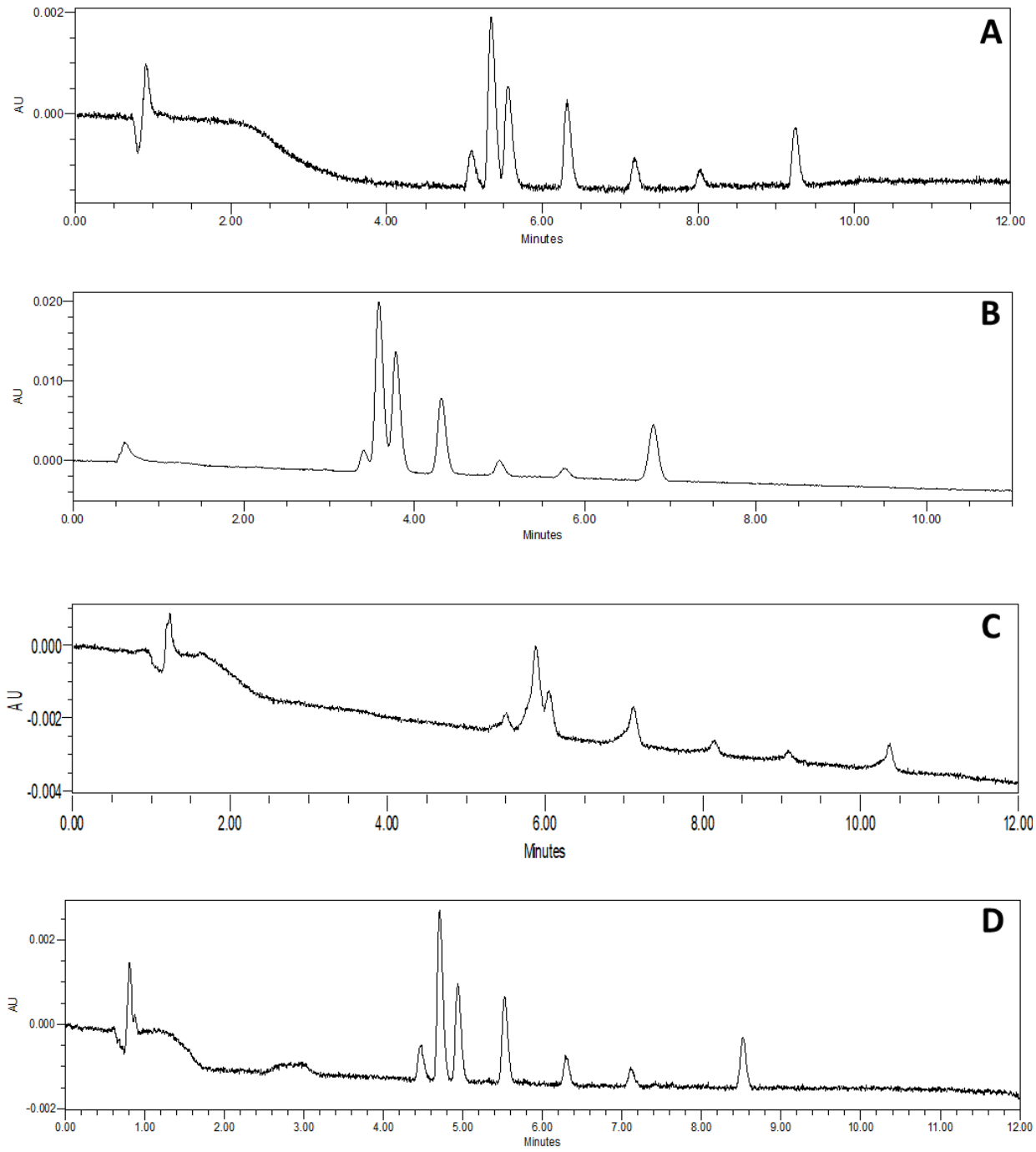

Figure S10. Comparison of the UHPLC-PDA chromatographic profiles of the different columns tested at 310 nm. A – CORTECS; B – BEH; C – CSH and D – HSS T3.

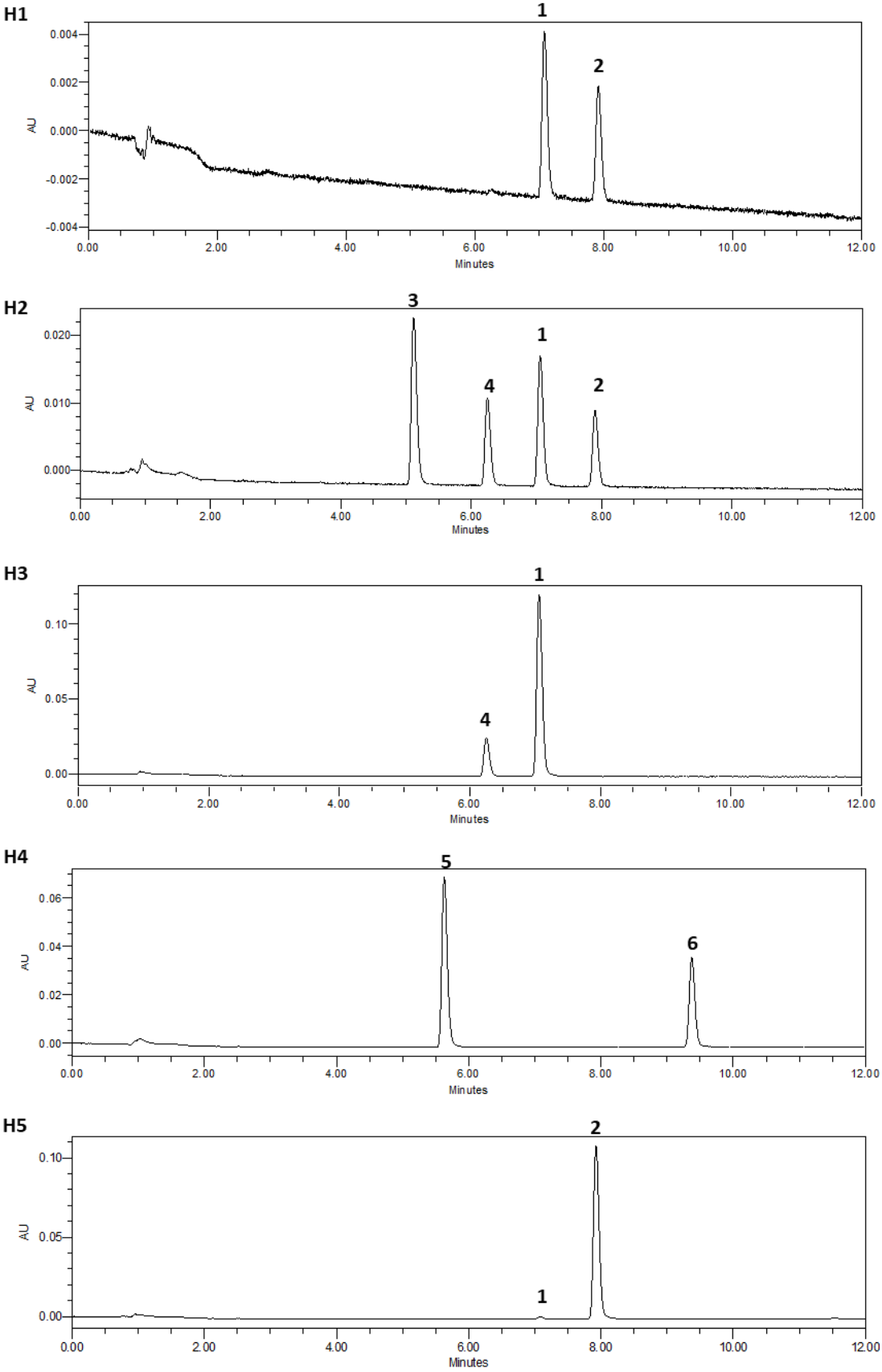
H1
1
2
AU
0.004
0.002
0.000
-0.002
-0.004
0.00
2.00
4.00
6.00
8.00
10.00
12.00
Minutes
H2
3
1
4
2
AU
0.020
0.010
0.000
Minutes
H3
1
4
AU
0.10
0.05
0.00
Minutes
H4
5
6
AU
0.06
0.04
0.02
0.00
Minutes
H5
2
1
AU
0.10
0.05
0.00
Minutes

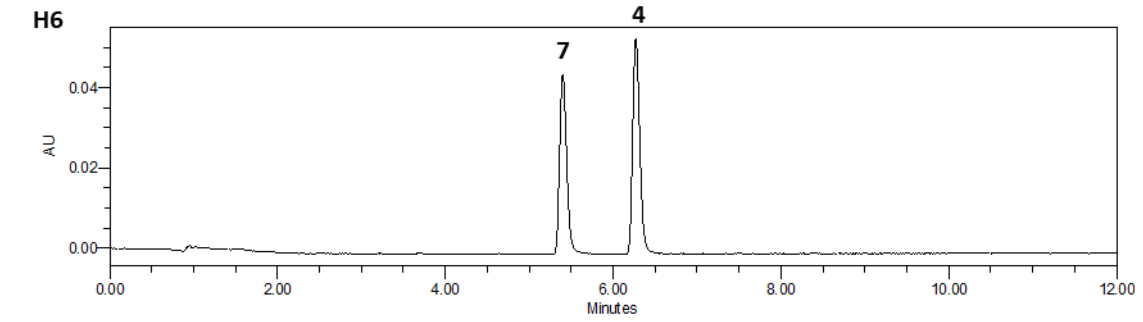
H6
7
4
AU
0.04
0.02
0.00
0.00
2.00
4.00
6.00
8.00
10.00
12.00
Minutes

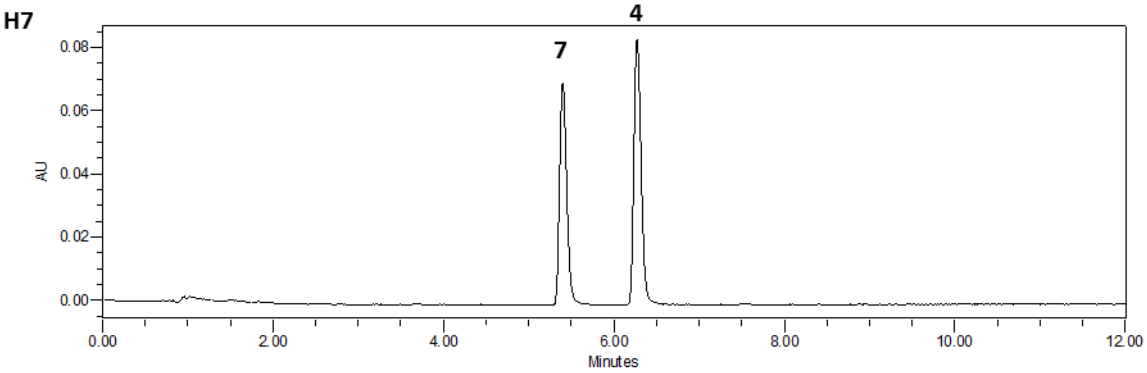
H7
7
4
AU
0.08
0.06
0.04
0.02
0.00
0.00
2.00
4.00
6.00
8.00
10.00
12.00
Minutes

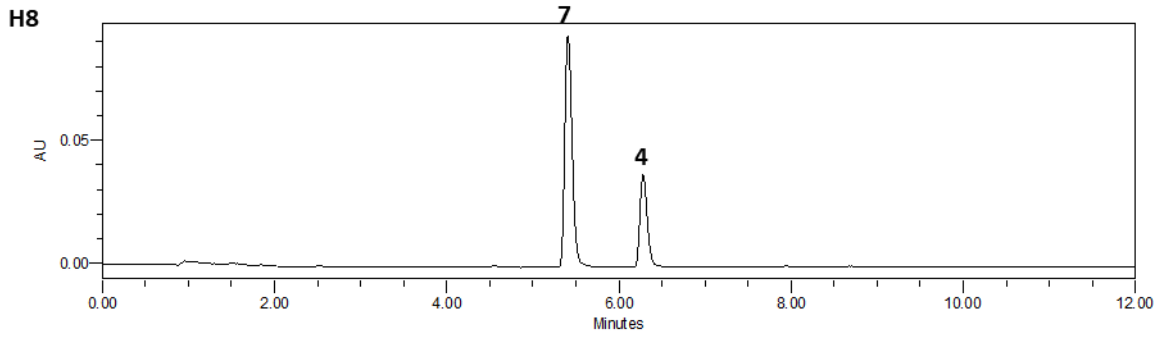
H8
7
4
AU
0.05
0.00
0.00
2.00
4.00
6.00
8.00
10.00
12.00
Minutes

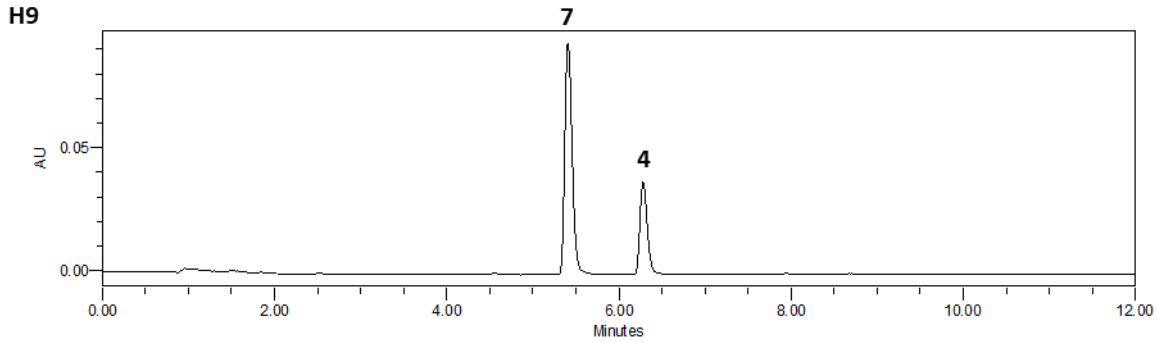
H9
7
4
AU
0.05
0.00
0.00
2.00
4.00
6.00
8.00
10.00
12.00
Minutes

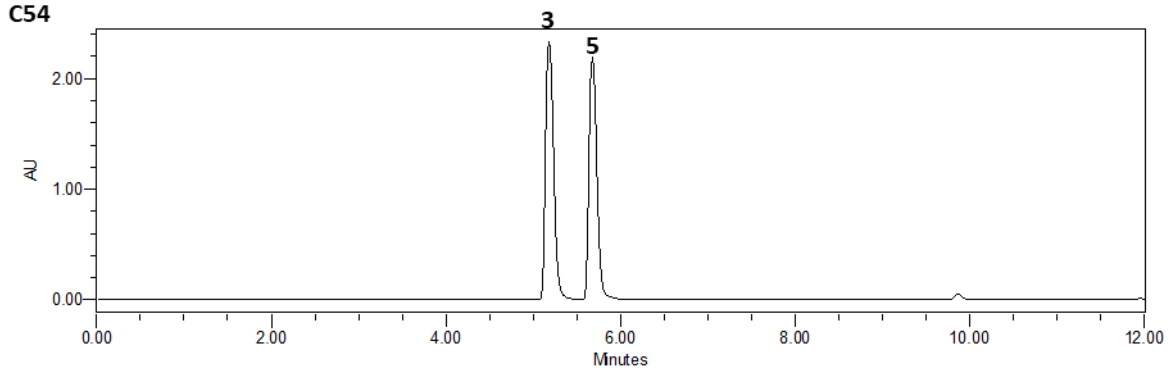
C54
3
5
AU
2.00
1.00
0.00
0.00
2.00
4.00
6.00
8.00
10.00
12.00
Minutes

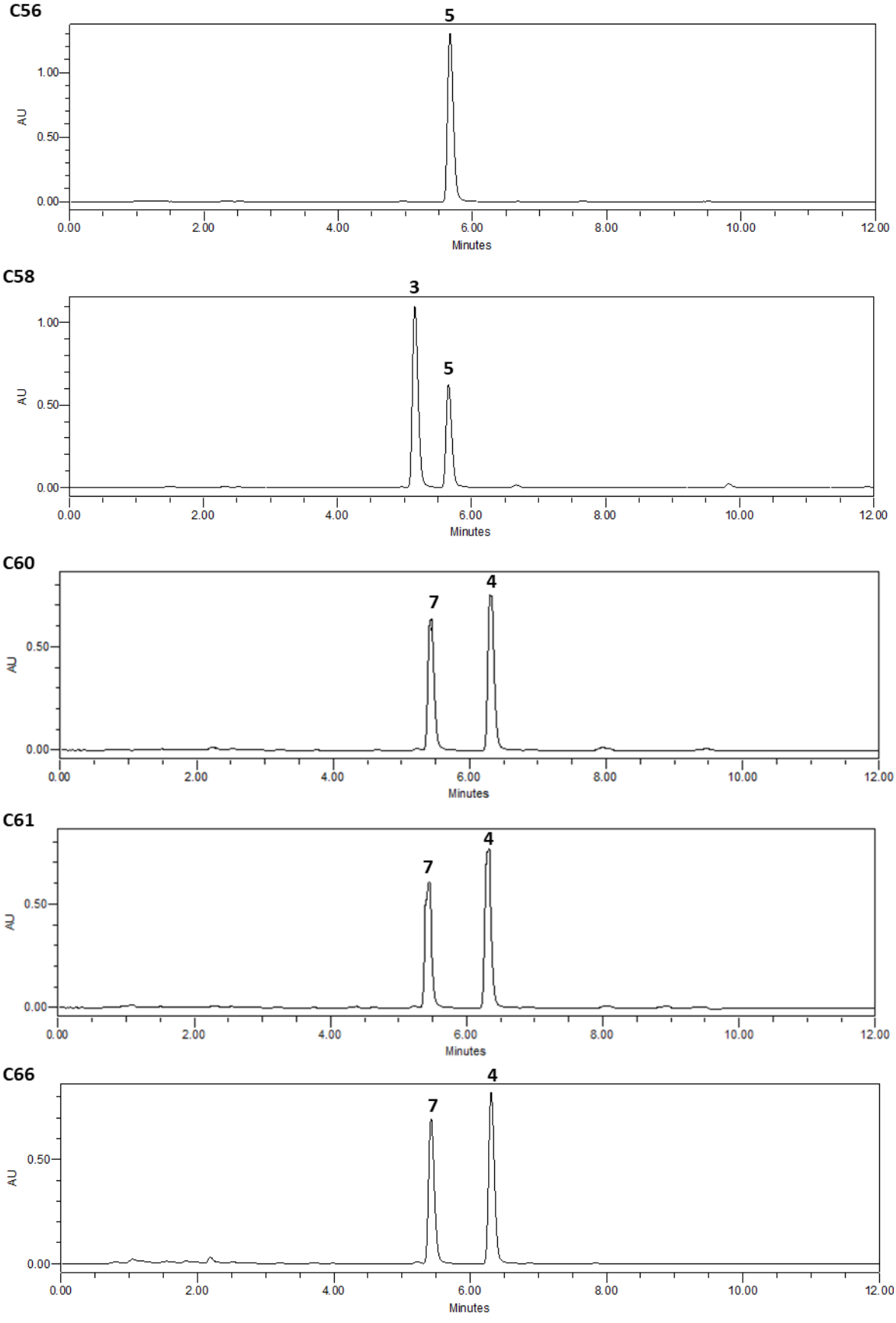
C56
5
AU
1.00
0.50
0.00
0.00
2.00
4.00
6.00
8.00
10.00
12.00
Minutes
C58
3
5
AU
1.00
0.50
0.00
0.00
2.00
4.00
6.00
8.00
10.00
12.00
Minutes
C60
7
4
AU
0.50
0.00
0.00
2.00
4.00
6.00
8.00
10.00
12.00
Minutes
C61
7
4
AU
0.50
0.00
0.00
2.00
4.00
6.00
8.00
10.00
12.00
Minutes
C66
7
4
AU
0.50
0.00
0.00
2.00
4.00
6.00
8.00
10.00
12.00
Minutes

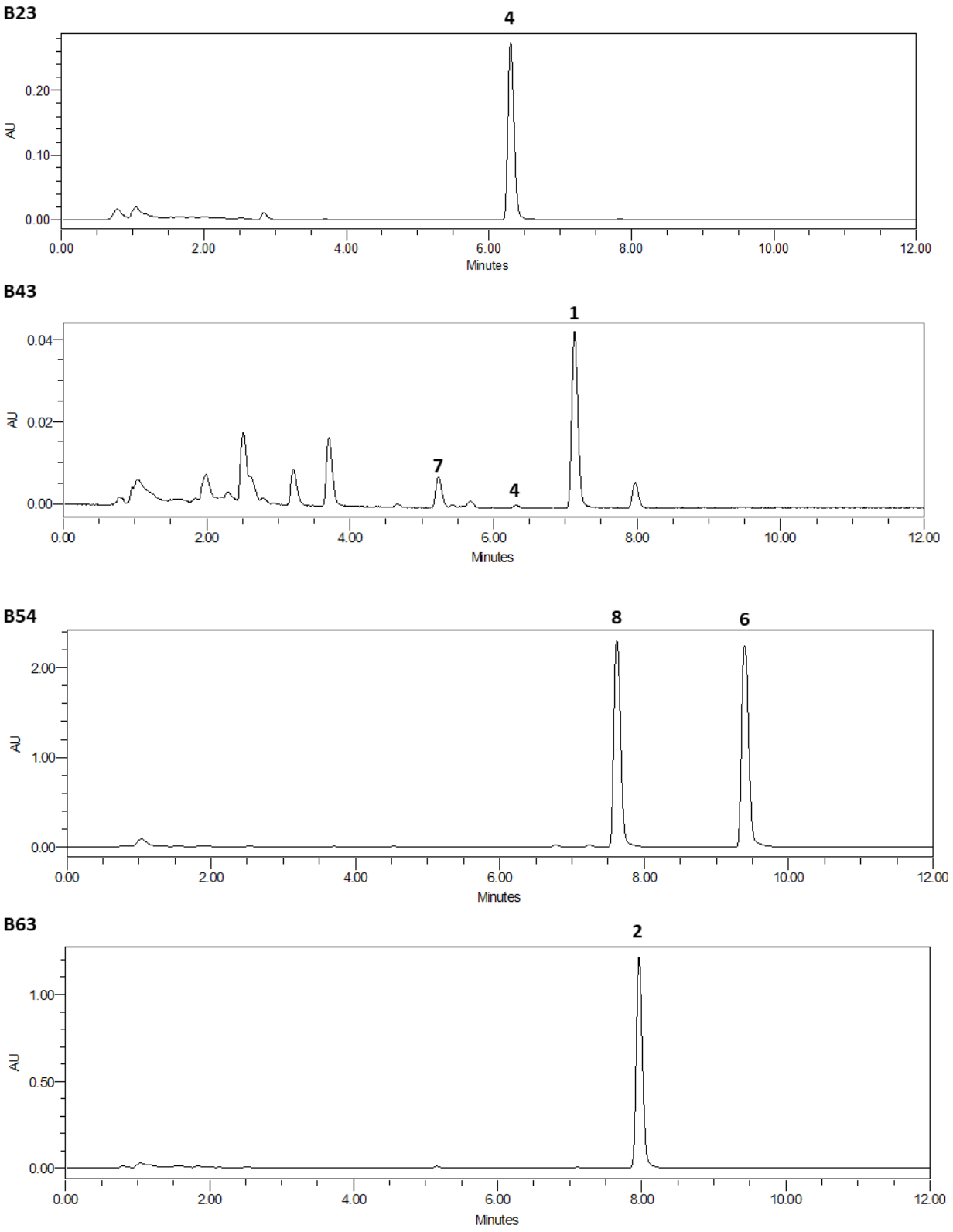

Figure S11.UHPLC-PDA chromatographic profiles of the different seized herbal extracts at 310 nm. Peak identification: 1 – JWH-122, 2 – JWH-210, 3 – MAM-2201, 4 – JWH-018, 5 – XLR-11, 6 – APINACA, 7 - JWH-073, 8 – UR-144.

MAM-2201

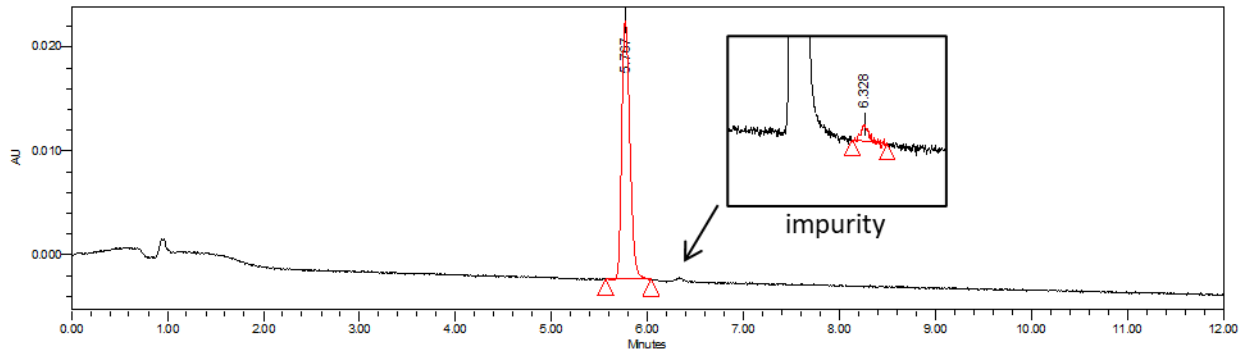

JWH-073

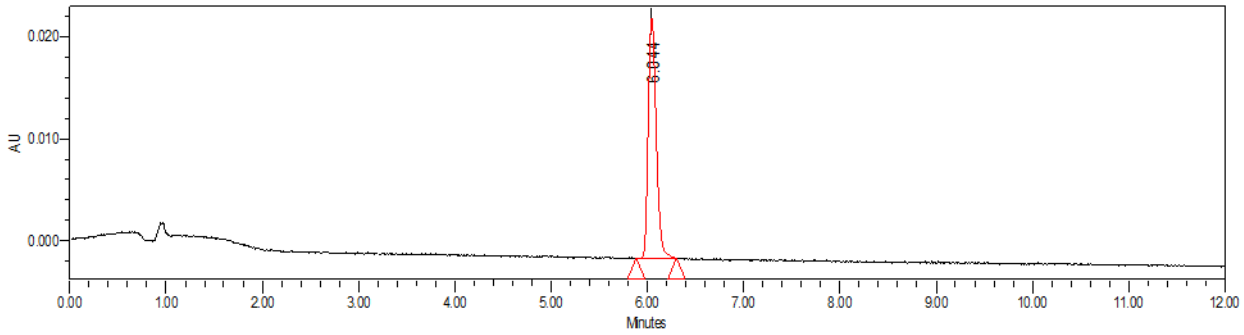

XLR-11

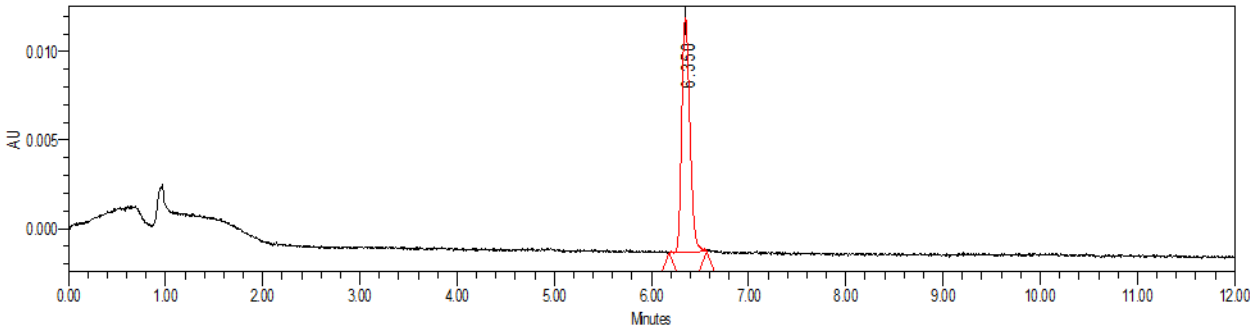

JWH-018

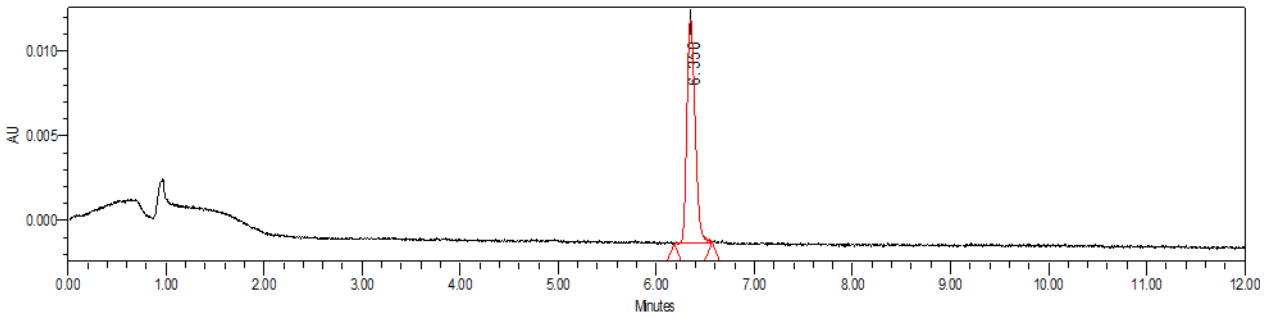

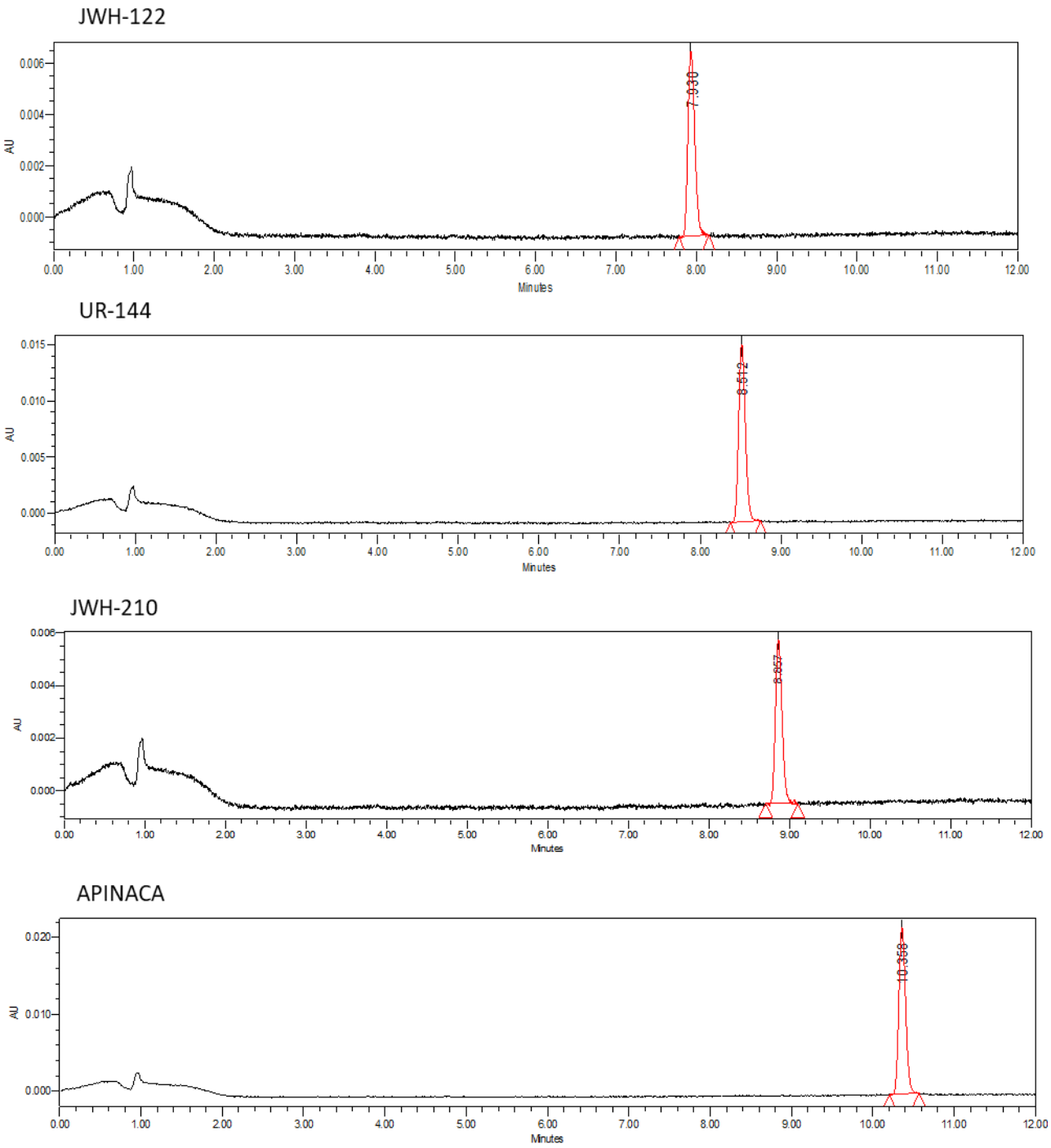

Figure S12. UHPLC-PDA chromatographic profiles of the isolated SCs at 310 nm.

MAM-2201

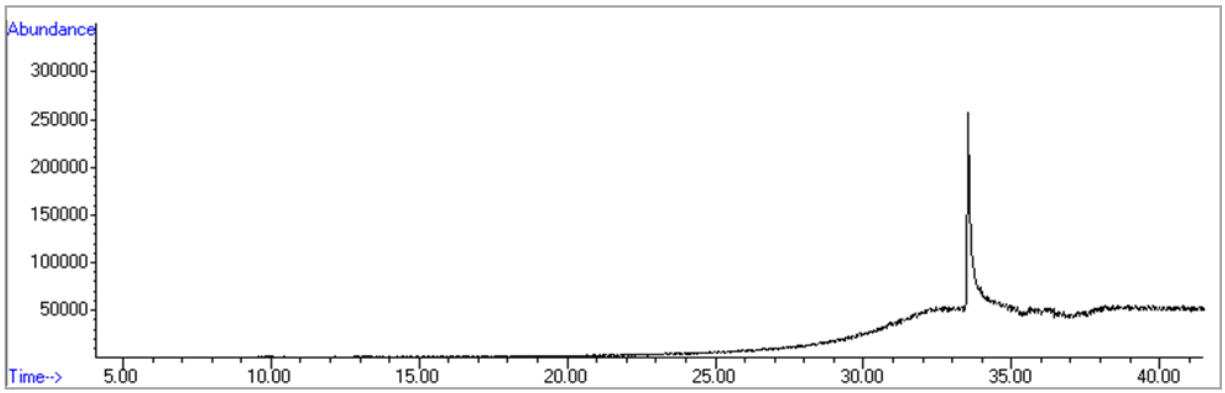

JWH-073

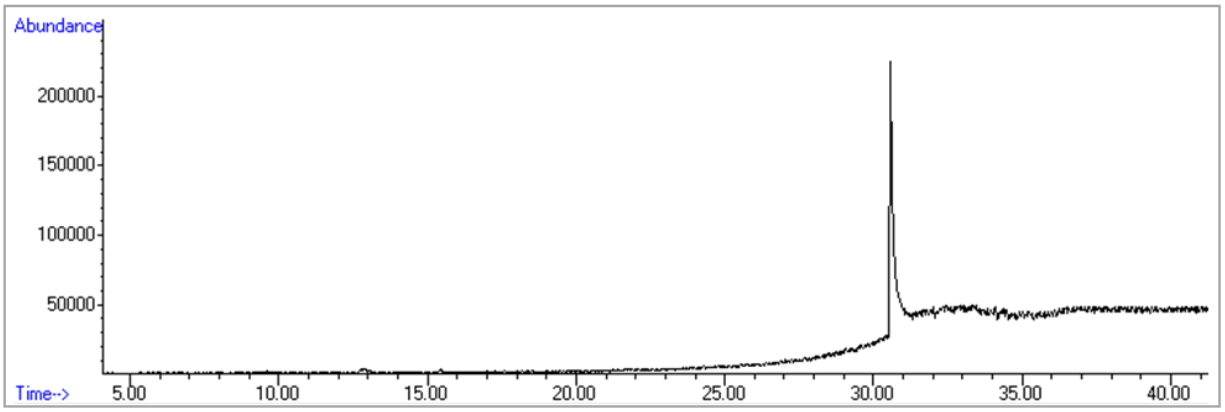

XLR-11

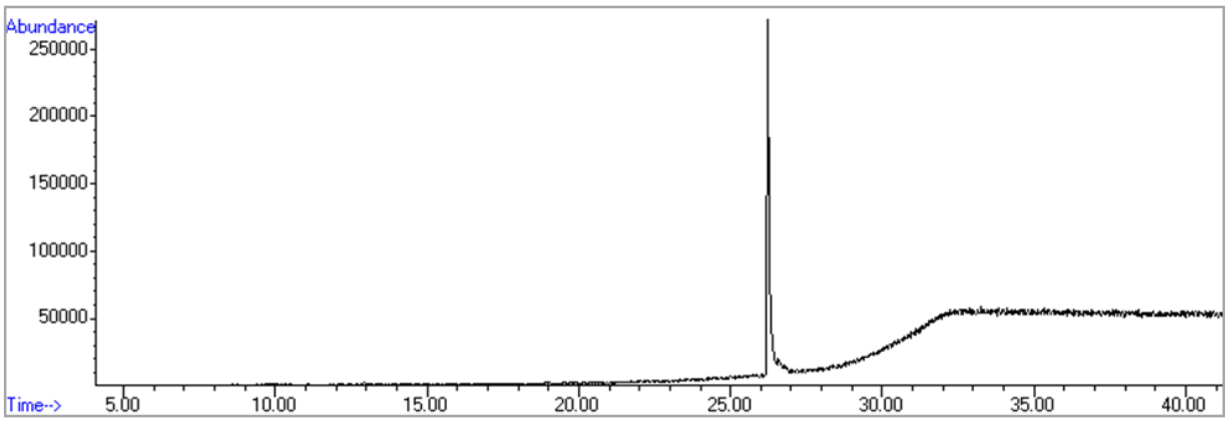

JWH-018

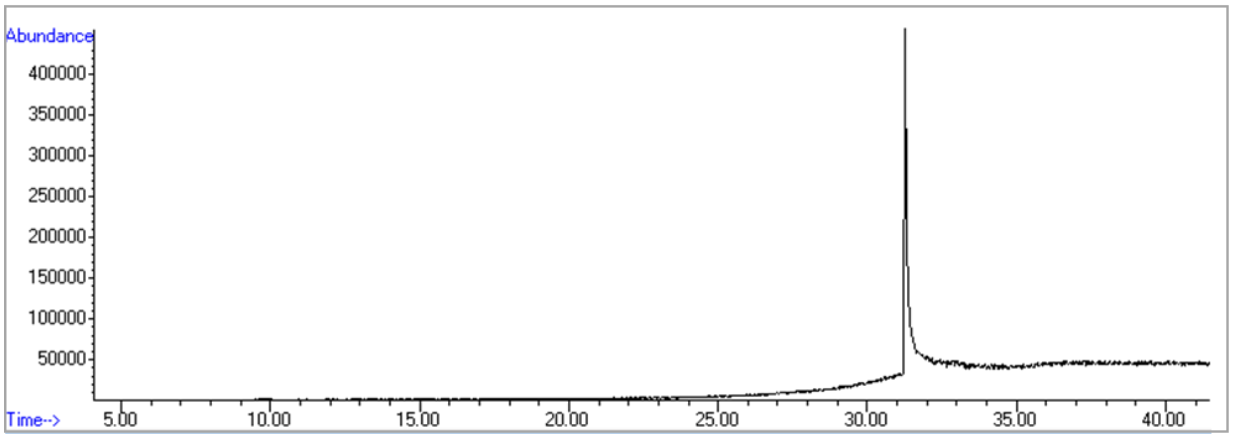

JWH-122

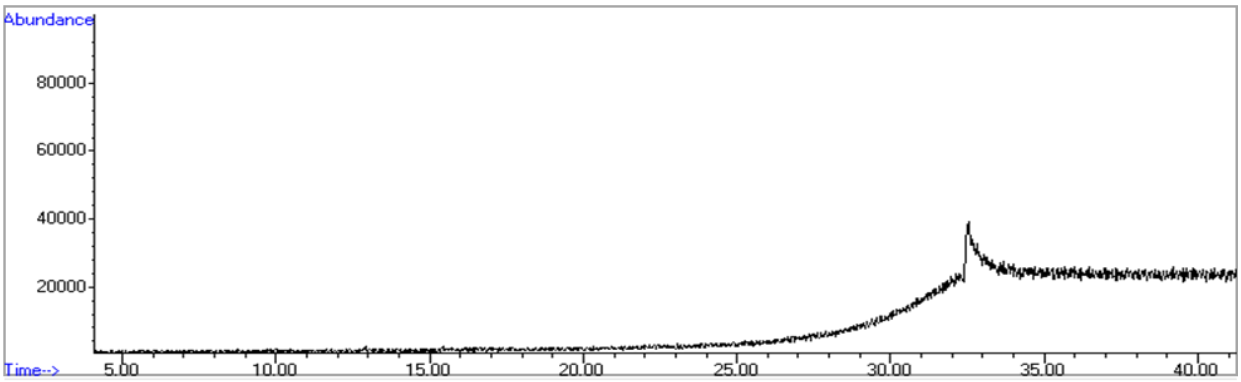

UR-144

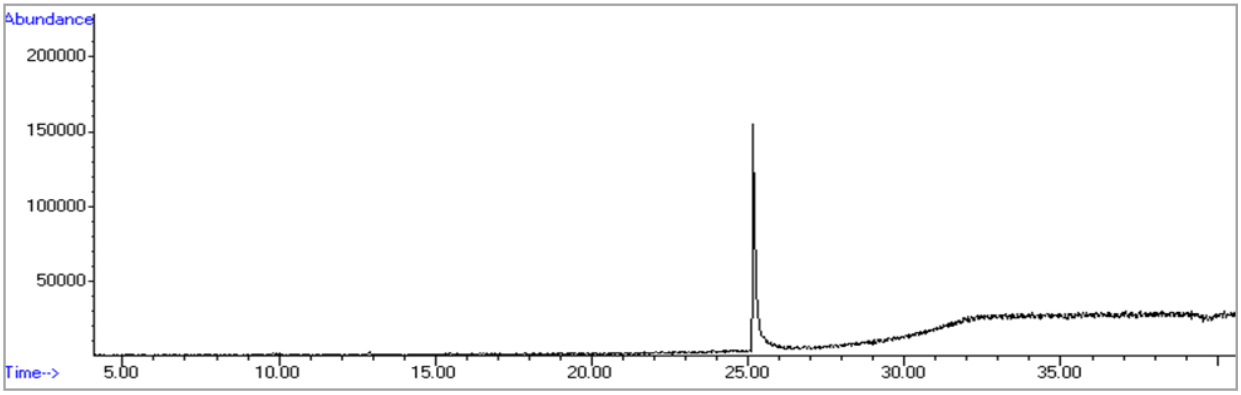

JWH-210

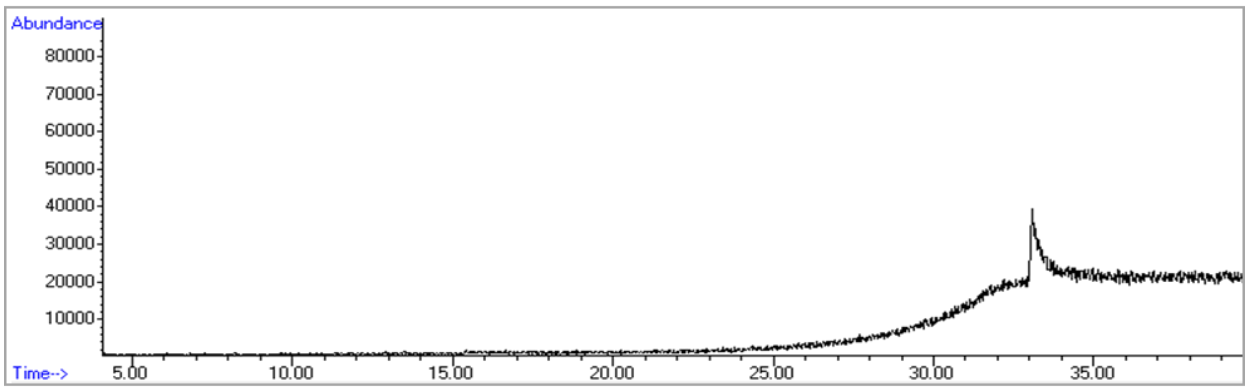

APINACA

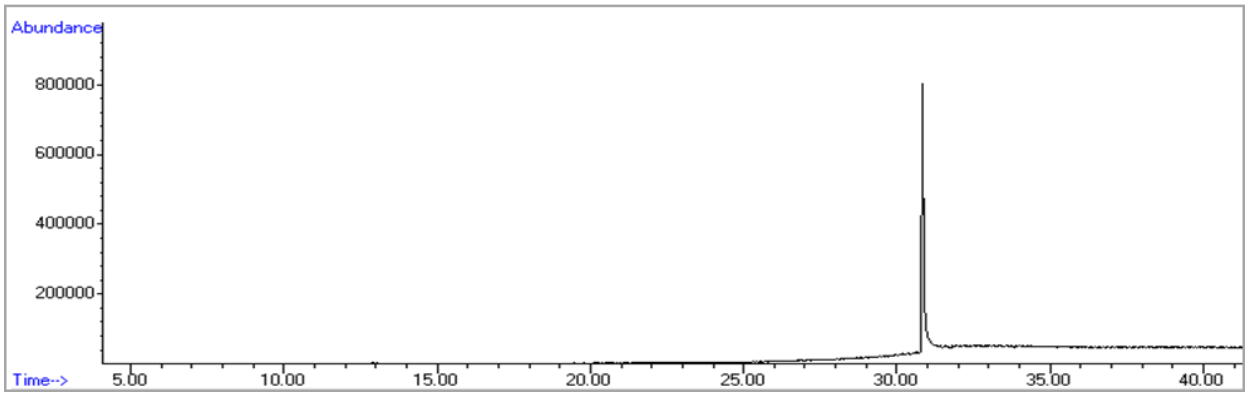

Figure S13. GC-MS chromatographic profiles of the isolated SCs.

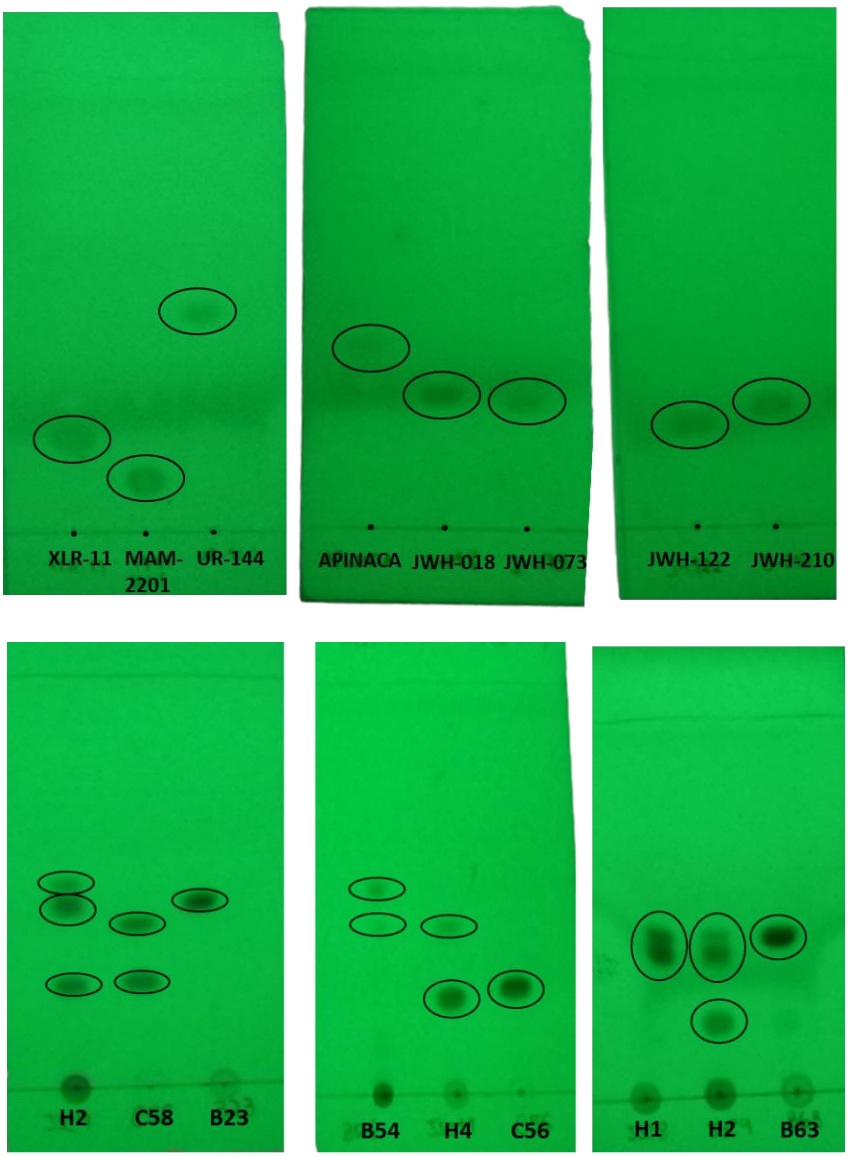

Figure S14. TLC plates of the isolated SCs and some sample extracts visualized under UV light (254 nm).

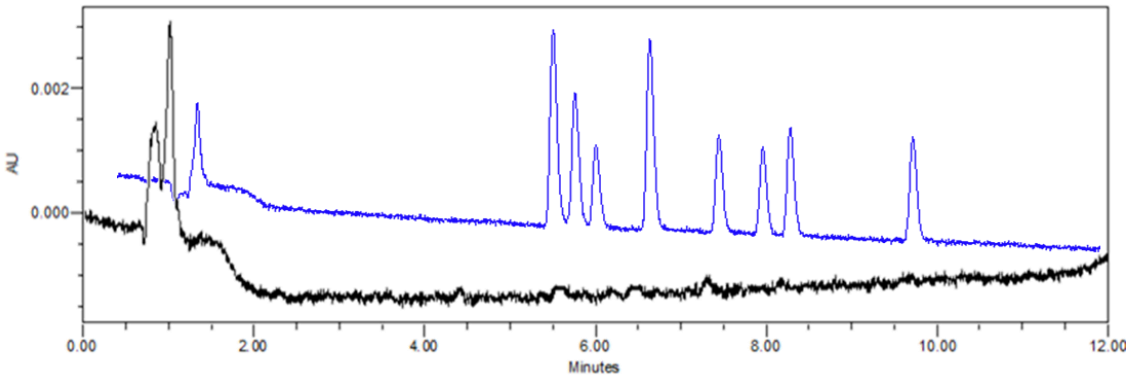

Figure S15. Chromatogram profiles of spiked oral fluid sample (in blue) and blank pool of oral fluid (in black) with MEPS procedure (at 310 nm).

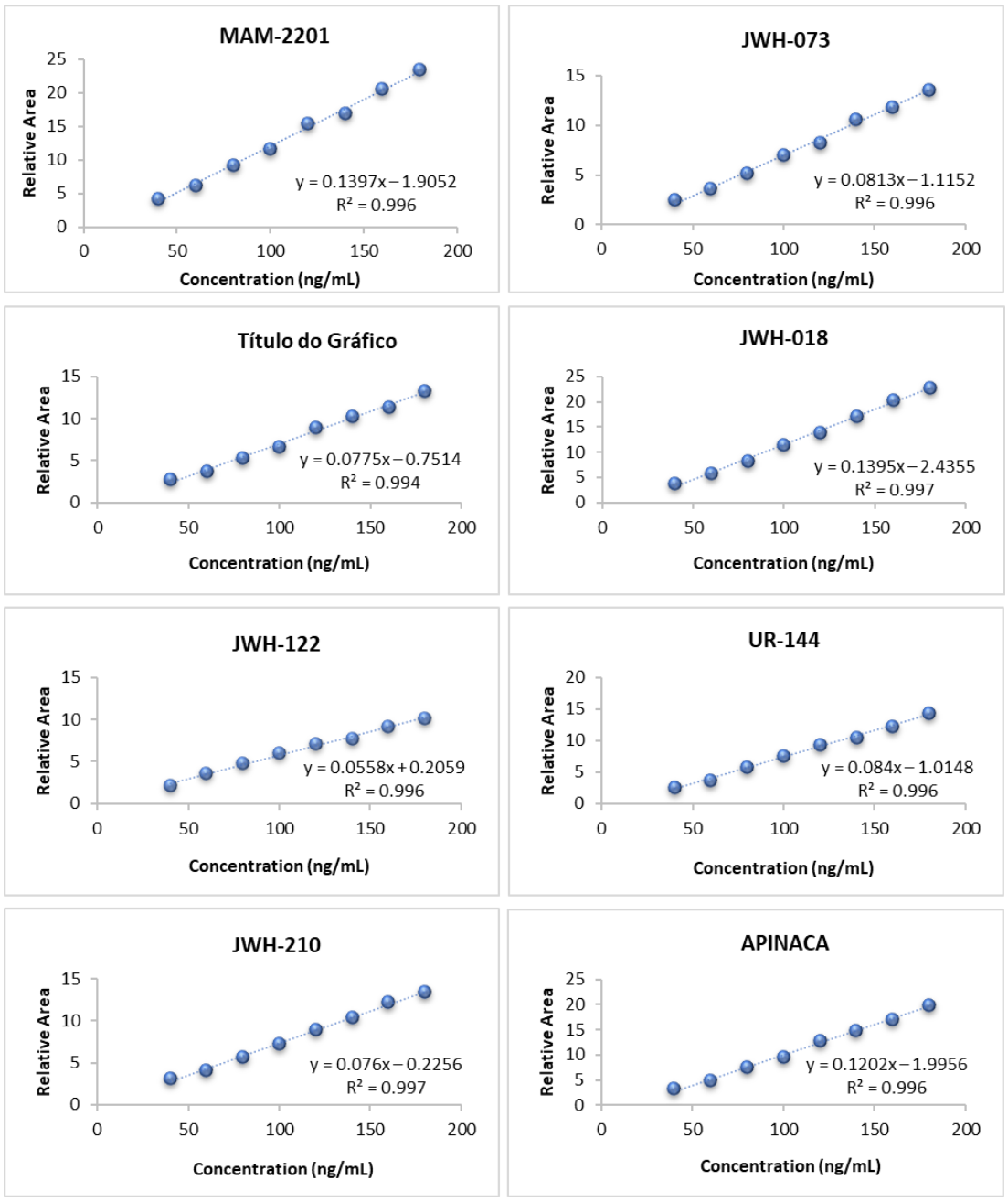

Figure S16. Calibration curve obtained for each synthetic cannabinoid by MEPS/UHPLC-PDA.

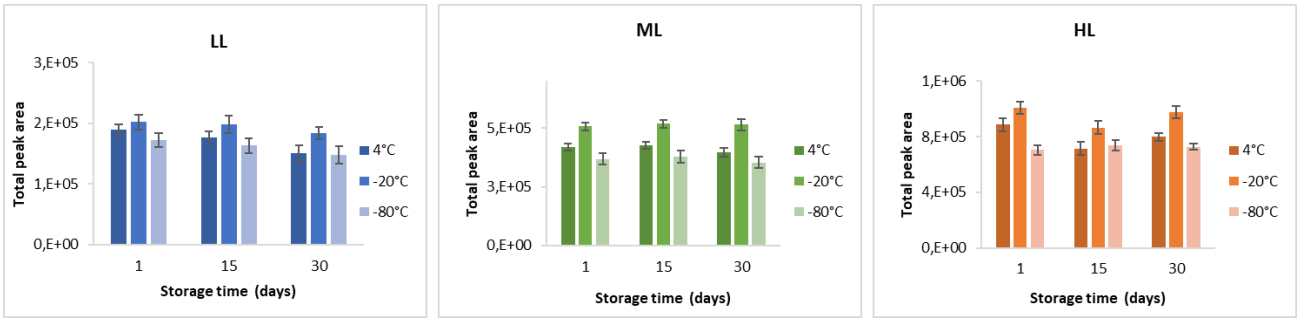

Figure S17. Stability tests using MEPS/UHPLC-PDA methodology.

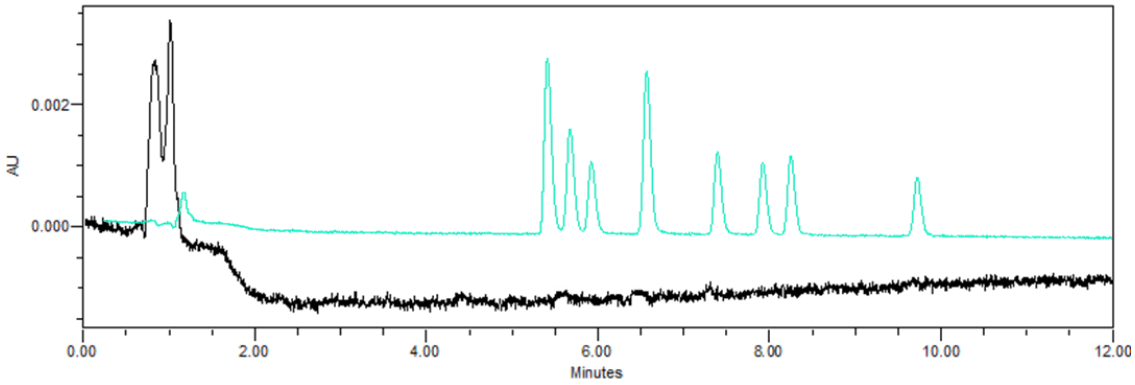

Figure S18. Chromatogram profiles of spiked oral fluid sample (in green) and blank pool of oral fluid (in black) with µSPEed procedure (at 310 nm).

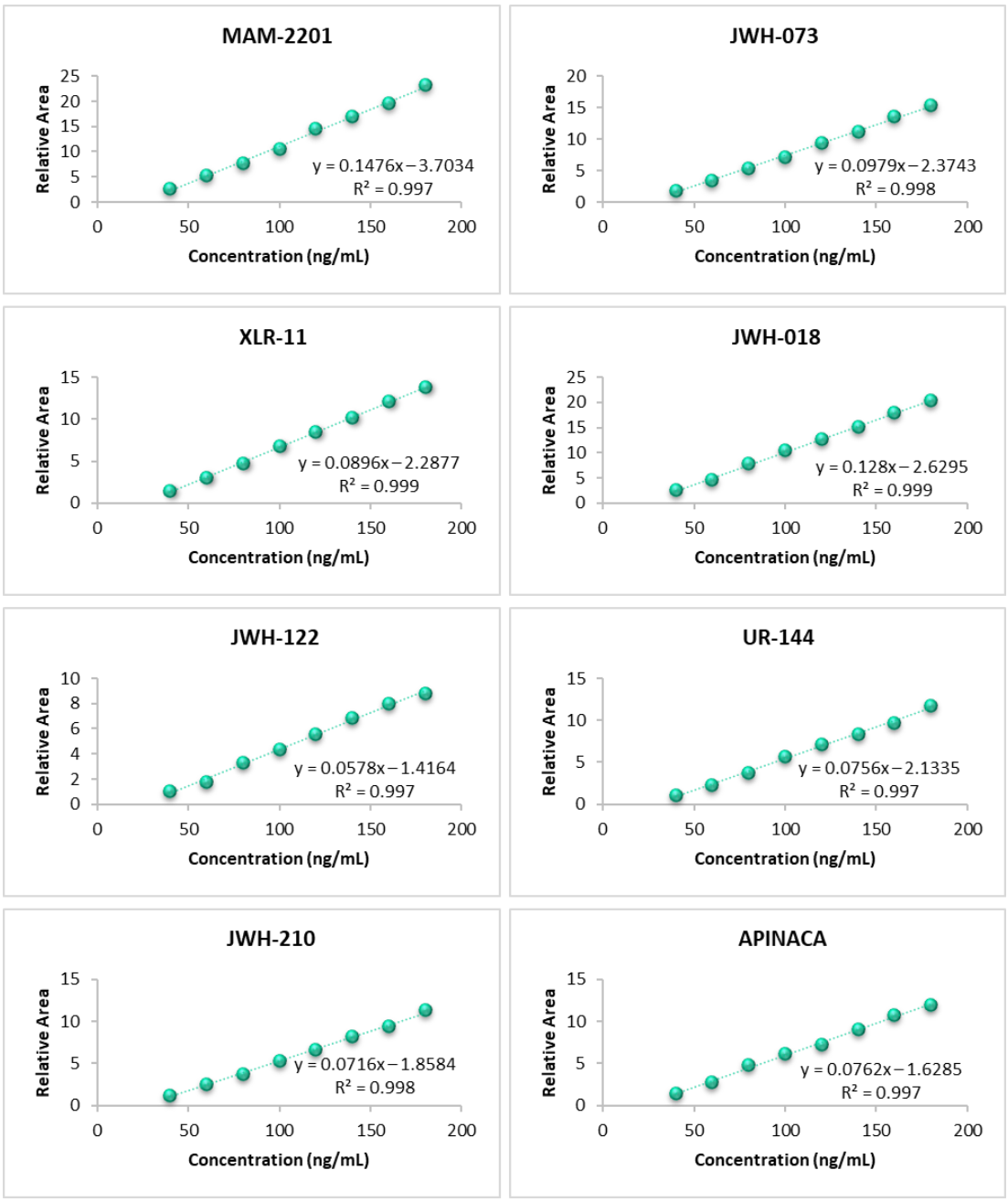

Figure S19. Calibration curve obtained for each synthetic cannabinoid by µSPEed/UHPLC-PDA.

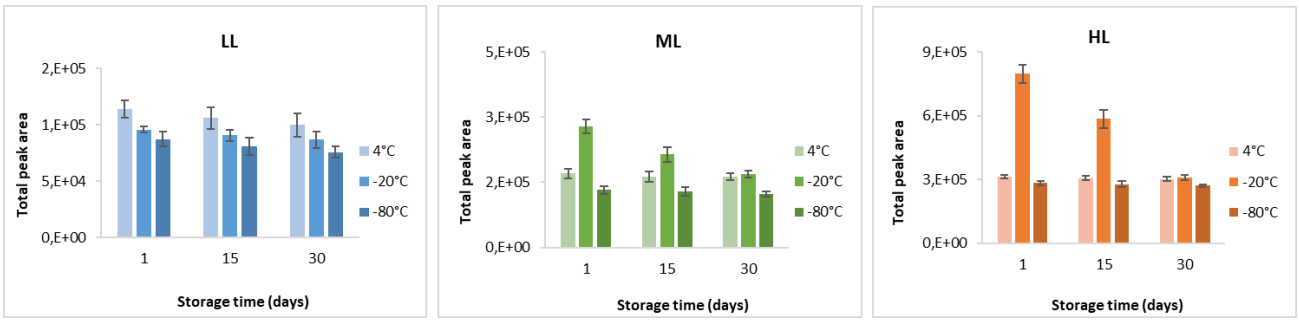

Figure S20. Stability tests using µSPEed/UHPLC-PDA methodology.

Supplementary Material III – Validation statistical studies

Table S1. Linearity statistical results of MAM-2201 by MEPS

Concentration (ng/mL)	Relative area
40	4.2
60	6.1
80	9.2
100	11.7
120	15.4
140	17.0
160	20.7
180	23.4

SUMMARY OUTPUT

Regression Statistics	
Multiple R	0,997899655
R Square	0,995803722
Adjusted R Square	0,994964466
Standard Error	0,440296041
Observations	7

ANOVA

	df	*SS*	*MS*	*F*	*Significance F*
Regression	1	230,0218061	230,0218	1186,532	3,87875E-07
Residual	5	0,969303017	0,193861		
Total	6	230,9911092			

	Coefficients	*Standard Error*	*t Stat*	*P value*	*Lower 95%*	*Upper 95%*
Intercept	-2,415962396	0,526254424	-4,59086	0,005889	-3,768742461	-1,063182332
40	0,143309669	0,004160407	34,44607	3,88E-07	0,132615004	0,154004335

RESIDUAL OUTPUT

Observation	*Predicted*	*Residuals*
1	6,182617751	-0,090838957
2	9,048811133	0,172365689
3	11,91500452	-0,252591438
4	14,7811979	0,62975791
5	17,64739128	-0,668155823
6	20,51358466	0,14060897
7	23,37977805	0,06885365

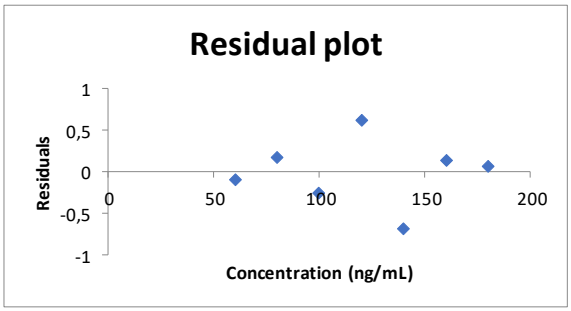

Table S2. Linearity statistical results of JWH-073 by MEPS

Concentration (ng/mL)	Relative area
40	2.5
60	3.6
80	5.2
100	7.0
120	8.3
140	10.6
160	11.9
180	13.6

SUMMARY OUTPUT

Regression Statistics	
Multiple R	0,998471319
R Square	0,996944975
Adjusted R Square	0,99633397
Standard Error	0,219101504
Observations	7

ANOVA

	df	*SS*	*MS*	*F*	*Significance F*
Regression	1	78,32802575	78,32803	1631,648	1,75344E-07
Residual	5	0,240027346	0,048005		
Total	6	78,56805309			

	Coefficients	*Standard Error*	*t Stat*	*P value*	*Lower 95%*	*Upper 95%*
Intercept	-1,444442914	0,261876386	-5,51574	0,002681	-2,117617595	-0,771268232
40	0,08362759	0,002070315	40,39366	1,75E-07	0,078305676	0,088949503

RESIDUAL OUTPUT

Observation	*Predicted*	*Residuals*
1	3,573212457	0,015369918
2	5,245764247	-0,050529209
3	6,918316037	0,125708252
4	8,590867828	-0,313087799
5	10,26341962	0,339703737
6	11,93597141	-0,082550552
7	13,6085232	-0,034614348

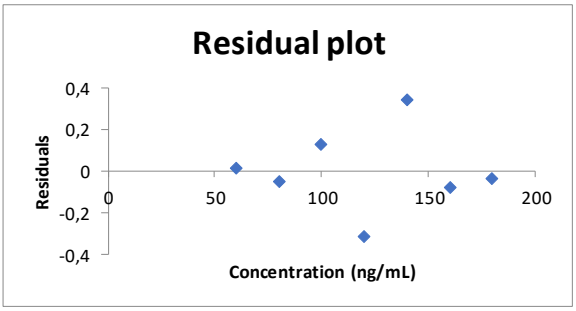

Table S3. Linearity statistical results of XLR-11 by MEPS

Concentration (ng/mL)	Relative area
40	2.7
60	3.7
80	5.3
100	6.6
120	8.9
140	10.3
160	11.4
180	13.3

SUMMARY OUTPUT

Regression Statistics	
Multiple R	0,997354004
R Square	0,99471501
Adjusted R Square	0,993658012
Standard Error	0,275520766
Observations	7

ANOVA

	df	*SS*	*MS*	*F*	*Significance F*
Regression	1	71,4386405	71,43864	941,0756	6,90734E-07
Residual	5	0,379558462	0,075912		
Total	6	71,81819896			

	Coefficients	*Standard Error*	*t Stat*	*P value*	*Lower 95%*	*Upper 95%*
Intercept	-1,08842229	0,329310302	-3,30516	0,021354	-1,93494137	-0,24190321
40	0,079865199	0,002603427	30,67696	6,91E-07	0,073172878	0,08655752

RESIDUAL OUTPUT

Observation	*Predicted*	*Residuals*
1	3,703489662	-0,026055529
2	5,300793647	0,017231591
3	6,898097631	-0,296936683
4	8,495401615	0,410468879
5	10,0927056	0,165901568
6	11,69000958	-0,305287824
7	13,28731357	0,034677997

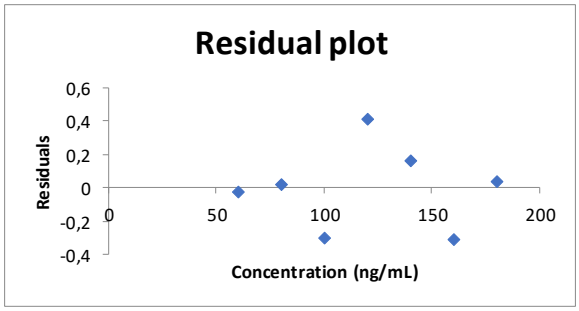

Table S4. Linearity statistical results of JWH-018 by MEPS

Concentration (ng/mL)	Relative area
40	3.8
60	5.8
80	8.1
100	11.5
120	13.9
140	17.1
160	20.3
180	22.7

SUMMARY OUTPUT

Regression Statistics	
Multiple R	0,999202325
R Square	0,998405285
Adjusted R Square	0,998086342
Standard Error	0,272722485
Observations	7

ANOVA

	df	*SS*	*MS*	*F*	*Significance F*
Regression	1	232,8283087	232,8283	3130,357	3,45012E-08
Residual	5	0,371887769	0,074378		
Total	6	233,2001965			

	Coefficients	*Standard Error*	*t Stat*	*P value*	*Lower 95%*	*Upper 95%*
Intercept	-3,092745592	0,325965717	-9,48795	0,00022	-3,930667142	-2,254824042
40	0,144181281	0,002576985	55,94959	3,45E-08	0,13755693	0,150805633

RESIDUAL OUTPUT

Observation	*Predicted*	*Residuals*
1	5,55813128	0,194750919
2	8,441756905	-0,304398203
3	11,32538253	0,185832067
4	14,20900815	-0,268479805
5	17,09263378	0,048320076
6	19,9762594	0,318956498
7	22,85988502	-0,174981552

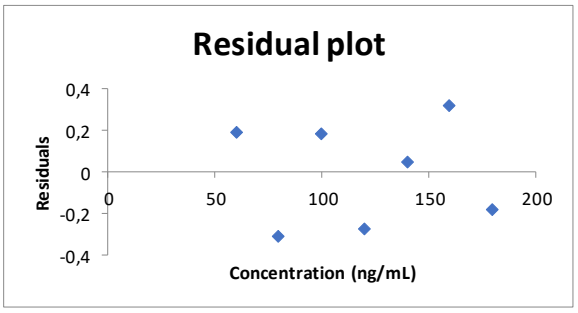

Table S5. Linearity statistical results of JWH-122 by MEPS

Concentration (ng/mL)	Relative area
40	2.2
60	3.6
80	4.8
100	6.0
120	7.1
140	7.8
160	9.2
180	10.1

SUMMARY OUTPUT

Regression Statistics	
Multiple R	0,998043829
R Square	0,996091484
Adjusted R Square	0,995309781
Standard Error	0,160329038
Observations	7

ANOVA

	df	*SS*	*MS*	*F*	*Significance F*
Regression	1	32,75531	32,75531	1274,258	3,24725E-07
Residual	5	0,128527002	0,025705		
Total	6	32,88383701			

	Coefficients	*Standard Error*	*t Stat*	*P value*	*Lower 95%*	*Upper 95%*
Intercept	0,450655386	0,191629853	2,351697	0,065422	-0,041944833	0,943255605
40	0,054079398	0,001514967	35,69675	3,25E-07	0,050185051	0,057973744

RESIDUAL OUTPUT

Observation	*Predicted*	*Residuals*
1	3,695419245	-0,096915108
2	4,777007198	0,015479379
3	5,858595151	0,116232838
4	6,940183104	0,142889312
5	8,021771057	-0,258241892
6	9,10335901	0,126978247
7	10,18494696	-0,046422776

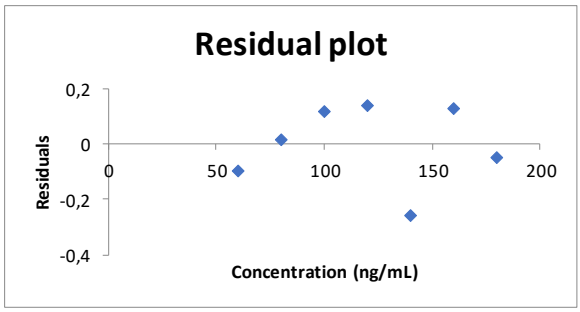

Table S6. Linearity statistical results of UR-144 by MEPS

Concentration (ng/mL)	Relative area
40	2.5
60	3.7
80	5.8
100	7.5
120	9.4
140	10.4
160	12.2
180	14.3

SUMMARY OUTPUT

Regression Statistics	
Multiple R	0,997308762
R Square	0,994624766
Adjusted R Square	0,99354972
Standard Error	0,295437906
Observations	7

ANOVA

	df	*SS*	*MS*	*F*	*Significance F*
Regression	1	80,7540602	80,75406	925,1921	7,20622E-07
Residual	5	0,436417781	0,087284		
Total	6	81,19047798			

	Coefficients	*Standard Error*	*t Stat*	*P value*	*Lower 95%*	*Upper 95%*
Intercept	-1,148815592	0,353115838	-3,25337	0,022611	-2,05652875	-0,241102434
40	0,084912802	0,002791626	30,41697	7,21E-07	0,077736699	0,092088905

RESIDUAL OUTPUT

Observation	*Predicted*	*Residuals*
1	3,945952529	-0,251411031
2	5,644208569	0,153591805
3	7,342464609	0,15323549
4	9,04072065	0,341677687
5	10,73897669	-0,309926028
6	12,43723273	-0,277615806
7	14,13548877	0,190447883

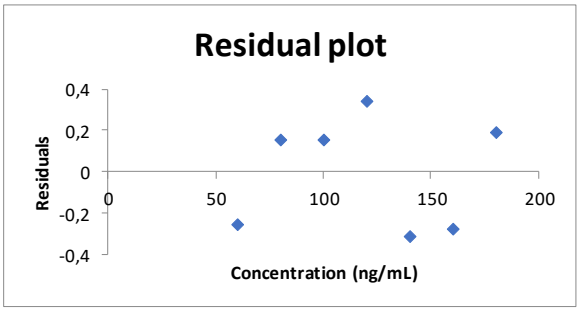

Table S7. Linearity statistical results of JWH-210 by MEPS

Concentration (ng/mL)	Relative area
40	3.2
60	4.1
80	5.7
100	7.2
120	8.9
140	10.4
160	12.2
180	13.4

SUMMARY OUTPUT

Regression Statistics	
Multiple R	0,999538504
R Square	0,99907722
Adjusted R Square	0,998892664
Standard Error	0,113063342
Observations	7

ANOVA

	df	*SS*	*MS*	*F*	*Significance F*
Regression	1	69,20136308	69,20136	5413,411	8,78551E-09
Residual	5	0,063916596	0,012783		
Total	6	69,26527968			

	Coefficients	*Standard Error*	*t Stat*	*P value*	*Lower 95%*	*Upper 95%*
Intercept	-0,586632115	0,135136541	-4,34103	0,007422	-0,934011652	-0,239252577
40	0,078604664	0,001068348	73,57589	8,79E-09	0,075858387	0,08135094

RESIDUAL OUTPUT

Observation	*Predicted*	*Residuals*
1	4,129647699	-0,029936482
2	5,70174097	0,004474812
3	7,273834241	-0,061846985
4	8,845927512	0,098710512
5	10,41802078	-0,027713902
6	11,99011405	0,163929035
7	13,56220733	-0,147616991

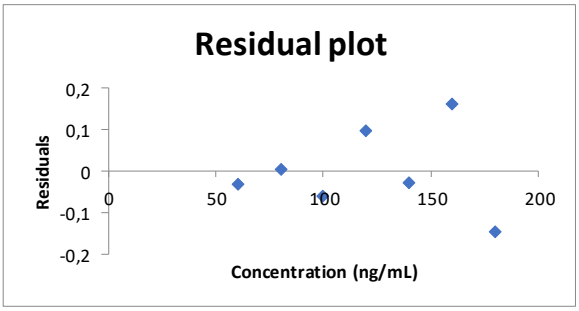

Table S8. Linearity statistical results of APINACA by MEPS

Concentration (ng/mL)	Relative area
40	3.4
60	4.8
80	7.5
100	9.5
120	12.7
140	14.8
160	17.1
180	19.9

SUMMARY OUTPUT

Regression Statistics	
Multiple R	0,998847974
R Square	0,997697274
Adjusted R Square	0,997236729
Standard Error	0,282956112
Observations	7

ANOVA

	df	*SS*	*MS*	*F*	*Significance F*
Regression	1	173,4461921	173,4462	2166,34	8,64653E-08
Residual	5	0,400320805	0,080064		
Total	6	173,8465129			

	Coefficients	*Standard Error*	*t Stat*	*P value*	*Lower 95%*	*Upper 95%*
Intercept	-2,596086764	0,33819724	-7,67625	0,000598	-3,465450445	-1,726723083
40	0,124443831	0,002673684	46,54396	8,65E-08	0,117570908	0,131316755

RESIDUAL OUTPUT

Observation	*Predicted*	*Residuals*
1	4,870543115	-0,035553112
2	7,359419742	0,15106826
3	9,848296368	-0,366755875
4	12,33717299	0,411749165
5	14,82604962	-0,034928964
6	17,31492625	-0,240388697
7	19,80380287	0,114809222

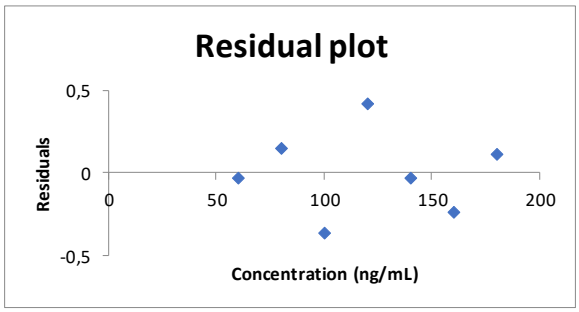

Table S9. Statistical results of intermediate precision for MAM-2201 by MEPS

Days	Day 1	Day 2	Day 3	Day 4	Day 5
R^2	0,9994	0,9937	0,9966	0,9984	0,9967
Slope	0,1380	0,1391	0,1374	0,1409	0,1418
Y_0	-1,3315	-0,9504	-0,6922	-1,3028	-1,7156
LL	**40**				
Replicated 1	40,3	36,2	36,1	41,7	43,0
Replicated 2	40,9	36,5	38,3	41,3	42,3
Replicated 3	42,2	36,3	37,6	42,6	42,7
$\overline{x}$	41,1	36,3	37,3	41,9	42,7
Recovery (%)	102,8	90,8	93,3	104,7	106,7
Mean Conc.	39,9				
Mean recovery (%)	99,6				
S_r	0,749				
S_{run}	2,813				
S_i	2,911				
RSD (%)	7,30				
ML	**100**				
Replicated 1	102,5	99,7	101,5	89,8	97,4
Replicated 2	94,8	110,1	106,8	100,7	92,8
Replicated 3	96,8	109,4	105,8	99,7	95,9
$\overline{x}$	98,0	106,4	104,7	96,7	95,3
Recovery (%)	102,0	98,8	99,4	106,4	104,1
Mean Conc.	100,2				
Mean recovery (%)	102,1				
S_r	4,48				
S_{run}	4,26				
S_i	6,18				
RSD (%)	6,16				
HL	**180**				
Replicated 1	178,1	174,1	178,3	183,8	180,5
Replicated 2	188,1	179,2	175,3	180,9	183,5
Replicated 3	176,3	178,4	180,4	179,5	182,0
$\overline{x}$	180,8	177,3	178,0	181,4	182,0
Recovery (%)	100,5	98,5	98,9	100,8	101,1
Mean Conc.	179,9				
Mean recovery (%)	99,9				
S_r	3,51				
S_{run}	0,67				
S_i	3,57				
RSD (%)	1,99				

Table S10. Statistical results of intermediate precision for JWH-073 by MEPS

Days	Day 1	Day 2	Day 3	Day 4	Day 5
R^2	0,9980	0,9976	0,9988	0,9998	1,0000
Slope	0,0787	0,0801	0,0768	0,0757	0,0763
Y_0	-0,3816	-0,7410	-0,5494	-0,5047	-0,4203
LL			**40**		
Replicated 1	36,3	39,7	39,5	38,3	39,4
Replicated 2	36,9	42,8	44,3	37,3	38,2
Replicated 3	40,6	44,2	41,0	42,3	43,2
$\bar{x}$	37,9	42,2	41,6	39,3	40,3
Recovery (%)	94,8	105,6	103,9	98,3	100,7
Mean Conc.			40,3		
Mean recovery (%)			100,7		
S_r			2,48		
S_{run}			0,97		
S_i			2,66		
RSD (%)			6,61		
ML			**100**		
Replicated 1	100,6	91,8	98,2	106,4	98,5
Replicated 2	102,1	96,4	97,2	98,8	99,2
Replicated 3	108,2	100,1	96,3	98,4	100,9
$\bar{x}$	103,6	96,1	97,2	101,2	99,5
Recovery (%)	98,2	102,9	99,5	96,8	97,7
Mean Conc.			99,5		
Mean recovery (%)			99,0		
S_r			3,35		
S_{run}			2,33		
S_i			4,08		
RSD (%)			4,10		
HL			**180**		
Replicated 1	179,5	182,3	179,4	178,4	179,6
Replicated 2	178,9	182,6	180,7	180,3	183,8
Replicated 3	177,1	180,1	182,8	180,4	177,2
$\bar{x}$	178,5	181,7	181,0	179,7	180,2
Recovery (%)	99,2	100,9	100,5	99,8	100,1
Mean Conc.			180,2		
Mean recovery (%)			100,1		
S_r			1,94		
S_{run}			0,49		
S_i			2,00		
RSD (%)			1,11		

Table S11. Statistical results of intermediate precision for XLR-11 by MEPS

Days	Day 1	Day 2	Day 3	Day 4	Day 5
R^2	0,9991	0,9993	0,9935	1,0000	0,9962
Slope	0,0773	0,0767	0,0777	0,0805	0,0775
Y_0	-0,4434	-0,6199	-0,7788	-0,7850	-0,9624
LL			**40**		
Replicated 1	40,4	42,8	44,9	40,0	42,9
Replicated 2	41,8	39,9	43,2	39,8	42,7
Replicated 3	42,0	40,9	43,1	39,6	42,9
$\overline{x}$	41,4	41,2	43,7	39,8	42,8
Recovery (%)	103,5	103,0	109,3	99,5	107,1
Mean Conc.			41,8		
Mean recovery (%)			104,5		
S_r			0,89		
S_{run}			1,44		
S_i			1,70		
RSD (%)			4,07		
ML			**100**		
Replicated 1	96,4	97,8	93,9	100,5	94,9
Replicated 2	99,6	96,4	93,5	100,7	95,5
Replicated 3	96,7	99,5	93,0	100,0	94,7
$\overline{x}$	97,6	97,9	93,5	100,4	95,0
Recovery (%)	103,2	99,9	101,1	104,4	99,0
Mean Conc.			96,9		
Mean recovery (%)			101,5		
S_r			1,10		
S_{run}			2,62		
S_i			2,84		
RSD (%)			2,93		
HL			**180**		
Replicated 1	181,7	180,3	181,2	179,9	181,5
Replicated 2	180,4	183,9	184,9	178,5	184,0
Replicated 3	181,0	178,5	182,3	181,1	181,3
$\overline{x}$	181,0	180,9	182,8	179,8	182,3
Recovery (%)	100,6	100,5	101,6	99,9	101,3
Mean Conc.			181,4		
Mean recovery (%)			100,8		
S_r			1,76		
S_{run}			0,59		
S_i			1,85		
RSD (%)			1,02		

Table S12. Statistical results of intermediate precision for JWH-018 by MEPS

Days	Day 1	Day 2	Day 3	Day 4	Day 5
R^2	0,9981	1,0000	1,0000	0,9994	0,9992
Slope	0,1413	0,1387	0,1432	0,1408	0,1340
Y_0	-2,3645	-2,6007	-2,9578	-3,0770	-2,8762
LL	**40**				
Replicated 1	38,4	39,5	40,6	41,9	39,3
Replicated 2	37,2	40,6	39,4	40,4	38,2
Replicated 3	38,4	40,5	39,6	41,0	38,4
$\bar{x}$	38,0	40,2	39,9	41,1	38,7
Recovery (%)	95,0	100,6	99,7	102,8	96,6
Mean Conc.	39,6				
Mean recovery (%)	98,9				
S_r	0,67				
S_{run}	1,19				
S_i	1,36				
RSD (%)	3,45				
ML	**100**				
Replicated 1	105,2	95,9	99,9	96,1	102,8
Replicated 2	103,4	102,2	99,5	99,8	101,7
Replicated 3	101,9	100,8	101,3	98,2	102,6
$\bar{x}$	103,5	99,6	100,2	98,0	102,4
Recovery (%)	99,8	103,1	96,5	96,6	95,7
Mean Conc.	100,7				
Mean recovery (%)	98,3				
S_r	1,93				
S_{run}	1,89				
S_i	2,70				
RSD (%)	2,68				
HL	**180**				
Replicated 1	177,5	179,4	178,9	181,3	177,4
Replicated 2	179,5	180,9	180,5	181,5	181,5
Replicated 3	178,5	180,2	180,3	179,5	178,0
$\bar{x}$	178,5	180,2	179,9	180,7	179,0
Recovery (%)	99,2	100,1	99,9	100,4	99,4
Mean Conc.	179,7				
Mean recovery (%)	99,8				
S_r	1,30				
S_{run}	0,50				
S_i	1,40				
RSD (%)	0,78				

Table S13. Statistical results of intermediate precision for JWH-122 by MEPS

Days	Day 1	Day 2	Day 3	Day 4	Day 5
R^2	0,9929	0,9998	0,9994	0,9994	0,9999
Slope	0,0563	0,0551	0,0578	0,0579	0,0556
Y_0	0,1141	0,0339	0,0059	-0,2191	-0,0519
LL			**40**		
Replicated 1	35,2	39,7	39,1	41,4	40,4
Replicated 2	36,3	39,1	38,8	41,1	40,9
Replicated 3	36,8	39,5	38,7	40,9	40,0
$\bar{x}$	36,1	39,4	38,9	41,1	40,4
Recovery (%)	90,3	98,6	97,2	102,8	101,1
Mean Conc.			39,2		
Mean recovery (%)			98,0		
S_r			0,48		
S_{run}			1,92		
S_i			1,98		
RSD (%)			5,04		
ML			**100**		
Replicated 1	106,6	98,2	103,0	94,4	99,6
Replicated 2	107,1	100,6	101,8	99,2	97,0
Replicated 3	106,7	104,2	101,1	100,4	101,2
$\bar{x}$	106,8	101,0	102,0	98,0	99,3
Recovery (%)	106,8	101,0	102,0	98,0	99,3
Mean Conc.			101,4		
Mean recovery (%)			101,4		
S_r			2,22		
S_{run}			3,14		
S_i			3,84		
RSD (%)			3,79		
HL			**180**		
Replicated 1	177,0	179,7	179,8	180,6	180,5
Replicated 2	177,4	179,0	178,7	181,2	180,4
Replicated 3	176,8	180,1	179,0	180,7	180,1
$\bar{x}$	177,1	179,6	179,1	180,8	180,3
Recovery (%)	98,4	99,8	99,5	100,5	100,2
Mean Conc.			179,4		
Mean recovery (%)			99,7		
S_r			0,42		
S_{run}			1,43		
S_i			1,49		
RSD (%)			0,83		

Table S14. Statistical results of intermediate precision for UR-144 by MEPS

Days	Day 1	Day 2	Day 3	Day 4	Day 5
R^2	0,9980	0,9979	0,9998	0,9975	0,9997
Slope	0,0859	0,0836	0,0846	0,0805	0,0808
Y_0	-0,7682	-1,1019	-0,8931	-0,5308	-0,6311
LL			**40**		
Replicated 1	37,6	42,0	40,7	42,0	41,0
Replicated 2	38,2	42,2	40,4	42,4	40,6
Replicated 3	37,9	42,1	40,8	42,5	40,9
$\bar{x}$	37,9	42,1	40,7	42,3	40,8
Recovery (%)	94,8	105,3	101,6	105,8	102,1
Mean Conc.			40,8		
Mean recovery (%)			101,9		
S_r			0,22		
S_{run}			1,75		
S_i			1,76		
RSD (%)			4,32		
ML			**100**		
Replicated 1	103,4	95,7	98,9	93,0	100,5
Replicated 2	103,9	96,6	99,0	98,3	93,7
Replicated 3	103,6	96,6	98,6	96,7	101,5
$\bar{x}$	103,6	96,3	98,8	96,0	98,6
Recovery (%)	103,6	96,3	98,8	96,0	98,6
Mean Conc.			98,7		
Mean recovery (%)			98,7		
S_r			2,27		
S_{run}			2,77		
S_i			3,58		
RSD (%)			3,63		
HL			**180**		
Replicated 1	177,5	181,8	180,8	183,7	179,6
Replicated 2	178,0	182,7	180,6	180,3	182,8
Replicated 3	179,8	180,3	180,1	181,2	179,5
$\bar{x}$	178,4	181,6	180,5	181,7	180,6
Recovery (%)	99,1	100,9	100,3	101,0	100,3
Mean Conc.			180,6		
Mean recovery (%)			100,3		
S_r			1,38		
S_{run}			1,04		
S_i			1,73		
RSD (%)			0,96		

Table S15. Statistical results of intermediate precision for JWH-210 by MEPS

Days	Day 1	Day 2	Day 3	Day 4	Day 5
R^2	0,9999	0,9999	0,9992	0,9994	0,9998
Slope	0,0738	0,0723	0,0724	0,0710	0,0703
Y_0	0,2136	0,1589	0,1856	0,2201	0,3153
LL			**40**		
Replicated 1	39,7	40,8	42,7	39,2	39,2
Replicated 2	39,5	40,5	40,6	38,9	39,1
Replicated 3	39,1	39,9	40,5	38,7	39,5
$\bar{x}$	39,4	40,4	41,3	38,9	39,3
Recovery (%)	98,6	101,0	103,2	97,3	98,2
Mean Conc.			39,9		
Mean recovery (%)			99,7		
S_r			0,62		
S_{run}			0,89		
S_i			1,08		
RSD (%)			2,72		
ML			**100**		
Replicated 1	101,8	94,1	96,1	101,9	99,2
Replicated 2	100,7	101,2	97,6	103,7	102,8
Replicated 3	100,4	102,6	99,6	100,1	101,8
$\bar{x}$	101,0	99,3	97,8	101,9	101,3
Recovery (%)	101,0	99,3	97,8	101,9	101,3
Mean Conc.			100,2		
Mean recovery (%)			100,2		
S_r			2,49		
S_{run}			0,87		
S_i			2,63		
RSD (%)			2,63		
HL			**180**		
Replicated 1	178,2	180,5	183,4	179,4	179,6
Replicated 2	180,5	180,3	179,8	179,8	178,8
Replicated 3	180,1	179,9	179,7	178,4	180,0
$\bar{x}$	179,6	180,2	181,0	179,2	179,5
Recovery (%)	99,8	100,1	100,5	99,5	99,7
Mean Conc.			179,9		
Mean recovery (%)			99,9		
S_r			1,18		
S_{run}			0,21		
S_i			1,20		
RSD (%)			0,67		

Table S16. Statistical results of intermediate precision for APINACA by MEPS

Days	Day 1	Day 2	Day 3	Day 4	Day 5
R^2	0,9972	0,9997	1,0000	0,9990	0,9989
Slope	0,1243	0,1229	0,1151	0,1220	0,1190
Y_0	-2,2881	-2,0594	-1,4574	-2,0765	-1,7147
LL			**40**		
Replicated 1	43,1	40,8	39,7	41,7	41,4
Replicated 2	42,3	41,1	39,8	41,3	41,5
Replicated 3	42,1	40,6	39,8	41,3	41,6
$\bar{x}$	42,5	40,8	39,8	41,4	41,5
Recovery (%)	106,2	102,1	99,4	103,6	103,8
Mean Conc.			41,2		
Mean recovery (%)			103,0		
S_r			0,29		
S_{run}			0,99		
S_i			1,03		
RSD (%)			2,50		
ML			**100**		
Replicated 1	95,8	98,5	100,3	98,6	97,5
Replicated 2	96,1	98,3	100,4	97,1	96,3
Replicated 3	95,3	98,8	100,6	96,7	98,3
$\bar{x}$	95,7	98,5	100,4	97,5	97,4
Recovery (%)	95,7	98,5	100,4	97,5	97,4
Mean Conc.			97,9		
Mean recovery (%)			97,9		
S_r			0,66		
S_{run}			1,69		
S_i			1,81		
RSD (%)			1,85		
HL			**180**		
Replicated 1	181,3	180,7	180,6	180,5	181,2
Replicated 2	181,7	180,3	179,4	181,5	180,7
Replicated 3	182,6	180,9	179,5	181,2	181,5
$\bar{x}$	181,8	180,6	179,8	181,1	181,1
Recovery (%)	101,0	100,4	99,9	100,6	100,6
Mean Conc.			180,9		
Mean recovery (%)			100,5		
S_r			0,53		
S_{run}			0,67		
S_i			0,86		
RSD (%)			0,47		

Table S17. Accuracy statistical results for MAM-2201 by MEPS

Days	Day 1	Day 2	Day 3	Day 4	Day 5
Equation	y = 0.1380x - 1.3315	y = 0.1391x - 0.9504	y = 0.1374x - 0.6922	y = 0.1409x - 1.3028	y = 0.1418x - 1.7156
Low Conc. (ng/mL)			40		
Mean concentration	41,1	36,3	37,3	41,9	42,7
Recovery (%)	102,8	90,8	93,3	104,7	106,7
Mean			39,9		
mean recovery (%)			99,6		
SD			7,11		
RSD (%)			7,14		
N (days)			5		
T_{exp}			0,11		
T_{crit}			2,78		
$U_{\%R}$			3,18		
U_R			0,03		
Bias (%)			-0,35		
Medium Conc. (ng/mL)			100		
Mean concentration	98,0	106,4	104,7	96,7	95,3
Recovery (%)	98,0	106,4	104,7	96,7	95,3
Mean			100,2		
mean recovery (%)			100,2		
SD			4,98		
RSD (%)			4,97		
N (days)			5		
T_{exp}			0,11		
T_{crit}			2,78		
$U_{\%R}$			2,23		
U_R			0,02		
Bias (%)			0,25		
High Conc. (ng/mL)			180		
Mean concentration	180,8	177,3	178,0	181,4	182,0
Recovery (%)	100,5	98,5	98,9	100,8	101,1
Mean			179,9		
mean recovery (%)			99,9		
SD			1,19		
RSD (%)			1,19		
N (days)			5		
T_{exp}			0,11		
T_{crit}			2,78		
$U_{\%R}$			0,53		
U_R			0,01		
Bias (%)			-0,06		

Table S18. Accuracy statistical results for JWH-073 by MEPS

Days	Day 1	Day 2	Day 3	Day 4	Day 5
Equation	y = 0.0787x - 0.3816	y = 0.0801x - 0.7410	y = 0.0768x - 0.5494	y = 0.0757x - 0.5047	y = 0.0763x - 0.4203
Low Conc. (ng/mL)			**40**		
Mean concentration	37,9	42,2	41,6	39,3	40,3
Recovery (%)	94,8	105,6	103,9	98,3	100,7
Mean			40,3		
mean recovery (%)			100,7		
SD			4,32		
RSD (%)			4,30		
N (days)			5		
T_{exp}			0,35		
T_{crit}			2,78		
$U_{\%R}$			1,93		
U_R			0,02		
Bias (%)			0,67		
Medium Conc. (ng/mL)			**100**		
Mean concentration	103,6	96,1	97,2	101,2	99,5
Recovery (%)	103,6	96,1	97,2	101,2	99,5
Mean			99,5		
mean recovery (%)			99,5		
SD			3,03		
RSD (%)			3,04		
N (days)			5		
T_{exp}			0,35		
T_{crit}			2,78		
$U_{\%R}$			1,35		
U_R			0,01		
Bias (%)			-0,47		
High Conc. (ng/mL)			**180**		
Mean concentration	178,4	181,7	181,2	179,5	180,2
Recovery (%)	103,6	96,1	97,2	101,2	99,5
Mean			180,2		
mean recovery (%)			99,5		
SD			3,03		
RSD (%)			3,04		
N (days)			5		
T_{exp}			0,35		
T_{crit}			2,78		
$U_{\%R}$			1,35		
U_R			0,01		
Bias (%)			0,11		

Table S19. Accuracy statistical results for XLR-11 by MEPS

Days	Day 1	Day 2	Day 3	Day 4	Day 5
Equation	y = 0.0773x - 0.4434	y = 0.0767x - 0.6199	y = 0.0777x - 0.7788	y = 0.0805x - 0.7850	y = 0.0775x - 0.9624
Low Conc. (ng/mL)			**40**		
Mean concentration	41,4	41,2	43,7	39,8	42,8
Recovery (%)	103,5	103,0	109,3	99,5	107,1
Mean			41,8		
mean recovery (%)			104,5		
SD			3,84		
RSD (%)			3,67		
N (days)			5		
T_{exp}			2,61		
T_{crit}			2,78		
$U_{\%R}$			1,72		
U_R			0,02		
***Bias* (%)**			4,47		
Medium Conc. (ng/mL)			**100**		
Mean concentration	97,6	97,9	93,5	100,4	95,0
Recovery (%)	97,6	97,9	93,5	100,4	95,0
Mean			96,9		
mean recovery (%)			96,9		
SD			2,69		
RSD (%)			2,77		
N (days)			5		
T_{exp}			2,61		
T_{crit}			2,78		
$U_{\%R}$			1,20		
U_R			0,01		
***Bias* (%)**			-3,13		
High Conc. (ng/mL)			**180**		
Mean concentration	181,0	180,9	182,8	179,8	182,1
Recovery (%)	100,6	100,5	101,6	99,9	101,2
Mean			181,3		
mean recovery (%)			100,7		
SD			0,64		
RSD (%)			0,63		
N (days)			5		
T_{exp}			2,61		
T_{crit}			2,78		
$U_{\%R}$			0,29		
U_R			0,003		
***Bias* (%)**			0,75		

Table S20. Accuracy statistical results for JWH-018 by MEPS

Days	Day 1	Day 2	Day 3	Day 4	Day 5
Equation	y = 0.1413x - 2.3645	y = 0.1387x - 2.6007	y = 0.1432x - 2.9578	y = 0.1408x - 3.0770	y = 0.1340x - 2.8762
Low Conc. (ng/mL)			40		
Mean concentration	38,0	40,2	39,9	41,1	38,7
Recovery (%)	95,0	100,6	99,7	102,8	96,6
Mean			39,6		
mean recovery (%)			98,9		
SD			3,13		
RSD (%)			3,16		
N (days)			5		
T_{exp}			0,75		
T_{crit}			2,78		
$U_{\%R}$			1,40		
U_R			0,01		
Bias (%)			-1,06		
Medium Conc. (ng/mL)			100		
Mean concentration	103,5	99,6	100,2	98,0	102,4
Recovery (%)	103,5	99,6	100,2	98,0	102,4
Mean			100,7		
mean recovery (%)			100,7		
SD			2,19		
RSD (%)			2,17		
N (days)			5		
T_{exp}			0,75		
T_{crit}			2,78		
$U_{\%R}$			0,98		
U_R			0,01		
Bias (%)			0,74		
High Conc. (ng/mL)			180		
Mean concentration	178,5	180,2	179,9	180,9	179,0
Recovery (%)	99,2	100,1	99,9	100,5	99,4
Mean			179,7		
mean recovery (%)			99,8		
SD			0,52		
RSD (%)			0,52		
N (days)			5		
T_{exp}			0,75		
T_{crit}			2,78		
$U_{\%R}$			0,23		
U_R			0,002		
Bias (%)			-0,18		

Table S21. Accuracy statistical results for JWH-122 by MEPS

Days	Day 1	Day 2	Day 3	Day 4	Day 5
Equation	y = 0.0563x + 0.1141	y = 0.0551x + 0.0339	y = 0.0578x + 0.0059	y = 0.0579x - 0.2191	y = 0.0556x - 0.0519
Low Conc. (ng/mL)			**40**		
Mean concentration	36,1	39,4	38,9	41,1	40,4
Recovery (%)	90,3	98,6	97,2	102,8	101,1
Mean			39,2		
mean recovery (%)			98,0		
SD			4,84		
RSD (%)			4,94		
N (days)			5		
T_{exp}			0,93		
T_{crit}			2,78		
$U_{\%R}$			2,17		
U_R			0,02		
***Bias* (%)**			-2,02		
Medium Conc. (ng/mL)			**100**		
Mean concentration	106,8	101,0	102,0	98,0	99,3
Recovery (%)	106,8	101,0	102,0	98,0	99,3
Mean			101,4		
mean recovery (%)			101,4		
SD			3,39		
RSD (%)			3,34		
N (days)			5		
T_{exp}			0,93		
T_{crit}			2,78		
$U_{\%R}$			1,52		
U_R			0,02		
***Bias* (%)**			1,41		
High Conc. (ng/mL)			**180**		
Mean concentration	177,1	179,6	179,1	180,8	180,3
Recovery (%)	98,4	99,8	99,5	100,5	100,2
Mean			179,4		
mean recovery (%)			99,7		
SD			0,81		
RSD (%)			0,81		
N (days)			5		
T_{exp}			0,93		
T_{crit}			2,78		
$U_{\%R}$			0,36		
U_R			0,004		
***Bias* (%)**			-0,34		

Table S22. Accuracy statistical results for UR-144 by MEPS

Days	Day 1	Day 2	Day 3	Day 4	Day 5
Equation	y = 0.0859x - 0.7682	y = 0.0836x - 1.1019	y = 0.0846x - 0.8931	y = 0.0805x - 0.5308	y = 0.0808x - 0.6311
Low Conc. (ng/mL)			**40**		
Mean concentration	37,9	42,1	40,7	42,3	40,8
Recovery (%)	94,8	105,3	101,6	105,8	102,1
Mean			40,8		
mean recovery (%)			101,9		
SD			4,38		
RSD (%)			4,30		
N (days)			5		
T_{exp}			0,98		
T_{crit}			2,78		
$U_{\%R}$			1,96		
U_R			0,02		
***Bias* (%)**			1,92		
Medium Conc. (ng/mL)			**100**		
Mean concentration	103,6	96,3	98,8	96,0	98,6
Recovery (%)	103,6	96,3	98,8	96,0	98,6
Mean			98,7		
mean recovery (%)			98,7		
SD			3,07		
RSD (%)			3,11		
N (days)			5		
T_{exp}			0,98		
T_{crit}			2,78		
$U_{\%R}$			1,37		
U_R			0,01		
***Bias* (%)**			-1,34		
High Conc. (ng/mL)			**180**		
Mean concentration	178,4	181,6	180,5	181,7	180,6
Recovery (%)	99,1	100,9	100,3	101,0	100,3
Mean			180,6		
mean recovery (%)			100,3		
SD			0,73		
RSD (%)			0,73		
N (days)			5		
T_{exp}			0,98		
T_{crit}			2,78		
$U_{\%R}$			0,33		
U_R			0,003		
***Bias* (%)**			0,32		

Table S23. Accuracy statistical results for JWH-210 by MEPS

Days	Day 1	Day 2	Day 3	Day 4	Day 5
Equation	y = 0.0738x + 0.2136	y = 0.0723x + 0.1589	y = 0.0724x + 0.1856	y = 0.0710x + 0.2201	y = 0.0703x + 0.3153
Low Conc. (ng/mL)			**40**		
Mean concentration	39,4	40,4	41,3	38,9	39,3
Recovery (%)	98,6	101,0	103,2	97,3	98,2
Mean			39,9		
mean recovery (%)			99,7		
SD			2,40		
RSD (%)			2,41		
N (days)			5		
T_{exp}			0,32		
T_{crit}			2,78		
$U_{\%R}$			1,07		
U_R			0,01		
***Bias* (%)**			-0,35		
Medium Conc. (ng/mL)			**100**		
Mean concentration	100,0	101,0	99,3	97,8	101,9
Recovery (%)	% rec 100	101,0	99,3	97,8	101,9
Mean			100,0		
mean recovery (%)			100,0		
SD			1,83		
RSD (%)			1,83		
N (days)			5		
T_{exp}			0,01		
T_{crit}			2,78		
$U_{\%R}$			0,82		
U_R			0,01		
***Bias* (%)**			-0,01		
High Conc. (ng/mL)			**180**		
Mean concentration	180,0	179,6	180,3	181,0	179,2
Recovery (%)	% rec 180	99,8	100,2	100,5	99,5
Mean			180,0		
mean recovery (%)			100,0		
SD			0,43		
RSD (%)			0,43		
N (days)			5		
T_{exp}			0,01		
T_{crit}			2,78		
$U_{\%R}$			0,19		
U_R			0,002		
***Bias* (%)**			0,002		

Table S24. Accuracy statistical results for APINACA by MEPS

Days	Day 1	Day 2	Day 3	Day 4	Day 5
Equation	y = 0.1243x - 2.2881	y = 0.1229x - 2.0594	y = 0.1151x - 1.4574	y = 0.1220x - 2.0765	y = 0.1190x - 1.7147
Low Conc. (ng/mL)			**40**		
Mean concentration	42,4	40,9	42,6	38,6	41,5
Recovery (%)	106,1	102,1	106,4	96,4	103,8
Mean			41,2		
mean recovery (%)			103,0		
SD			4,06		
RSD (%)			3,95		
N (days)			5		
T_{exp}			1,64		
T_{crit}			2,78		
$U_{\%R}$			1,82		
U_R			0,02		
***Bias* (%)**			2,98		
Medium Conc. (ng/mL)			**100**		
Mean concentration	95,7	98,5	100,4	98,0	97,4
Recovery (%)	95,7	98,5	100,4	98,0	97,4
Mean			98,0		
mean recovery (%)			98,0		
SD			1,71		
RSD (%)			1,74		
N (days)			5		
T_{exp}			2,63		
T_{crit}			2,78		
$U_{\%R}$			0,76		
U_R			0,01		
***Bias* (%)**			-2,01		
High Conc. (ng/mL)			**180**		
Mean concentration	181,8	180,6	179,8	186,6	181,1
Recovery (%)	101,0	100,4	99,9	103,7	100,6
Mean			182,0		
mean recovery (%)			101,1		
SD			1,49		
RSD (%)			1,48		
N (days)			5		
T_{exp}			1,68		
T_{crit}			2,78		
$U_{\%R}$			0,67		
U_R			0,007		
***Bias* (%)**			1,12		

Table S25. Linearity statistical results of MAM-2201 by µSPEed

Concentration (ng/mL)	Relative area
40	2.5
60	5.3
80	7.6
100	10.5
120	14.5
140	16.9
160	19.6
180	23.2

SUMMARY OUTPUT

Regression Statistics	
Multiple R	0,998616959
R Square	0,99723583
Adjusted R Square	0,996775135
Standard Error	0,411163863
Observations	8

ANOVA

	df	*SS*	*MS*	*F*	*Significance F*
Regression	1	365,9437091	365,9437	2164,633674	6,60686E-09
Residual	6	1,014334333	0,169056		
Total	7	366,9580434			

	Coefficients	*Standard Error*	*t Stat*	*P value*	*Lower 95%*	*Upper 95%*
Intercept	-3,703373285	0,378011027	-9,797	6,50978E-05	-4,628332947	-2,778413623
40	0,147588494	0,003172198	46,52562	6,60686E-09	0,139826405	0,155350583

RESIDUAL OUTPUT

Observation	*Predicted*	*Residuals*
1	2,200166485	0,338443432
2	5,151936371	0,179860632
3	8,103706256	-0,48677071
4	11,05547614	-0,507715407
5	14,00724603	0,446117687
6	16,95901591	-0,029669698
7	19,9107858	-0,262566302
8	22,86255568	0,322300366

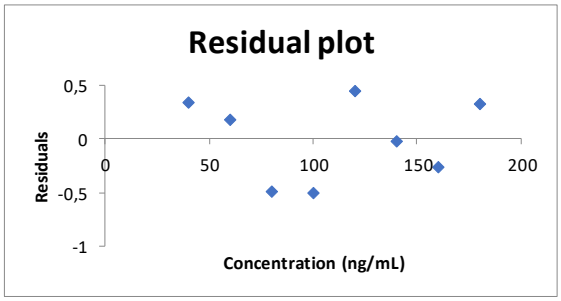

Table S26. Linearity statistical results of JWH-073 by µSPEed

Concentration (ng/mL)	Relative area
40	1.8
60	3.4
80	5.4
100	7.1
120	9.3
140	11.2
160	13.5
180	15.3

SUMMARY OUTPUT

Regression Statistics	
Multiple R	0,999063565
R Square	0,998128008
Adjusted R Square	0,997816009
Standard Error	0,224353577
Observations	8

ANOVA

	df	*SS*	*MS*	*F*	*Significance F*
Regression	1	161,0272607	161,0273	3199,141208	2,05148E-09
Residual	6	0,302007164	0,050335		
Total	7	161,3292678			

	Coefficients	*Standard Error*	*t Stat*	*P value*	*Lower 95%*	*Upper 95%*
Intercept	-2,374299319	0,206263569	-11,511	2,58292E-05	-2,879	-1,870
40	0,097902788	0,001730925	56,56095	2,05148E-09	0,093667367	0,10213821

RESIDUAL OUTPUT

Observation	*Predicted*	*Residuals*
1	1,54181222	0,303530644
2	3,49986799	-0,050603949
3	5,45792376	-0,051055471
4	7,415979529	-0,339296511
5	9,374035299	-0,055817435
6	11,33209107	-0,140873938
7	13,29014684	0,240572767
8	15,24820261	0,093543893

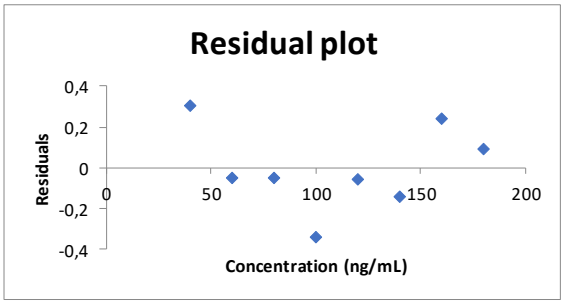

Table S27. Linearity statistical results of XLR-11 by µSPEed

Concentration (ng/mL)	Relative area
40	1.4
60	3.0
80	4.8
100	6.8
120	8.5
140	10.2
160	12.1
180	13.8

SUMMARY OUTPUT

Regression Statistics	
Multiple R	0,999679145
R Square	0,999358393
Adjusted R Square	0,999251458
Standard Error	0,120169588
Observations	8

ANOVA

	df	*SS*	*MS*	*F*	*Significance F*
Regression	1	134,9560426	134,956	9345,513924	8,25586E-11
Residual	6	0,08664438	0,014441		
Total	7	135,042687			

	Coefficients	*Standard Error*	*t Stat*	*P value*	*Lower 95%*	*Upper 95%*
Intercept	-2,287724489	0,110480112	-20,7071	8,25546E-07	-2,558	-2,017
40	0,08962755	0,000927129	96,6722	8,25586E-11	0,087358949	0,091896152

RESIDUAL OUTPUT

Observation	*Predicted*	*Residuals*
1	1,297377523	0,128578046
2	3,089928529	-0,135194427
3	4,882479535	-0,130912366
4	6,675030541	0,146518443
5	8,467581546	-0,005771243
6	10,26013255	-0,047892628
7	12,05268356	0,092707283
8	13,84523456	-0,048033108

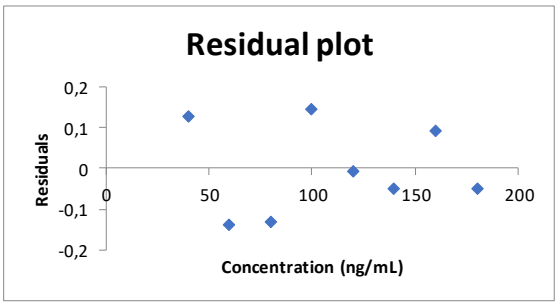

Table S28. Linearity statistical results of JWH-018 by µSPEed

Concentration (ng/mL)	Relative area
40	2.6
60	4.6
80	7.8
100	10.4
120	12.8
140	15.0
160	17.9
180	20.4

SUMMARY OUTPUT

Regression Statistics	
Multiple R	0,999373135
R Square	0,998746664
Adjusted R Square	0,998537774
Standard Error	0,239951436
Observations	8

ANOVA

	df	*SS*	*MS*	*F*	*Significance F*
Regression	1	275,2870096	275,287	4781,223143	6,15541E-10
Residual	6	0,345460149	0,057577		
Total	7	275,6324697			

	Coefficients	*Standard Error*	*t Stat*	*P value*	*Lower 95%*	*Upper 95%*
Intercept	-2,629518979	0,220603747	-11,9196	2,11127E-05	-3,169	-2,090
40	0,128008326	0,001851266	69,14639	6,15541E-10	0,123478442	0,13253821

RESIDUAL OUTPUT

Observation	*Predicted*	*Residuals*
1	2,490814061	0,121565861
2	5,050980581	-0,404568692
3	7,611147101	0,167406298
4	10,17131362	0,263703306
5	12,73148014	0,026618173
6	15,29164666	-0,244047623
7	17,85181318	0,09284714
8	20,4119797	-0,023524462

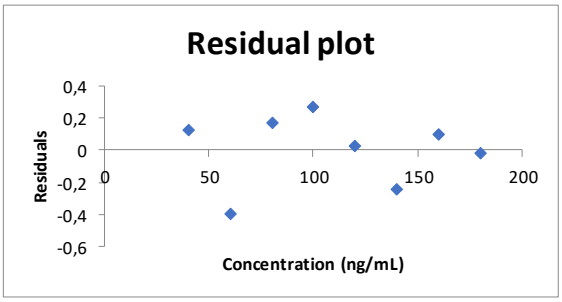

Table S29. Linearity statistical results of JWH-122 by µSPEed

Concentration (ng/mL)	Relative area
40	1.0
60	1.8
80	3.2
100	4.4
120	5.5
140	6.8
160	8.0
180	8.8

SUMMARY OUTPUT

Regression Statistics	
Multiple R	0,998333432
R Square	0,996669642
Adjusted R Square	0,996114583
Standard Error	0,176826425
Observations	8

ANOVA

	df	*SS*	*MS*	*F*	*Significance F*
Regression	1	56,144332	56,14433	1795,608222	1,15576E-08
Residual	6	0,187605508	0,031268		
Total	7	56,33193751			

	Coefficients	*Standard Error*	*t Stat*	*P value*	*Lower 95%*	*Upper 95%*
Intercept	-1,416371372	0,162568612	-8,71245	0,000126372	-1,814	-1,019
40	0,057809381	0,001364245	42,37462	1,15576E-08	0,054471192	0,061147569

RESIDUAL OUTPUT

Observation	*Predicted*	*Residuals*
1	0,896003865	0,1412036
2	2,052191484	-0,277987633
3	3,208379103	0,041215978
4	4,364566721	-0,000820474
5	5,52075434	0,017086116
6	6,676941959	0,133178612
7	7,833129577	0,159087029
8	8,989317196	-0,212963228

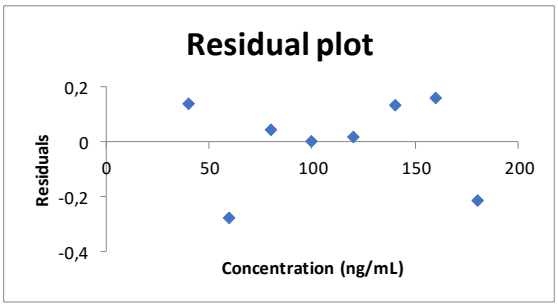

Table S30. Linearity statistical results of UR-144 by µSPEed

Concentration (ng/mL)	Relative area
40	1.1
60	2.3
80	3.7
100	5.6
120	7.1
140	8.3
160	9.7
180	11.7

SUMMARY OUTPUT

Regression Statistics	
Multiple R	0,998273826
R Square	0,996550632
Adjusted R Square	0,995975737
Standard Error	0,235494799
Observations	8

ANOVA

	df	*SS*	*MS*	*F*	*Significance F*
Regression	1	96,13327451	96,13327	1733,449114	1,2842E-08
Residual	6	0,332746801	0,055458		
Total	7	96,46602131			

	Coefficients	*Standard Error*	*t Stat*	*P value*	*Lower 95%*	*Upper 95%*
Intercept	-2,133465919	0,216506456	-9,85405	6,29812E-05	-2,663	-1,604
40	0,075645348	0,001816882	41,63471	1,2842E-08	0,071199599	0,080091098

RESIDUAL OUTPUT

Observation	*Predicted*	*Residuals*
1	0,892348014	0,157922432
2	2,40525498	-0,143550065
3	3,918161946	-0,198631336
4	5,431068912	0,175347267
5	6,943975878	0,20278338
6	8,456882844	-0,121531027
7	9,969789811	-0,31767711
8	11,48269678	0,245336458

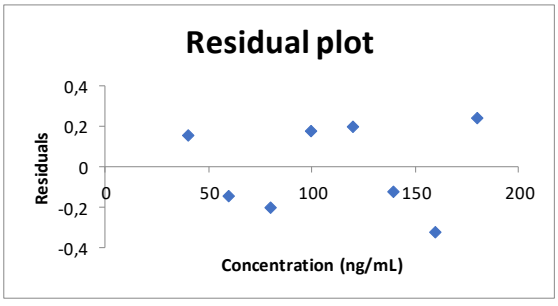

Table S31. Linearity statistical results of JWH-210 by µSPEed

Concentration (ng/mL)	Relative area
40	1.1
60	2.5
80	3.7
100	5.3
120	6.7
140	8.2
160	9.4
180	11.3

SUMMARY OUTPUT

Regression Statistics	
Multiple R	0,99907979
R Square	0,998160427
Adjusted R Square	0,997853831
Standard Error	0,162612555
Observations	8

ANOVA

	df	*SS*	*MS*	*F*	*Significance F*
Regression	1	86,08801483	86,08801	3255,626281	1,94671E-09
Residual	6	0,158657058	0,026443		
Total	7	86,24667189			

	Coefficients	*Standard Error*	*t Stat*	*P value*	*Lower 95%*	*Upper 95%*
Intercept	-1,858407358	0,14950083	-12,4307	1,65528E-05	-2,224	-1,493
40	0,071584123	0,001254583	57,0581	1,94671E-09	0,068514268	0,074653977

RESIDUAL OUTPUT

Observation	*Predicted*	*Residuals*
1	1,004957543	0,106512498
2	2,436639994	0,105773497
3	3,868322444	-0,16058748
4	5,300004894	-0,046874606
5	6,731687345	-0,058236337
6	8,163369795	-0,010180812
7	9,595052246	-0,194722006
8	11,0267347	0,258315247

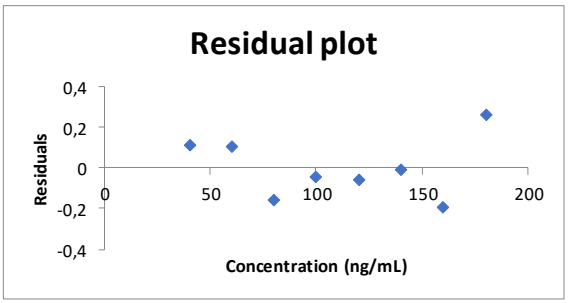

Table S32. Linearity statistical results of APINACA by µSPEed

Concentration (ng/mL)	Relative area
40	1.4
60	2.7
80	4.8
100	6.1
120	7.3
140	9.0
160	10.7
180	12.0

SUMMARY OUTPUT

Regression Statistics	
Multiple R	0,9984315
R Square	0,996865459
Adjusted R Square	0,996343036
Standard Error	0,226221633
Observations	8

ANOVA

	df	*SS*	*MS*	*F*	*Significance F*
Regression	1	97,65223126	97,65223	1908,156123	9,63569E-09
Residual	6	0,307057363	0,051176		
Total	7	97,95928862			

	Coefficients	*Standard Error*	*t Stat*	*P value*	*Lower 95%*	*Upper 95%*
Intercept	-1,628503141	0,207981001	-7,83006	0,000229166	-2,137	-1,120
40	0,076240624	0,001745338	43,68245	9,63569E-09	0,071969937	0,080511312

RESIDUAL OUTPUT

Observation	*Predicted*	*Residuals*
1	1,421121836	-0,021222911
2	2,945934325	-0,257522959
3	4,470746813	0,354614291
4	5,995559302	0,133169727
5	7,52037179	-0,240144601
6	9,045184279	-0,028265565
7	10,56999677	0,164912699
8	12,09480926	-0,105540681

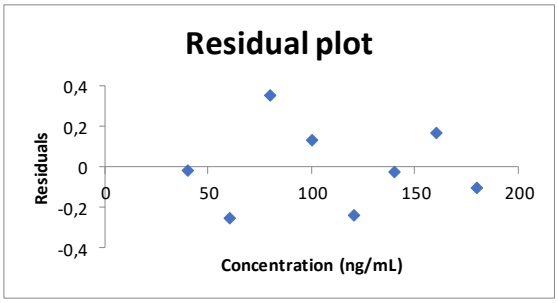

Table S33. Statistical results of intermediate precision for MAM-2201 by µSPEed

Days	Day 1	Day 2	Day 3	Day 4	Day 5
R^2	0,9994	0,9998	0,9999	0,9939	0,9974
Slope	0,1393	0,1538	0,1417	0,1400	0,1510
Y_0	-2,9853	-3,8280	-3,0960	-2,5623	-3,2489
LL	**40**				
Replicated 1	37,9	40,7	39,9	35,6	38,3
Replicated 2	40,9	40,5	41,5	36,4	37,3
Replicated 3	38,0	41,0	39,7	37,0	37,4
$\bar{x}$	38,9	40,7	40,4	36,4	37,6
Recovery (%)	97,2	101,8	100,9	90,9	94,1
Mean Conc.	38,8				
Mean recovery (%)	97,0				
S_r	0,97				
S_{run}	1,75				
S_i	2,00				
RSD (%)	5,15				
ML	**100**				
Replicated 1	102,7	99,6	100,6	105,1	102,3
Replicated 2	103,8	102,5	100,1	104,0	104,6
Replicated 3	99,6	94,4	97,6	110,1	105,3
$\bar{x}$	102,0	98,8	99,4	106,4	104,1
Recovery (%)	102,0	98,8	99,4	106,4	104,1
Mean Conc.	102,1				
Mean recovery (%)	102,1				
S_r	2,74				
S_{run}	2,74				
S_i	3,88				
RSD (%)	3,80				
HL	**180**				
Replicated 1	178,2	181,2	180,5	178,0	175,2
Replicated 2	177,5	179,1	182,2	175,1	181,3
Replicated 3	182,0	181,2	178,3	178,9	178,2
$\bar{x}$	179,2	180,5	180,3	177,3	178,2
Recovery (%)	99,6	100,3	100,2	98,5	99,0
Mean Conc.	179,1				
Mean recovery (%)	99,5				
S_r	2,22				
S_{run}	0,50				
S_i	2,27				
RSD (%)	1,27				

Table S34. Statistical results of intermediate precision for JWH-073 by µSPEed

Days	Day 1	Day 2	Day 3	Day 4	Day 5
R^2	0,9995	0,9987	1,0000	0,9984	0,9992
Slope	0,0995	0,0978	0,0962	0,1035	0,1115
Y_0	-2,2028	-1,9892	-2,1792	-2,6939	-3,0908
LL	**40**				
Replicated 1	40,5	39,0	41,7	41,9	40,4
Replicated 2	41,3	38,2	39,1	41,8	42,1
Replicated 3	41,2	37,6	40,2	41,9	41,3
$\bar{x}$	41,0	38,3	40,3	41,9	41,3
Recovery (%)	102,5	95,7	100,8	104,7	103,2
Mean Conc.	40,6				
Mean recovery (%)	101,4				
S_r	0,79				
S_{run}	1,31				
S_i	1,53				
RSD (%)	3,76				
ML	**100**				
Replicated 1	96,1	103,0	99,2	98,0	97,9
Replicated 2	101,4	103,3	97,8	94,9	96,6
Replicated 3	97,1	102,4	101,4	97,4	98,7
$\bar{x}$	98,2	102,9	99,5	96,8	97,7
Recovery (%)	98,2	102,9	99,5	96,8	97,7
Mean Conc.	99,0				
Mean recovery (%)	99,0				
S_r	1,75				
S_{run}	2,14				
S_i	2,77				
RSD (%)	2,80				
HL	**180**				
Replicated 1	181,7	179,6	180,0	182,1	181,0
Replicated 2	179,0	177,9	182,0	182,1	183,8
Replicated 3	181,7	178,8	178,7	179,9	178,3
$\bar{x}$	180,8	178,8	180,2	181,4	181,0
Recovery (%)	100,4	99,3	100,1	100,8	100,6
Mean Conc.	180,4				
Mean recovery (%)	100,2				
S_r	1,74				
S_{run}	0,09				
S_i	1,74				
RSD (%)	0,96				

Table S35. Statistical results of intermediate precision for XLR-11 by µSPEed

Days	Day 1	Day 2	Day 3	Day 4	Day 5
R^2	0,9984	1,0000	0,9998	0,9971	0,9998
Slope	0,0857	0,0930	0,0894	0,0894	0,0903
Y_0	-1,8646	-2,2850	-2,1384	-1,9363	-2,3047
LL	**40**				
Replicated 1	37,4	39,1	38,1	38,5	40,5
Replicated 2	38,1	39,6	40,2	37,4	40,6
Replicated 3	39,1	41,4	39,8	36,7	40,8
$\bar{x}$	38,2	40,0	39,4	37,5	40,6
Recovery (%)	95,5	100,0	98,4	93,8	101,6
Mean Conc.	39,1				
Mean recovery (%)	97,9				
S_r	0,92				
S_{run}	1,15				
S_i	1,48				
RSD (%)	3,78				
ML	**100**				
Replicated 1	101,5	101,7	102,0	106,6	101,1
Replicated 2	103,1	99,6	99,9	103,6	97,7
Replicated 3	105,0	98,4	101,4	103,0	98,3
$\bar{x}$	103,2	99,9	101,1	104,4	99,0
Recovery (%)	103,2	99,9	101,1	104,4	99,0
Mean Conc.	101,5				
Mean recovery (%)	101,5				
S_r	1,69				
S_{run}	2,01				
S_i	2,63				
RSD (%)	2,59				
HL	**180**				
Replicated 1	179,0	182,0	181,0	180,4	180,3
Replicated 2	177,9	178,6	179,4	176,7	182,1
Replicated 3	178,9	179,3	178,2	177,2	178,7
$\bar{x}$	178,6	180,0	179,5	178,1	180,4
Recovery (%)	99,2	100,0	99,7	98,9	100,2
Mean Conc.	179,3				
Mean recovery (%)	99,6				
S_r	1,58				
S_{run}	0,25				
S_i	1,60				
RSD (%)	0,89				

Table S36. Statistical results of intermediate precision for JWH-018 by µSPEed

Days	Day 1	Day 2	Day 3	Day 4	Day 5
R^2	1,0000	0,9986	0,9981	0,9983	0,9972
Slope	0,1420	0,1354	0,1448	0,1415	0,1315
Y_0	-2,7550	-2,4696	-3,3777	-2,9491	-2,7500
LL	**40**				
Replicated 1	40,2	39,2	43,5	40,9	41,4
Replicated 2	41,1	38,3	41,7	41,9	42,4
Replicated 3	39,1	37,5	40,9	42,8	43,6
$\bar{x}$	40,1	38,3	42,0	41,9	42,5
Recovery (%)	100,3	95,8	105,1	104,7	106,2
Mean Conc.	41,0				
Mean recovery (%)	102,4				
S_r	1,07				
S_{run}	1,61				
S_i	1,93				
RSD (%)	4,71				
ML	**100**				
Replicated 1	99,8	101,0	95,2	96,2	96,8
Replicated 2	98,6	103,8	96,3	96,3	95,7
Replicated 3	100,9	104,5	98,2	97,2	94,7
$\bar{x}$	99,8	103,1	96,5	96,6	95,7
Recovery (%)	99,8	103,1	96,5	96,6	95,7
Mean Conc.	98,3				
Mean recovery (%)	98,3				
S_r	1,31				
S_{run}	2,99				
S_i	3,27				
RSD (%)	3,32				
HL	**180**				
Replicated 1	180,6	178,4	181,9	179,5	179,7
Replicated 2	179,9	177,0	181,4	183,2	186,2
Replicated 3	179,6	180,7	181,2	181,6	179,6
$\bar{x}$	180,1	178,7	181,5	181,4	181,8
Recovery (%)	100,0	99,3	100,8	100,8	101,0
Mean Conc.	180,7				
Mean recovery (%)	100,4				
S_r	2,08				
S_{run}	0,53				
S_i	2,15				
RSD (%)	1,19				

Table S37. Statistical results of intermediate precision for JWH-122 by µSPEed

Days	Day 1	Day 2	Day 3	Day 4	Day 5
R^2	0,9987	0,9996	0,9998	0,9995	0,9963
Slope	0,0589	0,0593	0,0571	0,0617	0,0601
Y_0	-1,1445	-1,1936	-1,0105	-1,3711	-1,3787
LL			**40**		
Replicated 1	38,8	39,4	39,1	41,3	42,8
Replicated 2	38,1	38,5	39,5	41,0	43,3
Replicated 3	37,9	39,4	39,4	40,8	42,4
$\bar{x}$	38,3	39,1	39,3	41,0	42,8
Recovery (%)	95,7	97,7	98,3	102,6	107,1
Mean Conc.			40,1		
Mean recovery (%)			100,3		
S_r			0,39		
S_{run}			1,82		
S_i			1,86		
RSD (%)			4,64		
ML			**100**		
Replicated 1	105,6	95,1	97,7	102,4	97,6
Replicated 2	100,1	105,7	103,3	95,5	88,5
Replicated 3	103,1	104,0	102,6	96,7	99,0
$\bar{x}$	102,9	101,6	101,2	98,2	95,1
Recovery (%)	102,9	101,6	101,2	98,2	95,1
Mean Conc.			99,8		
Mean recovery (%)			99,8		
S_r			4,36		
S_{run}			1,91		
S_i			4,76		
RSD (%)			4,77		
HL			**180**		
Replicated 1	178,9	178,0	182,1	181,6	184,1
Replicated 2	177,1	180,3	178,6	180,6	183,3
Replicated 3	180,5	179,6	177,9	180,1	178,9
$\bar{x}$	178,9	179,3	179,5	180,7	182,1
Recovery (%)	99,4	99,6	99,7	100,4	101,2
Mean Conc.			180,1		
Mean recovery (%)			100,1		
S_r			1,89		
S_{run}			0,75		
S_i			2,03		
RSD (%)			1,13		

Table S38. Statistical results of intermediate precision for UR-144 by µSPEed

Days	Day 1	Day 2	Day 3	Day 4	Day 5
R^2	0,9995	0,9993	0,9998	0,9973	0,9986
Slope	0,0756	0,0778	0,0706	0,0798	0,0788
Y_0	-2,0273	-1,9094	-1,7540	-2,1254	-2,1149
LL	**40**				
Replicated 1	40,3	38,3	39,8	37,3	38,0
Replicated 2	41,5	39,0	40,8	37,7	37,6
Replicated 3	41,2	38,9	41,3	37,8	39,2
$\bar{x}$	41,0	38,8	40,7	37,6	38,3
Recovery (%)	102,5	96,9	101,6	94,0	95,7
Mean Conc.	39,3				
Mean recovery (%)	98,2				
S_r	0,62				
S_{run}	1,46				
S_i	1,59				
RSD (%)	4,04				
ML	**100**				
Replicated 1	95,8	102,4	103,3	101,2	96,5
Replicated 2	102,9	102,7	96,9	106,6	102,3
Replicated 3	96,0	101,4	96,3	104,9	110,3
$\bar{x}$	98,2	102,2	98,9	104,2	103,0
Recovery (%)	98,2	102,2	98,9	104,2	103,0
Mean Conc.	101,3				
Mean recovery (%)	101,3				
S_r	4,17				
S_{run}	1,06				
S_i	4,30				
RSD (%)	4,25				
HL	**180**				
Replicated 1	181,9	177,7	178,2	180,2	177,7
Replicated 2	179,2	181,1	181,9	176,8	180,9
Replicated 3	181,1	178,5	181,3	177,6	177,5
$\bar{x}$	180,7	179,1	180,5	178,2	178,7
Recovery (%)	100,4	99,5	100,3	99,0	99,3
Mean Conc.	179,4				
Mean recovery (%)	99,7				
S_r	1,78				
S_{run}	0,44				
S_i	1,83				
RSD (%)	1,02				

Table S39. Statistical results of intermediate precision for JWH-210 by µSPEed

Days	Day 1	Day 2	Day 3	Day 4	Day 5
R^2	0,9998	0,9997	1,0000	0,9994	0,9998
Slope	0,0741	0,0714	0,0719	0,0710	0,0703
Y_0	-1,7967	-1,7270	-1,7473	-1,7799	-1,6847
LL			**40**		
Replicated 1	39,7	39,6	40,8	39,2	39,2
Replicated 2	39,5	39,4	40,0	38,9	39,1
Replicated 3	39,1	38,8	39,9	38,7	39,5
$\bar{x}$	39,4	39,3	40,2	38,9	39,3
Recovery (%)	98,6	98,1	100,6	97,3	98,2
Mean Conc.			39,4		
Mean recovery (%)			98,6		
S_r			0,37		
S_{run}			0,44		
S_i			0,58		
RSD (%)			1,47		
ML			**100**		
Replicated 1	102,3	99,3	99,3	101,9	99,2
Replicated 2	100,5	100,9	97,4	103,7	102,8
Replicated 3	100,2	102,3	99,4	100,1	101,8
$\bar{x}$	101,0	100,8	98,7	101,9	101,3
Recovery (%)	101,0	100,8	98,7	101,9	101,3
Mean Conc.			100,7		
Mean recovery (%)			100,7		
S_r			1,51		
S_{run}			0,83		
S_i			1,73		
RSD (%)			1,71		
HL			**180**		
Replicated 1	179,3	179,1	180,4	179,4	179,6
Replicated 2	179,9	179,6	180,2	179,8	178,8
Replicated 3	179,5	179,3	180,0	178,4	180,0
$\bar{x}$	179,6	179,3	180,2	179,2	179,5
Recovery (%)	99,8	99,6	100,1	99,5	99,7
Mean Conc.			179,5		
Mean recovery (%)			99,7		
S_r			0,47		
S_{run}			0,26		
S_i			0,54		
RSD (%)			0,30		

Table S40. Statistical results of intermediate precision for APINACA by µSPEed

Days	Day 1	Day 2	Day 3	Day 4	Day 5
R^2	0,9992	0,9985	0,9990	0,9990	0,9993
Slope	0,0749	0,0722	0,0701	0,0690	0,0674
Y_0	-1,5157	-1,3897	-1,4683	-1,4792	-1,3544
LL	**40**				
Replicated 1	38,4	38,3	41,8	41,7	41,1
Replicated 2	38,6	38,5	41,3	41,4	41,2
Replicated 3	39,0	37,8	41,2	41,2	41,4
$\overline{x}$	38,7	38,2	41,4	41,4	41,2
Recovery (%)	96,8	95,5	103,6	103,6	103,1
Mean Conc.	40,2				
Mean recovery (%)	100,5				
S_r	0,29				
S_{run}	1,61				
S_i	1,63				
RSD (%)	4,06				
ML	**100**				
Replicated 1	102,5	103,5	97,1	97,5	98,6
Replicated 2	102,3	102,6	97,4	96,4	96,4
Replicated 3	102,0	103,4	97,9	98,6	98,4
$\overline{x}$	102,3	103,2	97,5	97,5	97,8
Recovery (%)	102,3	103,2	97,5	97,5	97,8
Mean Conc.	99,6				
Mean recovery (%)	99,6				
S_r	0,78				
S_{run}	2,79				
S_i	2,90				
RSD (%)	2,91				
HL	**180**				
Replicated 1	177,3	182,1	179,4	180,0	181,0
Replicated 2	178,9	177,1	180,5	181,9	180,2
Replicated 3	179,1	178,2	180,7	181,3	181,5
$\overline{x}$	178,4	179,1	180,2	181,1	180,9
Recovery (%)	99,1	99,5	100,1	100,6	100,5
Mean Conc.	180,0				
Mean recovery (%)	100,0				
S_r	1,38				
S_{run}	0,83				
S_i	1,61				
RSD (%)	0,89				

Table S41. Accuracy statistical results for MAM-2201 by µSPEed

Days	Day 1	Day 2	Day 3	Day 4	Day 5
Equation	y=0,1393x - 2,9853	y=0,1538x - 3,8280	y=0,1417x - 3,0960	y=0,1400x - 2,5623	y=0,1510x - 3,2489
Low Conc. (ng/mL)			40		
Mean concentration	38,9	40,7	40,4	36,4	37,6
Recovery (%)	97,2	101,7	100,9	90,9	94,1
Mean			38,8		
mean recovery (%)			97,0		
SD			4,54		
RSD (%)			4,68		
N (days)			5		
T_{exp}			1,50		
T_{crit}			2,78		
$U_{\%R}$			2,03		
U_R			0,02		
Bias (%)			-3,04		
Medium Conc. (ng/mL)			100		
Mean concentration	102,0	98,8	99,4	106,4	104,1
Recovery (%)	102,0	98,8	99,4	106,4	104,1
Mean			102,1		
mean recovery (%)			102,1		
SD			3,17		
RSD (%)			3,11		
N (days)			5		
T_{exp}			1,50		
T_{crit}			2,78		
$U_{\%R}$			1,42		
U_R			0,01		
Bias (%)			2,13		
High Conc. (ng/mL)			180		
Mean concentration	179,2	180,5	180,3	177,3	178,2
Recovery (%)	99,5	100,3	100,1	98,5	99,0
Mean			179,1		
mean recovery (%)			99,5		
SD			0,76		
RSD (%)			0,76		
N (days)			5		
T_{exp}			1,50		
T_{crit}			2,78		
$U_{\%R}$			0,34		
U_R			0,00		
Bias (%)			-0,51		

Table S42. Accuracy statistical results for JWH-073 by µSPEed

Days	Day 1	Day 2	Day 3	Day 4	Day 5
Equation	y=0,0995x - 2,2028	y=0,0978x - 1,9892	y=0,0962x - 2,1792	y=0,1035x - 2,6939	y=0,1115x - 3,0908
Low Conc. (ng/mL)			40		
Mean concentration	41,0	38,3	40,3	41,9	41,3
Recovery (%)	102,6	95,9	100,7	104,6	103,3
Mean			40,6		
mean recovery (%)			101,4		
SD			3,42		
RSD (%)			3,37		
N (days)			5		
T_{exp}			0,93		
T_{crit}			2,78		
$U_{\%R}$			1,53		
U_R			0,02		
Bias (%)			1,42		
Medium Conc. (ng/mL)			100		
Mean concentration	98,2	102,9	99,5	96,8	97,7
Recovery (%)	98,2	102,9	99,5	96,8	97,7
Mean			99,0		
mean recovery (%)			99,0		
SD			2,39		
RSD (%)			2,42		
N (days)			5		
T_{exp}			0,93		
T_{crit}			2,78		
$U_{\%R}$			1,07		
U_R			0,01		
Bias (%)			-0,99		
High Conc. (ng/mL)			180		
Mean concentration	180,8	178,8	180,2	181,4	181,0
Recovery (%)	98,2	102,9	99,5	96,8	97,7
Mean			180,4		
mean recovery (%)			99,0		
SD			2,39		
RSD (%)			2,42		
N (days)			5		
T_{exp}			0,93		
T_{crit}			2,78		
$U_{\%R}$			1,07		
U_R			0,01		
Bias (%)			0,24		

Table S43. Accuracy statistical results for XLR-11 by µSPEed

Days	Day 1	Day 2	Day 3	Day 4	Day 5
Equation	y=0,0857x - 1,8646	y=0,0930x - 2,2850	y=0,0894x - 2,1384	y=0,0894x - 1,9363	y=0,0903x - 2,3047
Low Conc. (ng/mL)			**40**		
Mean concentration	38,2	40,0	39,4	37,5	40,6
Recovery (%)	95,4	100,1	98,5	93,8	101,4
Mean			39,1		
mean recovery (%)			97,8		
SD			3,19		
RSD (%)			3,26		
N (days)			5		
T_{exp}			1,51		
T_{crit}			2,78		
$U_{\%R}$			1,43		
U_R			0,01		
***Bias* (%)**			-2,16		
Medium Conc. (ng/mL)			**100**		
Mean concentration	103,2	99,9	101,1	104,4	99,0
Recovery (%)	103,2	99,9	101,1	104,4	99,0
Mean			101,5		
mean recovery (%)			101,5		
SD			2,23		
RSD (%)			2,20		
N (days)			5		
T_{exp}			1,51		
T_{crit}			2,78		
$U_{\%R}$			1,00		
U_R			0,01		
***Bias* (%)**			1,51		
High Conc. (ng/mL)			**180**		
Mean concentration	178,6	180,0	179,5	178,1	180,4
Recovery (%)	99,2	100,0	99,7	99,0	100,2
Mean			179,4		
mean recovery (%)			99,6		
SD			0,53		
RSD (%)			0,53		
N (days)			5		
T_{exp}			1,51		
T_{crit}			2,78		
$U_{\%R}$			0,24		
U_R			0,002		
***Bias* (%)**			-0,36		

Table S44. Accuracy statistical results for JWH-018 by µSPEed

Days	Day 1	Day 2	Day 3	Day 4	Day 5
Equation	y=0,1420x - 2,7551	y=0,1354x - 2,4696	y=0,1448x - 3,3777	y=0,1415x - 2,9491	y=0,1315x - 2,7500
Low Conc. (ng/mL)			**40**		
Mean concentration	40,1	38,3	42,0	41,9	42,5
Recovery (%)	100,3	95,6	105,0	104,8	106,2
Mean			41,0		
mean recovery (%)			102,4		
SD			4,38		
RSD (%)			4,28		
N (days)			5		
T_{exp}			1,22		
T_{crit}			2,78		
$U_{\%R}$			1,96		
U_R			0,02		
Bias (%)			2,39		
Medium Conc. (ng/mL)			**100**		
Mean concentration	99,8	103,1	96,5	96,6	95,7
Recovery (%)	99,8	103,1	96,5	96,6	95,7
Mean			98,3		
mean recovery (%)			98,3		
SD			3,07		
RSD (%)			3,12		
N (days)			5		
T_{exp}			1,22		
T_{crit}			2,78		
$U_{\%R}$			1,37		
U_R			0,01		
Bias (%)			-1,67		
High Conc. (ng/mL)			**180**		
Mean concentration	180,1	178,7	181,5	181,4	181,8
Recovery (%)	100,1	99,3	100,8	100,8	101,0
Mean			180,7		
mean recovery (%)			100,4		
SD			0,73		
RSD (%)			0,73		
N (days)			5		
T_{exp}			1,22		
T_{crit}			2,78		
$U_{\%R}$			0,33		
U_R			0,003		
Bias (%)			0,40		

Table S45. Accuracy statistical results for JWH-122 by µSPEed

Days	Day 1	Day 2	Day 3	Day 4	Day 5
Equation	y=0,0589x - 1,1445	y=0,0593x - 1,1936	y=0,0571x - 1,0105	y=0,0617x - 1,3711	y=0,0601x - 1,3787
Low Conc. (ng/mL)			40		
Mean concentration	38,3	39,1	39,3	41,0	42,8
Recovery (%)	95,8	97,7	98,3	102,6	107,0
Mean			40,1		
mean recovery (%)			100,3		
SD			4,52		
RSD (%)			4,50		
N (days)			5		
T_{exp}			0,15		
T_{crit}			2,78		
$U_{\%R}$			2,02		
U_R			0,02		
Bias (%)			0,29		
Medium Conc. (ng/mL)			100		
Mean concentration	102,9	101,6	101,2	98,2	95,1
Recovery (%)	102,9	101,6	101,2	98,2	95,1
Mean			99,8		
mean recovery (%)			99,8		
SD			3,16		
RSD (%)			3,17		
N (days)			5		
T_{exp}			0,15		
T_{crit}			2,78		
$U_{\%R}$			1,41		
U_R			0,01		
Bias (%)			-0,21		
High Conc. (ng/mL)			180		
Mean concentration	178,8	179,3	179,5	180,8	182,1
Recovery (%)	99,3	99,6	99,7	100,4	101,2
Mean			180,1		
mean recovery (%)			100,0		
SD			0,75		
RSD (%)			0,75		
N (days)			5		
T_{exp}			0,15		
T_{crit}			2,78		
$U_{\%R}$			0,34		
U_R			0,003		
Bias (%)			0,05		

Table S46. Accuracy statistical results for UR-144 by µSPEed

Days	Day 1	Day 2	Day 3	Day 4	Day 5
Equation	y=0,0756x - 2,0273	y=0,0778x - 1,9094	y=0,0706x - 1,7540	y=0,0798x - 2,1254	y=0,00788x - 2,1149
Low Conc. (ng/mL)			**40**		
Mean concentration	41,0	38,8	40,7	37,6	38,3
Recovery (%)	102,5	96,9	101,6	94,0	95,7
Mean			39,3		
mean recovery (%)			98,2		
SD			3,76		
RSD (%)			3,83		
N (days)			5		
T_{exp}			1,10		
T_{crit}			2,78		
$U_{\%R}$			1,68		
U_R			0,02		
Bias (%)			-1,85		
Medium Conc. (ng/mL)			**100**		
Mean concentration	98,2	102,2	98,9	104,2	103,0
Recovery (%)	98,2	102,2	98,9	104,2	103,0
Mean			101,3		
mean recovery (%)			101,3		
SD			2,63		
RSD (%)			2,60		
N (days)			5		
T_{exp}			1,10		
T_{crit}			2,78		
$U_{\%R}$			1,18		
U_R			0,01		
Bias (%)			1,29		
High Conc. (ng/mL)			**180**		
Mean concentration	180,8	179,1	180,5	178,2	178,7
Recovery (%)	100,4	99,5	100,3	99,0	99,3
Mean			179,4		
mean recovery (%)			99,7		
SD			0,63		
RSD (%)			0,63		
N (days)			5		
T_{exp}			1,10		
T_{crit}			2,78		
$U_{\%R}$			0,28		
U_R			0,003		
Bias (%)			-0,31		

Table S47. Accuracy statistical results for JWH-210 by µSPEed

Days	Day 1	Day 2	Day 3	Day 4	Day 5
Equation	y=0,0741x - 1,7967	y=0,0714x - 1,7270	y=0,0719x - 1,7473	y=0,0710x - 1,7799	y=0,0703x - 1,6847
Low Conc. (ng/mL)			40		
Mean concentration	39,4	39,3	40,2	38,9	39,3
Recovery (%)	98,6	98,1	100,6	97,3	98,2
Mean			39,4		
mean recovery (%)			98,6		
SD			1,23		
RSD (%)			1,25		
N (days)			5		
T_{exp}			2,61		
T_{crit}			2,78		
$U_{\%R}$			0,55		
U_R			0,01		
Bias (%)			-1,44		
Medium Conc. (ng/mL)			100		
Mean concentration	101,0	101,3	99,6	101,9	101,3
Recovery (%)	101,0	101,3	99,6	101,9	101,3
Mean			101,0		
mean recovery (%)			101,0		
SD			0,86		
RSD (%)			0,85		
N (days)			5		
T_{exp}			2,61		
T_{crit}			2,78		
$U_{\%R}$			0,39		
U_R			0,00		
Bias (%)			1,01		
High Conc. (ng/mL)			180		
Mean concentration	179,6	179,4	180,2	179,2	179,5
Recovery (%)	99,8	99,7	100,1	99,5	99,7
Mean			179,6		
mean recovery (%)			99,8		
SD			0,21		
RSD (%)			0,21		
N (days)			5		
T_{exp}			2,61		
T_{crit}			2,78		
$U_{\%R}$			0,09		
U_R			0,001		
Bias (%)			-0,24		

Table S48. Accuracy statistical results for APINACA by µSPEed

Days	Day 1	Day 2	Day 3	Day 4	Day 5
Equation	y=0,0749x - 1,5157	y=0,0722x - 1,3897	y=0,0701x - 1,4683	y=0,0690x - 1,4792	y=0,0674x - 1,3544
Low Conc. (ng/mL)			**40**		
Mean concentration	38,7	38,2	42,2	40,7	41,2
Recovery (%)	96,8	95,5	105,6	101,6	103,1
Mean			40,2		
mean recovery (%)			100,5		
SD			4,28		
RSD (%)			4,26		
N (days)			5		
T_{exp}			0,27		
T_{crit}			2,78		
$U_{\%R}$			1,91		
U_R			0,02		
***Bias* (%)**			0,51		
Medium Conc. (ng/mL)			**100**		
Mean concentration	102,3	103,2	97,5	95,8	97,8
Recovery (%)	102,3	103,2	97,5	95,8	97,8
Mean			99,3		
mean recovery (%)			99,3		
SD			3,21		
RSD (%)			3,23		
N (days)			5		
T_{exp}			0,48		
T_{crit}			2,78		
$U_{\%R}$			1,44		
U_R			0,01		
***Bias* (%)**			-0,68		
High Conc. (ng/mL)			**180**		
Mean concentration	179,0	178,6	181,1	178,2	180,9
Recovery (%)	99,5	99,2	100,6	99,0	100,5
Mean			179,6		
mean recovery (%)			99,8		
SD			0,75		
RSD (%)			0,75		
N (days)			5		
T_{exp}			0,72		
T_{crit}			2,78		
$U_{\%R}$			0,33		
U_R			0,00		
***Bias* (%)**			-0,24		

Supplementary Material IV – Cytotoxicity studies

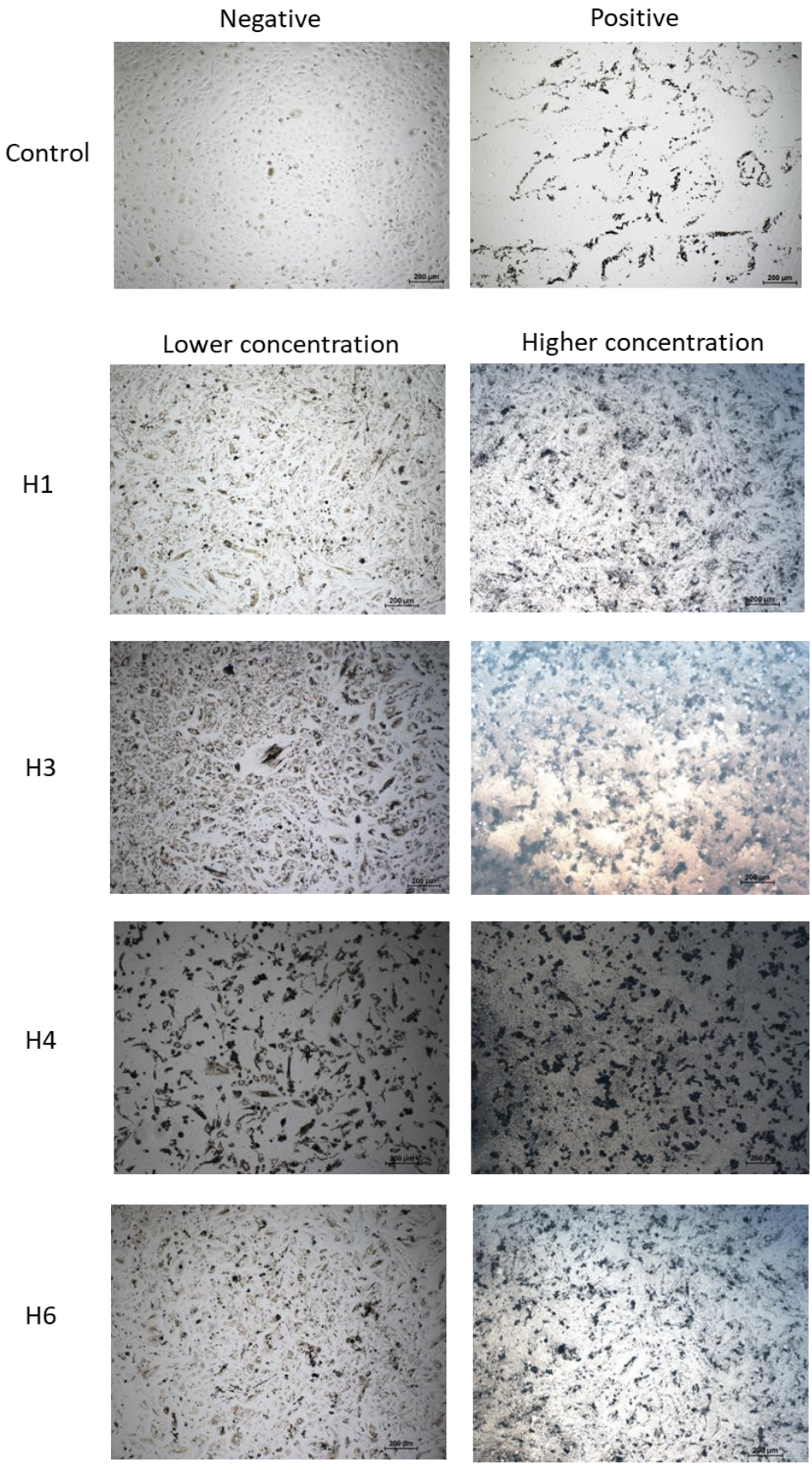

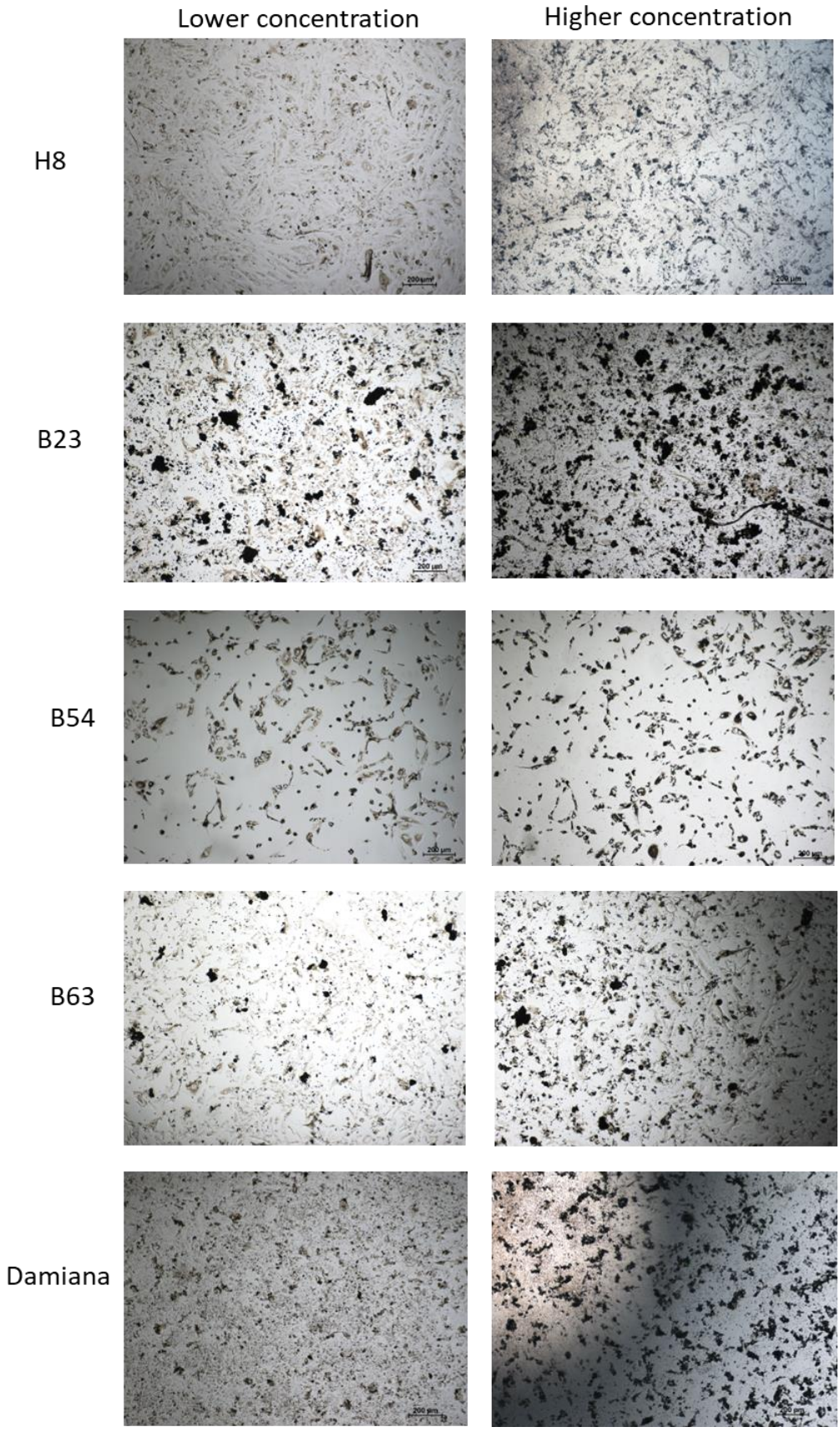

Figure S21. Microscopic images of A549 in a magnification of 40x of positive and negative controls and after 72h of exposure with herbal extracts.

Table S49. Parameters derived from nonlinear fits of herbal extracts concentration-response data to the asymmetric logit function, in the MTT reduction assay, in A549 lung cells after 48h and 72h of exposure (n = 4; P < 0.05).

Herbal extract	Estimated parameters for the best-fit regression model							IC_{50} (μg/mL)		IC_{25} (μg/mL)	
	Regression model	θ_1		θ_2		θ_{max}					
		48h	72h	48h	72h	48h	72h	48h	72h	48h	72h
H1	Logit	~7.11	2.92	~0.66	2.68	~40279	84.96	n.a.	833	n.a.	553
H3		~4.84	3.28	~1.66	0.96	~27907	196.7	n.a.	1888	n.a.	603
H4		2.33	3.10	1.29	1.39	101	197.2	214	1265	91	572
H6		~8.09	2.79	~0.33	2.15	~6870	93.02	n.a.	615	n.a.	369
H8		2.80	2.84	1.69	1.65	90.29	130.2	624	689	326	354
B23		3.14	3.12	7.72	4.12	84.93	118.8	1373	1326	1191	1015
B54		1.83	2.09	1.50	3.57	71.41	72.99	67	123	32	90
B63		~6.03	3.37	~0.92	2.82	~39433	299.4	n.a.	2338	n.a.	1584
Damiana		~-1.43	3.33	~0.44	1.52	~151.3	285.7	n.a.	2147	n.a.	1044

*n.a.: not available value; unable to calculate a complete confidence interval.